Methods in Molecular Biology™

VOLUME 232

Protein Misfolding and Disease

Principles and Protocols

Edited by

Peter Bross

Niels Gregersen

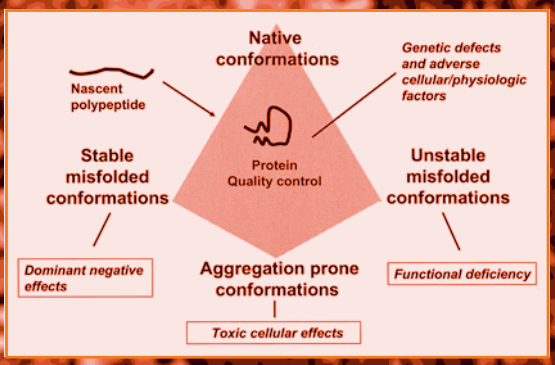

HUMANA PRESS

1

Protein Misfolding, Aggregation, and Degradation in Disease

Niels Gregersen, Lars Bolund, and Peter Bross

1. Introduction

During the last 5–10 years, it has been realized that a large number of diseases with very different pathologies at the cellular level can be discussed within a common framework of defective protein folding. Although the molecular mechanisms by which the pathologies develop are quite different, they can all be viewed as "conformational diseases." The original concept of conformational disease was developed in relation to disorders whose hallmark was intra- or extracellular accumulation of protein aggregates, such as seen in α-1-antitrypsin deficiency with liver pathology, Alzheimer's, Parkinson's, and Huntington's diseases (AD/PD/HD) ***(1–3)***. The basis for the pathology in these diseases is a cellular inability to degrade misfolded and damaged proteins and formation of cytotoxic intra- or extracellular oligomers and polymers/aggregates. The pathology in these diseases is predominantly determined by the cell damage associated with the aggregation process, thus exhibiting what can be considered a "gain-of-function" pathology.

Most cases with this type of conformational disease show a multifactorial etiology, involving genetic as well as physiological/environmental components. However, some cases are predominantly genetically determined, such as the early forms of Alzheimer's and Parkinson's diseases, and a few can be considered as classical monogenic disorders, such as HD and α-1-antitrypsin deficiency. To this last category of monogenic conformational diseases can be added a number of dominantly inherited diseases, such as hereditary forms of keratin- and collagen-disorders ***(4,5)*** as well as familial forms of cardiomyopa-

From: *Methods in Molecular Biology, vol. 232: Protein Misfolding and Disease: Principles and Protocols*
Edited by: P. Bross and N. Gregersen © Humana Press Inc., Totowa, NJ

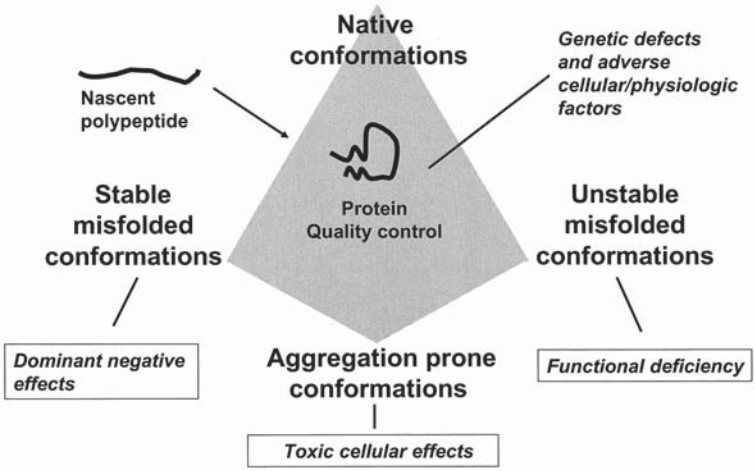

Fig. 1. Relationship between protein quality control and conformational diseases.

thies ***(6)***, where a misfolded protein coded from a defective gene exerts negative dominance in oligo- or multimeric complexes, thus compromising the function. Some cancers, such as the inherited Li-Fraumeni syndrome and some early onset cancers with p53 mutations, may be added to this negative dominant type of conformational diseases ***(7)***.

Yet, another group of diseases, where defective protein folding has been shown to play a central role in the pathology, comprises a large number of inherited autosomal recessive disorders ***(8–10)***, such as cystic fibrosis ***(11)***, phenylketonuria ***(12)***, the pulmonary form of α-1-antitrypsin deficiency ***(2,13)***, and the fatty acid oxidation defects ***(14)***, where misfolded mutant proteins are degraded rapidly, resulting in a "loss-of-function" pathology related to a decreased steady-state amount of the protein in question. The concept of conformational diseases with pathologies associated with negative dominance as well as with toxic accumulation and degradation of misfolded proteins is illustrated in **Fig. 1**.

In addition to the pathologies associated directly to protein misfolding, all the conformational diseases may develop pathological manifestations, which are specific to the particular protein or proteins that are misfolded. Such effects of the misfolding may be of determining importance for the pathological development of certain diseases, as it is documented in many metabolic disorders, where upstream accumulation of cellular components, e.g., substrates for enzymes or ligands for receptors, may contribute significantly to the pathological picture. These effects are not the theme of this book. The common framework is defective protein folding as the etiological factor and its consequences for the pathology. Selected aspects of this framework will be discussed

below, and illustrative experimental approaches to the investigations of the molecular cell pathology of protein folding diseases are the main theme of the book. To limit the number of citations in this chapter, most references are directed towards review papers discussing general or special aspects of protein folding diseases and in which references to the original literature can be found.

2. Pathogenesis of Conformational Diseases

Almost all proteins* must acquire a folded tertiary structure before they can function properly in the right place in the cell. To assist the folding and to supervise the maintenance of the folded structure, all organisms have evolved a set of protein quality-control systems, which consist of molecular chaperones and intracellular proteases. These components will be discussed in details in Chapter 2.

The proper acquisition and maintenance of the folded structure may be compromised by a number of genetically determined molecular and cellular/physiological factors. This chapter will discuss a number of these pathogenetic factors, the selection of which has been decided from the unifying view of protein misfolding. In this context it is important to discuss aspects of the genesis of misfolded proteins, which may be promoted by inherited amino acid alterations in the protein or/and associated with an intrinsic ability of the wild-type protein to acquire a misfolded conformation. Further, it is important for a pathogenetic understanding to discuss a number of other factors, which may be decisive for the genesis as well as for the consequences of misfolding. Here we have chosen to discuss cellular conditions, such as temperature and oxidative stress, as well as the cell's inherited or acquired ability to cope with misfolded and damaged proteins. This last aspect includes cell aging and inherited defects of folding and degradation systems.

2.1. Amino Acid Alterations as Determinants in Conformational Diseases

Genetic diseases are due to gene sequence alterations, the consequences of which may be quite different. A thorough discussion on the various types of sequence alterations is outside the scope of this chapter†, but in this connection it is interesting to note that about half of all sequence alterations in genetic disorders are missense mutations that change a single amino acid in the polypeptide chain ***(15)***. In most cases where missense mutations are involved the synthesized

---

*A number of cellular proteins do not possess a tertiary structure but are present in an unfolded form, e.g., α-synuclein, which is implicated in Parkinson's disease ***(28)***.

†A comprehensive treatment of mutation types and their consequences has been performed by Cooper and Krawczak ***(57)***.

amounts of mutant protein compared to wild-type (normal) are unimpaired* and the effect of the mutation is often structural, i.e., affecting the ability of the protein to fold to the functional conformation and/or the stability of this conformation. All types of conformational diseases are represented in this group.

2.1.1. Autosomal Recessive Disorders With Predominantly Loss-of-Function Pathology

As mentioned the pathogenesis of many autosomal recessive disorders are due to defective folding and elimination of the mutant protein, creating a loss-of-function pathology. Cystic fibrosis, phenylketonuria, and short-chain acyl-CoA dehydrogenase may serve as examples of diseases that affect the endoplasmic reticulum (ER), the cytosol, and the mitochondria, respectively. According to our present understanding, the mutated protein products in these disorders are degraded and the pathology is determined by functional deficiency and by redistribution of chloride, accumulation of phenylalanine, and accumulation of fatty acid oxidation intermediates, especially butyric acid, respectively. To what extent certain mutated proteins in these classically recessive disorders interfere with other cellular processes by occupying components of the protein quality-control systems, forming aggregates, or exerting negative dominance is not know at present, but certain indications suggest that it may sometimes be the case. The fact that the cystic fibrosis transmembrane conductance regulator (CFTR) protein contains a sequence that is prone to aggregation ***(16)*** indicates that some missense mutated CFTR in cells of cystic fibrosis patients may form aggregates, especially during cellular stress, which may add to the pathology ***(17)***. Although certain mutants of phenylalanine hydroxylase (PAH), which is defective in phenylketonuria (PKU), and some mutants of short-chain acyl-CoA dehydrogenase (SCAD), which are present in some patients with SCAD deficiency, have not been shown to form aggregates, they have been indicated to form complexes with components of the protein quality-control systems ***(18,19)***. Thus, certain SCAD mutant proteins have been shown to be associated with Hsp60 to a greater extent than the wild-type protein ***(9)***. The possible existence of symptomatic heterozygous patients with a number of fatty acid oxidation defects (SCAD, MCAD, VLCAD) (Andresen, B.S. and Gregersen, N. unpublished data) and CPTII deficiencies ***(20)*** also indicates that the degradation of the mutant protein may be slow and that negative dominance may come into action by integrating mutant proteins into the oligomeric enzyme complexes.

---

*Missense mutations may at certain positions alter the binding of protein factors involved in the splicing of pre-mRNA, resulting in aberrant spliced mRNA that may be rapidly degraded. Consequently the synthesised amounts of missense mutant protein may be decreased ***(58)***.

Despite the fact that there may be other effects of inherited mutations in metabolic disorders than the functional deficiency, the loss-of-function has until now attracted most attention. In the few diseases where mutant proteins have been studied, the main effect of missense mutations is prolonged interaction with the chaperones, which may target the mutant folding intermediates to degradation by intracellular proteases (*see* Chapter 2). Consequently, the amount of mutant protein will be decreased to a level that depends on the balance between folding and degradation. In the recessive diseases, the balance is shifted towards degradation. However, some mutations affect the folding to a lesser degree than others, which is reflected in the fact that the phenotype of many loss-of-function disorders may range from mild to severe ***(9,10)***. Moreover, the balance may be influenced by the cellular conditions. In some cases it has been shown that higher temperatures increase the misfolded fraction and that lower temperatures promote folding. This indicates that fever and other forms for folding stress may shift the balance to degradation, thereby eliminating a possible residual activity and worsening the clinical situation, as has been suggested to be the case in a number of autosomal recessively inherited diseases ***(8–10)***.

2.1.2. Dominant Inherited Diseases Showing Negative Dominant Gain-of-Function Pathology

The second type of consequences of inherited missense mutations is the genesis of misfolded proteins, which are not degraded but exert a negative effect by inhibiting the normal function of the protein in question. As mentioned this type of gain-of-function diseases is represented by disorders such as the keratin and collagen diseases, familial forms of cardiomyophaties, and others where the inheritance is dominant, reflecting that heterozygosity for mutations is disease-causing, and where a stable mutant protein exerts a dominant-negative effect on the wild-type protein. Again, depending on the nature and position of the mutations the condition may be mild or severe, as has been evidenced in the keratin disease Epidermolysis Bullosa Simplex ***(4)***, where mildly affected patients only suffer from bulla in the skin after stress and where severe phenotypes are characterized by chronic damage of epidermal cells.

Whether the cellular conditions in these cases may modulate the extent of negative dominance by promoting the degradation of misfolded mutant protein is not known at present, but it is likely that there exists a continuum between functional deficiency, as seen in the recessive disorders, and negative dominance, as seen in the dominant disorders.

2.1.3. Diseases With "Toxic" Aggregation-Type Gain-of-Function Pathology

The third type of structural consequences of missense mutant proteins is formation of insoluble oligomers and polymers/aggregates, which exert a toxic gain-

of-function effect on the cell, and in which cell damage/death is decisive for the clinical phenotype. Together with the amyloidoses and the late-onset (neuro)degenerative disorders, where a conformational change in a "normal" protein is the main disease-developing event, these are classical conformational diseases ***(21)***. Although the endpoint—the accumulation of aggregated proteins—is similar for the paradigmatic examples, α-1-antitrypsin deficiency, Huntington's, Parkinson's, and Alzheimer's diseases, the pathogenesis in these four diseases is quite different. In α-1-antitrypsin deficiency the prevalent Z-mutation hinders the proper folding in the ER of liver cells and the misfolded protein has an ability to form oligo- and polymers, which are targeted for degradation ***(2,13***; *see* Chapter 4***)***. In heterozygous carriers and in homozygous patients with the lung form of the disease the capacity of the degradation components of the protein quality-control system is sufficient to cope with the accumulated protein. However, owing to a yet undiscovered decrease in the degradation capacity in 10–15% of homozygous patients, the accumulated protein polymers cannot be eliminated in the liver cells of such individuals ***(22)*** and they develop cirrhosis-like liver damage and hepatocellular carcinoma. As was mentioned earlier, the cellular conditions may modulate the severity of the clinical phenotype, which has been suggested for the liver disease in α-1-antitrypsin deficiency ***(23)***.

The pathogenesis in HD is shared by at least nine other inherited neurological diseases where the pathogen is a string of glutamine amino acids, which is part of a large protein, huntingtin, of unknown function ***(24–26)***. In patients with HD, the repeat length may be more than 55, and the longer the repeat the more prone to aggregation is the fragment. This is reflected in earlier disease onset for patients with long repeats than in patients with shorter strings of glutamine ***(27)***.

The glutamine repeats share the tendency to self-aggregation with an unknown number of other amino acid strings in cellular proteins, among them α-synuclein and amyloid β-peptide, which are the considered pathogen in some cases of Parkinson's and Alzheimer's diseases, respectively ***(21)***. Early forms of these diseases are inherited due to mutations in the respective genes, which further promote the self-aggregation of the proteins/peptides. It is therefore appropriate to discuss this type of gain-of-function conformational diseases in relation to diseases (e.g., the late onset forms of Parkinson and Alzheimer's diseases) where self-aggregating proteins, due to an intrinsic conformational instability of the wild-type protein, accumulate and participate in the development of degenerative disorders.

2.2. The Significance of Intrinsic Conformational Instability

Normally a protein in its native state exists in a conformation, which is a balanced mixture of α-helices, β-sheets, and unstructured turns. As mentioned earlier, a minor fraction of cellular proteins are natively unfolded, as is the case

for α-synuclein ***(28)***. Furthermore, an unknown number of cellular proteins are prone to transition from the functional conformation to a conformation dominated by β-sheets, which may aggregate in the respective compartment where the particular protein is located or be excluded to form extracellular amyloid bodies. It is believed that intrinsic instability owing to a low transition energy to an unfolded state or/and relative stable folding intermediates, that escape the protein quality control systems is a precondition for aggregate formation ***(21)***. However, although all proteins under adverse in vitro or in vivo conditions may be able to aggregate, a further requirement for a protein to be pathogenic is a string of amino acids with high hydrophobicity and a high propensity to form β-sheets, which have a tendency to associate ***(21,29)***. The fact that the protein acylphosphatase, which has been used extensively in folding and aggregation studies, carries two short strings of aggregation prone amino acids ***(29)***, and the observation that a certain fragment of the CFTR protein forms aggregates when overexpressed in bronchial epithelial cells, but does not aggregate after mutation of two specific amino acid residues in the fragment, stress this point ***(16)***.

The aggregation mechanism is not known exactly. However, a conformation/polymerization mechanism, as reviewed by Soto ***(30)***, seems attractive. The process is initiated by a stochastic conformational change to an unfolded state with β-sheet propensity, followed by oligomerization and eventually further formation of larger oligomers/aggregates. This simple mechanism is attractive first of all because it is compatible with the hypothesis that the protein quality control in the healthy and young cell eliminates the molecules with non-native conformations before they can embark in oligomer assembly, and thereby prevents the oligomer/aggregate formation. Secondly, this mechanism is attractive because it has been strongly indicated from a number of experiments that early oligomers and not the finally visible aggregates themselves are the toxic species ***(31,32)***. In fact, aggregation and especially the formation of so-called aggresomes in the cytosol may be viewed as a cellular defense mechanism ***(17)***, and induction of an autophagic response may serve to eliminate these aggresomes as well as aggregates in other compartments ***(33,34)***.

Sequence alterations, as seen in α-1-antitrypsin, α-synuclein, and amyloid β-peptide, may further promote the structural transition and oligomerization. Likewise, mutations in proteins, which—maybe by complicated mechanisms—influence the steady-state level of the potential cytotoxic proteins, may accelerate aggregate formation. Mutations in presenilin-1 and presenilin-2, which are proteases associated with γ-secretase complexes ***(35)*** and involved in the formation of amyloid β-peptide, seem to confer susceptibility to amyloid formation in AD patients by elevating the cellular level of the β-peptide ***(36)***. Another instructive, but less clear, example of this phenomenon is the accumu-

lation of α-1-antitrypsin aggregates in liver cells of patients with the hepatic form of α-1-antitrypsin deficiency. In these patients there is a defect in the ER degradation apparatus, which in patients with the pulmonary form and in most individuals in the general population is able to clear the misfolded mutant α-1-antitrypsin *(22)*. Although the exact mechanism has not yet been identified, it is conceivable that a gene variation is responsible for the disability.

As mentioned earlier, it is not known to what extent mutant proteins in the loss-of-function recessive disorders may elude the protein quality-control systems and form oligo- and polymers, which may add to the pathology of the particular disease. Two examples, involving two different cellular compartments, suggest that this may turn out to be an important additional mechanism. Overexpression in cell culture of CFTR protein carrying the common δ-Phe508 mutation results in aggregate formation in the ER *(17)*, and the same mutant protein is able to release a stress response and activate a pro-inflammatory signal *(37)*. This may be induced by cell stress associated with the perturbed ion channels, but it is probable that toxic effects of oligomers/aggregates are involved. The other example is experimental. An in-frame deletion mutant gene of mitochondrial ornithine transcarbamylase, δ30-114OTC, was constructed and transfected into COS-7 cells. This procedure produced mitochondrial aggregates of the protein and elicited a stress response *(38)*. Whether naturally occurring mitochondrial mutant proteins may form aggregates is not known at present. It may depend on the protein in question, the nature of the mutation, and certainly on the cellular conditions.

2.3. The Cellular Conditions as Determinants in Conformational Disease

Elevated temperatures promote misfolding and decrease the residual activity in loss-of-function disorders, such as cystic fibrosis, phenylketonuria, and the fatty acid oxidation deficiencies. Elevated temperature has also been shown to increase the polymerization tendency of α-1-antitrypsin *(23)*, and the oligomerization tendency of α-synuclein is enhanced by temperature increase *(39)*. In general, elevated temperatures and other stress factors, like altered pH *(21)* and disturbed energy production may inhibit the acquisition of the folded state and promote the transition to an unfolded state, thus increasing the pathogenecity. Oxidative stress seems to be particularly harmful in this context *(25,40)*.

2.4. Oxidative Stress as Determinant in Conformational Diseases

Oxidative stress has been shown to contribute to the pathogenesis of many conformational diseases *(41)*. A cellular condition of oxidative stress develops

when the mitochondrial oxidative phosphorylation and the cell's antioxidative capacity become overloaded. In these situations reactive oxygen species (ROS) are generated in excessive amounts and damage to the cell and its DNA, RNA, lipid, and protein constituents may occur.

Misfolded proteins, including β-sheet oligo- and polymers, have been shown to provoke the development of oxidative stress ***(41)***. This might occur through an inability to clear misfolded proteins owing to perturbation of the proteasome degradation system ***(42)*** followed by an induction of the unfolded protein response ***(43)*** and a number of other stress responses ***(44)***. Dependent on the amount of insult, these responses are aimed at rescuing the cell or eliminating it by apoptosis or necrosis. An alternative or contributing mechanism may be that the misfolded proteins interact by hydrophobic forces and sequester other proteins, such as transcription factors and chaperones, which in turn elicit the stress responses ***(27,45)***.

Of special interest in this context is that misfolded and partly unfolded protein structures may be particularly susceptible to oxidative modifications, which may promote unfolding and thus increase the susceptibility to further modifications that exaggerate the stress responses ***(46)***. Despite the fact that the exact mechanisms and order of events may be quite different in the various conformational diseases, the endpoint seems similar: Chronic stress and eventually death to the cell. The mechanisms by which the cells are injured and the secondary consequences for the pathology in the various disorders are the focus of many investigations, some of which are discussed in this book with special focus on the methodologies used in the studies.

The involvement of oxidative stress associated with impairment of the oxidative phosphorylation and the induction of stress responses are well established for the gain-of-function neurodegenerative diseases. Deficient activity of components of the mitochondrial respiratory chain has been found in brain cells of patients with Alzheimer's, Parkinson's, and Huntington's diseases ***(25,41)***. The research in loss-of-function recessive disorders, on the other hand, has until now been focused on the functional deficiency and its consequences. However, the findings that misfolded mutant CFTR, α-1-antitrypsin, PAH, and SCAD proteins occupy those chaperones ***(9,18,47,48)*** that assist in the folding of the wild-type proteins for prolonged times and that the stress response in the ER and mitochondria may be induced by misfolded proteins indicate that unfolded protein induced oxidative stress may be of importance also in these diseases, especially for the progression of the pathology.

A dark horse in the aforementioned discussion is the cellular ability to cope with misfolded and damaged proteins, and thus inherited defects in components of the stress-response systems and cell aging become relevant in this context.

2.5. Decreased Ability to Cope With Misfolded and Damaged Proteins as Determinant in Conformational Diseases

The balance between the cellular capacity to eliminate misfolded and damaged proteins and the tendency of the particular protein to evade the system is a determining factor in the development and severity of conformational diseases. The outcome is often impossible to predict, but must be elucidated experimentally.

In healthy and young cells misfolded and damaged proteins are eliminated by the protease factors of the protein quality-control systems, but if these systems are overwhelmed, as may be the case in cells of patients with inherited defects of the defense systems and in aged cells, aberrant proteins may accumulate and cause all the problems discussed above ***(49–51)***.

In aged cells the resistance to oxidative stress as well as the capability to induce the activity of the protein quality control systems are decreased, which means that the cells may have difficulties in maintaining native protein conformations and elimination of misfolded and damaged proteins ***(49)***. Although the molecular mechanisms for these disabilities are still poorly defined they may contribute significantly to the pathogenesis of many of the age related conformational diseases.

In recent years, a number of diseases in which components of the cellular protein handling systems carry inherited defects have been identified ***(51)*** or indicated ***(22)*** and in some cases characterized at the molecular level ***(51–54)***. Without going into a detailed discussion about the pathogenesis in these diseases, suffice it to say that the molecular disability predominantly affects nondividing cells in the brain and muscles. Of particular relevance to the present discussion on conformational diseases is that there are diseases with distinct defects in general protein handling components, such as mitochondrial Hsp60 ***(54)*** and the ER degradation system ***(22)***, or in organ-specific components, such as crystallin ***(55)***.

Conformational diseases caused by defects in the oxidative defence systems, as for instance in superoxide dismutase (SOD) ***(56)***, have also been identified. These findings may forecast that more subtle deficiencies in the stress defense and protein handling systems may exist, which would add another susceptibility factor to the already known that should be included in the conceptional as well as experimental analyses of conformational diseases.

Acknowledgments

Work concerning protein misfolding as disease mechanism at Research Unit for Molecular Medicine and Institute of Human Genetics is supported by The Danish Medical Research Council; Danish Human Genome Centre; Karen

Elise Jensen Foundation; Aarhus County Research Initiative; Institute of Experimental Clinical Research, Aarhus University; Institute of Human Genetics, Aarhus University, and Aarhus University Hospital.

References

1. Carrell, R. W. and Lomas, D. A. (1997) Conformational disease. *Lancet* **350,** 134–138.
2. Carrell, R. W., and Lomas, D. A. (2002) Alpha1-antitrypsin deficiency: a model for conformational diseases. *N. Engl. J. Med.* **346,** 45–53.
3. Crowther, D. C. (2002) Familial conformational diseases and dementias. *Hum. Mutat.* **20,** 1–14.
4. Sørensen, C. B., Ladekjær-Mikkelsen, A. S., Andresen, B. S., Brandrup, F., Veien, N. K., Anton-Lamprecht, I., et al. (1999) Identification of novel and known mutations in the genes for keratin 5 and 14 in Danish patients with epidermolysis bullosa simplex. *J. Invest. Dermatol.* **112,** 184–190.
5. Baum, J. and Brodsky, B. (1999) Folding of peptide models of collagen and misfolding in disease. *Curr. Opin. Struct. Biol.* **9,** 122–128.
6. Burch, M. and Blair, E. (1999) The inheritance of hypertrophic cardiomyopathy. *Pediatr. Cardiol.* **20,** 313–316.
7. Monti, P., Campomenosi, P., Ciribilli, Y., Iannone, R., Inga, A., Abbondandolo, A., et al. (2002) Tumour p53 mutations exhibit promoter selective dominance over wild type p53. *Oncogene* **21,** 1641–1648.
8. Bross, P., Corydon, T. J., Andresen, B. S., Jørgensen, M. M., Bolund, L., and Gregersen, N. (1999) Protein misfolding and degradation in genetic disease. *Hum. Mutat.* **14,** 186–198.
9. Gregersen, N., Bross, P., Andresen, B. S., Pedersen, C. B., Corydon, T. J., and Bolund, L. (2001) The role of chaperone-assisted folding and quality control in inborn errors of metabolism: protein folding disorders. *J. Inherit. Metab. Dis.* **24,** 189–212.
10. Waters, P. J. (2001) Degradation of mutant proteins, underlying "loss of function" phenotypes, plays a major role in genetic disease. *Curr. Issues Mol. Biol.* **3,** 57–65.
11. Riordan, J. R. (1999) Cystic fibrosis as a disease of misprocessing of the cystic fibrosis transmembrane conductance regulator glycoprotein. *Am. J. Hum. Genet.* **64,** 1499–1504.
12. Waters, P. J., Parniak, M. A., Akerman, B. R., and Scriver, C. R. (2000) Characterization of phenylketonuria missense substitutions, distant from the phenylalanine hydroxylase active site, illustrates a paradigm for mechanism and potential modulation of phenotype. *Mol. Genet. Metab.* **69,** 101–110.
13. Perlmutter, D. H. (1999) Misfolded proteins in the endoplasmic reticulum. *Lab. Invest.* **79,** 623–638.
14. Gregersen, N., Andresen, B. S., Corydon, M. J., Corydon, T. J., Olsen, R. K., Bolund, L., and Bross, P. (2001) Mutation analysis in mitochondrial fatty acid oxidation defects: exemplified by acyl-CoA dehydrogenase deficiencies, with special focus on genotype-phenotype relationship. *Hum. Mutat.* **18,** 169–189.

15. Krawczak, M., Ball, E. V., Fenton, I., Stenson, P. D., Abeysinghe, S., Thomas, N., and Cooper, D. N. (2000) Human gene mutation database—a biomedical information and research resource. *Hum. Mutat.* **15,** 45–51.
16. Milewski, M. I., Mickle, J. E., Forrest, J. K., Stanton, B. A., and Cutting, G. R. (2002) Aggregation of misfolded proteins can be a selective process dependent upon peptide composition. *J. Biol. Chem.* **277,** 34462–34470.
17. Johnston, J. A., Ward, C. L., and Kopito, R. R. (1998) Aggresomes: a cellular response to misfolded proteins. *J. Cell Biol.* **143,** 1883–1898.
18. Gamez, A., Perez, B., Ugarte, M., and Desviat, L. R. (2000) Expression analysis of phenylketonuria mutations. Effect on folding and stability of the phenylalanine hydroxylase protein. *J. Biol. Chem.* **275,** 29,737–29,742.
19. Gregersen, N., Winter, V. S., Corydon, M. J., Corydon, T. J., Rinaldo, P., Ribes, A., et al. (1998) Identification of four new mutations in the short-chain acyl-CoA dehydrogenase (SCAD) gene in two patients: one of the variant alleles, 511C-->T, is present at an unexpectedly high frequency in the general population, as was the case for 625G-->A, together conferring susceptibility to ethylmalonic aciduria. *Hum. Mol. Genet.* **7,** 619–627.
20. Vladutiu, G. D. (1999) Biochemical and molecular correlations in carnitine palmitoyltransferase II deficiency. *Muscle Nerve* **22,** 949–951.
21. Dobson, C. M. (2001) The structural basis of protein folding and its links with human disease. *Philos. Trans. R. Soc. Lond. B Biol. Sci.* **356,** 133–145.
22. Wu, Y., Whitman, I., Molmenti, E., Moore, K., Hippenmeyer, P., and Perlmutter, D. H. (1994) A lag in intracellular degradation of mutant alpha 1-antitrypsin correlates with the liver disease phenotype in homozygous PiZZ alpha 1- antitrypsin deficiency. *Proc. Natl. Acad. Sci. USA* **91,** 9014–9018.
23. Lomas, D. A., Evans, D. L., Finch, J. T., and Carrell, R. W. (1992) The mechanism of Z alpha 1-antitrypsin accumulation in the liver. *Nature* **357,** 605–607.
24. Perutz, M. F. (1999) Glutamine repeats and neurodegenerative diseases: molecular aspects. *Trends Biochem. Sci.* **24,** 58–63.
25. Mattson, M. P., Chan, S. L., and Duan, W. (2002) Modification of brain aging and neurodegenerative disorders by genes, diet, and behavior. *Physiol. Rev.* **82,** 637–672.
26. Taylor, J. P., Hardy, J., and Fischbeck, K. H. (2002) Toxic proteins in neurodegenerative disease. *Science* **296,** 1991–1995.
27. Zoghbi, H. and Botas, J. (2002) Mouse and fly models of neurodegeneration. *Trends Genet.* **18,** 463–471.
28. Uversky, V. N. (2002) Natively unfolded proteins: a point where biology waits for physics. *Protein Sci.* **11,** 739–756.
29. Chiti, F., Taddei, N., Baroni, F., Capanni, C., Stefani, M., Ramponi, G., and Dobson, C. M. (2002) Kinetic partitioning of protein folding and aggregation. *Nat. Struct. Biol.* **9,** 137–143.
30. Soto, C. (2001) Protein misfolding and disease; protein refolding and therapy. *FEBS Lett.* **498,** 204–207.

31. Bucciantini, M., Giannoni, E., Chiti, F., Baroni, F., Formigli, L., Zurdo, J., et al. (2002) Inherent toxicity of aggregates implies a common mechanism for protein misfolding diseases. *Nature* **416,** 507–511.
32. Walsh, D. M., Klyubin, I., Fadeeva, J. V., Cullen, W. K., Anwyl, R., Wolfe, M. S., et al. (2002) Naturally secreted oligomers of amyloid beta protein potently inhibit hippocampal long-term potentiation in vivo. *Nature* **416,** 535–539.
33. Teckman, J. H., and Perlmutter, D. H. (2000) Retention of mutant alpha(1)-antitrypsin Z in endoplasmic reticulum is associated with an autophagic response. *Am. J. Physiol. Gastrointest. Liver Physiol.* **279,** G961–G974.
34. Earl, R. T., Mangiapane, E. H., Billett, E. E., and Mayer, R. J. (1987) A putative protein-sequestration site involving intermediate filaments for protein degradation by autophagy. Studies with transplanted Sendai-viral envelope proteins in HTC cells. *Biochem. J.* **241,** 809–815.
35. Weihofen, A., Binns, K., Lemberg, M. K., Ashman, K., and Martoglio, B. (2002) Identification of signal peptide peptidase, a presenilin-type aspartic protease. *Science* **296,** 2215–2218.
36. Yang, Y., Turner, R. S., and Gaut, J. R. (1998) The chaperone BiP/GRP78 binds to amyloid precursor protein and decreases Abeta40 and Abeta42 secretion. *J. Biol. Chem.* **273,** 25,552–25,555.
37. Weber, A. J., Soong, G., Bryan, R., Saba, S., and Prince, A. (2001) Activation of NF-kappaB in airway epithelial cells is dependent on CFTR trafficking and Cl- channel function. *Am. J. Physiol. Lung Cell Mol. Physiol.* **281,** L71–L78.
38. Zhao, Q., Wang, J., Levichkin, I. V., Stasinopoulos, S., Ryan, M. T., and Hoogenraad, N. J. (2002) A mitochondrial specific stress response in mammalian cells. *EMBO J.* **21,** 4411–4419.
39. Uversky, V. N., Lee, H. J., Li, J., Fink, A. L., and Lee, S. J. (2001) Stabilization of partially folded conformation during alpha-synuclein oligomerization in both purified and cytosolic preparations. *J. Biol. Chem.* **276,** 43,495–43,498.
40. Beal, M. F. (2000) Energetics in the pathogenesis of neurodegenerative diseases. *Trends Neurosci.* **23,** 298–304.
41. Butterfield, D. A. and Kanski, J. (2001) Brain protein oxidation in age-related neurodegenerative disorders that are associated with aggregated proteins. *Mech. Aging Dev.* **122,** 945–962.
42. Bence, N. F., Sampat, R. M., and Kopito, R. R. (2001) Impairment of the ubiquitin-proteasome system by protein aggregation. *Science* **292,** 1552–1555.
43. Imaizumi, K., Miyoshi, K., Katayama, T., Yoneda, T., Taniguchi, M., Kudo, T., and Tohyama, M. (2001) The unfolded protein response and Alzheimer's disease. *Biochim. Biophys. Acta* **1536,** 85–96.
44. Martindale, J. L. and Holbrook, N. J. (2002) Cellular response to oxidative stress: signaling for suicide and survival. *J. Cell Physiol.* **192,** 1–15.
45. Hughes, R. E. (2002) Polyglutamine disease: acetyltransferases awry. *Curr. Biol.* **12,** R141–R143.
46. Dukan, S., Farewell, A., Ballesteros, M., Taddei, F., Radman, M., and Nystrom, T. (2000) Protein oxidation in response to increased transcriptional or translational errors. *Proc. Natl. Acad. Sci. USA* **97,** 5746–5749.

47. Pind, S., Riordan, J. R., and Williams, D. B. (1994) Participation of the endoplasmic reticulum chaperone calnexin (P88, Ip90) in the biogenesis of the cystic fibrosis transmembrane conductance regulator. *J. Biol. Chem.* **269,** 12,784–12,788.
48. Qu, D., Teckman, J. H., Omura, S., and Perlmutter, D. H. (1996) Degradation of a mutant secretory protein, alpha1-antitrypsin Z, in the endoplasmic reticulum requires proteasome activity. *J. Biol. Chem.* **271,** 22,791–22,795.
49. Soti, C., and Csermely, P. (2000) Molecular chaperones and the aging process. *Biogerontology* **1,** 225–233.
50. Macario, A. J. and Conway, d. M. (2002) Sick chaperones and ageing: a perspective. *Aging Res. Rev.* **1,** 295–311.
51. Slavotinek, A. M. and Biesecker, L. G. (2001) Unfolding the role of chaperones and chaperonins in human disease. *Trends Genet.* **17,** 528–535.
52. Casari, G., De Fusco, M., Ciarmatori, S., Zeviani, M., Mora, M., Fernandez, P., et al. (1998) Spastic paraplegia and OXPHOS impairment caused by mutations in paraplegin, a nuclear-encoded mitochondrial metalloprotease. *Cell* **93,** 973–983.
53. Hazan, J., Fonknechten, N., Mavel, D., Paternotte, C., Samson, D., Artiguenave, F., et al. (1999) Spastin, a new AAA protein, is altered in the most frequent form of autosomal dominant spastic paraplegia. *Nat. Genet.* **23,** 296–303.
54. Hansen, J. J., Durr, A., Cournu-Rebeix, I., Georgopoulos, C., Ang, D., Nielsen, M. N., et al. (2002) Hereditary spastic paraplegia SPG13 is associated with a mutation in the gene encoding the mitochondrial chaperonin Hsp60. *Am. J. Hum. Genet.* **70,** 1328–1332.
55. Litt, M., Kramer, P., LaMorticella, D. M., Murphey, W., Lovrien, E. W., and Weleber, R. G. (1998) Autosomal dominant congenital cataract associated with a missense mutation in the human alpha crystallin gene CRYAA. *Hum. Mol. Genet.* **7,** 471–474.
56. Noor, R., Mittal, S., and Iqbal, J. (2002) Superoxide dismutase: applications and relevance to human diseases. *Med. Sci. Monit.* **8,** RA210–RA216.
57. Cooper, D. N. and Krawczak, M. (1993). Human Gene Mutation. Bios Scientific Publishers Ltd., Oxford, UK.
58. Cartegni, L., Chew, S. L., and Krainer, A. R. (2002) Listening to silence and understanding nonsense: exonic mutations that affect splicing. *Nat. Rev. Genet.* **3,** 285–298.

2

Basic Introduction to In Vivo Protein Folding and Its Defects

Peter Bross and Niels Gregersen

1. Introduction

The question on how proteins fold into their native structure has been a subject of intensive research since Anfinsen showed that a denatured protein could fold by itself in a test tube without any additional factors (reviewed in ***1***). In the last decade the field of research on protein folding has been further extended by the discovery of helper proteins—molecular chaperones—that assist protein folding in cells where adverse conditions for protein folding prevail. A comprehensive treatment of the huge body of knowledge on protein folding is not possible within the frame of this chapter. Our aim is to give a short introduction from the aspect of the conformational diseases (*see* Chapter 1) in which disturbances of protein folding are a major molecular pathological mechanism.

2. The Protein Folding Process

After assembly from the amino acid building blocks by the ribosome the linear polypeptide chain folds co- or post-translationally into its native conformation, the three-dimensional body that possesses the properties and activities for its cellular functions. Folding of the polypeptide chain may be understood as the sequential acquisition of all the interactions between atoms of the amino acid building blocks that are present in the native conformation. The information describing the exact three-dimensional structure resides in the amino acid sequence and naturally occurring proteins will usually with reasonable efficiency acquire their native conformation when produced in the appropriate biological environment.

From: *Methods in Molecular Biology, vol. 232: Protein Misfolding and Disease: Principles and Protocols*
Edited by: P. Bross and N. Gregersen © Humana Press Inc., Totowa, NJ

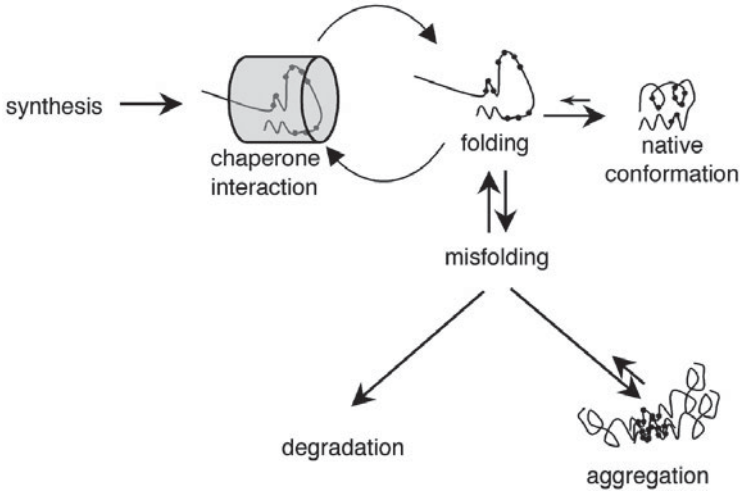

Fig. 1. The protein folding/misfolding process.

Theoretical considerations by Levinthal ***(2)*** had shown that proteins cannot explore all the possible combinations of interactions on the way to the native structure. This has led to the suggestion that pathways of protein folding exist. More recent research indicates that individual polypeptide chains from a given protein may pursue many different ways to reach the same native conformation, i.e., there is no fixed order for the acquisition of the various interactions. This "new view" of the protein folding process has been reviewed by Dinner et al. ***(3)***. Very briefly, folding is pictured in energy landscapes in which individual molecules, in a stochastic order, acquire increasing numbers of native interactions following a mainly downhill way of decreasing free energy, and finally ending up in the native conformation with the energy minimum for the molecule.

The folding process (*see* **Fig. 1**) is far from being perfect, which implies that individual molecules may form "wrong" interactions and be kinetically trapped in local energy minima. This process is described as misfolding. Misfolded molecules must usually partly unfold again to open up the "wrong" interactions before they can reinitiate folding with a potentially better outcome. Misfolded molecules may also form atomic interactions with other misfolded polypeptides, resulting in aggregation ***(4)***. It appears that aggregation occurs by specific interaction of certain conformations of folding intermediates of the same kind of protein rather than by nonspecific coaggregation of different proteins ***(5,6)***. Stretches of the polypeptide chain with a high propensity to form β-

sheet structures appear to play an important role in the aggregation process (*see* Chapter 1).

3. Protein Quality Control

Folding in the cell has to proceed under physicochemical conditions that are known to compromise folding in the test tube and in a highly crowded environment with many proteins, solutes, and other molecules ***(7)***. Although folding in vivo to a large degree follows the basic principles studied in in vitro folding experiments, the folding process in the cell must be protected from interferences by the cellular environment.

A large body of research in the last 15 years has shown that cells need and have systems—so-called protein quality-control systems—that supervise the last step in gene expression: production of the native conformation from translated proteins. Protein quality-control systems comprise molecular chaperones, proteases, and regulatory factors. These systems have to accomplish certain aims: 1) promote folding, 2) counteract aggregation, 3) select and eliminate polypeptides with a low folding capacity. In addition to occasionally misfolding proteins, gene transcription and translation themselves are flawed also in healthy cells and organisms resulting in the translation of aberrant proteins. That a surprisingly high percentage of newly synthesized proteins is sorted out even before synthesis is complete has been emphasized by a study that addressed the question of cotranslational degradation ***(8)***.

The sorting task of protein quality-control systems is dedicated to eliminate proteins with an increased probability to be in unfolded and misfolded conformations. The system is able to adapt to environmental stresses like changes in pH, temperature, and oxidative stress that all strongly affect protein folding. The energy level has a great impact for folding: many chaperones and proteases require ATP for their activity.

Adaptation of protein quality control to environmental challenges is in part accomplished by regulatory mechanisms involving transcriptional and translational responses. Adaptation to heat-shock (the heat-shock response ***[9]***) has been known for a long time and an adaptation to folding stress in specific cellular compartments like the endoplasmatic reticulum (ER) or mitochondria has been described as ER stress response ***(10)*** and mitochondrial stress response ***(11)***, respectively.

3.1. Molecular Chaperones

Molecular chaperones represent groups of phylogenetically conserved unrelated protein families that transitionally bind to proteins when they are in unfolded or partially unfolded conformations. Chaperones have been defined as

"proteins that assist the correct noncovalent assembly of other polypeptide-containing structures in vivo, but are not components of these assembled structures when they are performing their biological functions" ***(12)***. For a comprehensive discussion of different chaperones and their mechanisms of action, the reader is referred to **refs. *13–15***. We will in the following confine our discussion to some basic principles and a few instructive examples. Molecular chaperones typically bind exposed hydrophobic stretches of protein chains that are sequestered within the protein core once the native conformation has been adopted. Many molecular chaperones have originally been discovered as genes that are upregulated by heat shock and derive their nomenclature as heat-shock proteins (Hsps) from this fact. However, a number of chaperones are constitutively expressed and form part of the protein expression system under nonstress conditions.

One of the best-studied chaperone families are the Hsp70 chaperones, which may serve as a general example to illustrate chaperone function. In human cells, Hsp70 paralogues are found in the cytosol, mitochondria, and the ER. Hsp70s consist of a substrate-binding domain and an ATPase domain that communicate with each other. Cycles of ATP binding, hydrolysis, and ATP/ADP exchange in the ATPase domain drive switching between high- and low-affinity states of the substrate binding domain. This leads to controlled binding and release of exposed hydrophobic peptide segments of folding intermediates, gives the polypeptide undergoing folding a time window to resume folding while it is released, and counteracts aggregation as the sticky hydrophobic stretches are not available to interactions with other folding intermediates while the polypeptide is bound to the chaperone. Thus, chaperones do not catalyze the folding process in a classical way, but suppress side reactions that reduce the yield of correctly folded protein. The Hsp70 chaperone cycle of substrate binding and release is influenced by a large number of co-factors that stabilize either the high-affinity or the low-affinity conformation, facilitate ADP/ATP exchange or link the chaperone to the degradation machinery ***(16,17)***. These factors allow control of Hsp70 chaperone activity and adapt it to the actual needs.

A very intriguing group of chaperones has received its distinguishing designation as chaperonins with *Escherichia coli* GroELS as the most extensively studied representative ***(18)***. In human cells, chaperonins are present in the mitochondria (Hsp60/Hsp10) and the cytosol (TRiC/CCT). The chaperonins form barrel structures with an inner cavity in which entire substrate proteins, usually compact folding intermediates, are enclosed and may fold in an undisturbed environment. This architecture has also been described as the "folding cage." Timed cycling between high- and low-affinity states and opening and closure of the cavity are, as for the Hsp70 chaperones, orchestrated by ATP binding, hydrolysis, and ADP release.

Another example for ATP-dependent chaperones that has recently received great interest are chaperones that belong to the large and diverse group of AAA^+ domain proteins (AAA stands for ATPases associated with diverse cellular activities) that are involved in unfolding proteins (e.g., as subunits of proteases) or untangling complexes and aggregates ***(19)***. Many human representatives are known, and examples are subunits of the regulatory particle of the proteasome and mitochondrial ClpX.

Small heat-shock proteins (sHsps) are ATP-independent chaperones that bind unfolded proteins and serve as protected "resting places" for folding intermediates during stressful conditions like heat-shock until ATP-dependent Hsp70 chaperones are available to assist folding ***(20)***. Mutations in the sHsp α-crystallin that is involved in maintaining solubility of the eye lens crystallins cause a hereditary form of cataract ***(21)***.

The lectin chaperones calnexin and calreticulin of the ER exploit the presence and accessibility of certain sugar side-chains in the protein for recognition of incompletely folded chains ***(22)***. They bind proteins that contain one glucose unit in the N-glycosylated sugar branch. The binding site is abolished by glucosidases and reestablished by a glycosyl-transferase. As in the chaperone cycle of Hsp70, this leads to cycles of binding and release of the folding chain, and rebinding will not be abolished before reglycosylation is prevented because the site becomes buried inside the folded structure. Calnexin and calreticulin possess ER retention signals and association to these lectins therefore leads to retention in the ER. The lectin chaperones are associated with a proteindisulfide isomerase, ERp57, that facilitates correct formation of the cystin-bridges.

Besides the more general chaperones, there exist a series of protein-specific chaperones that only assist a specific protein in folding (reviewed in ***[23]***). An example of this is Hsp47, which stabilizes the correctly folded collagen helix for transport from the ER to the Golgi. It appears to recognize the triple-helical form of procollagen early in the secretory pathway and prevents the lateral aggregation of procollagen chains ***(24)***.

3.2. The Proteases of Protein Quality Control Systems

The architecture of proteases involved in general degradation in biological systems and as part of protein quality-control systems reflects that the conformational state is a decisive parameter for selection of proteins for degradation. The proteolytic active sites in such proteases are structurally sequestered inside barrel structures that, analogous to the chaperonins, enclose inner cavities. These proteases are designated "self-compartmentalizing" proteases ***(25)***. To be degraded, a protein has to be in an at least partially unfolded state that can pass through the narrow opening into the proteolytic cavity. The most promi-

nent protease of this kind is the proteasome ***(26)***, but mitochondrial (Lon, ClpXP) representatives are also known. ATP-dependent chaperone subunits or subdomains of the AAA^+ domain protein type are responsible for the transport of the substrate protein into the cavity and perform a gatekeeping role. As far as the proteasome is concerned, substrates are first tagged for degradation by the addition of multiple ubiquitin chains at lysine residues by the complex ubiquitin conjugation machinery ***(27)***.

Switching the balance between the folded state and unfolded states by covalent modifications like phosphorylation, ubiquitin-tagging, or cleavage at specific sites by sequence-specific proteases are frequently observed means to regulate turnover of regulatory proteins.

4. Mutations Compromising Folding and Stability

The protein sequences created in the evolutionary dice box have been selected for their ability to specify polypeptides with the capacity to fold to a functional conformation with a certain stability. On the other hand, the stability defined by the ensemble of atomic interactions must not be too high because proteins must be accessible to degradation to enable turnover and downregulation. The overall free-energy difference between unfolded and the native conformations typically is not very high ***(28)***. Many regulatory proteins for example must be available to fast regulated turnover in order to turn off signals. Naturally occurring proteins display a wide range of intrinsic folding capacities and conformational stabilities (*see* also Chapter 1). Mutations often change these intrinsic properties and may thus shift the balance between folding and misfolding towards the latter, resulting in molecular pathological effects like premature degradation or aggregation. On the other hand, certain "normal" proteins without mutations have an intrinsic tendency to misfold and do so under certain cellular conditions or owing to mild defects in protein quality-control system components. Premature degradation, misfolding, and aggregation occur to a certain degree in normal cells and organisms and it is only when these processes become unbalanced that conformational diseases develop (*see* Chapter 1).

In many monogenic diseases, missense mutations or one-amino acid-deletions or insertions in a particular gene lead to impaired folding and/or reduced conformational stability of the encoded protein. About half of the mutations recorded in the Cardiff-based Human Gene Mutation Database (HGMD; www.hgmd.org) are missense mutations ***(29)*** and increasing experimental evidence indicates that a majority of them has an effect on folding and/or stability of the native conformation thus shifting the balance between folded and partially folded/misfolded conformations towards the latter ***(30,31)***.

In spite of the great wealth of disease-causing mutations presently known, and the experimental investigations of a subset of these disease-causing mutations, it is possible only to a limited extent to predict securely the effects of an amino acid replacement on folding. Attempts to relate altered physico-chemical properties of observed mutations, and variations to their effect, have only been successful in a statistical way, i.e., the probability that a disease-causing missense mutation alters some of the evident properties involved in interactions in the native conformation is higher than the probability that a neutral single amino acid polymorphism does so ***(32,33).*** In a study, we addressed the question of whether disease-causing missense mutations can be distinguished from the ensemble of all possible amino acid replacements that can be induced by single base mutations in a series of genes ***(34)***. After modeling of the mutant structures, a large number of biophysical parameters were compared to those of the respective wild-type proteins. Statistical evaluation showed that a distinction between disease-causing and neutral mutations was possible only to a limited extent. This is probably owing to the current lack of understanding as to which amino acid residues are critical for protein folding, and it is hoped that future research will make it possible to pinpoint atomic interactions that are of special importance for the folding process.

Recent detailed studies of the effect of mutations on the aggregation propensity of a small single-domain protein (acylphosphatase) give an idea about potentially fruitful approaches to future work in this field. Chiti et al. ***(35)*** showed that mutations that significantly perturb the aggregation rate of acylphosphatase are localized in two regions with high hydrophobicity and propensity to adopt β-sheet structure. Furthermore, the observed changes in the aggregation rate correlated to the calculated changes in hydrophibicity and β-sheet propensity. The two regions are distinct from the regions that determine the rate of folding, the so-called folding nucleus, which consists of residues forming a critical contact network in the transition state to the native conformation ***(36,37)***. Only when it becomes possible to pinpoint folding nuclei and aggregation-prone regions in more complicated multidomain proteins will a rational explanation for intrinsic aggregation propensities and the prediction of effects of particular mutations on folding be found.

Acknowledgments

Work concerning the mitochondrial protein quality-control system has been supported by The Danish Medical Research Council; Danish Human Genome Centre; Karen Elise Jensen Foundation; Carlsberg Foundation; NOVO Nordisk Foundation; and Institute of Experimental Clinical Research, Aarhus University.

References

1. Anfinsen, C. B. (1973) Principles that govern the folding of protein chains. *Science* **181,** 223–230.
2. Levinthal, C. (1968) Are there pathways for protein folding? *J. Chim. Phys.* **85,** 44–45.
3. Dinner, A. R., Sali, A., Smith, L. J., Dobson, C. M., and Karplus, M. (2000) Understanding protein folding via free-energy surfaces from theory and experiment. *Trends Biochem. Sci.* **25,** 331–339.
4. Speed, M. A., King, J., and Wang, D. I. C. (1997) Polymerization mechanism of polypeptide chain aggregation. *Biotechnol. Bioeng.* **54,** 333–343.
5. Speed, M. A., Wang, D. I. C., and King, J. (1996) Specific aggregation of partially folded polypeptide chains: The molecular basis of inclusion body composition. *Nat. Biotechnol.* **14,** 1283–1287.
6. Rajan, R. S., Illing, M. E., Bence, N. F., and Kopito, R. R. (2001) Specificity in intracellular protein aggregation and inclusion body formation. *Proc. Natl. Acad. Sci. USA* **98,** 13060–13065.
7. Ellis, R. J. (2001) Macromolecular crowding: an important but neglected aspect of the intracellular environment. *Curr. Opin. Struct. Biol.* **11,** 114–119.
8. Turner, G. C. and Varshavsky, A. (2000) Detecting and measuring cotranslational protein degradation in vivo. *Science* **289,** 2117–2120.
9. Morimoto, R. I., Kline, M. P., Bimston, D. N., and Cotto, J. J. (1997) The heat-shock response: regulation and function of heat-shock proteins and molecular chaperones. *Essays Biochem.* **32,** 17–29.
10. Patil, C. and Walter, P. (2001) Intracellular signaling from the endoplasmic reticulum to the nucleus: the unfolded protein response in yeast and mammals. *Curr. Opin. Cell Biol.* **13,** 349–355.
11. Zhao, Q., Wang, J., Levichkin, I. V., Stasinopoulos, S., Ryan, M. T., and Hoogenraad, N. J. (2002) A mitochondrial specific stress response in mammalian cells. *EMBO J.* **21,** 4411–4419.
12. Ellis, R. J. (1993) The general concept of molecular chaperones. *Philos. Trans. R. Soc. Lond. B. Biol. Sci.* **339,** 257–261.
13. Beissinger, M. and Buchner, J. (1998) How chaperones fold proteins. *Biol. Chem.* **379,** 245–259.
14. Horwich, A. L., Fenton, W. A., and Rapoport, T. A. (2001) Protein folding taking shape: Workshop on molecular chaperones. *EMBO Rep.* **2,** 1068–1073.
15. Bukau, B. and Horwich, A. L. (1998) The Hsp70 and Hsp60 chaperone machines. *Cell* **92,** 351–366.
16. Brehmer, D., Rudiger, S., Gassler, C. S., Klostermeier, D., Packschies, L., Reinstein, J., et al. (2001) Tuning of chaperone activity of Hsp70 proteins by modulation of nucleotide exchange. *Nat. Struct. Biol.* **8,** 427–432.
17. Hohfeld, J., Cyr, D. M., and Patterson, C. (2001) From the cradle to the grave: molecular chaperones that may choose between folding and degradation. *EMBO Rep.* **2,** 885–890.
18. Ellis, R. J. (2001) Molecular chaperones: inside and outside the Anfinsen cage. *Curr. Biol.* **11,** R1038–R1040.

19. Maurizi, M. R. and Li, C. C. (2001) AAA proteins: in search of a common molecular basis: International meeting on cellular functions of AAA proteins. *EMBO Rep.* **2,** 980–985.
20. Ijssel, v. d. P., Norman, D. G., and Quinlan, R. A. (1999) Small heat shock proteins in the limelight. *Curr. Biol.* **9,** R103–R105.
21. Litt, M., Kramer, P., LaMorticella, D. M., Murphey, W., Lovrien, E. W., and Weleber, R. G. (1998) Autosomal dominant mutation of congenital cataract associated with a missense mutation in the alpha-crystallin gene CRYAA. *Hum. Mol. Genet.* **7,** 471–474.
22. Cabral, C. M., Liu, Y., and Sifers, R. N. (2001) Dissecting glycoprotein quality control in the secretory pathway. *Trends Biochem. Sci.* **26,** 619–624.
23. Tasab, M., Batten, M. R., and Bulleid, N. J. (2000) Hsp47: a molecular chaperone that interacts with and stabilizes correctly-folded procollagen. *EMBO J.* **19,** 2204–2211.
24. Tasab, M., Jenkinson, L., and Bulleid, N. J. (2002) Sequence-specific recognition of collagen triple helices by the collagen-specific molecular chaperone HSP47. *J. Biol. Chem.* **277,** 35007–35012.
25. Lupas, A., Flanagan, J. M., Tamura, T., and Baumeister, W. (1997) Self-compartmentalizing proteases. *Trends. Biochem. Sci.* **22,** 399–404.
26. Voges, D., Zwickl, P., and Baumeister, W. (1999) The 26S proteasome: a molecular machine designed for controlled proteolysis. *Annu. Rev. Biochem.* **68,** 1015–1068.
27. Glickman, M. H. and Ciechanover, A. (2002) The ubiquitin-proteasome proteolytic pathway: destruction for the sake of construction. *Physiol Rev.* **82,** 373–428.
28. Fersht, A. R. and Daggett, V. (2002) Protein folding and unfolding at atomic resolution. *Cell* **108,** 573–582.
29. Krawczak, M., Ball, E. V., Fenton, I., Stenson, P. D., Abeysinghe, S., Thomas, N., and Cooper, D. N. (2000) Human gene mutation database-a biomedical information and research resource. *Hum. Mutat.* **15,** 45–51.
30. Bross, P., Corydon, T. J., Andresen, B. S., Jørgensen, M. M., Bolund, L., and Gregersen, N. (1999) Protein misfolding and degradation in genetic diseases. *Hum. Mutat.* **14,** 186–198.
31. Gregersen, N., Bross, P., Andresen, B. S., Pedersen, C. B., Corydon, T. J., and Bolund, L. (2001) The role of chaperone-assisted folding and quality control in inborn errors of metabolism: protein folding disorders. *J. Inherit. Metab. Dis.* **24,** 189–212.
32. Sunyaev, S., Ramensky, V., Koch, I., Lathe, W., III, Kondrashov, A. S., and Bork, P. (2001) Prediction of deleterious human alleles. *Hum. Mol. Genet.* **10,** 591–597.
33. Wang, Z. and Moult, J. (2001) SNPs, protein structure, and disease. *Hum. Mutat.* **17,** 263–270.
34. Terp, B. N., Cooper, D. N., Christensen, I. T., Jorgensen, F. S., Bross, P., Gregersen, N., and Krawczak, M. (2002) Assessing the relative importance of the biophysical properties of amino acid substitutions associated with human genetic disease. *Hum. Mutat.* **20,** 98–109.

35. Chiti, F., Taddei, N., Baroni, F., Capanni, C., Stefani, M., Ramponi, G., and Dobson, C. M. (2002) Kinetic partitioning of protein folding and aggregation. *Nat. Struct. Biol.* **9,** 137–143.
36. Fersht, A. R. (1997) Nucleation mechanisms in protein folding. *Curr. Opin. Struct. Biol.* **7,** 3–9.
37. Vendruscolo, M., Paci, E., Dobson, C. M., and Karplus, M. (2001) Three key residues form a critical contact network in a protein folding transition state. *Nature* **409,** 641–645

3

Cystic Fibrosis

Premature Degradation of Mutant Proteins as a Molecular Disease Mechanism

Marina S. Gelman and Ron R. Kopito

1. Introduction

Cystic fibrosis (CF) is the most common autosomal recessive genetic disorder in the Caucasian population, with 1 out of every 2000 live births affected by this disease ***(1,2)***. The symptoms of CF appear in early childhood, and although the duration of the disease depends strongly on the severity of symptoms and availability of treatment options, it generally becomes fatal by the age of 30–40. The hallmark of the disease is the abnormal viscosity of mucous secretions resulting from the altered electrolyte transport across epithelial cell membranes. CF symptoms include pancreatic and gastrointestinal (GI) insufficiency, recurring lung infections, obstruction of sinuses, and male infertility. These pleiotropic symptoms arise as a result of mutations in a single gene, termed cystic fibrosis transmembrane conductance regulator *(CFTR)* ***(3–5)***. Understanding the mechanisms of biogenesis, folding, and degradation of the CFTR gene product is crucial for unraveling the molecular basis of CF pathogenesis, and will be the focus of this chapter.

Human CFTR functions as a Cl^- channel at the apical membranes of polarized epithelial cells, which line the mucosal surface of internal organs and glands. It is a large polytopic membrane protein composed of 1480 amino acids (approx 140 kDa) ***(3)***. The protein comprises two structurally similar halves, each consisting of six putative transmembrane helices and a nucleotide-binding domain (NBD). The two halves of the molecule are connected by a central cytosolic regulatory "R domain," which lacks a defined secondary structure. The gating of

From: *Methods in Molecular Biology, vol. 232: Protein Misfolding and Disease: Principles and Protocols*
Edited by: P. Bross and N. Gregersen © Humana Press Inc., Totowa, NJ

the channel is controlled by the binding of ATP to both NBDs and phosphorylation by the c-AMP dependent kinase (PKA) of multiple target sites within the "R domain" ***(6)***. According to the predicted structure, the bulk of amino acid residues that comprise CFTR are exposed to the cytosol or buried within the bilayer, with only short loops connecting pairs of transmembrane helices exposed to the exofacial surface of plasma membrane. Two potential sites for Asn-linked glycosylation are located at extracellular loop 4 (at residues 894 and 900), and acquisition of complex carbohydrates at these sites during Golgi processing increases the molecular weight of the protein to approx 160 kDa.

2. CFTR Biogenesis and the ΔF508 Mutation

Although over 1200 mutations and sequence variants in *CFTR* gene are associated with CF (CF Mutation Data Base http://www.genet.sickkids.on.ca/cftr/), the most prevalent mutation, responsible for over 70% of CF cases, is the deletion of a phenylalanine at position 508 (ΔF508) within the first NBD. At least one copy of ΔF508 allele is present in the chromosomes of a vast majority of CF patients in North America, and the disease is particularly severe in patients homozygous for this mutation ***(5)***. ΔF508 belongs to a class of mutants termed "temperature sensitive for folding," because it can achieve a correct tertiary structure only at permissive temperature (26°–30°C) but not at physiological temperature (37°C). As a consequence, both in CF patients and in cultured cells grown at physiological temperature, this mutant cannot leave the endoplasmic reticulum (ER) for delivery to the plasma membrane (***[7,8]***, but *see also* **ref. *9***). Pulse-chase experiments in heterologous cells expressing wild-type CFTR and the ΔF508 mutant established that in both cases CFTR is initially synthesized and inserted into the ER membrane as a approx 140 kDa core-glycosylated "immature" precursor, which is sensitive to digestion with endoglycosidase H (endo H) ***(10)***. In the case of CFTR, approx 25–30% of the nascent protein can be chased to a "mature" form, containing complex endo H-resistant oligosaccharides, which is deployed to the plasma membrane. The remainder of the wt CFTR (70–75%) and virtually all of ΔF508 (>99%) undergo rapid ER-associated degradation ***(11,12)***. The mechanism of this degradation will be discussed in greater detail below.

Several lines of evidence support the idea that ΔF508 is a folding mutant. First, Denning et al. demonstrated that incubation of ΔF508-expressing cells at low temperatures (26°–30°C) leads to expression of some ΔF508 at the cell surface ***(13)***. Cell-surface expression of ΔF508 is also detected after expression of ΔF508 mRNA in *Xenopus* oocytes, which are grown at low temperature ***(14)***. Second, co-translational folding of CFTR is mediated by several cytosolic molecular chaperones, such as heat-shock protein 70 (Hsp70), Hsp90, Hsc70 co-chaperone CHIP, Hdj2, and ER-resident chaperone calnexin ***(15–19)***. Inter-

action of some of these chaperones (Hsp70, calnexin) with ΔF508 was found to be aberrantly prolonged, compared to wt CFTR, suggesting that ΔF508 can reach an intermediate stage on the normal folding pathway of CFTR, but is not released from the chaperones to complete the folding process. Interestingly, treatment with geldanamycin, which disrupts ΔF508 interaction with Hsp90, does not promote the correct folding, but instead accelerates the degradation of this mutant ***(17)***. Finally, in vitro denaturation and refolding studies of a fragment corresponding to NBD1 demonstrated that although the stability of this fragment was not affected by deletion of ΔF508, the yield of properly folded ΔF508 NBD1 was substantially decreased when refolding was carried out at 37°C compared to 20°C ***(20)***. These results indicate that Phe^{508} is necessary for crucial interactions on the CFTR folding pathway, but does not significantly contribute to stability of the final folded form, at least insofar as this NBD fragment reflects the context of the intact protein. Furthermore, probing tertiary structures of ΔF508 and wt CFTR by limited proteolysis revealed that ΔF508 and immature form of wt CFTR have a similar proteolytic cleavage pattern (upon digestion with trypsin), whereas protease digestion of mature form of wt CFTR produces a different band pattern ***(21)***. These experiments suggest that the bulk of ER-retained ΔF508 resembles an intermediate of CFTR biogenesis rather than a distinct non-native variant, which follows a separate folding pathway. Despite evidence that ΔF508 is inefficiently folded and does not traffic properly, it is well-established that this mutant is able to form functional chloride channels. The conductance properties of ΔF508 channels are similar to those of the wild-type protein, as measured by patch-clamp analysis of intracellular membranes ***(22)***. Because of these observations and the evidence that ΔF508 molecules rescued to the plasma membrane retain at least partial function, strategies aimed at increasing the efficiency of ΔF508 folding, trafficking, and function are considered to be promising therapeutic approaches ***(23)***. Thus, a detailed understanding of the cellular mechanisms by which mutant CFTR molecules are recognized and degraded in cells is important to realizing this goal.

3. Degradation of Misfolded CFTR by Ubiquitin-Proteasome Pathway

Misfolded CFTR is the first integral membrane protein to be recognized as a substrate for degradation via the ubiquitin-proteasome pathway (UPS) ***(24,25)***. Both the immature form of wt CFTR and ΔF508 are degraded by this mechanism. The role for the UPS in CFTR turnover is supported by the following observations: 1) CFTR undergoes both co-translational and post-translational ubiquitylation when expressed in a cell-free system ***(26,27)***; 2) inhibition of proteasome function with specific chemical inhibitors such as MG132 or lactacystin leads to accumulation of multiubiquitylated, undegraded forms of

CFTR and ΔF508 ***(24,25)***; 3) co-expression of dominant-negative ubiquitin (K48R) inhibits degradation of misfolded CFTR and ΔF508 ***(24)***; and 4) degradation of ΔF508 in a cell-free system is blocked by inhibitors of both the 19S and 20S subunits of the proteasome ***(27,28)***. Degradation of the membrane-embedded CFTR by the cytosolic proteasomes is thought to occur following, or concomitantly with, the retrograde movement ("dislocation") of the protein via the Sec61 channel out of the ER membrane into the cytosol ***(29,30)***.

Despite the compelling evidence in support of a role for proteasomes in the degradation of misfolded CFTR, the effect of proteasome inhibition on the disappearance of ΔF508 from pulse-chase studies is modest. For example, the half-life of ΔF508 in cells treated with proteasome inhibitors is increased only about twofold compared to that in untreated cells ***(25,31)***. This observation led some investigators to suggest that additional proteases play an important role in disposal of misfolded CFTR ***(25)***. To resolve this apparent paradox, we used a fluorescent reporter consisting of a green fluorescent protein (GFP) fused to the amino-terminus of ΔF508, and examined the degradation of this construct in intact cells using noninvasive fluorescence-activated cell sorting (FACS)-based assay ***(31)***. We found that upon inhibition of protein synthesis, the rate of fluorescence decline in cells expressing GFP-ΔF508 corresponds to the degradation rate of this protein measured in pulse-chase experiments. Proteasome inhibition in these cells resulted in profound stabilization of GFP-ΔF508 fluorescence: over 70% of initial fluorescence was preserved after 4 h chase in the presence of MG132, an effect significantly stronger than stabilization of ΔF508 by proteasome inhibitors observed in pulse-chase experiments. This difference may be explained by the fact that the fluorescence-based method provides a more accurate measure of the undegraded substrate, because fluorescence readout is not affected by the change in the electrophoretic mobility of the substrate owing to polyubiquitylation or aggregation, and is not limited by the efficiency of protein recovery by immunoprecipitation. Furthermore, our studies revealed that proteolytic activities associated with individual β-subunits of the proteasome contribute to the degradation of misfolded CFTR independently. Thus, incubation of cells with a combination of epoxomicin, which inhibits predominantly the chymotryptic-like activity (CT-L) of the proteasome, and YU102, a derivative of epoxomicin selective for peptidyl-glutamyl hydrolyzing (PGPH) activity, resulted in augmentation of the overall ΔF508 stabilization compared with the effect of epoxomicin alone ***(31)***.

4. Correction of ΔF508 Folding Defect as Therapy for Cystic Fibrosis

It has become clear that inhibition of ΔF508 degradation with proteasome inhibitors or interference with the function of UPS, for example by co-transfection of dominant negative ubiquitin, are not viable options for increasing

cell-surface expression of ΔF508, because CFTR molecules covalently modified by ubiquitin attachment are irreversibly misfolded and committed to the degradation pathway ***(24,30)***. Instead, continuous proteasome inhibition results in accumulation of undegraded polyubiquitylated CFTR in aggresomes, pericentriolar accumulations of aggregated protein, surrounded by collapsed intermediate filaments ***(30)***. It is possible, however, that interference with the earliest steps in the process of recognition of misfolded CFTR molecules and targeting them for degradation will be effective in increasing folding and maturation of ΔF508. To this end, it is crucial to identify ubiquitin ligase(s), which recognize CFTR as a substrate for ER-associated degradation (ERAD) and catalyze transfer of ubiquitin to it. Ubiquitin ligases that participate in the degradation of misfolded proteins from the ER have been identified in yeast. For example, the RING-H2-finger protein Hrd1p/Der3p has been shown to function as a ubiquitin ligase (E3) during regulated degradation of misfolded carboxypeptidase Y ***(32)*** and an ER-resident enzyme Hmg-CoA reductase from the ER of *Saccharomyces cerevisiae* ***(33)***. In addition Doa10, an ER/nuclear envelope yeast E3 Ub ligase, was found to participate in the degradation of ER membrane proteins as well as of soluble transcription factor Mat α ***(34)***. Mammalian orthologs of these genes are potential candidates for recognition of misfolded ΔF508 molecules. Other Ub ligases that participate in ERAD remain to be identified. Perhaps development of strategies to prevent Ub conjugation to misfolded ΔF508 molecules may emerge as a strategy to increase the folding yield of this mutant.

A second strategy that is being explored is to identify small molecules which might improve ΔF508 folding, either by stabilizing ON-pathway intermediates or by increasing the energy barrier for certain folding intermediates to exit the folding pathway.

The temperature-dependent recovery of ΔF508 channels at the cell surface can be mimicked by treating cells with small molecules, termed "chemical chaperones" (*see also* Chapter 19), such as glycerol, dimethylsulfoxide (DMSO), trimethylamine-N-oxide (TMAO), or deuterated water ***(35–37)***. For example, treatment of cells expressing ΔF508 with high concentrations of glycerol increases the cAMP-dependent Cl^- currents by 8–10-fold ***(35)***. Chemical chaperones are thought to correct protein folding nonspecifically, by stabilizing both final structures and folding intermediates of mutant proteins and thus allowing them to escape ER quality control. Another class of folding modulators, pharmacological chaperones, includes compounds that specifically bind to unstable folding intermediates of mutant proteins and allow their release from the ER quality-control apparatus ***(38)***. For example, maturation of mutant P-glycoprotein is improved significantly in the presence of its transport substrates capsaicin, vinblastine, and verapamil ***(39)***, and selective cell-permeable antagonist of

mutant vasopressin receptor V2R can rescue its surface expression ***(40)***. In the case of CFTR, no such compounds have been identified to date. However, several pharmacological agents reportedly have an effect on improving the correct folding of ΔF508 in transfected and native epithelial cells. These include 4-phenylbutyrate (4-PB), deoxyspergualin, cyclopentylxanthine (CPX), doxorubicin, and benzo(c)quinolizimium compounds MPB-07 and MPB-91 ***(41–46)***. Some of these drugs, i.e., 4-PB, CPX and MPB compounds, have been reported to bind directly to ΔF508 to promote its maturation ***(43,44,46)***, but other, less specific mechanisms have not been ruled out ***(47)***. Interestingly, the combination of sodium butyrate and low temperature leads to a synergistic enhancement of cell surface ΔF508 expression (***[47]***; our unpublished observations). Furthermore, a recent study reported that a calcium-pump inhibitor, thapsigargin induced release of ER-retained ΔF508 to the cell surface both in cultured cells and in a CF mouse ***(48)***. An important caveat to pharmacological approaches focused on increasing delivery of ΔF508 to the cell surface is suggested by recent studies that indicate that the stability of rescued ΔF508 at the plasma membrane is considerably reduced compared with the wild-type protein ***(49,50)***. Thus, the best therapeutic effect may be achieved through a combination of treatments that increase expression of surface ΔF508, activate CFTR Cl^- channel, and stabilize plasma membrane-localized ΔF508.

Cell-based assays are being developed to facilitate drug discovery for CF therapy in a high-throughput screening format. A functional cell-based assay was developed by Verkman and colleagues ***(51)***, in which cells are doubly transfected with wild-type or mutant CFTR together with a yellow fluorescent protein (YFP)-based halide sensor, and cultured in a 96-well dish. CFTR activation is measured by increased halide permeability (and corresponding decrease in cellular YFP fluorescence) in response to extracellular addition of 100 m*M* I^- followed by stimulation with forskolin. This assay enabled identification of novel CFTR activators and an inhibitor ***(52)***. However, because it measures activation of chloride channels, this assay may identify compounds that activate latent anion channels other than CFTR; whether activation of such channels is of therapeutic value in treatment of the basic CF defect is yet to be established. Secondary screens can be implemented to verify the specificity of CFTR activation or to monitor ΔF508 surface expression. For example, we have developed a cell-based assay to measure wild-type CFTR or ΔF508 present in the plasma membrane of live cells using FACS (MG and RK, unpublished data). We have engineered cell lines expressing GFP-ΔF508-FLAG, a fusion protein between GFP-CFTR ***(53)*** and a CFTR variant containing a FLAG epitope in the 4th extracellular loop ***(54,55)***. Biogenesis, intracellular processing, and degradation of this fusion protein are virtually identical to those of ΔF508 ***(30,31)***. Appearance of GFP-ΔF508-FLAG on the cell surface is

monitored by the binding of fluorescent anti-FLAG antibody to intact cells, while GFP fluorescence reports on the total expression level of ΔF508 in these cells. In preliminary experiments, this assay showed a clear increase in the surface expression of GFP-ΔF508-FLAG upon incubation of cells at low temperature, and a synergistic effect when low temperature was combined with sodium butyrate treatment (our unpublished observations).

With the advent of high-throughput screening technology and improved sensitivity of ΔF508 detection at the cell surface, it should be possible to identify promising drug candidates for CF therapy.

References

1. Tsui, L. C., Rommens, J., Kerem, B., Rozmahel, R., Zielenski, J., Kennedy, D., et al. (1991) Molecular genetics of cystic fibrosis. *Adv. Exp. Med. Biol.* **290,** 9–17; discussion 17–18.
2. Jaffe, A., and Bush, A. (2001) Cystic fibrosis: review of the decade. *Monaldi Arch. Chest. Dis.* **56,** 240–247.
3. Riordan, J. R., Rommens, J. M., Kerem, B., Alon, N., Rozmahel, R., Grzelczak, Z., et al. (1989) Identification of the cystic fibrosis gene: cloning and characterization of complementary DNA. *Science* **245,** 1066–1073.
4. Rommens, J. M., Dho, S., Bear, C. E., Kartner, N., Kennedy, D., Riordan, J. R., et al. (1991) cAMP—inducible chloride conductance in mouse fibroblast lines stably expressing the human cystic fibrosis transmembrane conductance regulator. *Proc. Natl. Acad. Sci. USA* **88,** 7500–7504.
5. Kerem, E. and Kerem, B. (1995) The relationship between genotype and phenotype in cystic fibrosis. *Curr. Opin. Pulm. Med.* **1,** 450–456.
6. Gadsby, D. C. and Nairn, A. C. (1999) Control of CFTR channel gating by phosphorylation and nucleotide hydrolysis. *Physiol. Rev.* **79,** S77–S107.
7. Puchelle, E., Gaillard, D., Ploton, D., Hinnrasky, J., Fuchey, C., Boutterin, M. C., et al. (1992) Differential localization of the cystic fibrosis transmembrane conductance regulator in normal and cystic fibrosis airway epithelium. *Am. J. Respir. Cell Mol. Biol.* **7,** 485–491.
8. Bannykh, S. I., Bannykh, G. I., Fish, K. N., Moyer, B. D., Riordan, J. R., and Balch, W. E. (2000) Traffic pattern of cystic fibrosis transmembrane regulator through the early exocytic pathway. *Traffic* **1,** 852–870.
9. Kalin, N., Claass, A., Sommer, M., Puchelle, E., and Tummler, B. (1999) DeltaF508 CFTR protein expression in tissues from patients with cystic fibrosis. *J. Clin. Invest.* **103,** 1379–1389.
10. Cheng, S. H., Gregory, R. J., Marshall, J., Paul, S., Souza, D. W., White, G. A., et al. (1990) Defective intracellular transport and processing of CFTR is the molecular basis of most cystic fibrosis. *Cell* **63,** 827–834.
11. Lukacs, G. L., Mohamed, A., Kartner, N., Chang, X. B., Riordan, J. R., and Grinstein, S. (1994) Conformational maturation of CFTR but not its mutant counterpart (delta F508) occurs in the endoplasmic reticulum and requires ATP. *EMBO J.* **13,** 6076–6086.

12. Ward, C. L. and Kopito, R. R. (1994) Intracellular turnover of cystic fibrosis transmembrane conductance regulator. Inefficient processing and rapid degradation of wild-type and mutant proteins. *J. Biol. Chem.* **269,** 25,710–25,718.
13. Denning, G. M., Anderson, M. P., Amara, J. F., Marshall, J., Smith, A. E. and Welsh, M. J. (1992) Processing of mutant cystic fibrosis transmembrane conductance regulator is temperature-sensitive. *Nature* **358,** 761–764.
14. Drumm, M. L., Wilkinson, D. J., Smit, L. S., Worrell, R. T., Strong, T. V., Frizzell, R. A., et al. (1991) Chloride conductance expressed by delta F508 and other mutant CFTRs in Xenopus oocytes. *Science* **254,** 1797–1799.
15. Yang, Y., Janich, S., Cohn, J. A., and Wilson, J. M. (1993) The common variant of cystic fibrosis transmembrane conductance regulator is recognized by Hsp70 and degraded in a pre-Golgi nonlysosomal compartment. *Proc. Natl. Acad. Sci. USA* **90,** 9480–9484.
16. Pind, S., Riordan, J. R., and Williams, D. B. (1994) Participation of the endoplasmic reticulum chaperone calnexin (p88, IP90) in the biogenesis of the cystic fibrosis transmembrane conductance regulator. *J. Biol. Chem.* **269,** 12,784–12,788.
17. Loo, M. A., Jensen, T. J., Cui, L., Hou, Y., Chang, X. B., and Riordan, J. R. (1998) Perturbation of Hsp90 interaction with nascent CFTR prevents its maturation and accelerates its degradation by the proteasome. *EMBO J.* **17,** 6879–6887.
18. Meacham, G. C., Lu, Z., King, S., Sorscher, E., Tousson, A., and Cyr, D. M. (1999) The Hdj-2/Hsc70 chaperone pair facilitates early steps in CFTR biogenesis. *EMBO J.* **18,** 1492–1505.
19. Meacham, G. C., Patterson, C., Zhang, W., Younger, J. M., and Cyr, D. M. (2001) The Hsc70 co-chaperone CHIP targets immature CFTR for proteasomal degradation. *Nat. Cell Biol.* **3,** 100–105.
20. Qu, B. H., Strickland, E. H., and Thomas, P. J. (1997) Localization and suppression of a kinetic defect in cystic fibrosis transmembrane conductance regulator folding. *J. Biol. Chem.* **272,** 15,739–15,744.
21. Zhang, F., Kartner, N., and Lukacs, G. L. (1998) Limited proteolysis as a probe for arrested conformational maturation of delta F508 CFTR. *Nat. Struct. Biol.* **5,** 180–183.
22. Pasyk, E. A. and Foskett, J. K. (1995) Mutant (delta F508) cystic fibrosis transmembrane conductance regulator Cl- channel is functional when retained in endoplasmic reticulum of mammalian cells. *J. Biol. Chem.* **270,** 12,347–12,350.
23. Choo-Kang, L. R. and Zeitlin, P. L. (2000) Type I, II, III, IV, and V cystic fibrosis transmembrane conductance regulator defects and opportunities for therapy. *Curr. Opin. Pulm. Med.* **6,** 521–529.
24. Ward, C. L., Omura, S., and Kopito, R. R. (1995) Degradation of CFTR by the ubiquitin-proteasome pathway. *Cell* **83,** 121–127.
25. Jensen, T. J., Loo, M. A., Pind, S., Williams, D. B., Goldberg, A. L., and Riordan, J. R. (1995) Multiple proteolytic systems, including the proteasome, contribute to CFTR processing. *Cell* **83,** 129–135.
26. Sato, S., Ward, C. L., and Kopito, R. R. (1998) Cotranslational ubiquitination of cystic fibrosis transmembrane conductance regulator in vitro. *J. Biol. Chem.* **273,** 7189–7192.

27. Xiong, X., Chong, E., and Skach, W. R. (1999) Evidence that endoplasmic reticulum (ER)-associated degradation of cystic fibrosis transmembrane conductance regulator is linked to retrograde translocation from the ER membrane. *J. Biol. Chem.* **274,** 2616–2624.
28. Oberdorf, J., Carlson, E. J., and Skach, W. R. (2001) Redundancy of mammalian proteasome beta subunit function during endoplasmic reticulum associated degradation. *Biochemistry* **40,** 13,397–13,405.
29. Bebok, Z., Mazzochi, C., King, S. A., Hong, J. S., and Sorscher, E. J. (1998) The mechanism underlying cystic fibrosis transmembrane conductance regulator transport from the endoplasmic reticulum to the proteasome includes Sec61beta and a cytosolic, deglycosylated intermediary. *J. Biol. Chem.* **273,** 29,873–29,878.
30. Johnston, J. A., Ward, C. L., and Kopito, R. R. (1998) Aggresomes: a cellular response to misfolded proteins. *J. Cell Biol.* **143,** 1883–1898.
31. Gelman, M. S., Kannegaard, E. S., and Kopito, R. R. (2002) A principal role for the proteasome in ER-associated degradation of misfolded intracellular CFTR. *J. Biol Chem.* **277,** 11,709–11,714.
32. Bordallo, J., Plemper, R. K., Finger, A., and Wolf, D. H. (1998) Der3p/Hrd1p is required for endoplasmic reticulum-associated degradation of misfolded lumenal and integral membrane proteins. *Mol. Biol. Cell* **9,** 209–222.
33. Bays, N. W., Gardner, R. G., Seelig, L. P., Joazeiro, C. A., and Hampton, R. Y. (2001) Hrd1p/Der3p is a membrane-anchored ubiquitin ligase required for ER-associated degradation. *Nat. Cell Biol.* **3,** 24–29.
34. Swanson, R., Locher, M., and Hochstrasser, M. (2001) A conserved ubiquitin ligase of the nuclear envelope/endoplasmic reticulum that functions in both ER-associated and Matalpha2 repressor degradation. *Genes Dev.* **15,** 2660–2674.
35. Sato, S., Ward, C. L., Krouse, M. E., Wine, J. J., and Kopito, R. R. (1996) Glycerol reverses the misfolding phenotype of the most common cystic fibrosis mutation. *J. Biol. Chem.* **271,** 635–638.
36. Brown, C. R., Hong-Brown, L. Q., and Welch, W. J. (1997) Correcting temperature-sensitive protein folding defects. *J. Clin. Invest.* **99,** 1432–1444.
37. Brown, C. R., Hong-Brown, L. Q., Biwersi, J., Verkman, A. S., and Welch, W. J. (1996) Chemical chaperones correct the mutant phenotype of the delta F508 cystic fibrosis transmembrane conductance regulator protein. *Cell Stress Chaperones* **1,** 117–125.
38. Morello, J. P., Petaja-Repo, U. E., Bichet, D. G., and Bouvier, M. (2000) Pharmacological chaperones: a new twist on receptor folding. *Trends Pharmacol. Sci.* **21,** 466–469.
39. Loo, T. W. and Clarke, D. M. (1997) Correction of defective protein kinesis of human P-glycoprotein mutants by substrates and modulators. *J. Biol. Chem.* **272,** 709–712.
40. Morello, J. P., Salahpour, A., Laperriere, A., Bernier, V., Arthus, M. F., Lonergan, M., et al. (2000) Pharmacological chaperones rescue cell-surface expression and function of misfolded V2 vasopressin receptor mutants. *J. Clin. Invest.* **105,** 887–895.

41. Jiang, C., Fang, S. L., Xiao, Y. F., O'Connor, S. P., Nadler, S. G., Lee, D. W., et al. (1998) Partial restoration of cAMP-stimulated CFTR chloride channel activity in DeltaF508 cells by deoxyspergualin. *Am. J. Physiol.* **275,** C171–C178.
42. Andersson, C. and Roomans, G. M. (2000) Activation of deltaF508 CFTR in a cystic fibrosis respiratory epithelial cell line by 4-phenylbutyrate, genistein and CPX. *Eur. Respir. J.* **15,** 937–941.
43. Arispe, N., Ma, J., Jacobson, K. A., and Pollard, H. B. (1998) Direct activation of cystic fibrosis transmembrane conductance regulator channels by 8-cyclopentyl-1,3-dipropylxanthine (CPX) and 1,3-diallyl-8-cyclohexylxanthine (DAX). *J. Biol. Chem.* **273,** 5727–5734.
44. Zeitlin, P. L. (2000) Pharmacologic restoration of delta F508 CFTR-mediated chloride current. *Kidney Int.* **57,** 832–837.
45. Maitra, R., Shaw, C. M., Stanton, B. A., and Hamilton, J. W. (2001) Increased functional cell surface expression of CFTR and DeltaF508-CFTR by the anthracycline doxorubicin. *Am. J. Physiol. Cell Physiol.* **280,** C1031–1037.
46. Dormer, R. L., Derand, R., McNeilly, C. M., Mettey, Y., Bulteau-Pignoux, L., Metaye, T., et al. (2001) Correction of delF508-CFTR activity with benzo(c)quinolizinium compounds through facilitation of its processing in cystic fibrosis airway cells. *J. Cell Sci.* **114,** 4073–4081.
47. Heda, G. D. and Marino, C. R. (2000) Surface expression of the cystic fibrosis transmembrane conductance regulator mutant DeltaF508 is markedly upregulated by combination treatment with sodium butyrate and low temperature. *Biochem. Biophys. Res. Commun.* **271,** 659–664.
48. Egan, M. E., Glockner-Pagel, J., Ambrose, C. A., Cahill, P. A., Pappoe, L., Balamuth, N., et al. (2002) Calcium-pump inhibitors induce functional surface expression of DeltaF508-CFTR protein in cystic fibrosis epithelial cells. *Nat. Med.* **8,** 485–492.
49. Sharma, M., Benharouga, M., Hu, W., and Lukacs, G. L. (2001) Conformational and temperature-sensitive stability defects of the delta F508 cystic fibrosis transmembrane conductance regulator in post-endoplasmic reticulum compartments. *J. Biol. Chem.* **276,** 8942–8950.
50. Heda, G. D., Tanwani, M., and Marino, C. R. (2001) The Delta F508 mutation shortens the biochemical half-life of plasma membrane CFTR in polarized epithelial cells. *Am. J. Physiol. Cell Physiol.* **280,** C166–C174.
51. Galietta, L. V., Jayaraman, S., and Verkman, A. S. (2001) Cell-based assay for high-throughput quantitative screening of CFTR chloride transport agonists. *Am. J. Physiol. Cell Physiol.* **281,** C1734–C1742.
52. Galietta, L. J., Springsteel, M. F., Eda, M., Niedzinski, E. J., By, K., Haddadin, M. J., et al. (2001) Novel CFTR chloride channel activators identified by screening of combinatorial libraries based on flavone and benzoquinolizinium lead compounds. *J. Biol. Chem.* **276,** 19,723–19,728.
53. Moyer, B. D., Loffing, J., Schwiebert, E. M., Loffing-Cueni, D., Halpin, P. A., Karlson, K. H., et al. (1998) Membrane trafficking of the cystic fibrosis gene product, cystic fibrosis transmembrane conductance regulator, tagged with green fluorescent protein in madin-darby canine kidney cells. *J. Biol. Chem.* **273,** 21,759–21,768.

54. Howard, M., DuVall, M. D., Devor, D. C., Dong, J. Y., Henze, K., and Frizzell, R. A. (1995) Epitope tagging permits cell surface detection of functional CFTR. *Am. J. Physiol.* **269,** C1565–C1576.
55. Schultz, B. D., Takahashi, A., Liu, C., Frizzell, R. A., and Howard, M. (1997) FLAG epitope positioned in an external loop preserves normal biophysical properties of CFTR. *Am. J. Physiol.* **273,** C2080–C2089.

4

α1-Antitrypsin Deficiency

Liver Disease Associated With Retention of a Mutant Secretory Glycoprotein in the Endoplasmic Reticulum

David H. Perlmutter

1. Introduction

The classical form of α1-antitryspsin (α1AT) deficiency, homozygous for the α1ATZ allele, is associated with a mutant protein that is retained in the endoplasmic reticulum (ER) of liver cells rather than secreted into the blood and body fluids. Affected individuals are susceptible to liver injury and hepatocellular carcinoma. Most of the evidence in the literature suggests that liver disease is caused by

the toxic effects of the mutant α1ATZ molecule retained in the ER of the affected liver cells and, therefore, this inherited disorder is often considered a prototype human disease in which tissue damage results from a mutant protein.

α1AT is the archetype of serine protease inhibitor (SERPIN) supergene family. Its primary function is inhibition of destructive neutrophil proteases, including elastase, cathepsin G, and proteinase 3 ***(1)***. It is a glycoprotein secreted by liver cells and upregulated during the host response to inflammation/tissue injury, for which it has been termed a hepatic acute-phase reactant.

The α1AT deficiency state is relatively common, affecting 1 in 1800 live births in Northern European and North American populations ***(2)***. These homozygotes are predisposed to premature development of pulmonary emphysema by a loss-of-function mechanism, i.e., lack of α1AT in the lung permits uninhibited proteolytic damage of the connective tissue matrix ***(3,4)***. Cigarette smoking markedly increases the risk and rate of development of emphysema ***(5)***. One mechanism for this environmental risk factor involves the functional inactivation of residual α1AT by phagocyte-derived oxygen intermediates ***(3,4)***. However, a growing body of evidence suggests that there are other envi-

From: *Methods in Molecular Biology, vol. 232: Protein Misfolding and Disease: Principles and Protocols*
Edited by: P. Bross and N. Gregersen © Humana Press Inc., Totowa, NJ

ronmental factors and genetic traits that play a role in the incidence and severity of lung disease among α1AT-deficient individuals *(6)*.

Liver disease associated with α1AT deficiency may become evident in early infancy and childhood. In fact, α1AT deficiency is the most common genetic cause of liver disease in children *(6)*. It also predisposes adults to chronic liver disease and hepatocellular carcinoma *(7)*. However, in contrast to the pathobiology of lung disease, liver injury in this deficiency appears to involve a gain-of-function mechanism whereby retention of the mutant α1AT molecule in the ER triggers a series of events that are eventually hepatotoxic. The strongest evidence for a gain-of-function mechanism comes from studies in which mice transgenic for mutant human α1ATZ develop liver injury with many of the histopathologic hallmarks of the human condition *(8,9)*. Because there are normal levels of anti-elastases in these mice, as directed by endogenous genes, the liver injury cannot be attributed to a loss of function.

However, there is marked variation in the phenotypic expression of liver disease among homozygotes. Landmark nationwide prospective screening studies done by Sveger in Sweden have shown that only 10% of the homozygous population develops clinical significant liver disease over the first 30 years of life (*10,11*; Sveger, personal communication). It is not yet known what proportion of the remaining population has subclinical liver injury and what proportion will go on to have liver disease and/or hepatocellular carcinoma during adult life. Nevertheless, these data indicate that other genetic traits and/or environmental factors determine the severity of liver injury in α1AT deficiency.

2. The Mutant α1ATZ Molecule

The α1ATZ molecule is characterized by a point mutation that results in the substitution of lysine for glutamate 342 and accounts for defective secretion. This substitution reduces the stability of the monomeric form of the molecule and increases the likelihood that it will form polymers in the ER by the "loop-sheet" insertion mechanism *(12,13)*. This mutation opens the major β-sheet of the molecule, sheet A, in such a way that the reactive loop of another α1AT molecule can insert into a gap in sheet A to form a dimer (**Figs. 1**,**2**) *(61,62)*. This process presumably extends to form chains of polymers. Indeed polymers have been detected in the ER of hepatocytes by electron microscopic analysis of a liver biopsy from a PIZZ individual *(13)*. In vitro studies indicate that α1ATZ undergoes polymerization to a certain extent spontaneously and to a greater extent during relatively minor perturbations, such as a rise in temperature *(13)*. These observations have led Lomas et al. to speculate that increases in body temperature during systemic inflammation might exacerbate this tendency in vivo and that differences in incidence of severity of febrile illness might account for the variation in expression of liver disease among α1AT-deficient hosts *(13)*.

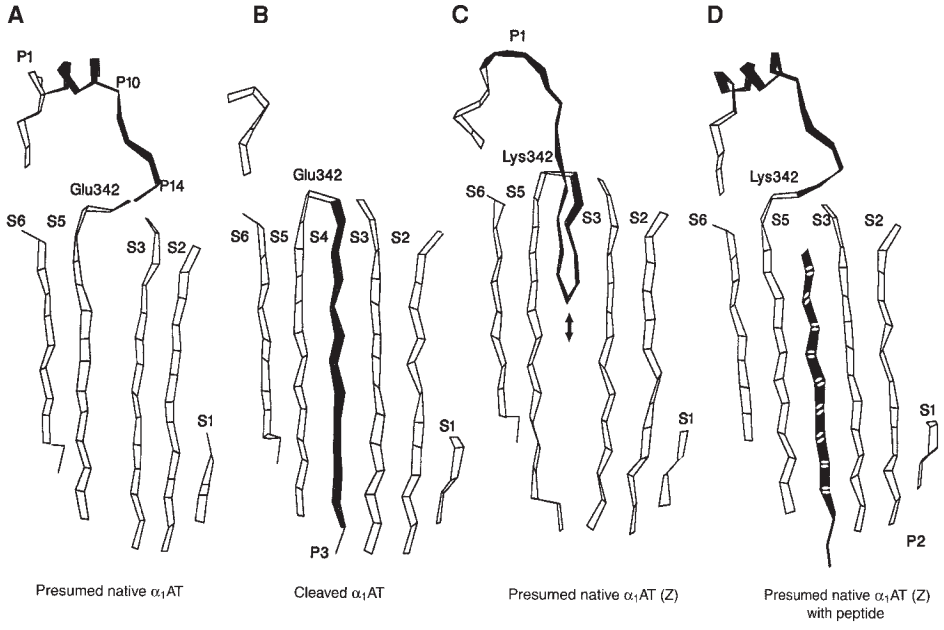

Fig. 1. Ribbon diagrams of the A-sheet and reactive-site loop of α1AT in several different states. The positions of the P1 residue in the reactive site loop and of glutamate 342 are indicated. (**A**) Presumed native α1AT. This state is presumed because it has not been crystallized. However, it is generated by computer models based on the crystal structures of cleaved α1AT and native ovalbumin. The reactive-site loop is shown in dark gray with residues P10-P14 numbered from the reactive-site methionine P1. The carboxyl-terminal fragment is shown as a white ribbon. α-helices of the A-sheet are shown in light gray and referred to as S1, S2, S3, S5 and S6. (**B**) Cleaved α1AT. The reactive site loop is cleaved and inserts into the A-sheet. It is referred to as S4 in between α-helices S1-S3, and S5-S6 of the A sheet. The positions of the P1 residue of the reactive site loop and of glutamate 342 are indicated. (**C**) Presumed native α1ATZ. The reactive-site loop simultaneously collapses into the gap in the A-sheet but because of the substitution of lysine at residue 342, it cannot fully insert. (**D**) Presumed native α1ATZ with peptide. A synthetic peptide that mimics the reactive site loop is shown in black with white stripes. The insertion of peptide would prevent insertion from an adjacent α1AT molecule and therein prevent polymerization. Adapted with permission from **ref. *61***. Copyright Macmillan Magazines Ltd.

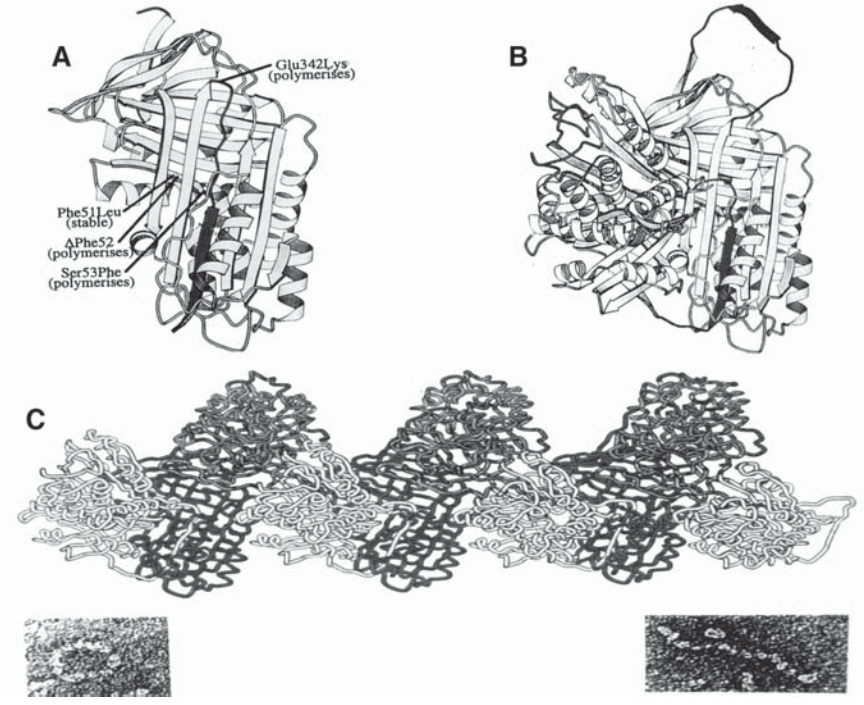

Fig. 2. Schematic representation of polymerization. (**A**) Cleaved α1AT. The cleaved reactive center loop (dark) is fully inserted into the A-sheet, stabilizing the molecule. The sites of substitutions that result in polymerogenic properties are indicated. (**B**) Dimerized α1ATZ. The reactive center loop (dark) cannot insert into the gap in A-sheet because of the substitution of bulky amino acid lysine for glutamate 342 at the hinge of the insertion movement and so the reactive center loop is stabilized in an extended β-sheet scaffold above the A-sheet. This leaves a gap in the A-sheet. The α1ATZ molecule on the left inserts its reactive center loop into the gap in the A-sheet of the α1ATZ molecule on the right. (**C**) Polymerized α1ATZ. Differently shaded α1ATZ molecules are shown in a well-ordered polymer. The insets show examples of these polymers by rotary shadowing EM. Adapted with permission from **ref. *62***. Copyright Macmillan Magazines Ltd.

The strongest evidence that polymerization causes retention of α1ATZ in the ER comes from studies in which the fate of α1ATZ is examined after the introduction of additional mutations into the molecule. For instance, Kim et al. ***(14)*** introduced a mutation into the α1AT molecule at amino acid 51, F51L. This mutation is remote from the Z mutation, E342K, but was predicted on the basis of structural characteristics to impede loop-sheet polymerization. Indeed the double-mutated F51L α1ATZ molecule was found to be less prone to polymerization and to fold more efficiently in vitro than α1ATZ. Moreover, the introduction of the F51L mutation partially corrected the intracellular retention properties of α1ATZ in microinjected Xenopus oocytes ***(15)*** and in yeast ***(16)***.

Further circumstantial evidence has come from studies of two families affected by autosomal dominantly inherited dementia ***(17)***. This dementia was associated with histological picture of unique neuronal inclusion bodies and characterized biochemically by polymers of a neuron-specific member of the SERPIN family, neuroserpin. Neuroserpin is a secretory protein, closely homologous to α1AT. The mutation in neuroserpin that was identified in one family is homologous to the mutation in the α1AT S_{iiyama} allele that is associated with polymerization and inclusions in the ER of liver cells ***(17)***.

In a recent study we found that a novel, naturally occurring variant of α1AT, bearing the mutation that characterizes α1ATZ as well as a mutation that results in carboxyl-terminal truncation, is retained in the ER for as long, or longer, than α1ATZ even though it does not polymerize ***(18)***. These results could indicate that there are mechanisms other than polymerization that determine whether mutant α1AT molecules are retained in the ER. An alternative explanation is that polymerization is not the cause of ER retention, but rather is its result.

It is still not entirely clear what proportion of the newly synthesized mutant α1ATZ molecules is converted to the polymeric state in the ER. In one cell-culture model system we have found that 17.0 +/– 1.9% of α1ATZ is in the insoluble fraction at steady state ***(18)***, but comparable in vivo data are not yet available. It is also not known whether polymeric molecules are degraded in the ER less rapidly than their monomeric counterparts or whether polymeric molecules, when retained in the ER, are more hepatotoxic than their monomeric counterparts. Indeed, recent studies on the effect of temperature on the fate of α1ATZ have indicated the high degree of complexity involved in these issues. Although Lomas et al. showed that a rise in temperature to 42°C increases the polymerization of purified α1ATZ in vitro ***(13)***, Burrows et al. found that a rise in temperature to 42°C resulted in increased secretion of α1ATZ as well as decreased intracellular degradation of α1ATZ in a model cell-culture system ***(19)***. In contrast, lowering the temperature to 27°C resulted in diminished intracellular degradation of α1ATZ without any change in the small amount of α1ATZ secreted ***(19)***. Consistent with the well-established

role that temperature plays in most biochemical processes, these results suggest that changes in temperature have the potential to affect multiple steps in the pathways by which α1ATZ is translocated through the secretory and degradative compartments/systems as well as affecting the relative proportions of αATZ in the monomeric and polymeric state. On the basis of these considerations, a long-standing clinical experience with α1AT-deficient children and other children with liver disease, and the lack of any substantive epidemiological evidence, it is very hard for this author to believe that there is a simple relationship between febrile episodes and phenotypic expression of liver disease in α1AT-deficient patients.

3. Fate of Mutant α1ATZ in ER

Several studies have shown that α1ATZ is degraded in the ER and that the proteasome is a key component of the degradation pathway ***(20–22)***. Degradation of α1ATZ is markedly reduced by specific proteasome inhibitors in yeast and mammalian cells ***(21,22)***. In a mammalian cell-free system degradation of α1ATZ is attributable, at least in part, to a pathway that involves interaction with the transmembrane ER chaperone calnexin, polyubiquitination of calnexin and targeting of the α1ATZ-polyubiquitinated calnexin complex by the proteasome ***(22)***. There is also evidence for the involvement of ubiquitin-independent proteasomal and nonproteasomal pathways in degradation of α1ATZ in the mammalian cell-free system ***(23)***. Autophagy may represent one nonproteasomal mechanism for degradation of α1ATZ ***(24)***. Because this is based on the effect of chemical inhibitors of autophagy which have other effects on cellular metabolism, definitive evidence for the role of autophagy in degradation of α1ATZ will require more detailed, probably genetic studies. Cabral et al. have recently provided evidence for a nonproteasomal degradation pathway that is sensitive to tyrosine phosphatase inhibitors ***(25)***. In their studies, degradation of α1ATZ in a hepatoma cell line was not affected by proteasome inhibitors but was reduced by tyrosine phosphatase inhibitors. Although this was originally interpreted to suggest that there were cell-type specific differences in the role of proteasomal and nonproteasomal degradation mechanisms and that nonproteasomal degradation mechanisms were more important in hepatocytes, subsequent studies have shown that the proteasome still plays a major role in degradation of α1ATZ in other hepatoma cell lines ***(26)***. This has led us to conclude that nonproteasomal mechanisms that are sensitive to tyrosine phosphatase inhibitors may be particularly important in specific cell lines rather than specific cell types. The relative importance of proteasomal and nonproteasomal mechanisms to the disposal of α1ATZ in vivo is still unknown.

The mechanism by which the proteasomal gains access from the cytoplasm to α1ATZ on the luminal side of the ER membrane is still unknown. Although

retrograde translocation from the ER to the cytoplasm has been demonstrated for some luminal substrates of the proteasome, there is very limited evidence for retrograde translocation of α1ATZ. Werner et al. detected α1ATZ free in the cytosolic fraction of yeast when the proteasome was inhibited ***(21)***, but it was only a small fraction of the total α1ATZ in the ER ***(21)*** and there has been no other evidence for retrotranslocation. Recent studies have provided evidence for extraction of substrates through the ER membrane by the proteasome ***(27)***. The AAA ATPase Cdc 48/p97 and its partners appear to play an important role in this process ***(28)***.

In order to determine whether the fate of α1ATZ is different in α1AT-deficient hosts susceptible to liver disease ("susceptible hosts") as compared to α1AT-deficient individuals who are protected from liver disease ("protected hosts"), Wu et al. transduced skin fibroblasts from PIZZ individuals, with or without liver disease, with amphotropic recombinant retroviral particles designed for constitutive expression of the mutant α1ATZ gene ***(29)***. The PIZZ individuals were carefully selected to ensure appropriate representation. Susceptible hosts were defined as having severe liver disease by clinical criteria. Protected hosts were discovered incidentally and never had clinical or biochemical evidence of liver disease. Human skin fibroblasts were selected because they do not express the endogenous α1AT gene but, presumably, express other genes involved in the postsynthetic processing of secretory proteins. The results showed that expression of the human α1AT gene was conferred on each fibroblast cell line. Compared with the same cell lines transduced with the wild-type α1AT gene, there was selective intracellular retention of the mutant α1ATZ protein in each case. However, there was a marked delay in degradation of the mutant α1ATZ protein after it accumulated in the fibroblasts from susceptible hosts as compared with protected hosts (**Fig. 3**). Thus, these data provide evidence that alterations in quality control mechanisms, such as the ER degradation pathway, can predispose α1AT-deficient hosts to liver injury and that further elucidation of the mechanisms by which the cell degrades and/or mounts protective cellular response pathways to mutant α1ATZ is critical for understanding the hepatotoxic effects of the aggregated protein.

4. Cellular Response to ER Retention of α1ATZ

Several recent studies have shown that there is a rather specific cellular response to ER retention of mutant α1ATZ with marked autophagy as its main feature. The autophagic response is thought to be a general mechanism whereby cytosol and intracellular organelles, such as ER, are first sequestered from the rest of the cytoplasm into newly formed vacuoles that then fuse with the lysosomes in such a way that the internal debris and cytosol are then degraded. It occurs in many cell types, especially during stress states, such as nutrient dep-

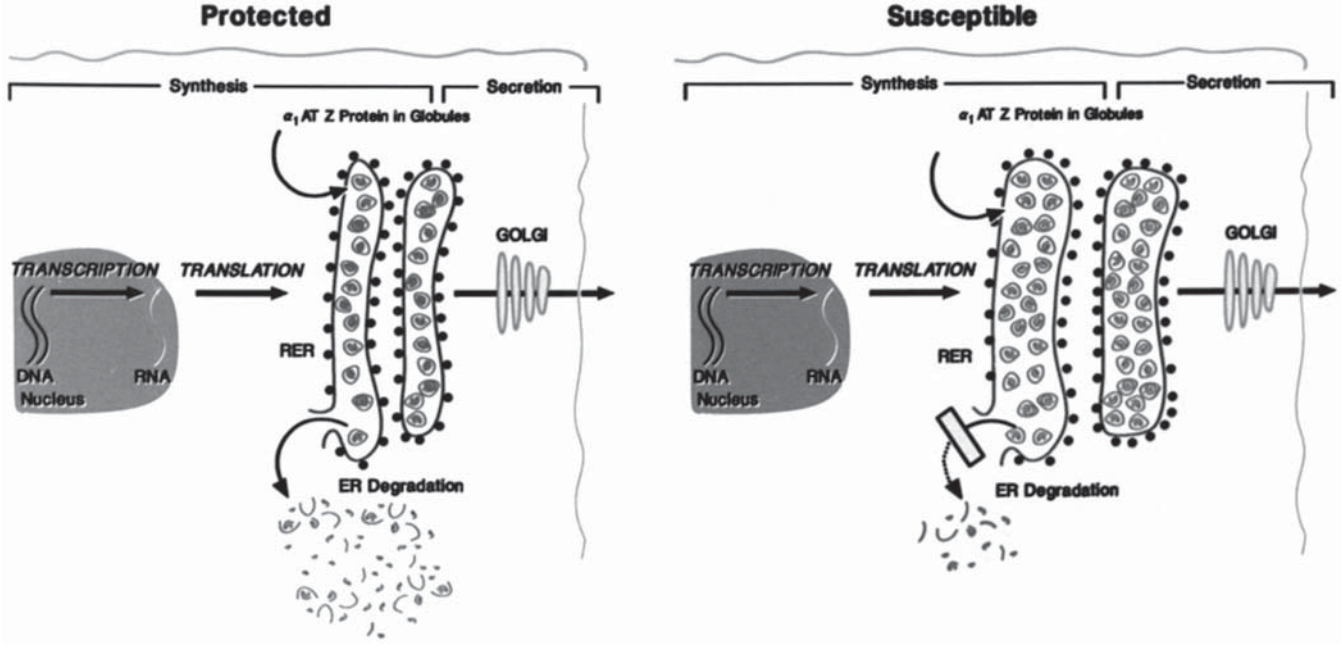

Fig. 3. Difference in ER degradation of α1ATZ in protected and susceptible hosts. In cells of the protected host α1ATZ is retained in the ER as globules and it is degraded from the cytoplasmic aspect of the ER. In cells of susceptible host, α1ATZ is retained in the ER in globules with even greater accumulation owing to a relative block in ER degradation.

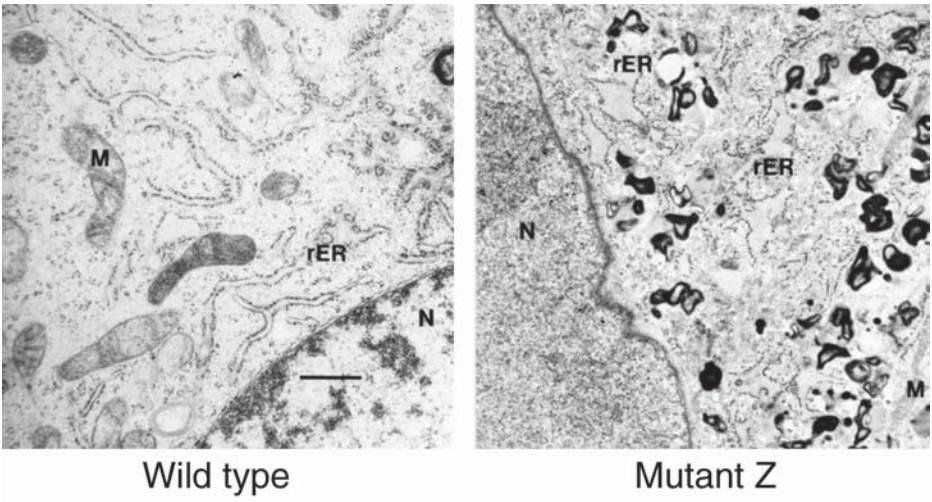

Fig. 4. Electron microscopic characteristics of the ER in genetically engineered fibroblast cell lines. A human fibroblast cell line engineered for stable expression of wild-type α1AT is shown in the left panel and the same cell line engineered for stable expression of mutant α1ATZ is shown in the right panel. Dilated ER is surrounded by electron-dense nascent and degradative autophagosomes in the right panel. N, nuclei; rER, rough ER; M, mitochondria.

rivation, and during the cellular remodeling that accompanies differentiation, morphogenesis and aging. Our studies show that autophagosomes develop in several different model cell culture systems genetically engineered to express α1ATZ, including human fibroblasts, murine hepatoma and rat hepatoma cell lines (**Fig. 4**). Moreover, in a HeLa cell line engineered for inducible expression of α1ATZ, autophagosomes appeared as a specific response to the expression of α1ATZ and its retention in the ER ***(24)***. There is a marked increase in autophagosomes in hepatocytes in transgenic mouse models of α1AT deficiency and a disease-specific increase in autophagosomes in liver biopsies from patients with α1AT deficiency. Mutant α1ATZ molecules can be detected in autophagosomes by immune electron microscopy, often together with the ER molecular chaperone calnexin. Intracellular degradation of α1ATZ is partially reduced by chemical inhibitors of autophagy, suggesting that autophagy also contributes to the quality control mechanism for disposal of α1ATZ ***(24)***. Taken together, these results have suggested that the autophagic response is induced to protect liver cells from the toxic effects of aggregated α1ATZ retained in the ER. We have also speculated about the role of autophagy in protecting liver cells from tumorigenesis. Several recent studies have shown that autophagic activity is decreased in tumors and that reconstitution of

autophagic activity inhibits tumorigenesis in vivo ***(30,31)***. In our studies, autophagosomes are predominantly found in liver cells with dilated ER in both human and transgenic mouse liver ***(24)***. Previous studies in transgenic mouse models of α1AT deficiency have shown that hepatocarcinogenesis evolves within nodular aggregates of hepatocytes that are negative for α1AT expression by immunofluorescent staining ***(32)***.

It is not yet clear whether the autophagic response is substrate-specific for α1ATZ or is a stereotypic response to all aggregated proteins that are retained in the ER or to aggregated luminal as opposed to membrane proteins. Autophagy has not been described in studies of mutant proteins that aggregate in the cytoplasm or nucleus. Although there is some mention of autophagic vacuoles around the aggresomes that form when CFTR ΔF508 accumulates in the presence of proteasomal inhibitors ***(33,34)***, the histologic picture in cells expressing α1ATZ is quite different than that in cells expressing CFTR ΔF508 ***(24)***. Autophagy is not induced by tunicamycin or thapsigargin, chemicals that cause a generalized form of "ER stress" (Mitzushima, N. personal communication). Russell bodies that have been described in cells that retain certain mutant immunoglobulin molecules in the ER ***(35)*** do have many characteristics of autophagosomes. Further studies of these structures may therefore shed additional light on whether the autophagic response is substrate-specific.

Recently we examined the autophagic response to ER retention of α1ATZ in vivo by testing the effect of fasting on the liver of the PiZ mouse model of α1ATZ deficiency ***(36)***. Starvation is a well-defined physiologic stimulus of autophagy as well as a known environmental stressor of liver disease in children. The results show that there is a marked increase in fat accumulation and in α1AT containing, ER-derived globules in the liver of the PiZ mouse induced by fasting. These changes were particularly exaggerated at 3–6 mo of age. Three-month-old PiZ mice had a significantly decreased tolerance for fasting compared to nontransgenic C57 black mice (mean time to death for PiZ = 64 h; for C57BL = 111 h). Although fasting induced a marked autophagic response in wild-type mice, the autophagic response was already activated in PiZ mice to levels that were twofold higher than those in the liver of fasted wild-type mice, and did not increase further during fasting. These results indicate that autophagy is constitutively activated in α1AT deficiency and that the liver is unable to mount an increased autophagic response to physiologic stressors. From our search of the literature, the only other condition in which there is accumulation of autophagic vacuoles under homeostatic condition is Danon disease ***(37)***. In contrast to α1AT deficiency, however, autophagosomes accumulate in Danon disease because of a genetic defect in the terminal phases of autophagy, i.e., the fusion of autophagic vacuoles with lysosomes and subsequent degradation within autolysosomes ***(37,38)***.

In the course of our ultrastructural studies of the liver of the PiZ mouse and of patients with α1AT deficiency, we have recently become struck by the degree of mitochondrial autophagy that is induced ***(39)***. A comparison of the liver from four α1AT-deficient patients to livers from eight patients with other liver diseases and four normal livers showed a marked significant increase in mitochondrial autophagy associated with α1AT deficiency. Even more interesting has been the observation that many mitochondria that are not surrounded by autophagic vacuolar membranes are damaged or in various phases of degeneration in liver cells from α1AT-deficient hosts. This damage is characterized by the formation of multilamellar structures within the limiting membrane, condensation of the cristae and matrix, and, in some cases, dissolution of the internal structures, often leaving only electron-dense debris compressed into a thin rim at the periphery of the mitochondrion. Although this second type of damaged mitochondria appears distinct from the mitochondria that are degenerating within autophagosomes, these mitochondria are sometimes seen in close proximity to, or even fusing with, autophagic vacuoles or lysosomes.

There is also marked mitochondrial autophagy and injury in the liver of the PiZ transgenic mouse model of α1AT deficiency. Immunofluorescence analysis shows the presence of activated caspase-3 in the PiZ mouse liver ***(39)***. Because cyclosporine A (CsA) has been shown to reduce mitochondrial injury ***(40)*** and inhibit starvation-induced autophagy ***(41)***, we examined the effect of CsA on PiZ mice. The results show that CsA mediates a marked significant reduction in hepatic mitochondrial injury, disappearance of activated caspase-3, and improvement in the capacity of the PiZ mouse to tolerate the stress of starvation. These results provide evidence for the novel concept that mitochondrial damage and caspase activation play a role in the mechanism of liver cell injury in α1AT deficiency and provide a proof-in-principle for mechanism-based therapeutic interventions such as CsA.

Although careful descriptive and quantitative analysis in this study suggests that there is mitochondrial injury that is separate from the autophagic process, we still cannot completely exclude the possibility that autophagy plays some role in all of the mitochondrial damage that is observed. This means that there are at least two possible explanations for mitochondrial damage in this deficiency. In the first, accumulation of α1ATZ in the ER is by itself responsible for mitochondrial dysfunction. There is now ample evidence in the literature that mitochondria are closely opposed to the cisternae of the ER physically ***(42)*** and that there are functional interactions between these two organelles ***(43)***. Recent studies show that specific signals are transmitted between these two intracellular compartments ***(44,45)***. Potentially even more relevant studies have shown that there is mitochondrial dysfunction, including release of cytochrome C and caspase-3 activation, when there is ER dilatation and/or "ER

stress" induced by brefeldin A, tunicamycin, or thapsigargin ***(46,47)***. It is not yet known, however, whether the mitochondrial dysfunction that was described in these last studies was owing to ER dilatation and/or ER stress or owing to an independent drug effect.

A second possible explanation envisages mitochondrial dysfunction as a result of the autophagic response to ER retention of α1ATZ. In this scenario, mitochondria are recognized nonspecifically by the autophagic response that is constitutively activated to somehow remove and degrade areas of the ER that are distended by aggregated mutant protein. Although our data indicates that CsA inhibits hepatic mitochondrial injury in vivo, this could be owing to the known effect of CsA on the mitochondrial permeability transition ***(40)*** or on autophagy ***(41)*** or both. Of course, these two scenarios are not mutually exclusive.

The results of experiments with CsA are also noteworthy for their therapeutic implications. They indicate that CsA can prevent mitochondrial damage even under circumstances in which α1ATZ is continuing to accumulate in the ER. Thus, these results provide a proof-in-principle for mechanism-based therapeutic approaches to liver disease in α1AT deficiency, i.e., pharmacological intervention directed as distal steps in the pathobiological pathway that leads to liver injury, such as the "mitochondrial" step, without correction of the primary defect and/or the more proximal steps in the pathobiology of this liver disease.

5. Other Potential Treatment Strategies

Several studies have shown that a class of compounds called chemical chaperones can reverse the cellular mislocalization or misfolding of mutant plasma membrane, lysosomal, nuclear, and cytoplasmic proteins including CFTRΔF508, prion proteins, mutant aquaporin molecules associated with nephrogenic diabetes insipidus, and mutant galactosidase A associated with Fabry disease ***(48–50)***. These compounds include glycerol, trimethylamine oxide, deuterated water and 4-phenylbutyric acid (PBA). We recently found that glycerol and PBA mediate an increase in the secretion of α1ATZ in a model cell-culture system ***(19)***. Moreover, oral administration of PBA was well-tolerated by PiZ mice (transgenic for the human α1ATZ gene) and consistently mediated an increase in blood levels of human α1AT, reaching 20% to 50% of the levels present in PiM mice and normal humans. PBA did not affect the synthesis or intracellular degradation of α1ATZ. The α1ATZ secreted in the presence of PBA was functionally active, in that it could form an inhibitory complex with neutrophil elastase. Because PBA has been used safely for years in children with urea cycle disorders as an ammonia scavenger and because clinical studies have suggested that only partial correction of the deficiency state is needed for the prevention of both liver and lung injury in

α1AT deficiency ***(4,7,51)***, it constitutes a candidate for chemoprophylaxis of target-organ injury in α1AT deficiency.

It also now appears that several iminosugar compounds may be potentially useful for chemoprophylaxis of liver and lung disease in α1AT deficiency. These compounds are designed to interfere with oligosaccharide side-chain trimming of glycoproteins and are now being examined as potential therapeutic agents for viral hepatitis and other types of infection ***(52,53)***. Initially we examined several of these compounds to determine the effect of inhibiting glucose or mannose trimming from the carbohydrate side chain of mutant α1ATZ on its fate in the ER, but found to our surprise that one glucosidase inhibitor, castanospermine (CST) and 2 α mannosidase I inhibitors, kifunensine (KIF) and deoxymannojirimicin (DMJ), actually mediate increased secretion α1ATZ ***(54)***. The α1ATZ that is secreted in the presence of these drugs retains partial functional activity. KIF and DMJ are less attractive candidates for chemoprophylactic trials because they delay degradation of α1ATZ in addition to increasing its secretion and therefore have the potential to exacerbate susceptibility to liver disease. However, CST has no effect on the degradation of α1ATZ and, therefore, may be targeted for development as a chemoprophylactic agent. The mechanism of action of CST on α1ATZ secretion is unknown. An interesting hypothesis for the mechanism of action of KIF and DMJ has mutant α1ATZ interacting with ERGIC-53 for transport from ER to Golgi when mannose trimming is inhibited.

Novoradovskaya et al. have suggested that inhibition of ER degradation of α1ATZ by proteasome inhibitor lactacystin and by protein synthesis inhibitor cycloheximide is associated with increased secretion of α1ATZ ***(55)***. We have been unable to confirm this result ***(19)***. Moreover, there are now several lines of evidence indicating that there is not a simple relationship between ER degradation of α1ATZ and its secretion such that perturbations that delay degradation are automatically accompanied by increased secretion. Some physiologic and pharmacologic perturbations are associated with delayed degradation without any change in secretion. Other perturbations increase secretion without any change in degradation. Increased temperature is associated with both delayed degradation and increased secretion ***(20)***.

Another potential treatment strategy is hepatocyte transplantation. Transplanted hepatocytes can repopulate the diseased liver in several mouse models ***(56,57)***, including a mouse model of a childhood metabolic liver disease termed hereditary tyrosinemia. Replication of the transplanted hepatocytes occurs only when there is injury and/or regeneration of the liver. The results provide evidence that it may be possible to use hepatocyte transplantation techniques to treat hereditary tyrosinemia and, perhaps, other metabolic liver diseases in

which the defect is cell-autonomous. For instance, α1AT deficiency involves a cell-autonomous defect and would be an excellent candidate for this strategy.

Alternative strategies for at least partial correction of α1AT deficiency may result from a more detailed understanding of the fate of the α1ATZ molecule in the ER. For instance, delivery of synthetic peptides to the ER to insert into the gap in the A-sheet or into a particular hydrophobic pocket of the α1AT molecule ***(58)*** and prevent polymerization of α1AT might result in release of the mutant α1ATZ molecules into the extracellular fluid and prevent accumulation in the ER. Although it is not yet entirely clear, there is some evidence from studies on the assembly of major histocompatibility complex (MHC) class I molecules that synthetic peptides may be delivered to the ER from the extracellular medium of cultured cells ***(59)***. There is also evidence that certain molecules may be transported retrograde to the ER by receptor-mediated endocytosis ***(60)***. Second, elucidation of the biochemical mechanism by which abnormally folded α1AT undergoes intracellular degradation might allow pharmacological manipulation of this degradative system, such as enhancing proteasomal activity with interferon-γ in the subpopulation of the PIZZ individuals predisposed to liver injury. It is now also possible to consider chemoprophylactic strategies involving combinations of drugs, perhaps even combinations of drugs that affect different steps in the pathobiology of liver injury. For instance, a combination of PBA that presumably affects the proximal part of the pathobiologic pathway, abnormal folding, and a CsA-like drug that presumably affects the distal part of the pathobiologic pathway by blocking the mitochondrial permeability transition could be tested.

References

1. Huber, R. and Carrell, R. W. (1990) Implications of the three-dimensional structure of α-1-antitrypsin for structure and function of serpins. *Biochemistry* **28,** 895–8966.
2. Perlmutter, D. H. (2001) α1-Antitrypsin deficiency, in *The Liver: Biology and Pathobiology* (Arias, I. M., Boyer, J. L., Fausto, N., Jakoky, W. B., Schachter, D. and Shafritz, D. A., eds.), Raven Press, New York, pp. 699–719.
3. Janoff, A. (1985) Elastases and emphysema: current assessment of the protease-antiprotease hypothesis. *Am. Rev. Respir. Dis.* **132,** 417–433.
4. Crystal, R. G. (1990) Alpha-1-antitrypsin deficiency, emphysema and liver disease: genetic basis and strategies for therapy. *J. Clin. Invest.* **95,** 1343–1352.
5. Janus, E. D., Phillips, N. T., and Carrell, R. W. (1985) Smoking, lung function and α-1-antitrypsin deficiency. *Lancet* **I,** 152–154.
6. Silverman, E. K., Province, M. A., Rao, D. C., Pierce, J. A., and Campbell, E. J. (1990) A family study of the variability of pulmonary function in α1-antitrypsin deficiency, quantitative phenotypes. *Am. Rev. Resp. Dis.* **142,** 1015–1021.
7. Eriksson, S., Carlson, J., and Velez, R. (1986) Risk of cirrhosis and primary liver cancer in α-1-antitrypsin deficiency. *N. Engl. J. Med.* **314,** 736–739.

8. Carlson, J. A., Rogers, B. B., Sifers, R. N., Finegold, M. J., Clift, S. M., DeMayo, F.J., et al. (1989) Accumulation of PiZ antitrypsin causes liver damage in transgenic mice. *J. Clin. Invest.* **83,** 1183–1190.
9. Dycaico, M. J., Grant, S. G., Felts, K., Nichols, S. W., Geller, S. A., and Sorge, J. A. (1988) Neonatal hepatitis induced by α-1-antitrypsin: a transgenic mouse model. *Science* **242,** 1409–1412.
10. Sveger, T. (1976) Liver disease in α1-antitrypsin deficiency detected by screening of 200,000 infants. *N. Engl. J. Med.* **294,** 1316–1321.
11. Sveger, T. (1995) The natural history of liver disease in α-1-antitrypsin deficient children. *Acta. Paediatr. Scand.* **77,** 847–851.
12. Carrell, R. W. and Lomas, D. A. (1997) Conformational disease. *Lancet* **350,** 134–138.
13. Lomas, D. A., Evans, D. L., Finch, J. T., and Carrell, R. W. (1992) The mechanism of Z α1-antitrypsin accumulation in the liver. *Nature* **357,** 605–607.
14. Kim, J., Lee, K. N., Yi, G. S., and Yu, M. H. (1995) A thermostable mutation located at the hydrophobic core of α1-antitrypsin suppresses the folding defect of the Z-type variant. *J. Biol. Chem.* **270,** 8597–8601.
15. Sidhar, S. K., Lomas, D. A., Carrell, R. W., and Foreman, R. C. (1995) Mutations which impede loop-sheet polymerization enhance the secretion of human α1-antitrypsin deficiency variants. *J. Biol. Chem.* **270,** 8393–8396.
16. Kang, H. A., Lee, K. N., and Yu, M.-H. (1997) Folding and stability of the Z and Siiyama genetic variants of human α1-antitrypsin. *J. Biol. Chem.* **272,** 510–516.
17. Davis, R. L., Shrimpton, A. E., Holohan, P. D., Bradshaw, C., Feiglin, D., Collins, G. H., et al. (1999) Familial dementia caused by polymerization of mutant neuroserpin. *Nature* **401,** 376–379.
18. Lin, L., Schmidt, B., Teckman, J., and Perlmutter, D. H. (2001) A naturally occurring non-polymerogenic mutant of α1-antitrypsin characterized by prolonged retention in the endoplasmic reticulum. *J. Biol. Chem.* **276,** 33,893–33,898.
19. Burrows, J. A. J., Willis, L. K., and Perlmutter, D. H. (2000) Chemical chaperones mediate increased secretion of mutant α1-antitrypsin (α1-AT) Z. A potential pharmacological strategy for prevention of liver injury and emphysema in α1-AT deficiency. *Proc. Natl. Acad. Sci. USA* **97,** 1796–1801.
20. McCracken, A. A. and Brodsky, J. L. (1996) Assembly of ER-associated protein degradation in vitro, dependence on cytosol, calnexin, and ATP. *J. Cell. Biol.* **132,** 291–298.
21. Werner, E. D., Brodsky, J. L., and McCracken, A. A. (1996) Proteasome-dependent endoplasmic reticulum-associated protein degradation, an unconventional route to a familiar fate. *Proc. Natl. Acad. Sci. USA* **93,** 13,797–13,801.
22. Qu, D., Teckman, J. H., Omura, S., and Perlmutter, D. H. (1996) Degradation of mutant secretory protein, α1-antitrypsin Z, in the endoplasmic reticulum requires proteasome activity. *J. Biol. Chem.* **271,** 22,791–22,795.

23. Teckman, J. H., Marcus, N., and Perlmutter, D. H. (2000) The role of ubiquitin in proteasomal degradation of mutant α1-antitrypsin Z in the endoplasmic reticulum. *Am. J. Physiol.* **278,** G39–G48.
24. Teckman, J. H. and Perlmutter, D. H. (2000) Retention of the mutant secretroy protein α1-antitrypsin Z in the endoplasmic reticulum induces autophagy. *Am. J. Physiol.* **279,** G961–G974.
25. Cabral, C. M., Choudhury, P., Liu, Y., and Sifers, R. N. (2000) Processing by endoplasmic reticulum mannosidases partitions a secretion-impaired glycoprotein into distinct disposal pathways. *J. Biol. Chem.* **275,** 25,015–25,022.
26. Teckman, J. H., Burrows, J., Hidvegi, T., Schmidt, B., Hale, P. D., and Perlmutter, D. H. (2001) The proteasome participants in degradation of mutant α1-antitrypsin Z in the endoplasmic reticulum of hepatoma-derived hepatocytes. *J. Biol. Chem.* **48,** 44,865–44,872.
27. Mayer, T., Braun, T., and Jentsch, S. (1998) Role of the proteasome in membrane extraction of a shortlived ER-transmembrane protein. *EMBO J.* **17,** 3251–3257.
28. Ye, Y., Meyer, H. H., and Rapoport, T. A. (2001) The AAA ATPase Cdc48/p97 and its partners transport proteins from the ER into the cytosol. *Nature* **414,** 652–656.
29. Wu, Y., Whitman, I., Molmenti, E., Moore, K., Hippenmeyer, P., and Perlmutter, D. H. (1994) A lag in intracellular degradation of mutant α1-antitrypsin correlates with the liver disease phenotype in homozygous PiZZ α1-antitrypsin deficiency. *Proc. Natl. Acad. Sci. USA* **91,** 9014–9018.
30. Kisen, G. O., Tessitore, L., Costelli, P., Gordon, P. B., Schwarze, P. E., Baccino, F. M., and Seglen, P. O. (1993) Reduced autophagic activity in primary rat hepatocellular carcinoma and ascites hepatoma cells. *Carcinogenesis* **14,** 2501–2505.
31. Liang, X. H., Jackson, S., Seaman, M., Brown, K., Kempkes, B., Hibshoosh, H., and Levine, B. (1999) Induction of autophagy and inhibition of tumorigenesis by beclin 1. *Nature* **402,** 672–676.
32. Geller, S. A., Nichols, W. S., Kim, S., Tolmachoff, T., Lee, S., Dycaico, M. J., Felts, K., and Sorge, J. A. (1994) Hepatocarcinogenesis is the sequel to hepatitis in Z #2 alpha-1-antitrypsin transgenic mice: histopathological and DNA ploidy studies. *Hepatology* **9,** 389–397.
33. Johnston, J. A., Ward, C. L., and Kopito, R. R. (1998) Aggresomes: a cellular response to misfolded proteins. *J. Cell. Biol.* **7,** 1883–1898.
34. Kopito, R. R. (2000) Aggresomes, inclusion bodies and protein aggression. *Trends Cell. Biol.* **10,** 524–527.
35. Kopito, R. R. and Sitia, R. (2000) Aggresomes and Russell bodies. Symptoms of cellular indigestion? *EMBO J.* **3,** 225–231.
36. Teckman, J. H., An, J.-K., Loethen, S., and Perlmutter, D. H. Fasting in α1-antitrypsin deficient liver: constitutive activation of autophagy. *Am. J. Physiol.* 2002; **283**:G1156–G1165.
37. Nishino, I., Fu, J., Tanji, K., Yamada, T., Shimojo, S., Koori, T., et al. (2000) Primary LAMP-2 deficiency causes X-linked vacuolar cardiomyopathy and myopathy (Danon disease). *Nature* **406,** 906–910.

38. Tanka, Y., Guhde, G., Suter, A., Eskelinen, E.-L., Hartmann, D., Lullmann-Rauch, R., et al. (2000) Accumulation of autophagic vacuoles and cardiomyopathy in LAMP-2-deficient mice. *Nature* **406,** 902–906.
39. Teckman, J. H., An, J.-K., Loethen, S., and Perlmutter, D. H. Mitochondrial autophagy and injury in the liver in alpha-1antitrypsin deficiency. *J. Clin. Invest.* (in review).
40. Lemasters, J. J., Nieminen, A. L., Qian, T., Trost, L. C., Elmore, S. P., Nishimura, Y., et al. (1998) The mitochondrial permeability transition in cell death: a common mechanism in necrosis, apoptosis and autophagy. *Biochim. Biophys. Acta* **1366,** 177–196.
41. Elmore, S. P., Qian T., Grissom, D. F., and Lemasters, J. J. (2001) The mitochondrial permeability transition initiates autophagy in rat hepatocytes. *FASEB J.* **15,** 2286–2287.
42. Perkins, G., Renken, C., Martone, M. E., Young, S. J., Ellisman, M., and Frey, T. (1997) Electrom tomography of neuronal mitochondria: three-dimensional structure and organization of cristae and membrane contacts. *J. Struct. Biol.* **119,** 260–272.
43. Achleitner, G., Gaigg, B., Krasser, A., Kainersdorfer, E., Kohlwein, S. D., Perktold, A., et al. (1999) Association between the endoplasmic reticulum and mitochondria of yeast facilitates intraorganelle transport of phospholipids through membrane contact. *Eur. J. Biochem.* **264,** 545–553.
44. Wang, H.-J., Guay, G., Pogan, L., Sauve, R., and Nabi, I. R. (2000) Calcium regulates the association between mitochondria and a smooth subdomain of the endoplasmic reticulum. *J. Cell. Biol.* **150,** 1489–1497.
45. Arnaudeau, S., Kelley, W. L., Walsh, J. V., and Demaurex, N. (2001) Mitochondria recycle Ca2+ to the endoplasmic reticulum and prevent the depletion of neighboring endoplasmic reticulum regions. *J. Biol. Chem.* **276,** 29,430–29,439.
46. Hacki, J., Egger, L., Conus, S., Rosse, T., Fellay, I., and Borner, C. (2000) Apoptotic crosstalk between the endoplasmic reticulum and mitochondria controlled by Bcl-2. *Oncogene* **19,** 2286–2295.
47. Wei, M. C., Zong, W.-X., Cheng, E. H.-Y., Lindsten,T., Panoutsakopoulou, V., Ross, A. J., et al. (2001) Proapoptotic BAX and BAK: A requisite gateway to mitochondrial dysfunction and death. *Science* **292,** 727–730.
48. Sato, S, Ward C. L., Krouse, M. E., Wine J. J., and Kopito, R. R. (1996) Glycerol reverses the misfolding phenotype of the most common cystic fibrosis mutation. *J. Biol. Chem.* **271,** 635–638.
49. Tamarappoo, B. and Verkman, A. S. (1998) Defective aquaporin-2 trafficking in nephrogenic diabetes insipidus and correction by chemical chaperones. *J. Clin. Invest.* **101,** 2257–2267.
50. Brown, C. R., Hong-Brown, L. Q., and Welch, W. J. (1997) Correcting temperature-sensitive protein folding defects. *J. Clin. Invest.* **101,** 2257–2267.
51. Campbell, E. J., Campbell, M. A., Boudedes, S. S., and Owens, C. A. (1999) Quantum proteolysis by neutrophils: implications for pulmonary emphysema in α1-antitrypsin deficiency. *J. Clin. Invest.* **99,** 1432–1444.
52. Jacob G. S. (1995) Gycosylation inhibitors in biology and medicine. *Curr. Opin. Struc. Biol.* **5,** 605–611.

53. Zitzmann, N., Mehta, A.S., Carrouee, S., Butters, T.D., Platt, F.J., McCauley, J., et al. (1999) Imino sugars inhibit the formation and secfretion of bovine viral diarrhea virus, a pestvirus model of hepatitis C virus: implications for the development of broad spectrum antihepatitis virus agents. *Proc. Natl. Acad. Sci. USA* **96,** 11,878–11,882.
54. Marcus, N. Y. and Perlmutter, D. H. (2000) Glucosidase and mannosidase inhibitors mediate increased secretion of mutant α1 antitrypsin Z. *J. Biol. Chem.* **275,** 1987–1992.
55. Novoradovskaya N., Lee J., Yu, Z. X., Ferrans, V. J., and Brantly, M. (1998) Inhibition of intracellular degradation increases secretion of a mutant for of α1-antitrypsin associated with profound deficiency. *J. Clin. Invest.* **1,** 2693–2701.
56. Rhim, J. A., Sandgen, E. P., Degen, J. L., Palmiter, R. D., and Brinster, R. L. (1994) Replacement of disease mouse liver by hepatic cell transplantation. *Science* **280,** 1593–1596.
57. Overturf K, Al-Dhalimy M, Tanguay R, Brantly, M., Ou, C. N., Finegold, M., and Crompe, M. (1996) Hepatocytes corrected by gene therapy are selected in vivo in a murine model of hereditary tyrosinaemia type I. *Nat. Genet.* **12,** 266–273.
58. Mahadeva, R., Dafforn, T. R., Carrell, R. W., and Lomas, D. A. (2002) 6-mer peptide selectively anneals to a pathogenic serpin conformation and blocks polymerizations: implications for the prevention of Z α1-antitrypsin-related cirrhosis. *J. Biol. Chem.* **277,** 6771–6774.
59. Day, P. M., Yewdell, J. W., Porgador A., Germain, R. N., and Bennink, J. R. (1997) Direct delivery of exogenous MHC class I molecule-binding oligopeptides to the endoplasmic reticulum of viable cells. *Proc. Natl. Acad. Sci. USA* **94,** 8064–8069.
60. Lord, J. M. and Roberts, L. M. (1998) Toxin entry: retrograde transport through the secretory pathway. *J. Cell Biol.* **140,** 733–736.
61. Carrell, R. W., Evans, D. L., and Stein, D. E. (1991) Mobile reactive centre of serpins and the control of thrombosis. *Nature* **353,** 576–578.
62. Elliott, P. R., Lomas, D. A., Carrell, R. W., and Abrahams, J. P. (1996) Inhibitory conformation of the reactive loop of α1-antitrypsin. *Nature Struct. Biol.* **2,** 676–681.

5

Parkinson's Disease

α-Synuclein and Parkin in Protein Aggregation and the Reversal of Unfolded Protein Stress

Lene Diness Jakobsen and Poul Henning Jensen

1. Introduction

Parkinson's disease (PD) is the second most common neurodegenerative disorder. The prevalence of PD increases dramatically with age, affecting 1–2% of the population above 65 years ***(1,2)***. PD is characterized by a progressive loss of dopaminergic neurons in the *substantia nigra*, *pars compacta* in the brain stem. The classical symptoms are tremor, rigidity, and slowness of movements. The symptoms appear when about 70% of the dopaminergic neurons are lost, demonstrating that the degenerative process is active long before the patients become aware of the disease. In the degenerating neurons, proteinaceous inclusions named Lewy bodies are found in the cell body and Lewy neurites in the neuronal processes ***(3)***. The inclusions exhibit filamentous protein aggregates with α-synuclein being a prominent component ***(4–7)***. The definitive diagnosis of PD requires both the clinical symptoms and post mortem examination. No preventive or neuroprotective therapies exist for PD, of which treatment primarily relies on substitution therapy with dopamine precursors or agonists. Genetic predispositions as well as environmental factors increase the risk of PD, but the etiology of PD is largely unknown. In rare familial cases, PD is linked to mutations in single genes encoding α-synuclein and parkin proteins. These cases have shed light on mechanisms leading to the selective dopaminergic cell loss.

The process of degeneration of the dopaminergic neurons leading to cell death is a focal point in PD research, as the ability to circumvent it will have the potential to bring forth neuroprotective strategies. Several features of the degenerative state have been described, such as oxidative stress, abnormal pro-

From: *Methods in Molecular Biology, vol. 232: Protein Misfolding and Disease: Principles and Protocols*
Edited by: P. Bross and N. Gregersen © Humana Press Inc., Totowa, NJ

teolysis, and increased caspase activity ***(8–11)***, but recent genetic evidence has placed two interrelated mechanisms in focus; first, protein aggregation leading to filament formation and second, a dysfunctional response to unfolded proteins. The importance of protein aggregation is highlighted by the pathogenic impact of: 1) α-synuclein mutations that lead to increased aggregation ***(12)***; 2) the presence of insoluble and aggregated α-synuclein species in PD tissue ***(7)***; 3) the presence of protein aggregates in a range of neurodegenerative disorders, e.g., Alzheimer's disease and Huntington's disease. The central position of unfolded protein stress and the ubiquitin-proteasome pathway is owing to: 1) the accumulation of unfolded proteins, often as filaments, in neurode-generative disorders; 2) the presence of ubiquitinated proteins in degenerating nerve cells in general, and in Lewy bodies in particular, indicating an imbalance in the formation and catabolism of unfolded proteins ***(7,13)***; 3) the linkage between familial PD and deletions or mutations in the gene of parkin, a ubiquitin-ligase, ***(14)*** and the gene of ubiquitin carboxy-terminal hydrolase L1 ***(15)***, both enzymes of importance for the degradation of ubiquitinated proteins. Degradation of proteins via the ubiquitin-proteasome pathway is a stepwise reaction beginning with the ATP-dependent activation of ubiquitin catalyzed by the ubiquitin-activating enzyme (E1). Ubiquitin is then transferred to cystein side chains of ubiquitin-conjugating enzymes (E2). The ubiquitin-ligases (E3) bind to certain substrates and mediate transfer of ubiquitin from the E2 to lysine side chains in these substrates. This is repeated and a polyubiquitin side chain on the substrate is formed, a sign that targets the substrate for degradation by the 26S proteasome followed by cleavage of the polyubiquitin chain to monomers by ubiquitin carboxy-terminal hydrolase L1. The specificity of the cascade regarding which proteins to degrade occurs at the level of E3 ligases ***(16)***. A reduced ubiquitination process results in diminished degradation of certain proteins, which therefore accumulate in the cell and might cause cell degeneration. Unfolded protein stress arises when unfolded proteins accumulate in the endoplasmic reticulum (ER) and induces an unfolded protein response, including upregulation of chaperones to facilitate refolding and of proteins involved in protein degradation ***(17)***. Parkin may play a role in the cellular response to unfolded protein stress ***(18–21)***.

The focus of this chapter will be on α-synuclein aggregation, parkin ubiquitin-ligase activity and its possible contribution to unfolded protein response in dopaminergic neurons.

2. α-Synuclein

α-synuclein consists of 140 amino acids with a random coil conformation in its native state ***(22)***. It has seven repeats of a conserved KTKEGV-motif, a hydrophobic middle region, and a negatively charged C-terminus ***(23)***. α-synuclein

Fig. 1. Illustration of the 140 amino acid α-synuclein protein. The black boxes indicate the seven conserved KTKEGV-repeats. The vesicle-binding and the ligand-binding domains are shown.

binds vesicles via regions in the N-terminus ***(24)***, whereas the C-terminal contains a ligand binding domain ***(11)*** (**Fig. 1**).

The function of α-synuclein is unknown, but its localization in presynaptic nerve terminals combined with the effect observed in gene knockout mice and antisense oligonucleotide-treated neurons suggests a role in neurotransmitter homeostasis ***(25–27)***. Cell-culture studies indicate that α-synuclein is degraded by the proteasome ***(28,29)*** although an unconventional mechanism degrading nonubiquitinated native α-synuclein by the 20S proteasome may be at play ***(30)***. The presence of *O*-glycosylated α-synuclein has been demonstrated in the human brain and this modified form is a substrate for ubiquitin ligases that may target α-synuclein to a conventional proteasomal degradation ***(31)***.

Two mutations in the α-synuclein gene are linked to autosomal dominant PD ***(32,33)*** and aggregated filamentous α-synuclein represents the unifying component of the neuronal inclusions, Lewy bodies and Lewy neurites, which are the pathoanatomical hallmark of all cases of PD ***(4–7)***. Accordingly, dysmetabolism of α-synuclein causes a dominant heritable disease that is compatible with a gain of toxic function. The mechanism whereby α-synuclein exerts its toxicity is yet unknown, but transgenic animal models mimic the development of PD to varying extents. The symptomatic phenotype is accompanied by a decreased solubility of α-synuclein ***(34)***. The transgenic *Drosophila* model overexpressing α-synuclein displayed a late-onset neurodegeneration that was augmented when α-synuclein contained the mutations linked to PD ***(35)***. These mutations cause an increase in α-synuclein's propensity for aggregation. The structure of α-synuclein displays a large plasticity because it, from its natively unfolded state, increases its α-helical content upon interaction with lipid membranes. Conversely, upon aggregation α-synuclein exhibits β-sheet characteristics like regular amyloid fibers ***(12)***. The fibrillation process of α-synuclein, which may be essential for the development of PD, is a nucleation-dependent process. Before monomeric α-synuclein forms regular filaments, there is an increase in so-called soluble oligomers ***(22,36)***. These oligomers might be more harmful to the cell than the filaments because pore-forming properties of the oligomers have been described ***(37)***. Thus, formation of filaments and Lewy bodies might be cytoprotective means of sequestering large amounts of unfolded proteins in a defined volume.

Several posttranslational modifications of α-synuclein have been described, including proteolytic truncations, phosphorylation, *O*-glycosylation, and oxidative damage ***(10,11,38,39)*** and all, except the *O*-glycosylation, increase the filamentogenic potential of α-synuclein. Moreover, C-terminally truncated α-synuclein has specifically been demonstrated in isolated Lewy bodies, as has α-synuclein phosphorylated on serine129 ***(11,38)***. The toxicity of aggregated α-synuclein may be subjected to modulation by endogenous factors, as coexpression of the human chaperone, heat-shock protein (Hsp)70, with α-synuclein reduced the neuronal loss in the α-synuclein transgenic *Drosophila* model, although the number, morphology, and distribution of protein inclusions were unaltered ***(40)***. Moreover, Hsp70 was found to be sequestered in 1–5% of all Lewy bodies in PD brains, indicating a human biological relevance of Hsp70 in relation to aggregation of α-synuclein ***(40)***. The mechanisms whereby aggregated α-synuclein implement its toxic properties are elusive but may depend on interactions between novel structures on the α-synuclein aggregates and vital proteins. Indeed, α-synuclein filament interacting proteins have been demonstrated, e.g., MAP-1B, which colocalize with α-synuclein in Lewy bodies and Lewy neurites ***(11)***.

3. Parkin

Parkin is a protein of 465 amino acids. The N-terminus consists of a ubiquitin-like domain and the C-terminus contains two RING-fingers with a cysteine-rich region between them denoted the In-Between-Rings (IBR) region ***(14)*** (**Fig. 2**).

Parkin is a member of the RING-finger containing E3 ubiquitin-ligase family ***(18,41,42)***. The RING-finger domains of parkin bind E2 ubiquitin-conjugating enzymes and show a preference for binding to Ubch7 ***(18,42)*** and Ubch8 ***(41,42)***, in addition to two ER-located E2 forms ***(19)***. No consensus has been achieved in detecting a single substrate binding site because both the ubiquitin-like domain and the RING-finger domains of parkin bind different substrates ***(19,31,43,41)***. The parkin gene was first described as responsible of Autosomal Recessive Juvenile Parkinsonism (AR-JP) ***(14)***. Mutations in the parkin gene were later associated with early-onset PD ***(44)***. The mutant parkin proteins had either no or very little E3 activity when investigated in cell lines or in vitro ***(18,41,43)***, in accordance with the recessive pattern of heredity observed in families with AR-JP. Parkin is widely expressed in the brain ***(45)***, however, loss of parkin function is associated with selective degeneration of dopaminergic neurons, indicating a higher degree of susceptibility towards accumulation of parkin substrates in these cells. Unfolded protein stress (UPS) might be con-

Fig. 2. Illustration of the 465 amino acid parkin protein. Ubl, Ubiquitin-like domain; R1 and R2, RING-finger domains; IBR, In-Between-Rings.

tributory to degeneration of dopaminergic neurons in PD, as the expression of the ER-chaperone BiP, an indicator of unfolded protein response (UPR), was observed in AR-JP brains ***(19)***. Parkin is part of the UPR, which has been demonstrated in the SHSY5Y cell line ***(18)*** and in rat primary astrocyte cultures, but not in rat hippocampal neurons ***(21)***. A parkin substrate, the PAEL-receptor, accumulates in AR-JP brains and induces UPS and subsequent cell death when overexpressed in cell lines. The viability of cells was ameliorated when the PAEL-receptor and parkin were coexpressed ***(19)***. Parkin forms a complex with the PAEL-receptor and the chaperone Hsp70 in transfected cell lines. Another binding partner of parkin, CHIP (carboxy terminus of the Hsc70-interacting protein), removes Hsp70 from the complex and induces an increase in parkin-mediated degradation of unfolded PAEL-receptor under UPS. CHIP might also exert its beneficial effect on parkin function by assisting in assembly of polyubiquitin chains ***(20)***.

A reduced parkin function may also be contributory in sporadic PD, since cleaved forms of parkin have been identified in PD brain extracts ***(10,46)***. These parkin fragments might be a result of caspase activity, as it has been demonstrated that parkin is a substrate of caspases in parkin transfected cell lines ***(47)*** and caspase activity is elevated in dopaminergic neurons of PD patients ***(9)***. Synphilin-1 is present in Lewy bodies ***(48)*** and it is a substrate of parkin ***(43)***, which might indicate a reduced parkin-mediated degradation. Only three other substrates of parkin have been found: the *O*-glycosylated form of α-synuclein ***(31)***, the PAEL-receptor ***(19)***, and the synaptic vesicle-associated protein CDCrel-1 ***(41)***. No *O*-glycosylated α-synuclein was detected in one patient with sporadic PD ***(31)***, but more investigations are needed to determine whether this or other parkin substrates accumulate in sporadic PD.

In line with the view that Lewy body development might be a cytoprotective mechanism sequestering unfolded proteins, it has been suggested that parkin participates in formation of Lewy bodies. This is based on the observation that AR-JP patients with parkin mutations lack Lewy bodies in the nigral neurons ***(46,49–52)***, although they have been observed in one patient ***(53)***. Furthermore, parkin, ubiquitin, and Ubch7 have been found in close association in Lewy bodies of PD patients, indicating parkin activity in Lewy bodies ***(10)***.

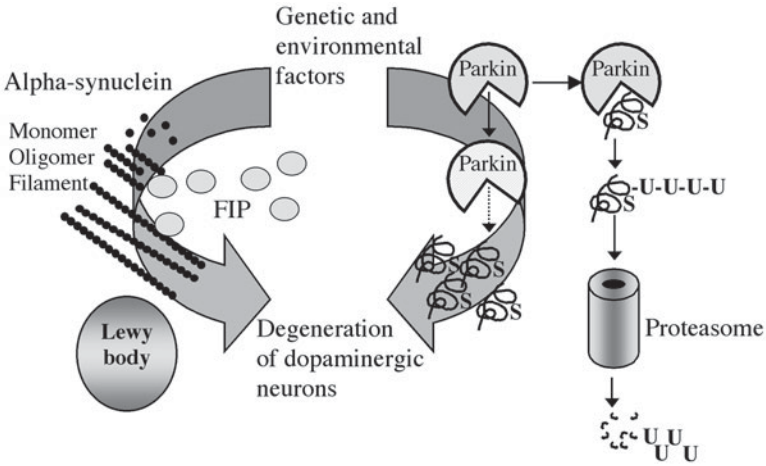

Fig. 3. Model of mechanisms leading to degeneration of dopaminergic neurons. Genetic or environmental factors induce alterations in the α-synuclein protein resulting in a gain of toxic function. This could reflect an interaction between polymeric forms of α-synuclein and cellular proteins with a subsequent loss of cellular functions and neurodegeneration. Lewy bodies might represent a later stage of protein sequestering. Additionally, abnormal modifications of parkin (shown as hatched) lead to loss of parkin function and subsequent accumulation of unfolded parkin substrates, which causes unfolded protein stress and neurodegeneration. Normal parkin function is shown to the right. FIP, Filament-interacting proteins; S, substrate of parkin; U, Ubiquitin.

4. Final Remarks

Changes in the α-synuclein protein result in a gain of toxic function, which involves increased tendency of α-synuclein to polymerize. Aggregates of α-synuclein might seize vital proteins and thereby cause cell degeneration. Loss of parkin function owing to pathogenic modifications, such as cleavage by caspases, will result in accumulation of unfolded proteins, which are toxic to the cell (*see* **Fig. 3**). Knowledge of posttranslational regulation of α-synuclein assembly and parkin function might lead to treatments that circumvent the degeneration of neurons and thereby the development of PD.

References

1. de Rijk, M. C., Tzourio, C., Breteler, M. M., Dartigues, J. F., Amaducci, L., Lopez-Pousa, S., et al. (1997) Prevalence of Parkinsonism and Parkinson's Disease in Europe: the EUROPARKINSON Collaborative Study. European Community Concerted Action on the Epidemiology of Parkinson's Disease. *J. Neurol. Neurosurg. Psychiatry* **62,** 10–15.

2. de Rijk, M. C., Launer, L. J., Berger, K., Breteler, M. M., Dartigues, J. F., Baldereschi, M., et al. (2000) Prevalence of Parkinson's Disease in Europe: a collaborative study of population-based cohorts. Neurologic Diseases in the Elderly Research Group. *Neurology* **54,** S21–S23.
3. Lang, A. E. and Lozano, A. M. (1998) Parkinson's disease. first of two parts. *N. Engl. J. Med.* **339,** 1044–1053.
4. Baba, M., Nakajo, S., Tu, P. H., Tomita, T., Nakaya, K., Lee, V. M., et al. (1998) Aggregation of alpha-synuclein in Lewy bodies of sporadic Parkinson's disease and dementia with Lewy bodies. *Am. J. Pathol.* **152,** 879–884.
5. Irizarry, M. C., Growdon, W., Gomez-Isla, T., Newell, K., George, J. M., Clayton, D. F., and Hyman, B. T. (1998) Nigral and cortical Lewy bodies and dystrophic nigral neurites in Parkinson's disease and cortical Lewy body disease contain alpha- synuclein immunoreactivity. *J. Neuropathol. Exp. Neurol.* **57,** 334–337.
6. Spillantini, M. G., Schmidt, M. L., Lee, V. M., Trojanowski, J. Q., Jakes, R., and Goedert, M. (1997) Alpha-synuclein in Lewy bodies. *Nature* **388,** 839–840.
7. Spillantini, M. G., Crowther, R. A., Jakes, R., Hasegawa, M., and Goedert, M. (1998) Alpha-synuclein in filamentous inclusions of Lewy bodies from Parkinson's disease and dementia with lewy bodies. *Proc. Natl. Acad. Sci. USA* **95,** 6469–6473.
8. Jenner, P. and Olanow, C. W. (1998) Understanding cell death in Parkinson's disease. *Ann. Neurol.* **44,** S72–S84.
9. Tatton, N. A. (2000) Increased caspase 3 and Bax immunoreactivity accompany nuclear GAPDH translocation and neuronal apoptosis in Parkinson's disease. *Exp. Neurol.* **166,** 29–43.
10. Schlossmacher, M. G., Frosch, M. P., Gai, W. P., Medina, M., Sharma, N., Forno, L., et al. (2002) Parkin localizes to the Lewy bodies of Parkinson disease and dementia with Lewy bodies. *Am. J. Pathol.* **160,** 1655–1667.
11. Jensen, P. H., Islam, K.; Kenney, J., Nielsen, M. S., Power, J., and Gai, W. P. (2000) Microtubule-associated protein 1B is a component of cortical lewy bodies and binds alpha-synuclein filaments. *J. Biol. Chem.* **275,** 21,500–21,507.
12. Narhi, L., Wood, S. J., Steavenson, S., Jiang, Y., Wu, G. M., Anafi, D., et al. (1999) Both familial Parkinson's disease mutations accelerate alpha-synuclein aggregation. *J. Biol. Chem.* **274,** 9843–9846.
13. Galvin, J. E., Lee, V. M., Schmidt, M. L., Tu, P. H., Iwatsubo, T., and Trojanowski, J. Q. (1999) Pathobiology of the Lewy body. *Adv. Neurol.* **80,** 313–324.
14. Kitada, T., Asakawa, S., Hattori, N., Matsumine, H., Yamamura, Y., Minoshima, S., et al. (1998) Mutations in the Parkin gene cause autosomal recessive juvenile parkinsonism. *Nature* **392,** 605–608.
15. Leroy, E., Boyer, R., Auburger, G., Leube, B., Ulm, G., Mezey, E., et al. (1998) The ubiquitin pathway in Parkinson's disease. *Nature* **395,** 451–452.
16. Hershko, A. and Ciechanover, A. (1998) The ubiquitin system. *Annu. Rev. Biochem.* **67,** 425–479.
17. Mori, K. (2000) Tripartite management of unfolded proteins in the endoplasmic reticulum. *Cell* **101,** 451–454.

18. Imai, Y., Soda, M., and Takahashi, R. (2000) Parkin suppresses unfolded protein stress-induced cell death through its E3 ubiquitin-protein ligase activity. *J. Biol. Chem.* **275,** 35,661–35,664.
19. Imai, Y., Soda, M., Inoue, H., Hattori, N., Mizuno, Y., and Takahashi, R. (2001) An unfolded putative transmembrane polypeptide, which can lead to endoplasmic reticulum stress, is a substrate of Parkin. *Cell* **105,** 891–902.
20. Imai, Y., Soda, M., Hatakeyama, S., Akagi, T., Hashikawa, T., Nakayama, K. I., and Takahashi, R. (2002) CHIP is associated with Parkin, a gene responsible for familial Parkinson's disease, and enhances its ubiquitin ligase activity. *Mol. Cell* **10,** 55–67.
21. Ledesma, M. D., Galvan C., Hellias B., Dotti C., and Jensen, P. H. (2002) Astrocytic but not neuronal increased expression and redistribution of parkin during unfolded protein stress. *J. Neurochem.* **83,** 1431–1440.
22. Conway, K. A., Harper, J. D., and Lansbury, P. T. (1998) Accelerated in vitro fibril formation by a mutant alpha-synuclein linked to early-onset Parkinson disease. *Nat. Med.* **4,** 1318–1320.
23. Ueda, K., Fukushima, H., Masliah, E., Xia, Y., Iwai, A., Yoshimoto, M.; et al. (1993) Molecular cloning of CDNA encoding an unrecognized component of amyloid in Alzheimer disease. *Proc. Natl. Acad. Sci. USA* **90,** 11,282–11,286.
24. Jensen, P. H., Nielsen, M. S., Jakes, R., Dotti, C. G., and Goedert, M. (1998) Binding of alpha-synuclein to brain vesicles is abolished by familial Parkinson's disease mutation. *J. Biol. Chem.* **273,** 26,292–26,294.
25. Abeliovich, A., Schmitz, Y., Farinas, I., Choi-Lundberg, D., Ho, W. H., Castillo, P. E., et al. (2000) Mice lacking alpha-synuclein display functional deficits in the nigrostriatal dopamine system. *Neuron* **25,** 239–252.
26. Murphy, D. D., Rueter, S. M., Trojanowski, J. Q., and Lee, V. M. (2000) Synucleins are developmentally expressed, and alpha-synuclein regulates the size of the presynaptic vesicular pool in primary hippocampal neurons. *J. Neurosci.* **20,** 3214–3220.
27. Jakes, R., Spillantini, M. G., and Goedert, M. (1994) Identification of two distinct synucleins from human brain. *FEBS Lett.* **345,** 27–32.
28. Bennett, M. C., Bishop, J. F., Leng, Y., Chock, P. B., Chase, T. N., and Mouradian, M. M. (1999) Degradation of alpha-synuclein by proteasome. *J. Biol. Chem.* **274,** 33,855–33,858.
29. Okochi, M., Walter, J., Koyama, A., Nakajo, S., Baba, M., Iwatsubo, T., et al. (2000) Constitutive phosphorylation of the Parkinson's disease associated alpha-synuclein. *J. Biol. Chem.* **275,** 390–397.
30. Tofaris, G. K., Layfield, R., and Spillantini, M. G. (2001) Alpha-synuclein metabolism and aggregation is linked to ubiquitin-independent degradation by the proteasome. *FEBS Lett.* **509,** 22–26.
31. Shimura, H., Schlossmacher, M. G., Hattori, N., Frosch, M. P., Trockenbacher, A., Schneider, R., et al. (2001) Ubiquitination of a new form of alpha-synuclein by Parkin from human brain: implications for Parkinson's disease. *Science* **293,** 263–269.

32. Polymeropoulos, M. H., Lavedan, C., Leroy, E., Ide, S. E., Dehejia, A., Dutra, A., et al. (1997) Mutation in the alpha-synuclein gene identified in families with Parkinson's disease. *Science* **276,** 2045–2047.
33. Kruger, R., Kuhn, W., Muller, T., Woitalla, D., Graeber, M., Kosel, S., et al. (1998) Ala30Pro mutation in the gene encoding alpha-synuclein in Parkinson's disease. *Nat. Genet.* **18,** 106–108.
34. Kahle, P. J., Neumann, M., Ozmen, L., Muller, V., Odoy, S., Okamoto, N., et al. (2001) Selective insolubility of alpha-synuclein in human Lewy body diseases is recapitulated in a transgenic mouse model. *Am. J. Pathol.* **159,** 2215–2225.
35. Feany, M. B. and Bender, W. W. (2000) A Drosophila model of Parkinson's disease. *Nature* **404,** 394–398.
36. Li, J., Uversky, V. N., and Fink, A. L. (2001) Effect of familial parkinson's disease point mutations A30P and A53T on the structural properties, aggregation, and fibrillation of human alpha-synuclein. *Biochemistry* **40,** 11,604–11,613.
37. Lashuel, H., Petre, B., Wall, J., Simon, M., Nowak, R., Walz, T., and Lansbury, P. (2002) Alpha-synuclein, especially the Parkinson's disease-associated mutants, forms pore-like annular and tubular protofibrils. *J. Mol. Biol.* **322,** 1089–1102.
38. Fujiwara, H., Hasegawa, M., Dohmae, N., Kawashima, A., Masliah, E., Goldberg, M. S., et al. (2002) Alpha-synuclein is phosphorylated in synucleinopathy lesions. *Nat. Cell Biol.* **4,** 160–164.
39. Giasson, B. I., Duda, J. E., Murray, I. V., Chen, Q., Souza, J. M., Hurtig, H. I., et al. (2000) Oxidative damage linked to neurodegeneration by selective alpha-synuclein nitration in synucleinopathy lesions. *Science* **290,** 985–989.
40. Auluck, P. K., Chan, H. Y., Trojanowski, J. Q., Lee, V. M., and Bonini, N. M. (2002) Chaperone suppression of alpha-synuclein toxicity in a Drosophila model for Parkinson's disease. *Science* **295,** 865–868.
41. Zhang, Y., Gao, J., Chung, K. K., Huang, H., Dawson, V. L., and Dawson, T. M. (2000) Parkin functions as an E2-dependent ubiquitin-protein ligase and promotes the degradation of the syaptic vesicle-associated protein, CDCrel-1. *Proc. Natl. Acad. Sci. USA* **97,** 13,354–13,359.
42. Shimura, H., Hattori, N., Kubo, S., Mizuno, Y., Asakawa, S., Minoshima, S., et al. (2000) Familial Parkinson disease gene product, Parkin, Is a ubiquitin-protein ligase. *Nat. Genet.* **25,** 302–305.
43. Chung, K. K., Zhang, Y., Lim, K. L., Tanaka, Y., Huang, H., Gao, J., et al. (2001) Parkin ubiquitinates the alpha-synuclein-interacting protein, synphilin- 1: implications for Lewy-body formation in Parkinson disease. *Nat. Med.* **7,** 1144–1150.
44. Lücking C., Düur A., Bonifati V., Vaughan J., de Michele G., Gasser T., et al. (2000) Association between early-onset Parkinson's disease and mutations in the Parkin gene. *N. Engl. J. Med.* **342,** 1560–1567.
45. Zarate-Lagunes, M., Gu, W. J., Blanchard, V., Francois, C., Muriel, M. P., Mouatt-Prigent, A., et al. (2001) Parkin immunoreactivity in the brain of human and non-human primates: an immunohistochemical analysis in normal conditions and in Parkinsonian syndromes. *J. Comp. Neurol.* **432,** 184–196.

46. Shimura, H., Hattori, N., Kubo, S., Yoshikawa, M., Kitada, T., Matsumine, H., et al. (1999) Immunohistochemical and subcellular localization of Parkin protein: absence of protein in autosomal recessive juvenile parkinsonism patients. *Ann. Neurol.* **45,** 668–672.
47. Kahns, S., Lykkebo, S., Jakobsen, L. D., Nielsen, M. S., and Jensen, P. H. (2002) Caspase-mediated Parkin cleavage in apoptotic cell death. *J. Biol. Chem.* **277,** 15,303–15,308.
48. Wakabayashi, K., Engelender, S., Yoshimoto, M., Tsuji, S., Ross, C. A., and Takahashi, H. (2000) Synphilin-1 is present in Lewy bodies in Parkinson's disease. *Ann. Neurol.* **47,** 521–523.
49. Mori, H., Kondo, T., Yokochi, M., Matsumine, H., Nakagawa-Hattori, Y., Miyake, T., et al. (1998) Pathologic and biochemical studies of juvenile parkinsonism linked to chromosome 6q. *Neurology* **51,** 890–892.
50 Hayashi, S., Wakabayashi, K., Ishikawa, A., Nagai, H., Saito, M., Maruyama, M., et al. (2000) An autopsy case of autosomal-recessive juvenile parkinsonism with a homozygous exon 4 deletion in the parkin gene. *Mov. Disord.* **15,** 884–888.
51. Takahashi, H., Ohama, E., Suzuki, S., Horikawa, Y., Ishikawa, A., Morita, T., et al. (1994) Familial juvenile parkinsonism: clinical and pathologic study in a family. *Neurology* **44,** 437–441.
52. van de Warrenburg, B. P., Lammens, M., Lucking, C. B., Denefle, P., Wesseling, P., Booij, J., et al. (2001) Clinical and pathologic abnormalities in a family with parkinsonism and parkin gene mutations. *Neurology* **56,** 555–557.
53. Farrer, M., Chan, P., Chen, R., Tan, L., Lincoln, S., Hernandez, D., et al. (2001) Lewy bodies and parkinsonism in families with parkin mutations. *Ann. Neurol.* **50,** 293–300.

6

Aberrant Protein Folding as the Molecular Basis of Cancer

Melissa D. Scott and Judith Frydman

1. Introduction

Under normal growth conditions, tumor-suppressor proteins and oncogenes play key roles in the tight regulation of cell division ***(1)***. Tumorigenesis often arises from mutations that interfere with the appropriate function of these regulatory proteins. Tumor-causing mutations may result in either an alteration of the catalytic activity of the protein, loss of a binding site for a partner or effector protein, or an alteration of the native folded conformation. There are a growing number of examples in which protein misfolding is associated with tumorigenesis. In some cases, misfolded tumor supressors are simply inactive and lead to cancer as a result of a loss-of-function phenotype, as in the case of tumor-suppressor proteins VHL and NF2. Alternatively, the mutated proteins may adopt an aberrant conformation that is regulated differently than the wild-type protein. Such mutations may lead to a dominant-negative inactivation of the wild-type tumor suppressor, as in the case of p53 and WT1, or to constitutive activation of an oncogenic protein, as in the case of the Src family kinases. Here we review a number of examples that illustrate how alterations in the folding of tumor-suppressor proteins or oncogenes lead to carcinogenesis. Most of the cases also involve altered interactions of these proteins with the components of the cellular folding machinery. Eukaryotic molecular chaperones such as TRiC/CCT, Hsp70, and Hsp90 play important roles in both assisting protein folding and in quality-control processes that recognize and target misfolded proteins for degradation by the Ubiquitin-26S Proteasome pathway ***(2,3)***.

From: *Methods in Molecular Biology, vol. 232: Protein Misfolding and Disease: Principles and Protocols*
Edited by: P. Bross and N. Gregersen © Humana Press Inc., Totowa, NJ

2. p53 Tumor Suppressor Protein

Often referred to as "guardian of the genome," p53 plays a role in cell-cycle arrest, DNA repair, and apoptosis (reviewed in **ref. *4***). Under normal conditions, p53 turnover in the cell is high. MDM2 Ubiquitin Ligase ubiquitinates p53, which targets it to the Ubiquitin-26S Proteasome system for degradation ***(5)***. In response to DNA damage, p53 is stabilized and transcriptionally upregulates p21, a cyclin-dependent kinase inhibitor ***(4)***. Elevated levels of p21 arrest cells in G_1 phase, allowing DNA repair to occur. If the DNA damage is not repaired, p53 activates genes involved in the cellular apoptosis, such as Bax ***(6)***.

Stabilization and overexpression of mutant p53 tumor-suppressor protein is observed in 50% of human tumors ***(4)***. Mutations in p53 result in sporadic tumors of the bladder, breast, colorectal, esophageal, liver, lung, ovarian carcinomas, brain tumors, sarcomas, lymphomas, and leukemias ***(4)***. In addition, Li Fraumeni patients inherit a mutated p53 allele and succumb to tumors early in life ***(7)***.

Active p53 is assembled into a homotetramer ***(8)***. The 393 amino acid p53 monomer contains N-terminal, central, and C-terminal domains, each with different functions ***(9)***. The N-terminal domain is involved in p53's transcriptional transactivation activity. The central DNA-binding core domain is comprised of amino acids 100–300 and contains nearly all of the inactivating p53 mutations. The C-terminal region contains the nuclear localization signal, p53 oligomerization domain, and regulatory phosphorylation sites. The structures of individual domains of p53 have been solved, yielding insight into the mechanism of tumorigenic mutants ***(10–13)***.

Folding defective p53 mutants can be classified into two groups ***(14)***. The first class includes temperature-sensitive conformational mutants that can display wild-type conformation and function but are inactivated at higher temperatures. Examples of this class of mutants include A135V and V143A, which disrupt the hydrophobic core of the central domain. The second type of folding mutant is constitutively inactive and is unable to adopt the wild-type conformation. The best characterized example of this type of mutation is R175H, which also disrupts the central core domain. These folding defective variants of p53 are not merely loss of function mutants, but appear to alter wild-type p53 function by a dominant-negative mechanism.

In contrast to wild-type p53, both classes of p53 conformational mutants have prolonged half-lives regardless of the presence of DNA damage ***(15,16)***. The stabilization of mutant p53 is thought to be mediated by binding to molecular chaperones ***(15–17)***. It was recently reported that Hsp90 forms a stable tertiary complex with the MDM2 Ubiquitin Ligase and the R175H p53 conformational mutant ***(18)***. This interaction increases the half-life of both R175H p53 and MDM2. Upon disruption of the tertiary complex by the Hsp90-

specific inhibitor geldanamycin, both R175H p53 and MDM2 are degraded rapidly. In addition to the role for Hsp90, Hsp70 binding may also contribute to mutant p53 stabilization ***(14)***. Unlike wild-type p53, both types of p53 conformational mutants bind Hsp70 ***(17,19,20)***. Although p53 contains Hsp70 binding sites in all three domains of p53, the sites with the highest affinity are found in the central domain ***(9)***. Interestingly, this is the same domain that harbors most of the tumorigenic p53 mutations ***(21)***. Thus, specific recognition of mutant p53 by Hsp70 may arise from increased exposure of the hydrophobic core of the misfolded protein ***(9)***.

Stabilization of mutant p53 in cells results in a dominant-negative inactivation of the wild-type copy of p53 ***(22,23)***. Mutant p53 forms mixed tetramers with wild-type p53 that are inactive, resulting in loss of tumor-suppressor function. When p53 function is lost, DNA damage can go unrepaired and cells continue multiplying unchecked ***(4)***. The results are catastrophic because loss of p53 activity can lead to the accumulation of mutations in the genome as a result of the improper repair of DNA lesions.

The key role of molecular chaperones Hsp90 and Hsp70 in the development of mutant p53-associated carcinomas affords a new potential target for pharmacological intervention, because the ansamycin family of Hsp90 inhibitors, which include geldanamycin, can restore rapid degradation of mutant p53 ***(15,18,24)***. Although treatment with geldanamycin cannot restore the transcriptional activity of mutant p53 ***(16)***, it may alleviate the dominant-negative effect of mutant p53, thereby releasing some of the endogenous wild-type p53 ***(25)***.

3. Wilms' Tumor

Wilms' tumor is a pediatric cancer of the kidney ***(26,27)***. It makes up about 7.5% of all childhood cancers, affecting 1 in 10,000 children, and can be inherited or sporadic. A portion of Wilms' tumor cases are caused by mutation of the *WT1* gene.

The WT1 protein is expressed primarily in glomerular precursors of the developing kidney ***(26)***. WT1 is a zinc-finger transcription factor but may also function in mRNA processing. Although there are numerous splice variants of this protein, WT1 is primarily found as two differentially spliced isoforms ***(28)***. The WT1(+KTS) variant is thought to be involved in post-transcriptional mRNA processing and localizes to the nucleus in a punctate pattern ***(29)***. The (–KTS) variant is identical to the (+KTS) variant but with three amino acids (K, T, and S) spliced out. This variant is thought to function as a transcription factor and localizes to the nucleus with a diffuse pattern ***(29)***.

It has recently been determined that both the (–KTS) and (+KTS) WT1 splicing variants bind to Hsp70 and co-localize with the chaperone in vivo ***(30)***. The involvement of Hsp70 in WT1 function has been explored through the use of

chimeric WT1 constructs ***(30)***. In these constructs, the Hsp70 binding sequence of WT1 was replaced with the Hsp70 binding sequence from a Hsp70 co-chaperone, DnaJ. The chimeric protein was competent to bind Hsp70. Other chimeras were constructed that did not bind Hsp70, either owing to point mutation or deletion of the transplanted Hsp70 binding domain. The chimeric protein that was competent to bind Hsp70 functioned identically to wild-type WT1 in an inhibition of colony-formation assay. Both also functioned equally to upregulate the expression of p21. In contrast, the chimeric proteins that could not bind Hsp70 failed to inhibit colony formation and did not upregulate expression of p21. These experiments suggest that Hsp70 may be required for WT1 function. Perhaps the requirement for the molecular chaperone Hsp70 in WT1 function is to maintain the protein in an active, folded conformation.

A tumorigenic WT1 inactivating mutation, WT/AR, appears to act through a dominant-negative gain-of-function mechanism ***(31)***. WT/AR is improperly spliced, resulting in a deletion of the third WT1 zinc-finger domain. The dominant-negative mechanism by which WT/AR is involved in tumorigenesis has not yet been determined. However, it seems as though the defect involves an aberrant conformation displayed by the WT/AR mutant, because this tumorigenic mutant can cooperate with the adenoviral E1A gene in an assay measuring the transformation of rat kidney cells. It is thought that mutant WT1 protein displays a unique conformation, because wild-type WT1 cannot cooperate with E1A. Although the molecular mechanisms by which Wilms' tumors develop are not clearly defined, these data indicate that proper WT1 folding and binding to the molecular chaperone Hsp70 are key to normal WT1 function.

4. VHL Tumor Suppressor Protein

Inactivating mutants of the von Hippel Lindau tumor-suppressor protein (VHL) lead to 80% of sporadic clear cell renal carcinomas, as well as pheochromocytomas, and vascular tumors of the central nervous system (CNS) and retina ***(32)***. VHL is a 213 amino acid tumor-suppressor protein that assembles with elongins B and C to form the VBC complex ***(33)***. This VBC complex further assembles with Cul2 and Rbx1 into an Ubiquitin Ligase that targets proteins involved in oxygen sensing for degradation ***(34,35)***. The best characterized substrate of the VHL Ubiquitin Ligase is the Hypoxia Inducible Factor HIF-1α subunit of the HIF-1 transcription factor ***(35)***. The HIF-1 transcription factor binds to hypoxia response elements to upregulate hypoxia-inducible genes such as vascular endothelial growth factor and glucose transporter 1. Under normoxic conditions, HIF-1α is ubiquitinated by the VHL Ubiquitin Ligase and degraded by the 26S Proteasome ***(36)***. Under hypoxic conditions, HIF1-α binds to HIF-1β to form the HIF-1 transcription factor ***(32)***. Without downregulation by the VHL Ubiquitin Ligase, HIF-1 is constitutively active and upregulates genes involved in vascularization of solid tumors.

Many tumorigenic mutants of VHL cannot form the correctly folded VBC complex ***(37)***. Some of these mutants cannot assemble in the appropriate complex because the binding site for elongin C has been disrupted. This is the case for mutations in the 157–166 amino acid helix that directly contacts elongin C, such as L158P ***(38,39)***. However, some of the VHL mutants that cannot form the VBC complex harbor no mutations in the elongin C binding region.

Molecular chaperones are also important for the formation of the VBC complex. In the absence of the eukaryotic chaperonin TRiC, wild-type VHL fails to assemble into the VBC complex ***(40)***. A 55-amino acid region of VHL was found to be both necessary and sufficient to mediate VHL binding to TRiC. This region harbors many naturally occurring tumor-causing point mutations, several of which appear to abolish binding to TRiC (Feldman, D. E. and Frydman, J., unpublished observation) manuscript in preparation. These same mutants cannot form the VBC complex, although the elongin C binding region remains intact. Because it appears that without the assistance of TRiC, VHL cannot assemble into the VBC complex, analysis of the mutations in the TRiC binding region of VHL may clarify whether decreasing the ability to bind to a chaperone results in loss of VHL function leading to development of tumors associated with VHL syndrome.

5. NF2

Neurofibromatosis type II (NF2) is an autosomal dominant disorder affecting one in every 30,000–42,000 births ***(41)***. NF2 is characterized by multiple tumors on the cranial and spinal nerves and by other lesions of the brain and spinal cord ***(42)***. The *nf2* gene encodes a tumor-suppressor protein known as Merlin, or Schwannomin. Merlin is a 65 kDa protein thought to act as a bridge between membrane-associated proteins and the actin cytoskeleton ***(41)***.

Merlin misfolding results in a loss-of-function phenotype that leads to the development of tumors concomitant with the progression of the NF2 disorder ***(43)***. Tumorigenic missense point mutations in the N-terminus of Merlin (L64P, L64R, and E106G) disrupt the folded conformation of Merlin ***(43)***. These mutants display a conformation that cannot dimerize but does not disrupt actin cytoskeleton-mediated events ***(43)***. In a separate study, a properly folded N-terminus was also shown to be critical for Merlin localization and function ***(44)***.

6. Src Kinase

Src family nonreceptor tyrosine kinases are a part of a larger tyrosine kinase family of proteins that participate in signal transduction ***(45,46)***. Unlike tumor suppressor proteins, Src family kinases are effectors of cell proliferation and are activated during cancer. Src family kinase members include: c-Src, Fgr, Fyn, Yes1, Blk, Hck, Lck, Lyn, Yrk, and Frk subfamily proteins. Overexpression of

c-Src is common in many tumor types, including pancreatic, breast, colon, lung, neural, ovarian, esophageal, gastric, melanoma, and Kaposi's sarcoma *(47)*. This overexpression is usually accompanied by an increase in specific activity of the Src kinase.

Proper folding by molecular chaperones, especially Hsp90, is an important part of the regulation of Src family kinases. Pulse-chase experiments indicate that Hsp90 is required for the maturation, but not the maintenance, of some wild-type Src family kinases such as Lck, Lyn, Hck, and c-Src *(48–51)*. In contrast, hyperactive mutants of these kinases such as Y505F Lck, ΔSH2 Lck, and Q499F Hck require Hsp90 for both maturation and maintenance of the mature structure. In addition to its role in folding, Hsp90 also appears to protect constitutively activated Src family kinase proteins from degradation by the Ubiquitin-Proteasome system *(48–51)*. In doing so, Hsp90 allows the accumulation of mutant activated Src family kinases associated with tumor development. Indeed, disruption of the interaction between Hsp90 and hyperactive mutant kinases by addition of geldanamycin leads to degradation of the mutant kinases. Thus, Hsp90 appears to have a role in both the proper function of wild-type Src family kinases and the stabilization of mutant kinases that leads to disease. As observed for p53, targeting the Hsp90-substrate interaction with the ansamycin family of Hsp90 inhibitors promotes the degradation of the mutant protein and thus may yield a potential target for pharmacological intervention in cancer patients with tumors containing stabilized, hyperactive Src family kinases *(52,53)*.

7. Conclusions

The aforementioned examples illustrate how defects in the folding of tumor-suppressor proteins or oncogenes can lead to cancer through multiple mechanisms. Mutations that cause misfolding may result in either dominant-negative gain of function, as seen for p53 and WT1; an aberrant conformation of a tumor-suppressor protein, as in the case of VHL and NF2; or constitutive activation of an oncogene, as observed for Src family kinases. Interestingly, it is becoming clear that the tumor-causing phenotype of many of these misfolding mutants involves altered interactions with the chaperone machinery. As the folding pathways of these tumor-suppressor proteins are elucidated, perhaps new mechanisms to correct the defects of misfolded variants will be uncovered. The possibility of targeting protein folding and chaperone-substrate interactions in cancer therapy is highlighted by the Phase I clinical trial currently underway to study the effect of analogs of the Hsp90 inhibitor geldanamycin in breast cancer *(54)*. Analogs of geldanamycin have already been shown to induce differentiation in human breast cancer cell lines positive for the growth factor receptor HER2 *(55)*, suggesting that Hsp90 may also

participate in the regulation of additional oncogenic proteins. Further characterization of the involvement of chaperones and protein folding in carcinogenesis will open up new avenues of investigation into novel cancer therapies.

Acknowledgments

Work in the Frydman lab is supported by the NIH and an award from the Keck foundation. M.D. Scott is supported by grant GM08294 from the NIH. We would like to thank A. Ballew, A. Dunn, A. McClellan, C. Speiss, and T. Tan for helpful discussion and critical reading of the manuscript.

References

1. Cooper, G. M. (1995) *Oncogenes*, 2nd ed. Jones and Bartlett Publishers, London.
2. Frydman, J. (2001) Folding of newly translated proteins in vivo: the role of molecular chaperones. *Annu. Rev. Biochem.* **70,** 603–647.
3. Glickman, M. H., and Ciechanover, A. (2002) The ubiquitin-proteasome proteolytic pathway: destruction for the sake of construction. *Physiol. Rev.* **82,** 373–428.
4. Vogelstein, B., Lane, D., and Levine, A. J. (2000) Surfing the p53 network. *Nature* **408,** 307–310.
5. Kubbutat, M. H., Jones, S. N., and Vousden, K. H. (1997) Regulation of p53 stability by Mdm2. *Nature* **387,** 299–303.
6. Miyashita, T., Krajewski, S., Krajewska, M., Wang, H. G., Lin, H. K., Liebermann, D. A., et al. (1994) Tumor suppressor p53 is a regulatory of bcl-2 and bax gene expression in vitro and in vivo. *Oncogene* **9,** 1799–1805.
7. Evans, S. C. and Lozano, G. (1997) The Li-Fraumeni syndrome: an inherited susceptibility to cancer. *Mol. Med. Today* **3,** 390–395.
8. Friedman, P. N., Chen, X., Bargonetti, J., and Prives, C. (1993) The p53 protein is an unusually shaped tetramer that binds directly to DNA. *Proc. Natl. Acad. Sci. USA* **90,** 3319–3323.
9. Fourie, A. M., Hupp, T. R., Lane, D. P., Sang, B. C., Barbosa, M. S., Sambrook, J. F., and Gething, M. J. (1997) HSP70 binding sites in the tumor suppressor protein p53. *J. Biol. Chem.* **272,** 19,471–19,479.
10. Cho, Y., Gorina, S., Jeffrey, P. D., and Pavletich, N. P. (1994) Crystal structure of a p53 tumor suppressor-DNA complex: understanding tumorigenic mutations. *Science* **265,** 346–355.
11. Jeffrey, P. D., Gorina, S., and Pavletich, N. P. (1995) Crystal structure of the tetramerization domain of the p53 tumor suppressor at 1.7 angstroms. *Science* **267,** 1498–1502.
12. Gorina, S. and Pavletich, N. P. (1996) Structure of the p53 tumor suppressor bound to the ankyrin and SH3 domains of 53BP2. *Science* **274,** 1001–1005.
13. Kussie, P. H., Gorina, S., Marechal, V., Elenbaas, B., Moreau, J., Levine, A. J., and Pavletich, N. P. (1996) Structure of the MDM2 oncoprotein bound to the p53 tumor suppressor transactivation domain. *Science* **274,** 948–953.

14. Zylicz, M., King, F. W., and Wawrzynow, A. (2001) Hsp70 interactions with the p53 tumour suppressor protein. *EMBO J.* **20,** 4634–4638.
15. Whitesell, L., Sutphin, P., An, W. G., Schulte, T., Blagosklonny, M. V., and Neckers, L. (1997) Geldanamycin-stimulated destabilization of mutated p53 is mediated by the proteasome in vivo. *Oncogene* **14,** 2809–2816.
16. Whitesell, L., Sutphin, P. D., Pulcini, E. J., Martinez, J. D., and Cook, P. H. (1998) The physical association of multiple molecular chaperone proteins with mutant p53 is altered by geldanamycin, an hsp90-binding agent. *Mol. Cell. Biol.* **18,** 1517–1524.
17. King, F. W., Wawrzynow, A., Hohfeld, J., and Zylicz, M. (2001) Co-chaperones Bag-1, Hop and Hsp40 regulate Hsc70 and Hsp90 interactions with wild-type or mutant p53. *EMBO J.* **20,** 6297–6305.
18. Peng, Y., Chen, L., Li, C., Lu, W., and Chen, J. (2001) Inhibition of MDM2 by hsp90 contributes to mutant p53 stabilization. *J. Biol. Chem.* **276,** 40,583–40,590.
19. Hainaut, P. and Milner, J. (1992) Interaction of heat-shock protein 70 with p53 translated in vitro: evidence for interaction with dimeric p53 and for a role in the regulation of p53 conformation. *EMBO J.* **11,** 3513–3520.
20. Akakura, S., Yoshida, M., Yoneda, Y., and Horinouchi, S. (2001) A role for Hsc70 in regulating nucleocytoplasmic transport of a temperature-sensitive p53 (p53Val-135). *J. Biol. Chem.* **276,** 14,649–14,657.
21. Hollstein, M., Sidransky, D., Vogelstein, B., and Harris, C. C. (1991) p53 mutations in human cancers. *Science* **253,** 49–53.
22. Milner, J., Medcalf, E. A., and Cook, A. C. (1991) Tumor suppressor p53: analysis of wild-type and mutant p53 complexes. *Mol. Cell. Biol.* **11,** 12–19.
23. Milner, J. and Medcalf, E. A. (1991) Cotranslation of activated mutant p53 with wild type drives the wild-type p53 protein into the mutant conformation. *Cell* **65,** 765–774.
24. Blagosklonny, M. V., Toretsky, J., Bohen, S., and Neckers, L. (1996) Mutant conformation of p53 translated in vitro or in vivo requires functional HSP90. *Proc. Natl. Acad. Sci. USA* **93,** 8379–8383.
25. Blagosklonny, M. V. (2002) p53: an ubiquitous target of anticancer drugs. *Int. J. Cancer* **98,** 161–166.
26. Scharnhorst, V., van der Eb, A. J., and Jochemsen, A. G. (2001) WT1 proteins: functions in growth and differentiation. *Gene* **273,** 141–161.
27. Dome, J. S., and Coppes, M. J. (2002) Recent advances in Wilms tumor genetics. *Curr. Opin. Pediatr.* **14,** 5–11.
28. Lee, S. B. and Haber, D. A. (2001) Wilms tumor and the WT1 gene. *Exp. Cell. Res.* **264,** 74–99.
29. Larsson, S. H., Charlieu, J. P., Miyagawa, K., Engelkamp, D., Rassoulzadegan, M., Ross, A., et al. (1995) Subnuclear localization of WT1 in splicing or transcription factor domains is regulated by alternative splicing. *Cell* **81,** 391–401.
30. Maheswaran, S., Englert, C., Zheng, G., Lee, S. B., Wong, J., Harkin, D. P., et al. (1998) Inhibition of cellular proliferation by the Wilms tumor suppressor WT1 requires association with the inducible chaperone Hsp70. *Genes Dev.* **12,** 1108–1120.

31. Haber, D. A., Timmers, H. T., Pelletier, J., Sharp, P. A., and Housman, D. E. (1992) A dominant mutation in the Wilms tumor gene WT1 cooperates with the viral oncogene E1A in transformation of primary kidney cells. *Proc. Natl. Acad. Sci. USA* **89,** 6010–6014.
32. Ivan, M. and Kaelin, W. G., Jr. (2001) The von Hippel-Lindau tumor suppressor protein. *Curr. Opin. Genet. Dev.* **11,** 27–34.
33. Duan, D. R., Pause, A., Burgess, W. H., Aso, T., Chen, D. Y., Garrett, K. P., et al. (1995) Inhibition of transcription elongation by the VHL tumor suppressor protein. *Science* **269,** 1402–1406.
34. Lonergan, K. M., Iliopoulos, O., Ohh, M., Kamura, T., Conaway, R. C., Conaway, J. W., and Kaelin, W. G., Jr. (1998) Regulation of hypoxia-inducible mRNAs by the von Hippel-Lindau tumor suppressor protein requires binding to complexes containing elongins B/C and Cul2. *Mol. Cell. Biol.* **18,** 732–741.
35. Maxwell, P. H., Wiesener, M. S., Chang, G. W., Clifford, S. C., Vaux, E. C., Cockman, M. E., et al. (1999) The tumour suppressor protein VHL targets hypoxia-inducible factors for oxygen-dependent proteolysis. *Nature* **399,** 271–275.
36. Tanimoto, K., Makino, Y., Pereira, T., and Poellinger, L. (2000) Mechanism of regulation of the hypoxia-inducible factor-1 alpha by the von Hippel-Lindau tumor suppressor protein. *EMBO J.* **19,** 4298–4309.
37. Clifford, S. C., Cockman, M. E., Smallwood, A. C., Mole, D. R., Woodward, E. R., Maxwell, P. H., et al. (2001) Contrasting effects on HIF-1alpha regulation by disease-causing pVHL mutations correlate with patterns of tumourigenesis in von Hippel-Lindau disease. *Hum. Mol. Genet.* **10,** 1029–1038.
38. Kibel, A., Iliopoulos, O., DeCaprio, J. A., and Kaelin, W. G., Jr. (1995) Binding of the von Hippel-Lindau tumor suppressor protein to Elongin B and C. *Science* **269,** 1444–1446.
39. Stebbins, C. E., Kaelin, W. G., Jr., and Pavletich, N. P. (1999) Structure of the VHL-ElonginC-ElonginB complex: implications for VHL tumor suppressor function. *Science* **284,** 455–461.
40. Feldman, D. E., Thulasiraman, V., Ferreyra, R. G., and Frydman, J. (1999) Formation of the VHL-elongin BC tumor suppressor complex is mediated by the chaperonin TRiC/CCT. *Mol. Cell* **4,** 1051–1061.
41. Reed, N. and Gutmann, D. H. (2001) Tumorigenesis in neurofibromatosis: new insights and potential therapies. *Trends Mol. Med.* **7,** 157–162.
42. Bashour, A. M., Meng, J. J., Ip, W., MacCollin, M., and Ratner, N. (2002) The neurofibromatosis type 2 gene product, merlin, reverses the F-actin cytoskeletal defects in primary human Schwannoma cells. *Mol. Cell. Biol.* **22,** 1150–1157.
43. Gutmann, D. H., Hirbe, A. C., and Haipek, C. A. (2001) Functional analysis of neurofibromatosis 2 (NF2) missense mutations. *Hum. Mol. Genet.* **10,** 1519–1529.
44. Brault, E., Gautreau, A., Lamarine, M., Callebaut, I., Thomas, G., and Goutebroze, L. (2001) Normal membrane localization and actin association of the NF2 tumor suppressor protein are dependent on folding of its N-terminal domain. *J. Cell Sci.* **114,** 1901–1912.
45. Thomas, S. M. and Brugge, J. S. (1997) Cellular functions regulated by Src family kinases. *Annu. Rev. Cell. Dev. Biol.* **13,** 513–609.

46. Brown, M. T. and Cooper, J. A. (1996) Regulation, substrates and functions of src. *Biochim. Biophys. Acta* **1287,** 121–149.
47. Irby, R. B. and Yeatman, T. J. (2000) Role of Src expression and activation in human cancer. *Oncogene* **19,** 5636–5642.
48. Hartson, S. D., Barrett, D. J., Burn, P., and Matts, R. L. (1996) Hsp90-mediated folding of the lymphoid cell kinase p56lck. *Biochemistry* **35,** 13,451–13,459.
49. Yorgin, P. D., Hartson, S. D., Fellah, A. M., Scroggins, B. T., Huang, W., Katsanis, E., et al. (2000) Effects of geldanamycin, a heat-shock protein 90-binding agent, on T cell function and T cell nonreceptor protein tyrosine kinases. *J. Immunol.* **164,** 2915–2923.
50. Bijlmakers, M. J. and Marsh, M. (2000) Hsp90 is essential for the synthesis and subsequent membrane association, but not the maintenance, of the Src-kinase p56(lck). *Mol. Biol. Cell* **11,** 1585–1595.
51. Scholz, G. M., Hartson, S. D., Cartledge, K., Volk, L., Matts, R. L., and Dunn, A. R. (2001) The molecular chaperone Hsp90 is required for signal transduction by wild-type Hck and maintenance of its constitutively active counterpart. *Cell Growth Differ.* **12,** 409–417.
52. Smith, D. F., Whitesell, L., and Katsanis, E. (1998) Molecular chaperones: biology and prospects for pharmacological intervention. *Pharmacol. Rev.* **50,** 493–514.
53. Neckers, L. (2002) Hsp90 inhibitors as novel cancer chemotherapeutic agents. *Trends Mol. Med.* **8,** S55–S61.
54. Zheng, F. F., Kuduk, S. D., Chiosis, G., Munster, P. N., Sepp-Lorenzino, L., Danishefsky, S. J., and Rosen, N. (2000) Identification of a geldanamycin dimer that induces the selective degradation of HER-family tyrosine kinases. *Cancer Res.* **60,** 2090–2094.
55. Munster, P. N., Srethapakdi, M., Moasser, M. M., and Rosen, N. (2001) Inhibition of heat shock protein 90 function by ansamycins causes the morphological and functional differentiation of breast cancer cells. *Cancer Res.* **61,** 2945–2952.

7

Yeast as a Model System to Investigate Protein Conformational Diseases

Christina M. Coughlan and Jeffrey L. Brodsky

1. Introduction

The yeast *Saccharomyces cerevisiae* has long served as a model euakaryote by virtue of the plethora of tools with which it can be manipulated genetically. Importantly, genetic dissections of yeast physiology have led serendipitously to significant advances in our understanding of several human diseases, most notably cancer, via the seminal studies performed by Hartwell and colleagues ***(1)*** on the regulation of the cell cycle. More recently, however, the genetic and biochemical tools available in yeast have been co-opted for the purpose of directly examining the molecular basis and to aid in the treatment of several human diseases. First, yeast has served as a "bio-factory" for the over-expression and purification of insulin and granulocyte-macrophage colony-stimulating factor (GM-CSF) and for the production of the antigen for the hepatitis B vaccine. Second, large-scale screening methods have been used to identify novel pharmacological targets produced in yeast or, via the two-hybrid screen, to obtain protein partners of medically-relevant gene-products. Finally, the heterologous expression of proteins in yeast that lead to human disease has been used to uncover physiological responses to these proteins; yeast also encode homologues of several disease-causing proteins. In particular, the expression of specific proteins in yeast that fail to adopt their proper conformations and/or whose conformation lead to a pathological state has helped us to understand how "conformational diseases" ***(2)*** arise, and how eukaryotic cells respond to aberrant polypeptides.

Here, we describe a subset of the diseases that affect humans for which defects in protein conformation play a role in the etiology of the malady and for

From: *Methods in Molecular Biology, vol. 232: Protein Misfolding and Disease: Principles and Protocols*
Edited by: P. Bross and N. Gregersen © Humana Press Inc., Totowa, NJ

which studies in *S. cerevisiae* have helped us to understand the genesis or progression of the disease. Owing to space constraints, more detailed backgrounds than we present on each disease can be obtained elsewhere in this volume.

2. Cystic Fibrosis

The most common lethal, inherited disease in Caucasians in North America and Europe is cystic fibrosis (CF), which is evidenced by airway disease, pancreatic insufficiency, increased chloride in the sweat, and male infertility (*see also* Chapter 3). Although more than 900 unique mutations in the gene encoding the cystic fibrosis transmembrane conductance regulator (CFTR) have been described (http://www.genet.sickkids.on.ca/cftr/), the deletion of a single phenylalanine at position 508 in CFTR (ΔF508) accounts for approx 70% of all mutations.

CFTR is a polytopic membrane protein that functions as a chloride transporter and resides in the plasma membrane of epithelial cells. However, ΔF508 prevents the folding and subsequent transit of the protein to the plasma membrane; it has also been suggested that the ΔF508 variant of CFTR may be less stable, once folded (reviewed in **refs. *3*,*4***). In any event, the mutant protein is exported from the endoplasmic reticulum (ER) and degraded by the cytoplasmic proteasome ***(5*,*6)***. This degradative aspect of ER protein quality control, which we have named ER-Associated Degradation (ERAD; ***[7]***), ensures that potentially toxic misfolded or aberrant secreted proteins are excluded from their ultimate destinations. Interestingly, a significant majority of even wild-type CFTR is degraded by the proteasome ***(8)***, suggesting that it too folds poorly in the ER.

Key mediators of ERAD are molecular chaperones, a family of proteins that recognize mis- or unfolded polypeptide domains and help retain polypeptides in solution by interacting with amino acid arrays exhibiting hydrophobic character (*also see* below). Studies in mammalian cells have determined that several chaperones associate with both wild-type and the ΔF508 variant of CFTR during its biogenesis ***(9–12)***. The chaperones are liberated from the wild-type protein when it achieves its native conformation, but remain associated with immature forms of both mutant and wild-type CFTR until degradation ensues. Because of limits on the ability to modify chaperone activity in mammalian cells, it has been unclear whether these chaperones associate with CFTR because they are helping the protein to fold, or because they catalyze its degradation.

To examine this question, we established a yeast expression system for CFTR because of the availability of a large number of strains defective for the activities of specific chaperones. As anticipated, ER-associated CFTR was degraded by the proteasome in yeast. When CFTR was expressed in yeast containing a rapid-acting thermosensitive allele of a cytosolic Hsp70 chaperone,

we discovered that degradation was attenuated when the mutant, but not the wild-type, strain was shifted to elevated temperatures ***(13)***. These results indicate that Hsp70 facilitates CFTR degradation. Interestingly, CFTR was degraded proficiently in yeast lacking a functional form of calnexin, an ER lumenal chaperone that, like Hsp70, associates with CFTR in mammals ***(9,10)***, suggesting that calnexin aids in CFTR folding, but not in its degradation.

Future uses of the yeast system include the following, which we hope will help us to understand better the biogenesis of CFTR and ultimately yield novel small molecule facilitators of CFTR folding. First, the spectrum of CFTR-interacting proteins can be identified by large-scale expression of CFTR in yeast, immune precipitation, and mass spec analysis. Yeast deleted for the corresponding protein partners of CFTR can then be screened rapidly for their ability to support CFTR degradation, thus uncovering CFTR-interactors that play a role in its maturation. Second, Hsp70-modulating drugs have been identified that can be analyzed in yeast for their effects on CFTR maturation, activity and stability ***(14–16)***. This concept is supported by the observation that changing the levels of Hsp70 chaperones may augment CFTR maturation and that protein-stabilizing osmolytes, also known as "chemical chaperones," improve CFTR folding and trafficking in mammalian cells ***(4,17,18)***. Current efforts are being directed toward expanding the number of such compounds with the goal of establishing large-scale screening regimens.

3. Antitrypsin Deficiency (ATD)

The most common cause of liver disease in juveniles is expression of the aggregation-prone Z variant of α1-antitrypsin (ATZ, also known as A1Pi-Z; reviewed in **ref. *19***; *see also* Chapter 4). Children homozygous for ATZ exhibit antitrypsin deficiency (ATD), present early-onset emphysema, and accumulate misfolded AT in the hepatic ER, which may aggregate and give rise to liver failure. To clear the ER of the misfolded AT, much of the protein is handled by ERAD; that is, it is "retro-translocated" from the ER back to the cytoplasm and degraded by the proteasome ***(20)***. In theory, improving the clearance of AT from the ER would offset the occurrence of liver disease. Thus, as with CFTR, facilitating the folding and/or solubility of ATZ could alleviate several symptoms associated with ATD. As a first step toward this goal, it was found that a fraction of ATZ became secreted from ATZ-expressing cells in the presence, but not in the absence, of chemical chaperones ***(21)***.

Surprisingly, only one ER chaperone has been reported to be associated with ATZ or other mutated forms of AT ***(20,22,23)***. This chaperone, known as calnexin, is a lectin that recognizes trimmed ER glycans on incompletely folded polypeptides, and thus serves as a primary determinant of the ER quality-control machinery. Release from calnexin occurs only if the polypeptide has

folded, or if folding is unlikely, in which case the polypeptide is delivered to the cytoplasm for proteasomal degradation ***(24,25)***. Although the association of additional chaperones and ATZ has been observed (B. Schmid and D. Perlmutter, personal communication), whether the complete spectrum of ATZ-associated factors has been defined and how these chaperones function during ATZ biogenesis is unclear.

To rectify this deficit in our knowledge, an ATZ yeast-expression system was established ***(26)***. As anticipated, the degradation of ER-retained ATZ was mediated by the proteasome ***(27)***. Surprisingly, mutations in the gene encoding the ER lumenal Hsp70, BiP, slowed ATZ degradation ***(28)***, although a direct association between BiP and ATZ had not been reported in mammalian cells. These data suggest either that yeast rely more on BiP than on calnexin to mediate protein quality control and/or that the interaction between ATZ and BiP is transient and thus cannot be detected by traditional biochemical methods. Nevertheless, by screening for ATZ-expressing, mutagenized yeast that harbored increased levels of ATZ at steady-state, several *A*1PiZ *D*egradation *D*efective (*ADD*) mutants were isolated ***(29)***. The cloning of the genes that complement the *add* mutants will undoubtedly improve our understanding of how this disease-causing ERAD substrate is handled by the protein quality-control machinery in the secretory pathway.

4. Prion-Related Disease

Prions are proteinaceous, pathogenic agents that initiate a group of mammalian infectious neurodegenerative diseases, the transmissible spongiform encephalopathies (TSEs). The human TSEs can appear in epidemic form (kuru), a familial form (Gerstmann-Straussler-Scheinker disease), and most commonly, a spontaneous form (Creutzfeld-Jacob disease).

The concept of an infectious protein arose from studies on the scrapie prion, which infects sheep and is extraordinarily resistant to treatments such as heat or formaldehyde-fixation. The benign cellular scrapie protein (PrPc) is a 27- to 30-kDa species that is partially protease-sensitive and that is composed primarily of α-helical secondary structure. In contrast, PrPsc, the infectious form of PrPc, is protease resistant, aggregation-prone, and β-sheet-rich. Importantly, PrPsc has been both conformationally altered and simultaneously has acquired the ability to influence PrPc to adopt the prion conformation. Although, in theory, purified PrPsc should be sufficient to induce the disease in any PrPc-expressing organism, this has not been directly demonstrated in mammals. In addition, it is still not completely clear how a protein shifts between the latent and prion states in the cell, and whether there are specific chaperones for this process.

To begin to address these questions, several research laboratories turned to yeast as a model system to investigate the "protein-only" prion hypothesis and to uncover how the balance between wild-type and conformationally altered forms of prions is mediated in the cell ***(30,31)***. Yeast proved invaluable for these studies as yeast prions only change the metabolic state of the cell and, unlike mammalian prions, do not damage the cell ***(32,33)***. This benefit has permitted the use of both genetic and pharmacological tools to examine prion function in vivo.

Recently, the Weissman laboratory examined the protein-only hypothesis by introducing a purified, bacterially produced yeast prion into *S. cerevisiae* by liposome-mediated transformation ***(34)***. Using biochemical, microscopic, and genetic tools, these investigators determined that the introduction of the *S. cerevisiae* prion, but not a prion from a distantly related species of yeast, was sufficient to induce the prion phenotype in the transformed cells. These data establish that yeast prions are infectious, species-specific agents, and support the protein-only hypothesis.

To examine in vivo what factors may prevent or accelerate conversion from the latent to the prion state, the status of endogenous yeast prions has been examined in a number of wild-type strains and in yeast mutated for specific molecular chaperones. The logic behind these studies was that because chaperones mediate the attainment of protein conformation in the cell, they might catalyze or attenuate the conversion of yeast prions. Indeed, it has been found that chaperones of the Hsp70, Hsp40, and Hsp104 classes all impact the efficiency of propagation or loss ("curing") of prions ***(35–40)***. Hsp70 chaperones bind and hydrolyze ATP concomitant with the association and dissociation of bound polypeptide substrates. The ATPase activity, and thus polypeptide binding affinity of Hsp70s, is augmented by the Hsp40s (also known as J domain-containing chaperones). Hsp104 is a yeast chaperone that has been shown to disaggregate polypeptide inclusions in vivo ***(41)***. Based on these characteristics, it may not be surprising that Hsp70, Hsp40, and Hsp104 chaperones modulate the transmission of the prion phenotype. What is surprising, however, is that not all chaperones affect prion propagation similarly. For example, a yeast Hsp70 (Ssb) facilitates Hsp104-mediated prion curing, whereas overexpression of another yeast Hsp70 (Ssa) hinders Hsp104-mediated curing ***(35)***. These studies underscore the variability of chaperone action in the cell, and point to the complexity with which prions are maintained in vivo. Clearly, there is much more to be learned by using genetic tools to examine prion maintenance. In addition, because some mammalian prions are subjected to protein quality control and degraded via ERAD after interacting with conserved, ER-associated chaperones ***(42)***, yeast may also provide a means to screen for the spectrum of chaperones that mediate prion degradation.

5. Huntington's Disease (HD)

Huntington's Disease (HD) is characterized by a complex and variable set of symptoms that have psychological, motor, and cognitive components, and is one of an increasing number of human neurodegenerative disorders caused by polyglutamine (polyQ) expansions. The hallmark of HD is the proteolytic production of an N terminal fragment of the Huntingtin (Ht) protein, containing the polyQ repeat, which forms aggregates in the nucleus and cytoplasm of affected neurons ***(43)***.

The mutation underlying HD has been identified as a CAG/polyglutamine expansion in the first exon of the Ht-encoding gene. To date, the cellular function of Ht is unclear. The toxicity of Ht in specific neurons correlates with the length of the glutamine expansion, but the mechanism of toxicity is also unknown. PolyQ expansions of up to approx 35 residues are benign, whereas expansions of >40 residues are pathogenic, with earlier disease onset associated with longer repeats. The molecular mechanism of this delayed onset is mysterious, as is the basis for the fact that in HD, like other polyQ expansion diseases, the protein may be expressed widely in the brain and other tissues, yet only a highly specific group of neurons is affected ***(44)***.

To begin to determine the factors that affect Ht aggregation, yeast were engineered to express an N terminal fragment of Ht with polyQ repeat lengths of 25, 47, 72, or 103 residues, fused to green fluorescent protein (GFP) ***(45)***. In these studies it was shown that the reporter protein aggregated when 72 or 103 glutamines were present, and coalesced into distinct, punctate "spots" in vivo. Neither aggregation (as monitored by centrifugation of cellular extracts) nor coalescence (as monitored by fluorescence microscopy) was observed when the constructs containing shorter polyQ tracks were expressed. Given the involvement of chaperones in the aggregation of and phenotypes associated with yeast prions (*see* above), the impact of overexpressing or removing the activities of distinct chaperones on these phenotypes was next examined. It was found that overexpression of a yeast Hsp40, Sis1p, or a cytosolic Hsp70 altered the number and intensity of Ht aggregates containing the longer repeats in the cell; similar results were obtained by others ***(46)***. Overexpressed Hsp104 induced a similar phenotype. Most striking, and in accordance with the data on yeast prion conversion described earlier, cells lacking Hsp104 exhibited only a diffuse fluorescence pattern and aggregates were undetected by centrifugation of cellular lysates. Consistent with these results, Meriin et al. reported recently that mutations in the genes encoding Hsp104, cytosolic Hsp70, or one of two cytosolic Hsp40s alters either the seeding or expansion of polyQ-containing Ht in yeast ***(47)***. These investigators also found that the cytotoxicity of Ht required the presence of an endogenous yeast prion; other examples of interactions between

multiple prions have now been uncovered in yeast ***(48,49)*** and suggest cross-seeding phenomena. Overall, these studies suggest critical roles for several chaperones in the etiology of intracellular protein aggregation. Although mammalian homologues of Hsp104 may exist (http://www.proteome.com), whether these homologues or mammalian Hsp104 analogues play a role in Ht solubility has not been reported.

6. Alzheimer's Disease (AD)

The Aβ peptide fragment, which results from the cleavage of full-length amyloid precursor protein (APP), plays a central role in the development of Alzheimer's disease (AD) ***(50)***. APP, the precursor protein, exists in three main isoforms, namely 695, 751, and 770, which result from alternative splicing of the APP pre mRNA ***(51–54)***. APP is cleaved by members of the α and β and γ secretase family. Because it is believed that the generation of Aβ requires cleavage by the β secretase(s) and γ secretase(s) acting sequentially, a significant research effort has been devoted to identifying the proteins that comprise the secretase family, and to understanding their substrate specificity and site(s) of action.

The participation of Aβ in AD is underscored by many observations. First, Down's Syndrome (DS) is caused by trisomy 21, the same chromosome on which APP resides, and all people with DS ultimately show signs of AD ***(55)***. Second, mutations in APP predispose people to AD ***(56)***. Third, all familial AD (FAD) results from APP processing aberrations ***(57)***. Fourth, Aβ might activate an immune response that converts the diffuse plaques into the neuritic form because vaccination with Aβ 1-42 (the more aggregation-prone version of Aβ) appears to dissolve plaques and/or prevent their formation ***(50)***. Finally, Aβ has been shown to be an activator of neuronal apoptosis ***(58)***.

Aβ is produced in two main forms, 1-40 and 1-42, depending on the site of cleavage by the γ secretase enzyme(s). Three intracellular sites of Aβ generation have been identified in mammalian cells: the endosomal/lysosomal pathway (thought to play a minor role) ***(59)***; the trans-Golgi network, which is the main route for secreted Aβ ***(60)***; and the ER/intermediate compartment (IC) ***(60–63)***. It was previously thought that when Aβ was secreted from the cell at critical concentrations it aggregated and was toxic. However, the 1-42 form that is generated in the ER has been found to be more prone to aggregation, is retained within the cell, and is toxic ***(64)***. Because the presenilins, PS1 and PS2 in their holoprotein form, are also localized in the ER ***(65,66)*** and mutations in PS1 and PS2 are responsible for the majority of early-onset AD (their main intracellular effect being the elevation of the ratio of Aβ 1-42/1-40 ***[67,68]***) alterations in Aβ production play an important role in AD pathogenesis.

As this discussion indicates, there have been problems identifying the cellular site(s) of action of the secretases that give rise to Aβ in mammalian cells. With a few notable exceptions, factors that cooperate with the secretases are largely unknown, as is the reaction of the cell to the sudden or chronic accumulation of specific proteolytic fragments of APP. Unfortunately, there are notable difficulties in obtaining answers to these questions using mammalian cells, but in each case, yeast may provide a suitable model system with which to surmount these problems. First, it is difficult to assay transport between and residence within intracellular compartments in mammalian cell systems, whereas in yeast mutations that rapidly block transport to specific intracellular compartments are readily available. Second, silencing the expression of APP is not trivial. In contrast, yeast can be designed to selectively express APP under the control of inducible promoters to vary the levels of expression. Third, because of the extreme redundancy in the human genome, the abundance of secretases in mammals has made it difficult to assess their relative contributions in the biogenesis of APP.

To begin to develop yeast as a model system for the study of APP biogenesis, inducible APP expression systems have been developed and genetic screens have been designed to better define the proteases that act on APP. Two structurally and functionally related glycosyl-phosphatidylinositol (GPI)-linked yeast aspartyl proteases, Mkc7p and Yap3p (collectively termed "yapsin"), both of which reside at least in part on the cell membrane, were identified as being responsible for an α-secretase-mediated cleavage of APP expressed in the yeast *S. cerevisiae* ***(69,70)***. Importantly, the cleaved APP fragments can be released into the extracellular space, as occurs in mammalian cells. In the future it will be interesting to identify protein partners of these factors in yeast using genetic selections and introduced libraries encoding the yeast and mammalian genomes.

S. cerevisiae has also been used to establish a genetic screen for mammalian proteases that act at the caspase cleavage site. Upon transformation of a mammalian expression library into the strain, plasmids encoding caspase-3 and caspase-8 were obtained, confirming the efficacy of the screen ***(71)***. Strikingly, endogenous α, β, and γ secretase activities have been found to be conserved in *Picchia pastoris* ***(72)***, a budding yeast amenable to genetic analyses and with a more defined compartmental structure than *S. cerevisiae*. *P. pastoris* also has a higher secretory capacity than *S. cerevisiae*, suggesting that this yeast may prove quite valuable in the future to define the sites of action, proteases, and protease-partners that mediate secretase-like cleavage in eukaryotic cells.

7. Summary

Although this field is still in its infancy, it is hoped that the development of yeast expression systems to examine the diseases described in this chapter will further elucidate how the corresponding proteins mature and/or are degraded in the cell. The ability to use yeast to analyze the specific effects of cellular factors on a protein's conformation and maturation and to screen yeast with small molecule inhibitors or activators suggest that future pharmacological attacks will also prove successful. Finally, the genetic screens described in this report represent only the beginning of novel attacks that may identify additional players in the onset of conformational diseases. We suggest that only by fully understanding how misfolded proteins are handled in the cell and with whom they associate will we be able to rectify the intracellular protein folding problem without harming the host cell.

References

1. Hartwell, L. H., Culotti, J., Pringle, J. R., and Reid B. J. (1974) Genetic control of the cell division cycle in yeast. *Science* **183,** 46–51.
2. Carrell, R. W. and Lomas, D. A. (1997) Conformational disease. *Lancet* **350,** 134–138
3. Kopito, R. R. (1999) Biosynthesis and degradation of CFTR. *Physiol. Rev.* **79,** S167–S173.
4. Brodsky, J. L. (2001) Chaperoning the maturation of the cystic fibrosis transmembrane conductance regulator. *Am. J. Physiol. Lung Cell Mol. Physiol.* **281,** L39–L42.
5. Jensen, T. J., Loo, M. A., Pind, S., Williams, D. B., Goldberg, A. L., and Riordan, J. R. (1995) Multiple proteolytic systems, including the proteasome, contribute to CFTR processing. *Cell* **83,** 129–135.
6. Ward, C. L., Omura, S., and Kopito, R. R. (1995) Degradation of CFTR by the ubiquitin proteasome pathway. *Cell* **83,** 121–127.
7. McCracken, A. A. and Brodsky, J. L. (1996) Assembly of ER-associated protein degradation in vitro: dependence on cytosol, calnexin, and ATP. *J. Cell Biol.* **132,** 291–298.
8. Cheng, S. H., Gregory, R. J., Marshall, J., Paul, S., Souza, D. W., White, G. A., et al. (1990) Defective intracellular transport and processing of CFTR is the molecular basis of most cystic fibrosis. *Cell* **63,** 827–834.
9. Yang, Y., Janich, S., Cohn, J. A., and Wilson, J. M. (1993) The common variant of cystic fibrosis transmembrane conductance regulator is recognized by Hsp70 and degraded in a pre-Golgi nonlysosomal compartment. *Proc. Natl. Acad. Sci. USA* **90,** 9480–9484.

10. Pind, S., Riordan, J. R., and Williams, D. B. (1994) Participation of the endoplasmic reticulum chaperone calnexin (p88, IP90) in the biogenesis of the cystic fibrosis transmembrane conductance regulator. *J. Biol. Chem.* **269,** 12,784–12,788.
11. Meacham, G. C., Lu, Z., King, S., Sorscher, E., Tousson, A., and Cyr, D. M. (1999) The Hdj-2/Hsc70 chaperone pair facilitates early steps in CFTR biogenesis. *EMBO J.* **18,** 1492–1505.
12. Meacham, G. C., Patterson, C., Zhang, W., Younger, J. M., and Cyr, D. M. (2001) The Hsc70 co-chaperone CHIP targets immature CFTR for proteasomal degradation. *Nature Cell Biol.* **3,** 100–105.
13. Zhang, Y., Nijbroek, G., Sullivan, M. L., McCracken, A. A., Watkins, S. C., Michaelis, S., and Brodsky, J. L. (2001) Hsp70 molecular chaperone facilitates endoplasmic reticulum-associated protein degradation of cystic fibrosis transmembrane conductance regulator in yeast. *Mol. Biol. Cell* **12,** 1303–1314.
14. Nadler, S. G., Tepper, M. A., Schacter, B., and Mazzucco, C. E. (1992) Interaction of the immunosuppressant deoxyspergualin with a member of the Hsp70 family of heat shock proteins. *Science* **258,** 484–486.
15. Rubenstein, R. C. and Zeitlin, P. L. (2000) Sodium 4-phenylbutyrate downregulates Hsc70: implications for intracellular trafficking of DeltaF508-CFTR. *Am. J. Physiol. Cell Physiol.* **278,** C259–C267.
16. Fewell, S. W., Day, B. W., and Brodsky, J. L. (2001) Identification of an inhibitor of hsc70-mediated protein translocation and ATP hydrolysis. *J. Biol. Chem.* **276,** 910–914.
17. Brown, C. R., Hong-Brown, L. Q., Biwersi, J., Verkman, A. S., and Welch, W. J. (1996) Chemical chaperones correct the mutant phenotype of the delta F508 cystic fibrosis transmembrane conductance regulator protein. *Cell Stress Chap.* **1,** 117–125.
18. Sato, S., Ward, C. L., Krouse, M. E., Wine, J. J., and Kopito, R. R. (1996) Glycerol reverses the misfolding phenotype of the most common cystic fibrosis mutation. *J. Biol. Chem.* **271,** 635–638.
19. Teckman, J. H., Qu, D., and Perlmutter, D. H. (1996) Molecular pathogenesis of liver disease in alpha1-antitrypsin deficiency. *Hepatology* **24,** 1504–1516.
20. Qu, D., Teckman, J. H., Omura, S., and Perlmutter, D. H. (1996) Degradation of a mutant secretory protein, alpha1-antitrypsin Z, in the endoplasmic reticulum requires proteasome activity. *J. Biol. Chem.* **271,** 22,791–22,795.
21. Burrows, J. A., Willis, L. K., and Perlmutter, D. H. (2000) Chemical chaperones mediate increased secretion of mutant alpha 1- antitrypsin (alpha 1-AT) Z: A potential pharmacological strategy for prevention of liver injury and emphysema in alpha 1-AT deficiency. *Proc. Natl. Acad. Sci. USA* **97,** 1796–1801.
22. Le, A., Steiner, J. L., Ferrell, G. A., Shaker, J. C., and Sifers, R. N. (1994) Association between calnexin and a secretion-incompetent variant of human alpha 1-antitrypsin. *J. Biol. Chem.* **269,** 7514–7519.
23. Ware, F. E., Vassilakos, A., Peterson, P. A., Jackson, M. R., Lehrman, M. A., and Williams, D. B. (1995) The molecular chaperone calnexin binds Glc1Man9GlcNAc2 oligosaccharide as an initial step in recognizing unfolded glycoproteins. *J. Biol. Chem.* **270,** 4697–4704.

24. Cabral, C. M., Liu, Y., and Sifers, R.N. (2001) Dissecting glycoprotein quality control in the secretory pathway. *Trends Biochem. Sci.* **26,** 619–624.
25. Ellgaard, L. and Helenius, A. (2001) ER quality control: towards an understanding at the molecular level. *Curr. Opin. Cell Biol.* **13,** 431–437.
26. McCracken, A. A. and Kruse, K. B. (1993) Selective protein degradation in the yeast exocytic pathway. *Mol. Biol. Cell.* **4,** 729–736.
27. Werner, E. D., Brodsky, J. L., and McCracken, A. A. (1996) Proteasome-dependent endoplasmic reticulum-associated protein degradation: an unconventional route to a familiar fate. *Proc. Natl. Acad. Sci. USA* **93,** 13,797–13,801.
28. Brodsky, J. L, Werner, E. D., Dubas, M. E., Goeckeler, J. L., Kruse, K. B., and McCracken, A. A. (1999) The requirement for molecular chaperones during endoplasmic reticulum-associated protein degradation demonstrates that protein export and import are mechanistically distinct. *J. Biol. Chem.* **274,** 3453–3460.
29. McCracken, A. A., Karpichev, I. V., Ernaga, J. E., Werner, E. D., Dillin, A. G., and Courchesne, W. E. (1996) Yeast mutants deficient in ER-associated degradation of the Z variant of alpha-1-protease inhibitor. *Genetics* **144,** 1355–1362.
30. Lindquist, S., Krobitsch, S., Li, L., and Sondheimer, N. (2001) Investigating protein conformation-based inheritance and disease in yeast. *Philos. Trans. R. Soc. Lond. B. Biol. Sci.* **356,** 169–176.
31. Wickner, R. B., Taylor, K. L., Edskes, H. K., Maddelein, M. L., Moriyama, H. and Roberts, B. T. (1999) Prions in Saccharomyces and Podospora spp.: protein-based inheritance. *Microbiol. Mol. Biol. Rev.* **63,** 844–861.
32. Lacroute, F. (1971) Non-Mendelian mutation allowing ureidosuccinic acid uptake in yeast. *J. Bacteriol.* **106,** 519–522.
33. Cox, B. S. (1965) A cytoplasmic suppressor of super-suppressor in yeast. *Heredity* **24,** 505–521.
34. Sparrer, H. E., Santoso, A., Szoka, F. C., Jr., and Weissman, J. S. (2000) Evidence for the prion hypothesis: induction of the yeast [PSI+] factor by in vitro- converted Sup35 protein. *Science* **289,** 595–599.
35. Newnam, G. P., Wegrzyn, R. D., Lindquist, S. L., and Chernoff, Y. O. (1999) Antagonistic interactions between yeast chaperones Hsp104 and Hsp70 in prion curing. *Mol. Cell. Biol.* **19,** 1325–1333.
36. Chernoff, Y. O., Lindquist, S. L., Ono, B., Inge-Vechtomov, S. G., Liebamn, S. W. (1995) Role of the chaperone protein Hsp104 in propagation of the yeast prion-like factor [psi+]. *Science* **268,** 880–884.
37. Chernoff, Y. O., Newnam, G. P., Kumar, J., Allen, K., and Zink, A. D. (1999) Evidence for a protein mutator in yeast: role of the Hsp70-related chaperone ssb in formation, stability, and toxicity of the [PSI] prion. *Mol. Cell. Biol.* **19,** 8103–8112.
38. Moriyama, H., Edskes, H. K., and Wickner, R. B. (2000) [URE3] prion propagation in Saccharomyces cerevisiae: requirement for chaperone Hsp104 and curing by overexpressed chaperone Ydj1p. *Mol. Cell. Biol.* **20,** 8916–8922.
39. Kushnirov, V. V., Kryndushkin, D. S., Boguta, M., Smirnov, V. N., and Ter-Avanesyan, M. D. (2000) Chaperones that cure yeast artificial [PSI+] and their prion-specific effects. *Curr. Biol.* **10,** 1443–1446.

40. Sondheimer, N., Lopez, N., Craig, E. A., and Lindquist, S. (2001) The role of Sis1 in the maintenance of the [RNQ+] prion. *EMBO J.* **20,** 2435–2442.
41. Parsell, D. A., Kowal, A. S., Singer, M. A., and Lindquist, S. (1994) Protein disaggregation mediated by heat-shock protein Hsp104. *Nature* **372,** 475–478.
42. Jin, T., Gu, Y., Zanusso, G., Sy, M., Kumar, A., Cohen, M., Gambetti, P., and Singh, N. (2000) The chaperone protein BiP binds to a mutant prion protein and mediates its degradation by the proteasome. *J. Biol. Chem.* **275,** 38699–38704.
43. Reddy, P. H., Williams, M., and Tagle, D. A. (1999) Recent advances in understanding the pathogenesis of Huntington's disease. *Trends Neurosci.* **22,** 248–255.
44. Ross, C. A. (1995) When more is less: pathogenesis of glutamine repeat neurodegenerative diseases. *Neuron* **15,** 493–496.
45. Krobitsch, S. and Lindquist, S. (2000) Aggregation of huntingtin in yeast varies with the length of the polyglutamine expansion and the expression of chaperone proteins. *Proc. Natl. Acad. Sci USA* **97,** 1589–1594.
46. Muchowski, P. J., Schaffar, G., Sittler, A., Wanker, E. E., Hayer-Hartl, M. K., and Hartl, F. U. (2000) Hsp70 and Hsp40 chaperones can inhibit self-assembly of polyglutamine proteins into amyloid fibrils. *Proc. Natl. Acad. Sci. USA* **97,** 7841–7846.
47. Meriin, A. B., Zhang, X., He, X., Newnam, G. P., Chernoff, Y. O., and Sherman, M. Y. (2002) Huntington toxicity in yeast model depends on polyglutamine aggregation mediated by a prion-like Rnq1. *J. Cell Biol.* **157,** 997–1004.
48. Schwimmer, C. and Masison, D. C. (2002) Antagonistic interactions between yeast [PSI(+)] and [URE3] prions and curing of [URE3] by Hsp70 protein chaperone Ssa1p but not by Ssa2p. *Mol. Cell. Biol.* **22,** 3590–3598.
49. Derkatch, I. L., Bradley, M. E., Hong, J. Y., and Liebman, S. W. (2001) Prions affect the appearance of other prions: the story of [PIN(+)]. *Cell* **106,** 171–182
50. Selkoe, D. J. (1994) Alzheimers disease: a central role for amyloid. *J. Neuropathol. Exp. Neurol.* **53,** 438–447.
51. Ponte, P., Gonzalez-DeWhitt, P., Schilling, J., Miller, J., Hsu, D., Greenberg, B., et al. (1988) A new A4 amyloid mRNA contains a domain homologous to serine proteinase inhibitors. *Nature* **331,** 525–527.
52. Tanzi, R. E., McClatchey, A. I., Lamperti, E. D., Villa-Komaroff, L., Gusella, J. F., and Neve, R. L. (1988) Protease inhibitor domain encoded by an amyloid protein precursor mRNA associated with Alzheimer's disease. *Nature* **331,** 528–530.
53. Kang, J., Lemaire, H. G., Unterbeck, A., Salbaum, J. M., Masters, C. L., Grzeschik, K. H., et al. (1987) The precursor of Alzheimer's disease amyloid A4 protein resembles a cell-surface receptor. *Nature* **325,** 733–736.
54. Kitaguchi, N., Takahashi, Y., Tokushima, Y., Shiojiri, S., and Ito, H. (1988) Novel precursor of Alzheimer's disease amyloid protein shows protease inhibitory activity. *Nature* **331,** 530–532.
55. Mann, D. M. A., Yuonis, N., Jones, D., and Stoddart, R.W. (1992) The time course of pathological events in Down's syndrome with particular reference to the involvement of microglial cells and deposits of b/A4. *Neurodegeneration* **1,** 201–215.
56. Benson, M. D. (1991) Inherited amyloidosis. *J. Med. Genet.* **28,** 73–78.
57. Mullan, M. and Crawford, F. (1993) Genetic and molecular advances in Alzheimers disease. *Trends Neurosci.* **16,** 398–403.

58. Marx, J. (2001) New leads on the "How" of Alzheimers. *Science* **293,** 2192–2194.
59. Koo, E. H. and Squazzo, S. L. (1994) Evidence that production and release of amyloid beta-protein involves the endocytic pathway. *J. Biol. Chem.* **269,** 17386–17389.
60. Xu, H., Sweeney, D., Wang, R., Thinakaran, G., Lo, A. C., Sisodia, S. S., et al. (1997) Generation of Alzheimer beta-amyloid protein in the trans-Golgi network in the apparent absence of vesicle formation. *Proc. Natl. Acad. Sci. USA* **94,** 3748–3752.
61. Chyung, A. S. C., Greenberg, B. D., Cook, D. G., Doms, R. W., and Lee, V. M.-Y. (1997) Novel β-secretase cleavage of β-amyloid precursor protein in the endoplasmic reticulum/intermediate compartment of NT2N cells. *J. Cell Biol.* **138,** 671–680.
62. Cook, D. G., Forman, M. S., Sung, J. C., Leight, S., Kolson, D. L., Iwatsubo, T., et al. (1997) Alzheimers Abeta1-42 is generated in the endoplasmic reticulum/intermediate compartment of NT2N cells. *Nature Med.* **3,** 1021–1023.
63. Hartmann, T., Bieger, S. C., Bruhl, B., Tienari, P. J., Ida, N., Allsop, D., et al. (1997) Distinct sites of intracellular production for Alzheimer's disease A beta40/42 amyloid peptides. *Nature Med.* **3,** 1016–1020.
64. Skovronsky, D. M., Pijak, D. S., Doms, R. W., and Lee, V. M. (2000) A distinct ER/IC gamma-secretase competes with the proteasome for cleavage of APP. *Biochemistry* **39,** 810–817.
65. Cook, D. G., Sung, J. C., Golde, T. E., Felsenstein, K. M., Wojczyk, B. S., Tanzi, R. E., et al. (1996) Expression and analysis of presenilin 1 in a human neuronal system: localization in cell bodies and dendrites. *Proc. Natl. Acad. Sci. USA* **93,** 9223–9228.
66. Kovacs D. M, Fausett, H. J., Page, K. J., Kim, T. W., Moir, R. D., Merriam, D. E., et al. (1996) Alzheimer associated pres.enilins 1 and 2: neuronal expression in brain and localization to intracellular membranes in mammalian cells. *Nature Med.* **2,** 224–229.
67. Borchelt, D. R., Thinakaran, G., Eckman, C. B., Lee, M. K., Davenport, F., Ratovitsky, T., et al. (1996) Familial Alzheimer's disease-linked presenilin 1 variants elevate Abeta1-42/1-40 ratio in vitro and in vivo. *Neuron* **17,** 1005–1013.
68. Scheuner, D., Eckman, C., Jensen, M., Song, X., Citron, M., Suzuki, N., et al. (1996) Secreted amyloid beta-protein similar to that in the senile plaques of Alzheimer's disease is increased in vivo by the presenilin 1 and 2 and APP mutations linked to familial Alzheimer's disease. *Nature Med.* **2,** 864–870.
69. Zhang, W., Espinoza, D., Hines, V., Innis, M., Mehta, P., and Miller, D. L. (1997) Characterization of beta-amyloid peptide precursor processing by the yeast Yap3 and Mkc7 proteases. *Biochim Biophys Acta* **1359,** 110–122.
70. Komano, H., Seeger, M., Gandy, S., Wang, G. T., Krafft, G. A., and Fuller, R. S. (1998) Involvement of cell surface glycosyl-phosphatidylinositol-linked aspartyl proteases in alpha-secretase-type cleavage and ectodomain solubilization of human Alzheimer beta-amyloid precursor protein in yeast. *J. Biol. Chem.* **273,** 31,648–31,651.

71. Gunyuzlu, P. L., White, W. H., Davis, G. L., Hollis, G. F., and Toyn, J. H. (2000) A yeast genetic assay for caspase cleavage of the amyloid-beta precursor protein. *Mol. Biotechnol.* **15,** 29–37.
72. Le Brocque, D., Henry, A., Cappai, R., Li, Q.-X., Tanner, J.E., Galatis, D., et al. (1998) Processing of the Alzheimers Disease Amyloid Precursor Protein in Pichia pastoris: Immunodetection of α-, β-, and γ-secretase products. *Biochemistry* **37,** 14,958–14,965.

8

Expression of Recombinant Proteins

An Introduction

Jane Nøhr, Karsten Kristiansen, and Anne-M. Krogsdam

1. Introduction

To better understand and characterize the function (or lack thereof) of proteins—wild-type vs mutants—it is advantageous to be able to express these proteins in a controlled, chosen setup. For downstream applications such as enzymatic assays, X-ray crystallography/nuclear magnetic resonance (NMR), raising antibodies, or characterization of physical interaction with other proteins, it may furthermore be desirable to obtain large quantities of pure protein.

Some overall considerations are addressed in this chapter. *Escherichia coli* and yeast expression systems including relevant procedures are described in detail in the following two chapters. Examples for expression of mutant proteins in *E. coli*, yeast, and mammalian cells are given in following chapters. We will here confine ourself to discuss the general considerations when choosing an expression system and a vector design and briefly mention some background and general aspects relevant for baculovirus and mammalian expression systems.

2. Choosing an Expression System

Many different expression host systems are technically within reach, ranging from bacteria, yeasts, insect cells, mammalian cell cultures, plants, frog eggs (*Xenopus*), and filamentous fungi to goat-milk, nematodes (*Caenorhabditis elegans*), and transgenic rodents.

From: *Methods in Molecular Biology, vol. 232: Protein Misfolding and Disease: Principles and Protocols*
Edited by: P. Bross and N. Gregersen © Humana Press Inc., Totowa, NJ

For the purpose of lab-scale production of recombinant protein, single-cell organisms are generally a first choice because they offer the advantages of speed and simplicity combined with genetic and physiological malleability.

When choosing an expression system two main concerns should be addressed:

1. The nature of the protein. (Does it require extensive posttranslational modification? Does it contain hydrophobic stretches [impairing secretion]? Is it potentially harmful to certain hosts?)
2. The purpose of the expression. (Do downstream applications require large amounts of protein? Is biological activity an imperative? Is authenticity of the posttranslational modifications important?)

The choice of host affects these parameters very differently (*see* **Table 1**). Generally, biological activity and complex processing is inversely correlated with ease of handling and high yield. If very large quantities of protein are required for downstream applications such as crystallization for X-ray structure analysis, it is favorable to express the protein in a bio-reactor setup. This allows for very controlled growth conditions leading to high cell density at optimal conditions regarding nutrients, pH, and so on, and easily results in recombinant protein production in the gram scale. For other applications where yields in the μg/low milligram protein range suffice, batch cultivation is recommended because it is by far the simplest and fastest way of achieving the desired protein. Therefore in this chapter we will focus on production by batch cultivation. As an alternative means of obtaining high protein yields, we introduce expression in the yeast *Pichia pastoris* (Chapter 10), a methylotrophic yeast strain that combines the ease of manipulation, short doubling times, and high yield found in bacteria with the posttranslational modifications (as glycosylations), resulting in correct folding of mammalian proteins difficult to achieve in the prokaryotic systems ***(1)***. The *P. pastoris* expression system also has the advantage of a strong inducible promoter and is less prone to hyperglycosylation than the related *Saccharomyces* system.

3. General Considerations When Choosing a Vector for Stable Expression: *Vector Design/Elements (for Bacterial/Yeast/Mammalian Unicellular Systems)*

The expression vector should contain origin of replication, selectable marker, promoter, transcription terminator, and optimized mRNA translational signals and translation termination codon (**Fig. 1**). If a shuttle vector is used, origin of replication and selectable markers for *E. coli* must be included.

Table 1
Important Considerations When Choosing an Expression System

System/organism	Advantage	Drawback
E. coli	Easily obtainable large scale production (often approaching 30–50% of total cell protein) Well-developed procedures for purification of tagged proteins Easy and fast recombination DNA manipulations Much experience available for refolding protein from inclusion bodies	Large proteins (approx limit: 50 kDa) are poorly produced and largely misfolded. No posttranslational processing (e.g., glycosylation) Only a fraction of the protein exhibits natural biological activity. High endotoxin content in gram-negative bacteria Protein often ends up in inclusion bodies Refolding may be required.
Yeasts and fungi	Easy manipulation Low cost media More complex processing possible (including some glycosylation and disulfide bond formation). Functional analysis often possible directly in the cells (incl. membrane proteins) Generally regarded as safe (GRAS) Well-established large-scale production (high yield possible) Null-background possible Well-defined procedures for purification of tagged proteins	Glycosylation pattern differs from mammalian cells
Baculovirus/insect cells	Glycosylation possible Large amounts of protein can be produced and is largely correctly folded.	Cumbersome procedures for recombination and selection Complex media
Mammalian cell culture	"Native" processing background generally can be expected to support functional analysis Many vector types available Refolding not necessary.	Large-scale production and purification is costly and difficult. Null-background often difficult to achieve Low productivity Complex media

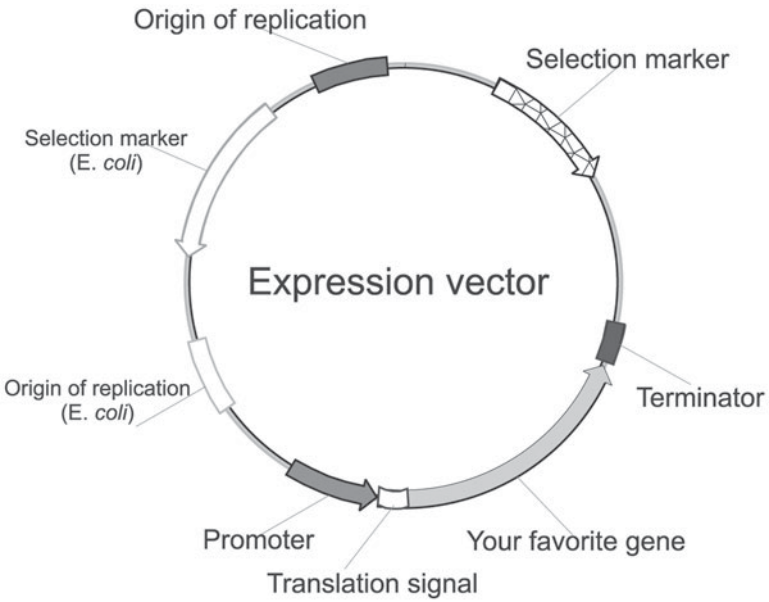

Fig. 1. Basic design of an expression (shuttle) vector.

Additionally, genetic elements for specific applications such as affinity fusion moieties, signal sequences for secretion, and protease cleavage sites may be included.

3.1. Origin of Replication (Table 2)

The origin of replication ensures that the vector is replicated along with the host genome during cell division and thus propagated in every new generation of the host cell. The origin of replication also determines the vector copy number. A high copy number may be favorable if a high production yield is to be obtained. In *E. coli*, high copy number increases vector stability when the random partitioning occurs during cell division. On the downside, maintaining a high copy number slows the growth rate of the host cells, thus favoring culture domination by cells with fewer vector copies. Alternatively, in runaway vectors, temperature-sensitive origins (i.e., R1-derived [dependent on the dnaK heat-shock protein] or ColE1-derived) allow the copy number to be greatly varied simply by altering the growth temperature ***(2)***. In yeast and mammalian systems, the low copy number vectors are generally more stable than the high copy number vectors. The origins of these low copy number vectors are centromere derived and/or contain scaffold attachment sequences, which allow the vector to be propagated as an extra chromosome and hence decrease the

Table 2
Origins of Replication

Host	Typical origins of replication used in expression vector design
E. coli	pBR322 derived (25–50 copies)
	pUC derived (150–200 copies)
	R1 or ColE1 derived (inducible copynumber)
Yeast	ARS/CEN (1–2 copies)
	2μ derived (>30 copies)
Mammalian[a]	OriP (only active in primate and canine cells)
	OriSV40+S/MAR(hINFβ) (< 20 copies)

[a]It should be noted that many mammalian expression vectors rely on transient expression or genomic integration and thus do not contain origins of replication.

risk of uneven partitioning during cell division. As in *E. coli*, the high copy number directing origins are generally derived from naturally occurring circular DNA (plasmids) (i.e., the 2μ circle in yeast) or viruses.

3.2. Selectable Marker

A selectable marker is required to allow identification of transformed cells and, upon cultivation of the transformants, to ensure selective pressure favoring cells harboring the expression vector (thus preventing growth of cells experiencing vector loss). A number of different selectable markers exist, thus allowing coexpression of several proteins by applying multiple selective pressures on the cultured cells. Genes encoding antibiotic resistance are among the most commonly used selective markers, and include genes conferring resistance to ampicillin (the β-lactamase gene), tetracycline, hygromycin, chloramphenichol, and various kanamycin variants. They are all very efficient for short-term batch production of recombinant proteins, but it should be noted that ampicillin is a poor choice for longer growth periods, because the β-lactamase inactivates the antibiotic, thereby gradually conditioning the medium for nonselective growth. Alternative selective markers often used in *E. coli* and yeast include a number of heterotrophies induced by deletion in the host genome of genes encoding essential proteins. The intact gene is then included on the expression vector and selection is obtained by excluding from the growth medium the essential ingredient produced by the protein encoded by the selective marker gene. Some common examples include the *HIS3* and *LEU2* genes. They encode enzymes required for endogenous production of histidine and leucine. Cells lacking these genes are counter selected (nonviable) when grown in defined medium lacking these amino acids. The genes conferring the selectivity

are generally identical between different expression vectors, but the promoter controlling the expression of the genes determines host specificity.

3.3. Promoter

The promoter directing expression of the protein of interest should be recognized by the host polymerase initiation complex, and therefore often is derived from active genomic host sequences (i.e., promoters for genes involved in basal metabolism). Promoter choice depends on the nature and purpose of the expressed protein. Some proteins may be toxic in high dose or require some limiting posttranslational modification, in which case a weak promoter may be preferred. Moreover, if the protein is to be analyzed in a cell-based assay, it may be favorable to have a low expression level to avoid nonspecific interactions or squelching effects. For production of large quantities of protein for downstream in vitro analysis, it is often desirable to choose a tightly regulated promoter to ensure a high growth rate under noninduced conditions and to avoid early production of protein that may then be partly degraded by the time the culture is harvested.

3.4. Transcription Terminator

A transcription terminator ensures proper termination of the transcript of the inserted gene. This will often increase the stability of the transcript and prevent a toxic effect of a very long transcript encompassing a large portion of noncoding vector sequence. The best terminators are often derived from genes highly expressed in the host. Particularly in prokaryotes, a strong terminator sequence plays a crucial role in regulating gene expression ***(3)***.

3.5. Translation Signals

Translational signals inherent in the mRNA transcript are required for optimal assembly, initiation, and termination of the ribosomal translational machinery. A host-optimized initiation signal will typically be placed immediately before the translation start codon. In *E. coli* the consensus signal is a stretch of about 30 bases, with a purine-rich core sequence resembling: UAAGGAGGU (Shine-Dalgarno sequence). In yeast no consensus sequence has been determined, but by comparison of a broad range of very active metabolic promoters from *Saccharamyces cerevisiae*, it has been concluded that optimal activity coincides with very AT rich sequence immediately before and after the translational start codon (consensus: (A/U)A(A/C)A(A/C)AaugUC(U/C), ***[4,5]***). In mammalian cells the optimal sequence is very GC-rich and has the consensus: GCCGCC(A/G)CCaugG (Kozak sequence) ***(6)***. Yet, it should be noted that although an optimized translation signal may increase an otherwise poor protein yield, good expression levels have been found to occur even in the absence

of the host-optimized initiation signal. Although the translation stop codons conform to the UGA/UAG/UAA consensus in *E. coli*, yeast, and mammalian cells, different preferences exist, i.e., the optimal stop codon in *E. coli* is UAA preceeded by an "A," whereas in mammalian cells a stop codon immediately followed by a purine is the most efficient. In general, different organisms have different levels of the different tRNAs and thus to acquire optimized expression it is advantageous to avoid stretches of codons requiring tRNAs that are rare in the expression host ***(7)***. Several databases exist for optimal codon usage in various hosts ***(8)***.

4. Baculovirus Expression Systems

Baculovirus-based expression systems in combination with insect cell-culture hosts are among the major recombinant DNA expression systems used for production of a wide variety of heterologous proteins. Compared to expression in yeast, the ability of insect cells to posttranslationally modify large quantities of expressed proteins is even closer to mammalian processing. Because the high expression levels often lead to aggregation of accumulated, unprocessed protein, efforts are continuously made to engineer improved secretion from the insect cells ***(9)***.

Establishing a baculovirus-insect cell expression setup involves packing of the circular expression vector into virus-like particles, which are then titrated for optimal infection of the insect cells. This is a rather elaborate process compared to the production of protein in bacteria and yeast and has thus so far been chosen mainly for production of protein that was poorly processed in the other two host types, or protein that was required aplenty for a longer study period. It should be noted that with the new baculovirus derived vector systems that have been developed for expression in insect cells several of the virus-dependent intermediate steps are circumvented. Moreover, relatively simple bioreactors can now be purchased at reasonable cost specifically for eased production of recombinant protein in insect cells.

For further description as well as practical guidelines (particularly with respect to the improved transformation system) *see* **ref. *10***.

5. Mammalian Expression Systems

For cell-based analysis of protein function, as well as for production of protein for downstream in vitro analyses, it can be advantageous /necessary to express the protein in a "native" background ***(11)***. Key advantages of expression in mammalian systems are the ability to correctly fold, glycosylate, and otherwise modify the expressed proteins. Moreover, interaction with a broad spectrum of more or less well-defined endogenous proteins may be required for elucidation of particular aspects of protein function. Not surprisingly, a very

large number of expression vectors therefore are available for mammalian expression (more than 2600 vectors), including several viral vectors as well as baculovirus-derived vectors. The in-cell analysis of expressed protein is thus rather straightforward, using transient transfection, viral transduction, or stable gene expression systems, because a large number of options for optimization exist. High-level production of protein in mammalian cell culture remains slightly more tricky because it requires high compatibility of vector (+ gene of interest) with host cell. However some very good results have been obtained using COS cells (derived from African green monkey kidney (CV-1) cells), HEK-293 (human embryonic kidney), BHK (baby hamster kidney) cells, and CHO (Chinese hamster ovary cells). The details of this topic is beyond the scope of this chapter but the reader is referred to excellent, in depth, detailed reviews on this field (*see* **refs. *12–17***; for examples, *see* Chapters 12, 16, 18–20).

Acknowledgments

This work was conducted within the Danish Biotechnology Instrument Center (DABIC) and the center "Relationship between Architecture and Functionality of Glycosylated Multidomain Polysaccharide-Hydrolases with Emphasis on Covalent Structure, Conformational Stability, and Binding Site Cooperativity (RAPFUS)," and supported by the Danish Natural Science Research Council and the Danish Research Councils' Committee on Biotechnology (No. 9502014).

References

1. Psaridi-Linardaki, L., Mamalaki, A., Remoundos, M., and Tzartos, S. J. (2002) Expression of soluble ligand- and antibody-binding extracellular domain of human muscle acetylcholine receptor alpha subunit in yeast *Pichia pastoris*. Role of glycosylation in alpha-bungarotoxin binding. *J. Biol. Chem.* **277,** 26,980–26,986.
2. Giraldo-Suarez, R., Fernandez-Tresguerres, E., Diaz-Orejas, R., Malki, A., and Kohiyama, M. (1993) The heat-shock *DnaK* protein is required for plasmid R1 replication and it is dispensable for plasmid ColE1 replication. *Nucleic Acids Res.* **21,** 5495–5499.
3. Gusarov, I. and Nudler, E. (2001) Control of intrinsic transcription termination by N and NusA: the basic mechanisms. *Cell* **107,** 437–449.
4. Hamilton, R., Watanabe, C. K., and de Boer, H. A. (1987) Compilation and comparison of the sequence context around the AUG startcodons in *Saccharomyces cerevisiae* mRNAs. *Nucleic Acids Res.* **15,** 3581–3593.
5. Cigan, A. M. and Donahue, T. F. (1987) Sequence and structural features associated with translational initiator regions in yeast: a review. *Gene* **59,** 1–18
6. Kozak, M. (1989) The scanning model for translation: an update. *J. Cell. Biol.* **108,** 229–241.

7. Gilbert, M. and Albala, J. S. (2002) Accelerating code to function: sizing up the protein production line. *Curr. Opin. Chem. Biol.* **6,** 102–105.
8. (http://www.kazusa.or.jp/codon/). (2002)
9. Ailor, E. and Betenbaugh, M. J. (1998) Overexpression of a cytosolic chaperone to improve solubility and secretion of a recombinant IgG protein in insect cells. *Biotechnol. Bioeng.* **58,** 196–203.
10. http://www.invitrogen.com:80/content.cfm?pageid=3440&nv=1. (2002)
11. Morton, C. L. and Potter, P. M. (2000) Comparison of *Escherichia coli*, *Saccharomyces cerevisiae*, *Pichia pastoris*, *Spodoptera frugiperda*, and COS7 cells for recombinant gene expression. Application to a rabbit liver carboxylesterase. *Mol. Biotechnol.* **16,** 193–202.
12. Makrides, S. C. (1999) Components of vectors for gene transfer and expression in mammalian cells. *Protein. Expr. Purif.* **17,** 183–202.
13. Rossi, F. M. and Blau, H. M. (1998) Recent advances in inducible gene expression systems. *Curr. Opin. Biotechnol.* **9,** 451–456.
14. Trill, J. J., Shatzman, A. R., and Ganguly, S. (1995) Production of monoclonal antibodies in COS and CHO cells. *Curr. Opin. Biotechnol.* **6,** 553–560.
15. Wurm, F. and Bernard, A. (1999) Large-scale transient expression in mammalian cells for recombinant protein production. *Curr. Opin. Biotechnol.* **10,** 156–159.
16. Edwards, C. P. and Aruffo, A. (1993) Current applications of COS cell based transient expression systems. *Curr. Opin. Biotechnol.* **4,** 558–563.
17. Anson, D. S. (2001) Retroviral-mediated gene transduction. *Methods. Mol. Biol.* **175,** 471–494.

9

Expression in *E. coli* Systems

Anne-M. Krogsdam, Karsten Kristiansen, and Jane Nøhr

1. Introduction

Owing to cost advantage, speed of production, and often high product yield (up to 50% of total cell protein), expression in *Escherichia coli* is generally the first choice when attempting to express a recombinant protein. Expression systems exist to produce recombinant protein intracellularly (soluble or in inclusion bodies), secreted to the periplasm, or to the surrounding medium. When deciding on a genetic design strategy, it is important to consider the nature of the recombinant protein. The mildest and thus the obvious first-choice expression strategy is to attempt to express the protein intracellularly in soluble form. In *E. coli*, proteins containing disulfide bonds are best produced by secretion because the disulfide forming foldases reside in the periplasm. Likewise, a correct N-terminus is more likely to be obtained upon secretion. Moreover, potentially toxic proteins are more likely to be produced in high yield if secreted from the cell. Secretion eases later purification of the product as the host secretes relatively few of its own proteins. Although tags exist that will direct the protein to the periplasm, only a few reports exist of successfully tagging the protein for extracellular secretion ***(1)***. As another strategy to avoid toxicity to the host, or if the recombinant protein is very susceptible to cellular proteases, some protection is obtained by targeting the protein to light-refractile aggregates known as inclusion bodies ***(2,3)***. Several different strategies exist for subsequent recovery and folding of the protein, which notably must be able to withstand the denaturing–renaturing process. Unfortunately, this strategy is only applicable for proteins that can be refolded adequately. Instead of targeting the protein to inclusion bodies, the opposite strategy namely to increase the solubility of the protein, may be employed. This may be done, for example, by coexpressing interacting proteins; fusing the protein to a highly soluble tag;

From: *Methods in Molecular Biology, vol. 232: Protein Misfolding and Disease: Principles and Protocols*
Edited by: P. Bross and N. Gregersen © Humana Press Inc., Totowa, NJ

coexpressing foldases or chaperones; or by altering the temperature, pH, or osmotic stress of the growth medium.

The next step in designing a genetic strategy for expression requires consideration of downstream purification methods. If a high-affinity ligand or antibody is available, this will greatly ease the purification, given that a method exists to release the purified protein without resorting to harsh/denaturing treatment. Alternatively, an affinity-fusion strategy may be applied. A large number of affinity-fusion systems have been developed and thoroughly tested and documented to facilitate the recovery of recombinant proteins. The basic concept of these systems involves binding of the fusion protein to a high-affinity ligand (specific for the affinity fusion tag), coupled to a gel matrix. The fusion protein is then extracted from the total protein mix by simple centrifugation. (Alternatively, the affinity material may be packed into a column and the cell extract simply passed through.) These systems include several different types of fusion tags. When choosing a system, it is important to ensure that the tag is suitable for the intended type of purification (i.e., some tags such as the GST do not withstand denaturation as well as a poly-histidine or FLAG-peptide tag). Also the size of the tag should be considered, because the total size of the fusion protein should not exceed 75–100 kDa if a reasonable yield of intact protein is to be obtained. Unfortunately, some of the tags providing the highest degree of purification are among the largest (the GST and ProteinA tags). On the other hand, it appears that some of the novel gel-matrixes (i.e., acrylamide or silica-based gels) for attachment of the fusion ligands may allow better purification with smaller tags such as the poly-His, thus holding promise for improved purification procedures in the near future. Further advantages of the fusion systems include increased solubility of the protein and quite often also increased yield and stability. By combining different tags, an expressed double-tagged protein can moreover often be obtained at higher purity following a two-step purification process (double-tag vectors are commercially available from Novagen; *see also*: http://www.embl-heidelberg.de/ExternalInfo/geerlof/draft_frames/flowchart/clo_vector/vector.html). Once a fusion system is chosen, some consideration should be given when deciding whether the fusion should be N-terminal or C-terminal to the recombinant protein, because direct fusion to an active domain may sometimes impair the activity of this domain. Although most tags eventually can be enzymatically or chemically released, the initial folding of the active domain may still be affected.

Most of the commercially available affinity fusion vectors have fairly strong promoters, which can be directly or indirectly induced by the synthetic lactose substitute isopropyl β-D-thiogalactopyranoside (IPTG). For expression of potentially toxic proteins, it is important to use promoters that are tightly shut in the absence of induction (i.e., the pET vector systems). Because the directly

inducible systems are not completely tight, it is important to consider carefully the manufacturer's notes when choosing a vector system. On the other hand, the tightness of the directly inducible systems is more easily manipulated. For instance, the low basal expression from the wild-type *lac* promoter can be reduced by inclusion of 2% glucose in the growth medium. It should be noted, though, that most commercially available systems employ a modified, glucose-nonresponsive, T5 *lac* operator (for a further, more detailed review we recommend **refs**. ***4*** and ***5*)**.

The following procedure is a good first choice for expression of a recombinant protein by fusion to a GST affinity tag.

2. Materials

1. LB (Luria or Lenox Broth): 10% (w/v) tryptone, 5% (w/v) yeast extract, 10% (w/v) NaCl
2. IPTG (isopropyl β-D-thiogalactopyranoside). (NB: toxic.)
3. PBS (Phosphate-buffered saline): 137 m*M* NaCl, 2.7 m*M* KCl, 4.3 m*M* Na_2HPO_4, 1.4 m*M* KH_2PO_4, pH ~7.3.
4. PIC (Protease Inhibitor Cocktail™ (tablets obtainable from Boehringer-Mannheim).
5. Buffer A: PBS + PIC (1 tablet pr. 25 mL), 1 m*M* PMSF.
6. 0.9% NaCl, sterilize by autoclaving.
7. French press.
8. Triton X-100, detergent.
9. Glutathione-coupled Sepharose beads (e.g., Glutathione Sepharose™ 4B, from Amersham-Pharmacia Biotech AB).
10. Glutathione. Dissolve in Buffer A before use.
11. Benzonase, a potent, almost inactivatable nuclease.
12. Antibiotic (ampicillin).
13. Phenylmethylsulfonic fluoride (PMSF) (NB: toxic), temperature-sensitive (25 m*M* solution can be stored at –20°C). Owing to its labile nature PMSF should be added to the buffer immediately before use.
14. Sodium dodecylsulfate (SDS)-sample buffer (1X): 62.5 m*M* Tris-HCl, pH 6.8, 2.5% SDS, 10% glycerol, 0.02% bromophenol-blue, 1 m*M* DTE. If prepared without DTE, the buffer may be stored at –20°C for several years. Once DTE has been added, the buffer may be stored at –20°C for a month.

3. Method

This is a basic procedure for expression and purification of GST-fusion proteins using an IPTG-inducible expression system such as, among others, the pGEX systems (Amersham Pharmacia Biotech). For further advice on methodology, we recommend **ref. *6***.

Please note that several similar commercially available, well-documented systems exist.

(Because general cloning is a prerequisite for implementing an expression vector design, and transformation of *E. coli* is a central part thereof, we will assume that the reader must already be familiar with this step.)

1. Prepare 20 mL LB media with appropriate antibiotic (100 μg/mL ampicillin). Inoculate with an *E. coli* culture harboring an expression vector for the recombinant protein of interest and incubate overnight at 37°C, with moderate shaking.
2. The following day, dilute the culture in 200 mL LB media (75 μg/mL ampicillin) to obtain a final OD_{600} = 0.25 and incubate at 30°C. When OD_{600} = 0.5, induce expression of recombinant protein by adding IPTG to a final concentration of 100 μ*M* (*see* **Note 1**).
3. Incubate 2–2½ h until OD_{600} = 0.8–1.2
4. Harvest the cells in 250-mL bottles by spinning in a JA14 rotor at 5500*g*, 10 min at 4°C (*see* **Note 2**).
5. Wash the pellet twice in approx 100 mL 0.9% NaCl (4°C) (*see* **Note 2**). Add 20 mL cold buffer A and carefully resuspend the cells. Transfer the resuspended cells to a JA20 harvest vial (*see* **Note 2**).
6. French press the cells twice at 1000 psi (*see* **Note 3**).
7. Add Triton X-100 to a final concentration of 1% and rotate 10 min at 4°C. Attach the tube onto the end-over so that sideways rotation will occur.
8. If the solution is viscous add a few μL of Benzonase.
9. Clear-spin in a JA-20 rotor at 20000*g*, 35 min, 4°C to remove cellular debris.
10. Transfer the supernatant to a 50 mL test tube with screw-on lid, and add 10% glycerol (final concentration) (*see* **Note 4**).
11. Prepare for purification of the GST protein: equilibrate the glutathione-coupled Sepharose beads as follows:
    a. Add 300 μL beads suspension to a microfuge reaction tube (*see* **Note 5**).
    b. Spin down briefly (max. 4 s !) in a table centrifuge at max speed.
    c. Discard the supernatant and add 1 mL buffer A. Invert the tube to gently resuspend the beads and spin again.
    d. Add the beads to the supernatant from **step 10**.
12. Incubate the supernatant and beads in an end-over for 2 h at 4°C (or overnight). Attach the tube onto the end-over so that sideways rotation will occur.
13. Spin in the table centrifuge at 1000*g* for 3–5 min, transfer the beads into a 1.5 mL microfuge reaction tube, and wash three times with buffer A.
14. After the final wash, add 200 μL of buffer A and store at 4°C for up to a week.
15. To evaluate the recombinant protein yield or to identify steps where the yield may be improved, monitor the amount of recombinant protein present at the different steps by sampling at harvest, after French press (both debris pellet and supernatant) and after affinity binding. Boil the samples in SDS sample buffer (the SDS sample buffer should preferentially constitute at least half of the final sample volume) and compare by SDS-polyacrylamide gel-electrophoresis (PAGE) (*see* **Notes 6–9**).

16. At this step the proteins can be eluted by incubation with 10 m*M* glutathione in buffer A, or cleaved from the GST-tag using appropriate enzymes.

4. Notes

1. For aeration, the volume of the incubation flask must always be at least 5 times the culture volume. Therefore use a 1-L baffled-bottom flask for the incubation of a 200-mL culture.
2. At this step you can freeze the cells at –80°C for later use.
3. Alternatively lysis can be performed by addition of lysozyme 1–4 mg/mL followed by repeated freezing and thawing or by sonication with 4 × 15 s repeated cycles (on ice).
4. At this step the supernatant may be frozen at –80°C for later use.
5. When pipetting Sepharose beads: always cut off the distal 3–4 mm of the pipet tip before use, in order not to crush the beads.
6. If low amounts of protein are bound to the beads, there are several possible causes. These include: 1) the affinity of the fused GST (steric hindrance) for the beads is impaired, 2) the expression may be low, or 3) the majority of the expressed protein is insoluble. Impaired affinity can be compensated by resuspending the cell pellet in a smaller volume in **step 7**. Alternatively, because different lysis procedures have different efficiencies with respect to release of soluble protein, choosing a different lysis procedure may increase the concentration of the protein without decreasing the volume (decreased volume unfortunately also leads to more unspecific capture of host protein on the beads, as the concentration of the nontagged *E. coli* protein increases). It should be noted that if it is desired that a large fraction of the extracted protein retain biological activity, a very "efficient" lysis procedure releasing a lot of protein into the soluble fraction tends not to be a good choice, possibly because it brings into solution a larger fraction of poorly folded (less soluble) protein, solubilized as a side effect of the strong lysis conditions. Low expression level or insolubility may be helped by altering the concentration of the IPTG, the temperature, or the time period of induction. Addition of a small amount of glucose (<2%) at the time of incubation at 30°C may also be beneficial. Also even minor variations in the OD_{600} at the time of induction may greatly affect the biological activity of the expressed protein; thus it is important to try to find the optimal conditions for the protein in question.
7. The general stability and/or solubility of the protein is often increased by coexpression of interacting proteins/"foldases." Examples include coexpression of molecular chaperones, such as GroES-GroEL, DnaK-DnaJ-GrpE, or ClpB ***(7–9)***. The positive effect of coexpression of a partner protein has been seen in the case where nuclear receptor dimer coexpression enhances solubility and biological activity of the expressed protein ***(10)***. Coexpression of proteins that participate in regulation of expression may also be advantageous, i.e., the T7 lysozyme expressed from the pLysS and pLysE vectors ***(11)***. Strains containing these coexpression vectors are commercially available.

8. The choice of host strain may influence the expression level.
9. If expression levels are low, check for possible loop formation in the 5' of the mRNA transcript; inserting synthetic 5' secondary structure may possibly improve expression ***(12)***.
10. For further aid in troubleshooting or application of alternative expression systems in *E. coli* we recommend **ref. *13***.

Acknowledgments

This work was conducted within the Danish Biotechnology Instrument Center (DABIC) and the center "Relationship between Architecture and Functionality of Glycosylated Multidomain Polysaccharide-Hydrolases with Emphasis on Covalent Structure, Conformational Stability, and Binding Site Cooperativity (RAPFUS)," and supported by the Danish Natural Science Research Council and the Danish Research Councils' Committee on Biotechnology (No. 9502014).

References

1. Tan, S. (2001) A modular polycistronic expression system for overexpressing protein complexes in *Escherichia coli*. *Protein Expr. Purif.* **21,** 224–234.
2. Windsor, L. J. and Steele, D. L. (1902) Expression of recombinant matrix metalloproteinases in *Escherichia coli*. *Methods Mol. Biol.* **151,** 191–205.
3. Ellis, R. J. and Pinheiro, T. J. (2002) Medicine: danger–misfolding proteins. *Nature* **416,** 483–484.
4. Jonasson, P., Liljeqvist, S., Nygren, P. A., and Stahl, S. (2002) Genetic design for facilitated production and recovery of recombinant proteins in *Escherichia coli*. *Biotechnol. Appl. Biochem.* **35,** 91–105.
5. Balbas, P. (2001) Understanding the art of producing protein and nonprotein molecules in *Escherichia coli*. *Mol. Biotechnol.* **19,** 251–267.
6. Amersham Pharmacia Biotech AB. (2000) *The Recombinant Protein Handbook.* Protein Amplification and Simple Purification.
7. Schlieker, C., Bukau, B., and Mogk, A. (2002) Prevention and reversion of protein aggregation by molecular chaperones in the *E. coli* cytosol: implications for their applicability in biotechnology. *J. Biotechnol.* **96,** 13–21.
8. Ben-Zvi, A. P. and Goloubinoff, P. (2001) Review: mechanisms of disaggregation and refolding of stable protein aggregates by molecular chaperones. *J. Struct. Biol.* **135,** 84–93.
9. Kedzierska, S. and Matuszewska, E. (2001) The effect of co-overproduction of DnaK/DnaJ/GrpE and ClpB proteins on the removal of heat-aggregated proteins from *Escherichia coli* [Delta]clpB mutant cells: new insight into the role of Hsp70 in a functional cooperation with Hsp100. *FEMS Microbiol. Lett.* **204,** 355–360
10. Li, C., Schwabe, J. W., Banayo, E., and Evans, R. M. (1997) Coexpression of nuclear receptor partners increases their solubility and biological activities. *Proc. Natl. Acad. Sci. USA* **94,** 2278–2283.

11. Studier, F. W. (1991) Use of bacteriophage T7 lysozyme to improve an inducible T7 expression system. *J. Mol. Biol.* **219,** 37–44.
12. Carrier, T. A. and Keasling, J. D. (1999) Library of synthetic 5' secondary structures to manipulate mRNA stability in *Escherichia coli*. *Biotechnol. Prog.* **15,** 58–64.
13. http//www.apbiotech.com/technical/technical_index.html. (2002)

10

Protein Expression in Yeasts

Jane Nøhr, Karsten Kristiansen, and Anne-M. Krogsdam

1. Introduction

Yeasts are attractive hosts for production of mammalian proteins requiring posttranslational processing, because yeasts offer advantages of both eukaryotic expression mechanisms and bacteria-like growth and handling. Thus for the past 22 years yeasts have been used to overcome the shortcomings of bacterial expression systems. As in *Escherichia coli* yeasts can provide intracellular as well as secreted expression. By applying short signaling sequences, the expressed proteins can be directed to extracellular secretion or to distinct compartments of the cell ***(1)***. Because *Saccharomyces cerevisiae* tends to hyperglycosylate secreted proteins, this strain is primarily used for intracellular production. Other yeast strains (i.e., *Pichia pastoris*, *Hansenula polymorpha*, *Schizosaccharomyces pompe*, *Klyveromyces lactis*, or *Yarrowia lipolytica*) are more suited for secretion ***(2)***.

Among the best-developed systems for large-scale protein production is *P. pastoris*-based expression. A notable advantage of *Pichia pastoris* compared with *S. cerevisiae* is that *Pichia pastoris* may produce levels 10–100-fold higher of heterologous protein ***(3–5)*** and that *Pichia pastoris* does not hyperglycosylate as *S. cerevisiae* does upon secretion. Both yeasts have a majority of N-linked glycosylation of the high-mannose type, but in *Pichia* the average length of the oligosaccharide chain is 8–14 mannose residues per side chain, whereas in *Saccharomyces* it is between 50–150 mannoses ***(6)***. In addition, *S. cerevisiae* core oligosaccharides have terminal α1,3 glycan linkages, and *P. pastoris* has none. The α1,3 glycan linkage is believed to be responsible for the antigenic nature of proteins produced by secretion from *S. cerevisiae*.

From: *Methods in Molecular Biology, vol. 232: Protein Misfolding and Disease: Principles and Protocols*
Edited by: P. Bross and N. Gregersen © Humana Press Inc., Totowa, NJ

1.1. Expression in Pichia pastoris

Pichia pastoris is a methylotrophic yeast, able to grow on methanol as the only carbon-source. The first step in the methanol metabolism is the oxidation of methanol to formaldehyde, catalyzed by an alcohol oxidase. This reaction generates formaldehyde and hydrogen peroxide. To avoid the toxic effect of the hydrogen peroxide, the methanol metabolism takes place in specialized organelles called peroxisomes, which sequesters toxic by-products from the rest of the cell. The enzyme alcohol oxidase has a poor affinity for O_2 and *Pichia pastoris* compensates for this by generating large amounts of the enzyme, typically more than 30%, of the total soluble protein in cells grown with methanol as carbon source.

Two genes, *AOX1* and *AOX2*, code for alcohol oxidase in *Pichia pastoris*. The *AOX1* expression is tightly regulated at the level of transcription. The regulation is a two-step process: a repression/derepression mechanism and an induction mechanism. Glucose represses transcription even in the presence of methanol, whereas methanol is needed for induction. *AOX2* is constitutively expressed at much lower levels than *AOX1*. Loss of the *AOX1* gene results in loss of most of the cell's alcohol oxidase activity. This results in a reduction in the cell's ability to metabolize methanol, and, consequently, to slow growth on methanol medium. This slow growth allows the isolation of the Mut^s strains (Methanol utilization slow). This phenotype is used to evaluate *Pichia* transformants for integration of the gene of interest into the *AOX1* gene, as the integration disables the gene (giving the Mut^s phenotype).

Expression of recombinant protein in *P. pastoris* can be intracellular or secreted. Secretion requires the presence of a signal peptide for targeting the expressed protein to the secretory pathway. Many different signal peptides have been used successfully, e.g., signal sequences from *S. cerevisiae* α-mating factor prepro peptide and the signal peptide from the *P. pastoris* acid phosphatase gene *(PHO1)* **(*7*)**.

An advantage of expressing heterologous proteins as secreted proteins is that *Pichia* secretes very low levels of its endogenous proteins, and that the minimal media for *Pichia* growth contains low amounts of protein. Hence, the secreted recombinant protein comprises the majority of the total protein in the medium, and the secretion by itself serves as the first step in purification of the protein. For further information about expression and optimizing expression in *Pichia pastoris* we recommend **ref. *8***.

1.1.1. Pichia pastoris *Expression Vectors*

Plasmid vectors for recombinant protein expression in *P. pastoris* have several common features. One is the foreign gene-expression cassette which is

composed of the DNA sequences containing the *AOX1* promoter (or the promoter from the constitutively expressed glyceraldehyde-3-phosphate dehydrogenase gene [GAP]), followed by a linker containing cloning sites for insertion of the gene of interest, and the transcriptional termination sequence from *AOX1* that directs 3' processing and polyadenylation of the mRNAs. Some vectors contain the *AOX1* 3' flanking sequence, which can be used for integration of the gene-expression cassette into the *AOX1* locus by gene replacement or gene insertion 3' to the *AOX1* gene.

The vectors also contain sequences required for plasmid replication and maintenance in bacteria (e.g., ColE1 replication origin and the ampicillin-resistance gene), and the HIS4 gene for selection vectors with dominant drug-resistance markers (i.e., the bacterial kanamycin-resistance gene or the ble gene conferring resistance for Zeocin) that allow for enrichment of strains with multiple copies of foreign gene-expression cassettes through increased antibiotic pressure and vectors with sequences encoding the His_6 and myc epitopes for easy epitope-tagging of the C terminal of the protein have also been developed (e.g., the Multi-Copy Pichia Expression Kit, or the pPICZ/pPICZ-E vectors, Invitrogen).

Transformation of *P. pastoris* occurs through integration of the transforming DNA into the host genome by a single crossover event or by gene replacement. The site of integration can be determined by linearization of the expression vector generating 5' and 3' ends homologous to the corresponding chromosomal site of integration. These sites can be, for example, the *HIS4* gene, the *AOX1* gene, or the glyceraldehyde-3-phosphate dehydrogenase promoter P_{GAP} ***(9)***. Integration at the 5' and 3' regions of the *AOX1* leads to replacement of the gene, and results in a Mut^s phenotype (slow growth on methanol as sole carbon source). A single crossover event within the *AOX1*, *HIS4*, or *GAP* gene results in transformants with a Mut^+ phenotype (wild-type growth on methanol). Which crossover event gives the highest expression level of a given protein is unpredictable. The main practical difference therefore is that the double crossover transformants can be easily selected owing to their slow growth on methanol, whereas the single crossover transformants are more difficult to select but exhibit faster growth rate and less rigorous methanol addition regimens.

1.2. Expression in S. cerevisiae

Baker's yeast—*S. cerevisiae* being a genetically and functionally well-defined, batch-grown, easily handled eukaryotic cell—has become a choice model organism for the establishment of a number of methods for expression and analysis of protein function.

1.2.1. Cell-Based Assays

S. cerevisiae-based models have been established/developed for investigating the molecular details of, i.e., eukaryotic cell division ***(10–13)***, expression, and analysis of mammalian transmembrane receptors ***(14)***, and nuclear receptor function ***(15)***. Yeast does not contain homologues of mammalian nuclear receptors and therefore has proven useful for investigation of various receptor mutants and/or for ligand screens in a receptor null background. Thus, expression of mutant yeast proteins and their mammalian homologues continually provides information on their functions in health and disease. In addition to the models for direct functional analysis, several protein–protein interaction assays have been developed in yeast. The most famous assay is the two-hybrid system ***(16)***, where two proteins of interest are expressed as hybrids with the GAL4 transcription factor DNA binding and transactivating domains, respectively. If the proteins physically interact, they will form a connection between the two GAL4 domains, which will then be capable of forming a transactivating unit on a GAL4 response element containing promoter site. Coupling cDNA libraries to the GAL4 transactivating domain, and then screening for interaction using a bait protein coupled to the GAL4 DNA binding domain, subsequently expanded this assay to allow screening for protein-interaction partners. Additionally, several alternative versions of the original two-hybrid system have been developed, i.e., to allow detection of interaction taking place outside of the cell nucleus (reviewed in **ref. *17***).

1.2.2. In Vitro Assays

Most recently the ease of using this organism for high-throughput analysis of complex protein formations, large-scale phosphoprotein mapping, and mapping of various protein–protein interaction networks has made *S. cerevisiae* a favorite at the frontline of today's proteomics ***(18–20)***. These approaches are generally based on the ability of expressing protein targets of interest in the yeast. Subsequently, cell extracts containing the trans-expressed protein are then used for in vitro analysis of its function/interacting partners.

Depending on the downstream application, the vector may include an affinity tag fused to the protein, i.e., GST, FLAG. Some of these applications require that the expressed proteins retain full biologic activity. Hence, it can be advantageous to express the protein at low level to ensure that the host capacity of expression/folding is not exceeded. Because low-level expression impairs the purity that may be obtained upon affinity purification of a single-tagged protein, double-tagged expression systems have been devised and have lately proven rather successful for functional analysis of proteins expressed in yeast. Some double-tag systems are commercially available but currently the best-

documented system is the TAP (Tandem Affinity Purification) system devised at EMBL ***(21–23)***.

1.2.3. Choosing a Yeast Expression Vector

Four different basic types of yeast expression vectors exist in common use. The YEp (yeast episomal plasmid) is replicated in the host cell at high copy number because it carries the replication origin of the yeast 2μ circle. It is generally the first choice for expression of recombinant protein for downstream in vitro analysis. In combination with a strong promoter, it may yield in extreme cases as much as 5% of total cell protein. Because the main focus in production of recombinant protein in yeast is quality rather than quantity, it is sometimes preferable to choose a low copy vector for expression because it may increase the ability of the cell to correctly fold the recombinant protein. For this purpose, the YCp (yeast centromere plasmid) is a good choice. It carries a yeast autonomous replicating sequence (ARS) and is furthermore stabilized by a yeast centromere sequence. This is also the optimal choice for expression of proteins to be assayed within the cell, because stability in vector copy number along with low protein yield ensures high reproducibility, low clonal variation and reduces squelching of endogenous factors that may influence the analysis of, for example, nuclear receptor function. If even more stable propagation of the recombinant gene is desired, the YIp (yeast integrating plasmids) can be used. These are unable to replicate and function through integration into the host genome. Finally, for propagation of very large DNA sequences (up to 1000 kb) (mainly for library purposes) the YACs (yeast artificial chromosomes) are vectors carrying a centromere, an ARS, and two telomeres.

1.2.4. Choosing a Promoter

When choosing a promoter for expression of recombinant protein in *S. cerevisiae*, several options exist. Basically the many different options are related by being derived from genomic yeast promoters and can be distinguished by promoter strength and degree of inducibility. For expression in the context of a cell-based assay, a relatively weak, constitutive promoter is often advantageous. The promoters P_{CYC1} (cytochrome C1) or the truncated P_{ADH2} (alcohol dehydrogenase 2) found in the original yeast two-hybrid vectors (BD Biosciences) have often been found to be a good choice. For production of larger amounts of protein for downstream in vitro applications or purification, some of the strong promoters derived from genes encoding glycolytic enzymes are generally chosen. These are semi-inducible because they are several-folds upregulated when grown on a medium with glucose as the carbon source. Examples of promoters used in industrial-scale production include the P_{GPD} (glycerolphosphate dehy-

drogenase), the P_{PGK} (phosphoglycerokinase), and the P_{TPI} (triose phosphate isomerase). The latter was for many years used for commercial production of a Pro-Insulin precursor molecule ***(24)***. Alternatively, a truncated version of the P_{THX7} (glucose transporter) may be used, as it is also very powerful and is only affected by very high levels of glucose ***(25)***. If a cell-based assay requires analysis in the absence and presence of a given protein, or if the protein is potentially harmful to the host, an inducible promoter may be chosen. The most commonly used inducible promoter in *S. cerevisiae* is the P_{GAL} (galactosidase). It is a relatively high-level expression promoter, which is induced by switching from raffinose-containing medium to growth on galactose as the carbon source. Unfortunately, this is a relatively cumbersome and expensive means of induction. If a very tight regulation is required (e.g., for the production of a known toxic protein) a more creative solution has been devised in the form of the P*GEV* (GAL4.ER.VP16) system ***(26)***. It relies on vector based constitutive expression of a GAL4 (DNA binding domain)-Estrogen receptor ***(27)***-VP16 (virally derived activator domain) hybrid. Upon addition of β-estradiol to the medium, the hybrid activates transcription from an otherwise silent UAS*GAl10* (upstream activating sequence from a gene involved in galactose metabolism)-containing promoter, controlling expression of the recombinant protein of interest ***(26)***. If the desired feature of the inducibility is to be able to grade the expression level, the simplest, easiest, and most sensitive system most likely is the P_{CUP1} (copper inducible metallothionein) controlled system. This system allows for differential expression levels without exchanging promoter system, and moreover, allows dosage-dependence analysis of the recombinant protein in, for example, cell-based transactivation assays. The promoter is regulated by an endogenous copper-binding transcription factor, and thus is induced simply by adding $CuSO_4$ to the growth medium. The promoter generally responds at very low copper levels and gradually increases in strength until a cytotoxic level of copper is reached (for an example, *see* **Fig. 1**).

1.2.5. Selective Markers

Most vectors available from commercial sources (including the ATCC) rely on heterotrophic selection in the absence of uracil (the *URA3* marker), leucine (*LEU2*), tryptophane (*TRP1*), or histidine (*HIS3*) from the medium. However, other markers do exist including the *LYS2* (lysine), *MET3*/*MET14* (methionine), and *ADE2* (adenine). It should be noted though that the corresponding *ade2* genomic mutation generally is leaky. *ADE2* thus should not be used as an exclusive marker. Additionally a number of antibiotic-resistance genes can be used in yeast. These include genes encoding resistance to kanamycin, zeocin, blasticidin, and also more recently hygromycin B, nourseothricin, and bialaphos ***(28)***. Although the heterotropic markers are the easiest and cheapest solutions, given a corresponding mutated host strain is available, the antibi-

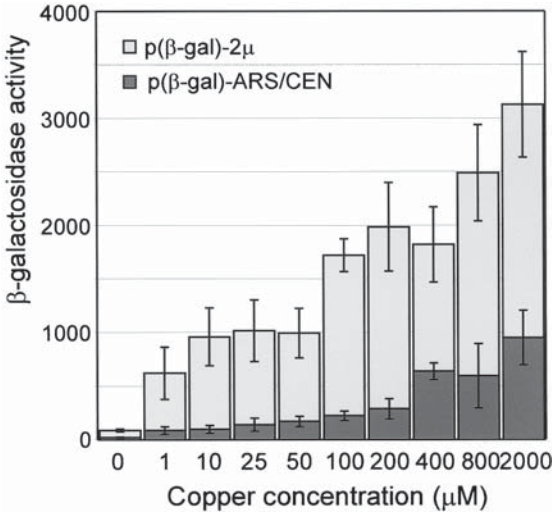

Fig. 1. Copper-inducible expression. The β-galactosidase gene was expressed in the S. cerevisiae strain Y700 from a high copy (2μ) and a low copy (ARS/CEN) vector. Expression was under control of the PCUP1 and induced at increasing levels of copper added to the growth medium. β-galactosidase activity was determined by a quantitative liquid culture-based assay.

otic-resistance genes are generally applicable and certainly broaden the spectrum of proteins that can be simultaneously expressed in a host cell.

2. Materials

2.1. P. pastoris

All solutions, tubes, and bottles should be sterile. All solutions should be kept on ice.

1. An appropriate *P. pastoris* host strain.
2. Electroporator (e.g., BIORAD GenePulser™).
3. 0.2 cm Electroporation cuvets (e.g., BIORAD GenePulser™).
4. 1 *M* Sorbitol, 4°C.
5. YEPD media: 1% yeast extract, 2% peptone, 2% dextrose. Store at 4°C. Stable for several months.
6. Sterile water, 4°C.
7. Linearized DNA (5–20 μg in 5–10 μL TE buffer).
8. Minimal dextrose (MD) plates: 0.9 g yeast nitrogen base (without amino acids and $(NH_4)_2SO_4$), 2.5 g $(NH_4)_2SO_4$, 7.5 g agar, 10 g D-glucose, 0.5 mL 0.02% biotin, in 500 mL H_2O.
9. 30°C incubator.

10. MD agar plates: 0.9 g yeast nitrogen base (without amino acids and $(NH_4)_2SO_4$), 2.5 g $(NH_4)_2SO_4$, 7.5 g agar, 10 g D-glucose, in 500 mL H_2O. After autoclaving add 0.5 mL 0.02% biotin. Store at 4°C. Stable for several months.
11. Minimal methanol (MM) agar plates: 0.9 g yeast nitrogen base (without amino acids and $(NH_4)_2SO_4$), 2.5 g $(NH_4)_2SO_4$, 7.5 g agar, in 500 mL H_2O. After autoclaving add 0.5 mL 0.02% Biotin and 2.5 mL 99% methanol. Store at 4°C. Stable for several months.
12. Sterile toothpicks and scoring template.
13. BMGY media: 5 g yeast extract, 10 g peptone, 0.9 g yeast nitrogen base (without amino acids and $(NH_4)_2SO_4$), 2.5 g $(NH_4)_2SO_4$, 5.9 mL 85% glycerol, H_2O to 449 mL. Autoclave. Add 50 mL 1 *M* potassium buffer, pH 6.0 +/– 0.1, and 1 mL 500X biotin. Store at 4°C. Stable for 2 mo. (*see* **Note 1**.)
14. BMMY media: 5 g yeast extract; 10 g peptone, 0.9 g yeast nitrogen base (without amino acids and $(NH_4)_2SO_4$), 2.5 g $(NH_4)_2SO_4$, H_2O to 446.5 mL. Autoclave. Add 50 mL 1 *M* potassium buffer, pH 6.0 +/- 0.1, 1 mL 500X biotin, and 2.5 mL 99% Methanol. Store at 4°C, stable for 2 mo.
15. 500X Biotin: 20 mg biotin in 100 mL H_2O, filter-sterilize, stable for 1 yr at 4°C.
16. 1 *M* Potassium buffer, pH 6.0 +/– 0.1: Mix 132 mL 1 *M* K_2HPO_4 and 868 mL 1 *M* KH_2PO_4; adjust pH with H_3PO_4 or KOH to 6.0 +/– 0.1; Autoclave, stable at RT for 1 yr.
17. 99% Methanol (NB: toxic).
18. Baffled flasks.
19. Thermostated shaker (200–300 rotations/min, 30°C).

2.2. Saccharomyces cerevisiae

1. YEPD-medium: 10% (w/v) yeast extract, 20% (w/v) peptone, 20% (w/v) dextrose). Autoclave and store at 4°C.
2. Selective media (-uracil): 3X DropOut solution (-uracil), 1X minimal medium, 2% (w/v) glucose. Prepare fresh before use.
3. 100X DropOut solution (-uracil): 0.2% (w/v) arginine, 0.1% (w/v) histidine, 0.4% (w/v) lysine, 0.1% (w/v) DL-methionine, 0.6% (w/v) phenylalanine, 0.5% (w/v) threonine, 0.4% (w/v) tryptophane, 0.6% (w/v) leucine. Dissolve in distilled water by heating at 70°C. Filter-sterilize and store at 4°C in dark bottle (tryptophan is light-unstable).
4. 2X Minimal medium: 16% (w/v) yeast nitrogen base (w/o amino acids [aa], w/ammonium sulfate), 0.11% (w/v) adenine, 0.11% (w/v) tyrosine. Autoclave (gently, in order not to destroy the adenine!) Store at 4°C.
5. Selective agar plates: 2% (w/v) granulated agar, 1X selective medium (-uracil). Autoclave a 4% (w/v) agar solution (in H_2O) cool to 55°C, add selective medium components, and pour into petri dishes (approx 20 mL pr dish).
6. Plate mixture, 1 mL: 800 µL 50% (w/v) PEG4000, 100 µL 1 *M* Li OAc, 100 µL "10X TE" (0.1 *M* Tris-HCl, pH 8.0, 10 m*M* ethylenediamine tetraacetic acid [EDTA]). Prepare plate mixture fresh on the day of use.

7. 0.5 *M* Dithioerythritol (DTE) (dissolved in H_2O and stored at –20°C).
8. Yeast strain with deletion of the *URA1* gene (preferably also protease deficient, several such strains are available from commercial sources).
9. Copper-inducible yeast expression vector containing the *URA1* gene and a DNA sequence encoding the protein of interest.
10. Salmon sperm DNA 10 mg/mL, sonicated. Store at –20°C. Before use: denature by boiling 3 times for 2 min interchanged with placing on ice for 2 min.
11. $CuSO_4$, a filter-sterilized, aqueous solution may be stored almost indefinitely.
12. Selective media (-uracil): 3X DropOut solution (-uracil), 1X minimal medium, 2% (w/v) glucose. Prepare fresh before use.
13. High salt buffer: 0.4 *M* NaCl, 20 m*M* Tris-HCl, pH 7.5, 20% glycerol, 2 m*M* $MgCl_2$ (or 2 m*M* EDTA), 2 m*M* DTE.
14. Protease inhibitors: one "complete" cocktail-tablet (Boehringer PIC™) pr. 25 mL buffer, (optional: phenylemethylsulfonyl fluoride [PMSF] to 0.5 m*M*).
15. Liquid nitrogen.
16. French press.

3. Methods

3.1. P. pastoris

(For further protocols, *see* **ref. *3***)

3.1.1. Electroporation of P. pastoris

1. Grow *P. pastoris* in 5 mL of YEPD in a 50-mL conical flask at 30°C, 200 rotations per min, overnight.
2. Inoculate 500 mL fresh YEPD with 0.1–0.5 mL of the overnight culture in a 2.5-L flask. Grow overnight at 30°C to an OD_{600} = 1.3–1.5.
3. Harvest the cells by centrifugation at 1500*g* for 5 min at 4°C. Resuspend the pellet with 500 mL of 4°C sterile water.
4. Centrifuge the cells as in **step 3**, then resuspend in 250 mL 4°C sterile water.
5. Centrifuge the cells as in **step 3**, then resuspend in 20 mL 4°C 1 *M* sorbitol solution.
6. Centrifuge the cells as in **step 3**, then resuspend the pellet in 1 mL of ice-cold 1 *M* sorbitol for a final volume of approx 1.5 mL (*see* **Note 2**).
7. Mix 80 µL of the cells from **step 6** with 5–20 µg linearized DNA (in 5–10 µL TE buffer) and transfer to an ice-cold 0.2 cm electroporation cuvet (*see* **Note 3**).
8. Incubate the cuvet with the cells on ice for 5 min.
9. Pulse the cells according to the parameters for yeast suggested by the manufacturer of the specific electroporation device being used (*see* **Note 4**).
10. Immediately add 1 mL ice-cold 1 *M* sorbitol to the cuvet. Transfer the cuvet contents to a sterile microcentrifuge tube.
11. Spread 200 µL aliquots on five selection plates.
12. Incubate the plates at 30°C until colonies appear (approx 3 d).

3.1.2. Screening for AOX1 Disrupted Transformants in Pichia pastoris

Use the plates from the electroporation containing the His^+ transformants and screen for the Mut^s or Mut^+ phenotype:

1. Using a sterile toothpick, pick one colony from the transformation plate and streak or patch out in a regular pattern on both a MM and a MD plate (*see* **Note 5**).
2. Use a new sterile toothpick for each transformant, and patch 100 transformants.
3. Incubate the plates at 30°C for 2 d (*see* **Note 6**).
4. Score the plates. Mut^+ transformants will grow on both plates, whereas Mut^s transformants will show little or no growth on the MM plates (*see* **Note 7**).

3.1.3. Expression in Pichia pastoris

This is a basic procedure for recombinant protein expression in the methanolytic *P. pastoris* system:

1. Make a preculture by inoculating from a selected transformant into 50 mL of YEPD in a 500 mL baffled flask (*see* **Note 8**). Grow at 30°C (*see* **Note 9**) in a shaking incubator (250 rotations per min) until OD_{600} = 2–6 (*see* **Note 10**). The cells will be in log phase growth.
2. Transfer 5 × 10 mL culture from the preculture to 5 × 1 l BMGY in 5 L flasks. Cover the flasks with two layers of sterile cheesecloth and return to incubator to continue growth for 20 h, 250 rotations per min, 30°C.
3. Harvest cells by centrifugation: 1500*g*, 10 min, room temperature. Resuspend cell pellet in 2 × 0.5 L BMMY, and grow in 5 L flasks covered with cheesecloth, 250 rotations per min, 30°C.
4. Add 99% methanol to a final concentration of 0.5% every 24 h to maintain induction (*see* **Note 11**). Take out aliquots at 0, 6, 12, 18, 24, 36, 48, 60, 72, 84, and 96 h, and determine the optimal time after induction for harvest.
5. Harvest by centrifugation; 1500*g*, 10 min at room temperature (*see* **Note 12**).
6. Freeze pellet; prepare cell extract as described in **Subheading 3.2.2., steps 8–12**.

3.2. Saccharomyces cerevisiae

3.2.1. Transformation of Host Culture (Modified Lithium Acetate Yeast Transformation; Modified from ref. 27)

1. Inoculate yeast culture in YEPD and grow at 30°C with strong agitation (or on a wheel) to saturation (overnight) (*see* **Notes 13** and **14**).
2. In a microfuge tube, spin down 1 mL of cells (5 s) for each transformation.
3. Decant and shake once, leaving cells and 50–100 µL of liquid.
4. Add 2 µL of 10 mg/mL salmon sperm DNA, resuspending cells with pipet tip.
5. Add approx 1 µg of your vector DNA and vortex.
6. Add 0.5 mL of PLATE mixture and 40 µL of 0.5 *M* DTE and vortex.
7. Incubate on benchtop for 2–24 h.
8. Heat-shock the cells for 10 min at 42°C.

9. Spin down for 2 min at 1200*g* in benchtop microfuge centrifuge. Remove supernatant using a pipet. Add 200 µL 1X TE.
10. Plate cells on selective media and incubate for 2 d at 30°C. Expect approx 1000 transformants per µg of DNA. (Only transformed cells will survive and form colonies.) (*See* **Notes 15–17**.)

3.2.2. Induced Expression and Preparation of High-Salt, Whole-Cell Yeast Extract

High-salt extracts are primarily useful for extraction of nuclear protein such as nuclear receptors ***(30)*** or other DNA-binding proteins.

1. Inoculate appropriate selective medium with yeast clone.
2. The following day dilute the overnight culture to $OD_{600} = 0.3$ in a total volume of minimum 100 mL.
3. At $OD_{600} = 0.4–0.5$ add $CuSO_4$ to a final concentration of 200 µ*M* (*see* **Note 18**).
4. Grow 5 h past $OD_{600} = 0.5$ (or overnight). Harvest cells by centrifugation, 2000*g*, and 22°C, 5 min in a Beckman JA14 rotor. Wash once in approx ½ volume of distilled H_2O.
5. Place the cells on ice and keep them on ice from hereon.
6. Resuspend in high-salt buffer + protease inhibitors. Use two volumes of buffer pr. volume of cells. Transfer to JA20 polypropylene tubes.
7. Snap-freeze in liquid nitrogen (*see* **Note 19**).
8. Thaw on ice.
9. Destroy cells by passing the thawed solutions five times through an ice-cold French press at 1300 psi. Keep the solution on ice between passes (*see* **Note 20**).
10. Precipitate cell-debris by centrifugation at 20,000*g*, 4°C, 30 min in a Beckman JA20 rotor.
11. Pipet the supernatant into a clean tube (on ice) and store in liquid nitrogen.
12. The resulting extracts will be in: 267 m*M* NaCl, 13 m*M* TrisHCl, 13% glycerol, 1.33 m*M* MgCl, 2 m*M* DTE, and contain 7–10 µg total cell protein/µL (*see* **Notes 21** and **22**).

4. Notes

1. BMGY/BMMY (buffered complex glycerol or methanol media) are usually used for expression of secreted proteins, particular if the pH is important for the activity of the expressed protein. They are buffered with a phosphate buffer and, because *P. pastoris* is able to grow at a wide range of pH values, it is possible to optimize the conditions for the protein. BMGY/BMMY contain yeast extract and peptone, which may help stabilize secreted proteins and prevent or decrease proteolysis of secreted proteins.
2. The cells may be frozen down in 80 µL aliquots at –80°C for later use. This will make the transformation efficiency decrease.
3. Make two control transformations: One with empty expression vector to determine the intracellular protein background and one without DNA to determine the number of "natural revertants."

4. For Biorad GenePulser™: 1.5 kV, 200Ω, 25 μFD.
5. It is important to patch the MM plate before patching on the MD plate.
6. Add 100 μL 100% methanol to the lid of the inverted MM plate every day to compensate for the loss owing to evaporation and consumption.
7. A transformant may be selected owing to the $His4^+$ and Mut^S phenotype, without expressing the integrated gene. Additional assays for selection of transformants expressing the protein are made based on the specific protein and its characteristics, the existence of antibodies or tags ***(5,31)***.
8. A very important parameter for efficient expression in *P. pastoris* is adequate aeration during growth and especially during methanol induction. As a general rule for growth of *P. pastoris*, never allow cultures to be more than 10–30% of the total volume of the flask. If possible, use baffled flasks, and cover these with cheesecloth (2–3 layers) or a loose cover.
9. All expressions are done at 30°C, in a shaking incubator. It is critical that the temperature does not exceed 30°C. If the incubator temperature fluctuates, set the temperature at 28°C.
10. For cultures inoculated from fresh plates, this takes approx 16 h.
11. The optimal methanol percentage for induction varies from protein to protein (in the range 0.25–1.4%).
12. For secreted expression, the cells can be resuspended after harvest, and expression continued several times with only slight decreases in expression level ***(4)***. For intracellular expression, decant the supernatant and store the pellet at –80°C until ready for purification.
13. Instead of an overnight culture, a toothpickful of cells directly from a fresh plate of cells can be dissolved directly in the plate mixture.
14. Late log cells yield a higher level of transformants than stationary phase cells.
15. Alternative procedures exist, including spheroblasting or electroporation. None of these techniques are as efficient as lithium acetate transformation. Nevertheless, they may be useful, e.g., cells for electroporation can be stored in a –70°C freezer, which makes this procedure slightly faster (although with more "hands-on" time). For extensive review of transformation procedures, *see* **ref. *32***.
16. Transformed cells may be kept on sealed plates in a cold room for several months. For longer storage, prepare frozen stock: inoculate selective medium with a transformant colony. Grow overnight until saturation. Add glycerol to 15% and store at –70°C.
17. Be aware that if a heterologous selection is used in a strain that does not contain a deletion but merely point mutation(s) in the endogenous gene, some nontransformed background revertants may also occur and form colonies on the selective plate.
18. For higher protein yield, try increasing the copper concentration. Be aware that different yeast strains have different levels of copper sensitivity depending on the copy numbers of the genomic metallothionein genes.
19. The cells may be stored in liquid nitrogen for later use.

20. If a French press is not at hand, alternative procedures may include glass-bead disruption. This procedure can be performed with the same buffer (or a low-salt buffer if different kinds of protein is expressed) but is best-suited for small sample volumes. The cells may also be disrupted by enzymatic spheroblasting followed by dounce homogenization.
21. If the expressed protein is fused to an affinity partner, the extract may be diluted to approx 10X the original cell volume in approx 200 m*M* salt and applied to affinity material for purification (basically like that described for *E. coli* in Chapter 9, this volume). Because the tagged protein represents at best a few percent of the total cell protein to achieve better purification, it is often advantageous to include more than one affinity tag. Submitting the protein to more than one type of affinity extraction often decreases the amount of unspecifically bound/co-purified yeast proteins.
22. Co-expression of partner proteins may increase the stability and thereby increase yield as well as biological activity. (Personal observation upon expression of mammalian nuclear receptors.)

Acknowledgments

This work was conducted within the Danish Biotechnology Instrument Center (DABIC) and the center "Relationship between Architecture and Functionality of Glycosylated Multidomain Polysaccharide-Hydrolases with Emphasis on Covalent Structure, Conformational Stability, and Binding Site Co-operativity (RAPFUS)" and supported by the Danish Natural Science Research Council and the Danish Research Councils' Committee on Biotechnology (No. 9502014).

References

1. Schuster, M., Einhauer, A., Wasserbauer, E., Sussenbacher, F., Ortner, C., Paumann, M., et al. (2000) Protein expression in yeast: comparison of two expression strategies regarding protein maturation. *J. Biotechnol.* **84,** 237–248.
2. Muller, S., Sandal, T., Kamp-Hansen, P., and Dalboge, H. (1998) Comparison of expression systems in the yeasts *Saccharomyces cerevisiae*, *Hansenula polymorpha*, *Klyveromyces lactis*, *Schizosaccharomyces pombe*, and *Yarrowia lipolytica*. Cloning of two novel promoters from Yarrowia lipolytica. *Yeast* **14,** 1267–1283.
3. www.invitrogen.com:80/Content/Tech-Online/molecular_biology/manuals_ppr/pich_man.pdf. (2002)
4. Fierobe, H. P., Mirgorodskaya, E., Frandsen, T. P., Roepstorff, P., and Svensson, B. (1997) Overexpression and characterization of *Aspergillus awamori* wild-type and mutant glucoamylase secreted by the methylotrophic yeast *Pichia pastoris*: comparison with wild-type recombinant glucoamylase produced using *Saccharomyces cerevisiae* and *Aspergillus niger* as hosts. *Protein. Expr. Purif.* **9,** 159–170.
5. Rosenfeld, S. A. (1999) Use of *Pichia pastoris* for expression of recombinant proteins. *Methods. Enzymol.* **306,** 154–169.

6. Grinna, L. S. and Tschopp, J. F. (1989) Size distribution and general structural features of N-linked oligosaccharides from the methylotrophic yeast, *Pichia pastoris*. *Yeast* **5,** 107–115.
7. Scorer, C. A., Buckholz, R. G., Clare, J. J., and Romanos, M. A. (1993) The intracellular production and secretion of HIV-1 envelope protein in the methylotrophic yeast *Pichia pastoris*. *Gene* **136,** 111–119.
8. Sreekrishna, K., Brankamp, R. G., Kropp, K. E., Blankenship, D. T., Tsay, J. T., Smith, P. L., et al. (1997) Strategies for optimal synthesis and secretion of heterologous proteins in the methylotrophic yeast *Pichia pastoris*. *Gene* **190,** 55–62.
9. Waterham, H. R., Digan, M. E., Koutz, P. J., Lair, S. V., and Cregg, J. M. (1997) Isolation of the *Pichia pastoris* glyceraldehyde-3-phosphate dehydrogenase gene and regulation and use of its promoter. *Gene* **186,** 37–44.
10. Blow, J. J. (1991) Cell cycle control of DNA replication by p34cdc2. *Semin. Cell. Biol.* **2,** 243–250.
11. Guarente, L. and Bermingham-McDonogh, O. (1992) Conservation and evolution of transcriptional mechanisms in eukaryotes. *Trends Genet.* **8,** 27–32.
12. Resnick, M. A. and Cox, B. S. (2000) Yeast as an honorary mammal. *Mutat. Res.* **451,** 1–11.
13. Defossez, P. A., Park, P. U., and Guarente, L. (1998) Vicious circles: a mechanism for yeast aging. *Curr. Opin. Microbiol.* **1,** 707–711.
14. Bill, R. M. (2001) Yeast: a panacea for the structure-function analysis of membrane proteins? *Curr. Genet.* **40,** 157–171.
15. McEwan, I. J. (2001) Bakers yeast rises to the challenge: reconstitution of mammalian steroid receptor signalling in *S. cerevisiae*. *Trends. Genet.* **17,** 239–243.
16. Fields, S. and Song, O. (1989) A novel genetic system to detect protein-protein interactions. *Nature* **340,** 245–246.
17. Serebriiskii, I. G., Khazak, V., and Golemis, E. A. (2001) Redefinition of the yeast two-hybrid system in dialogue with changing priorities in biological research. *BioTechniques* **30,** 634–636, 638, 640.
18. Delneri, D., Brancia, F. L., and Oliver, S. G. (2001) Towards a truly integrative biology through the functional genomics of yeast. *Curr. Opin. Biotechnol.* **12,** 87–91.
19. Ficarro, S. B., McCleland, M. L., Stukenberg, P. T., Burke, D. J., Ross, M. M., Shabanowitz, J., et al. (2002) Phosphoproteome analysis by mass spectrometry and its application to *Saccharomyces cerevisiae*. *Nat. Biotechnol.* **20,** 301–305.
20. Ho, Y., Gruhler, A., Heilbut, A., Bader, G. D., Moore, L., Adams, S. L., et al. (2002) Systematic identification of protein complexes in *Saccharomyces cerevisiae* by mass spectrometry. *Nature* **415,** 180–183.
21. The Séraphin TAP page, EMBL. http://www-db.embl-heidelberg.de/jss/servlet/de.embl.bk.wwwTools.GroupLeftEMBL/ExternalInfo/seraphin/TAP.html. (2002)
22. Rigaut G., Shevchenko A., Rutz B., Wilm M., Mann M., and Seraphin B. (1999) A generic protein purification method for protein complex characterization and proteome exploration. *Nat. Biotechnol.* **17,** 1030–1032.

23. Puig O, Caspary F, Rigaut G, et al. (2001) The tandem affinity purification (TAP) method: a general procedure of protein complex purification. *Methods* **24,** 218–229.
24. Kjeldsen, T. (2000) Yeast secretory expression of insulin precursors. *Appl. Microbiol. Biotechnol.* **54,** 277–286.
25. Hauf, J., Zimmermann, F. K., and Muller, S. (2000) Simultaneous genomic overexpression of seven glycolytic enzymes in the yeast *Saccharomyces cerevisiae*. *Enzyme Microb. Technol.* **26,** 688–698.
26. Gao, C. Y. and Pinkham, J. L. (2000) Tightly regulated, beta-estradiol dose-dependent expression system for yeast. *BioTechniques* **29,** 1226–1231.
27. Psaridi-Linardaki, L., Mamalaki, A., Remoundos, M., and Tzartos, S. J. (2002) Expression of soluble ligand- and antibody-binding extracellular domain of human muscle acetylcholine receptor alpha subunit in yeast *Pichia pastoris*. Role of glycosylation in alpha-bungarotoxin binding. *J. Biol. Chem.* **277,** 26,980–26,986.
28. Goldstein, A. L., and McCusker, J. H. (1999) Three new dominant drug resistance cassettes for gene disruption in *Saccharomyces cerevisiae*. *Yeast* **15,** 1541–1553.
29. Elble, R. (1992) A simple and efficient procedure for transformation of yeasts. *BioTechniques* **13,** 18–20.
30. Nordhoff, E., Krogsdam, A. M., Jorgensen, H. F., Kallipolitis, B. H., Clark, B. F., Roepstorff, P., and Kristiansen, K. (1999) Rapid identification of DNA-binding proteins by mass spectrometry. *Nat. Biotechnol.* **17,** 884–888.
31. http://www.invitrogen.com:80/content.cfm?pageid=3440&nv=1. (2002)
32. Gietz, R. D. and Woods, R. A. (2001) Genetic transformation of yeast. *BioTechniques* **30,** 816–6, 828.

11

Site-Directed Mutagenesis

Jane Nøhr and Karsten Kristiansen

1. Introduction

Site-directed mutagenesis (SDM) is a powerful tool for analyzing protein structure and function, protein folding, and enzyme mechanism ***(1)***. Several protocols for SDM by using polymerase chain reaction (PCR) are available ***(2–4)***, resulting in protocols that are faster, more efficient, and less tedious. The major problem encountered in site-directed mutagenesis is, however, not the introduction of the mutations but the separation of the mutagenized DNA from the wild-type DNA that served as a template. One of the fastest and most powerful mutagenesis and selection strategies is QuikChange™ developed by Stratagene Inc. (La Jolla, CA). The protocol shown in this chapter was developed from this method and allows rapid introduction of mutations (insertions, deletions, and exchanges) into a sequence of interest, using one or two complementary mutagenesis primers to amplify the entire plasmid in a single PCR reaction. This is followed by the destruction of the parental wild-type template by *Dpn*I digestion and the direct transformation into *Escherichia coli* cells. This strategy allows introduction and selection of desired mutants in as little as 24 h.

The strategy is based on the properties of two enzymes. The first critical step is the generation of the mutagenized DNA without introducing additional undesired mutations. A DNA polymerase with proofreading activity, as the thermostable DNA polymerase isolated from *Pyrococcus furiosis* (*Pfu* polymerase, Stratagene, Piscataway, NJ), is extremely well-suited to amplify DNA with high fidelity. The second critical step in this mutagenesis/selection protocol is the discrimination between wild-type DNA template and mutagenized DNA. A very simple approach is to take advantage of the fact that the wild-type DNA differs from the mutated DNA, not only because of the introduced mutation, but also because the mutated DNA is synthesized in vitro and there-

From: *Methods in Molecular Biology, vol. 232: Protein Misfolding and Disease: Principles and Protocols*
Edited by: P. Bross and N. Gregersen © Humana Press Inc., Totowa, NJ

fore not methylated as the wild-type DNA synthesized in vivo. This difference is owing to the fact that most bacteria have a species-specific modification/restriction system that secures recognition and destruction/removal of foreign DNA. Thus, wild-type DNA purified from almost all common *E. coli* strains will be methylated whereas the mutagenized DNA synthesized in a PCR reaction will not. This difference can be exploited to remove the methylated template. The sequence GATC is the recognition sequence of the *dam* methylation system in *E. coli*, which specifically methylates the adenosine at N6. The restriction enzyme *Dpn*I recognizes only fully or hemimethylated 5'-G^{m6}ATC-3' DNA sequences. Because the recognition sequence is short (only four bases), it will occur by chance in high numbers in all sequences and therefore *Dpn*I will digest the methylated wild-type template into small fragments.

In conclusion: high fidelity in vitro mutagenesis can be carried out using *Pfu* polymerase to generate mutated DNA, and treatment with *Dpn*I is subsequently used to remove the wild-type DNA template. The mutagenized DNA is then transformed directly into *E. coli*.

2. Materials

1. PCR cycler.
2. Thin-walled PCR tubes.
3. Template plasmid containing the gene of interest (50 ng/µL).
4. PCR primer (125 ng/µL) (*see* **Notes 1** and **2**).
5. DNA polymerase with proofreading activity, e.g., *Pfu* polymerase (Stratagene, La Jolla, CA).
6. 10X Polymerase buffer (as supplied with the polymerase).
7. 10 m*M* Deoxyribonucleoside triphosphate (dNTP) stock solution (each 2.5 m*M*).
8. Restriction endonuclease *Dpn*I (New England Biolabs Inc., Beverly, MA).
9. 10X *Dpn*I restriction enzyme buffer (New England Biolabs Inc.).
10. 37°C Incubator.
11. Competent *E. coli* cells.

3. Method

3.1. PCR Reactions

1. Pipet into the appropriately labeled tubes according to Table 1 and in the given order.
2. Mix the contents of the tubes very carefully. Give the tubes a quick spin in a tabletop centrifuge, and add 1.0 µL (2.5 U/µL) *Pfu* polymerase (*see* **Note 4**) to each reaction tube except for the control tube. Immediately after adding the polymerase to the reaction tubes, mix well, but gently (try not to make air bubbles), and transfer the tubes to the PCR cycler.
3. PCR conditions are:
   a. Heated lid: 110°C
   b. Preliminary denaturation: 95°C, 30 s

Table 1
Schema for PCR Reactions

Solutions	Test tube 1 (mutation)	Test tube 2 (control)
H_2O	17.5 μL (18.5 μL for single primer SDM; *see* **Note 2**)	(18.5 μL (19.5 μL for single primer SDM; *see* **Note 2**)
10X *Pfu* buffer	2.5 μL	2.5 μL
10 m*M* dNTP	1.0 μL	1.0 μL
Oligo 1	1.0 μL (125 ng)	1.0 μL (125 ng)
Oligo 2	1 μL (125 ng) (0.0 μL for single primer SDM)	1 μL (125 ng) (0.0 μL for single primer SDM)
Template DNA	1.0 μL (50 ng)	1.0 μL (50 ng)

c. Cycles: 16
d. Denaturation: 95°C, 30 s
e. Annealing: 50–60°C (*see* **Note 3**), 1 min
f. Extension: 68°C, 2 min/kb plasmid length (>15 min)

3.2. Dpn*I Digestion*

Add 2.9 μL 10X *Dpn*I buffer to each PCR tube. Mix well. Add 1 μL (20 U) *Dpn*I to each tube, mix well, but gently. Spin down in tabletop centrifuge and transfer the restriction enzyme reaction to new tubes (*see* **Note 5**). Incubate at 37°C for 2 h (or more).

3.3. Transformation of E. coli

1. Use 1–2 μL (*see* **Note 6** and **7**) from the *Dpn*I-digested PCR reactions for transformation into 50 μL competent *E. coli* cells using standard protocols ***(5)***. Streak out on selective Luria broth (LB) agar plates containing an appropriate antibiotic. Incubate overnight (*see* **Note 8**).
2. Isolate plasmid DNA from bacterial clones, and sequence or digest to confirm that the desired mutation has been introduced. Typically, >80% of the colonies will contain the mutation (*see* **Note 9**).

4. Notes

1. The PCR is primed by two mutagenic primers that are completely complementary. The primers have to fulfill certain requirements. The annealing temperature, a function of length and base composition, should not be too low or too high. Typically, 15–17 nucleotides on either side of the mutation will be appropriate. Because the template DNA and the mutation to be introduced dictate the primer

sequence, the choice of the base composition is not at will. Although the genetic code is degenerate, one might expect any codon will be fine as long as the desired amino acid is encoded. However, certain codons for a particular amino acid are preferred over other codons. If possible, the most preferred codon should be used in the design of the mutagenic primer. The preference for different codons can be found in codon frequency tables for highly expressed genes for particular organisms (e.g., http://www.kazusa.or.jp/codon/).

2. It is possible to make SDM with only one mutagenic primer ***(6)***. It is the same setup as for the traditional PCR-based SDM, but only one mutagenic primer is used. This results in a primer extension, which is treated the same way as the protocol involving two primers for PCR. For some primers/types of mutation, the single primer reactions actually work better than the normal two primers primed reactions. For example, for the construction of large deletions, insertions, and exchanges (>20 bases), the single primer protocol is recommended.
3. The annealing temperature can be determined as the temperature 2°C higher than the melting temperature (T_m) of the part of the primer complementary to the region downstream of the mutation.
   T_m is calculated manually by the "4 + 2 rule" (T_m (°C) = (numbers of G + C) × 4 + (numbers of A + T) × 2) or by use of one of the utilities available on the internet (e.g., http://alces.med.umn.edu/rawtm.html). In cases when T_m exceeds the extension temperature, perform a two-step PCR with annealing and extension at 68°C. For optimal primer annealing, we recommend to design primers with G or C as start and end nucleotide if possible.
4. The *Pfu* polymerase can be exchanged with other proofreading polymerases as long as they are performing well at high temperatures over long periods, because the long extension times needed make the PCR programs very long. If the PCR reaction fails, it is worth trying different polymerases (e.g., Platinum Pfx [LifeTechnologies]) instead of starting optimization of the PCR conditions/buffers.
5. The transfer of the reaction to a new tube after the addition of DpnI gives fewer colonies arising from undigested template.
6. It is important only to use a small amount of the PCR-*Dpn*I mixture for transformation because this mixture contains several compounds, particularly the dNTPs, which are known to negatively influence the transformation efficiency.
7. It is possible to clean up the PCR-*Dpn*I reaction (either by standard phenol:chloroform extraction or a commercial PCR purification kit as, e.g., GFX™ PCR DNA and Gel Band Purification Kit, Amersham Pharmacia Biotech Inc., Piscataway, NJ) prior to transformation. This improves the transformation efficiency.
8. The transformation efficiency of the competent cells needs to be high for a successful experiment. The tubes with *Pfu* polymerase should result in tens to hundreds of colonies. The control tube without *Pfu* polymerase should result in zero to only very few colonies.
9. If the *Dpn*I digest of the PCR reaction for some reason fails, the wild-type template in the transformation will result in hundreds of colonies of wild type

transformants. The control tube made without *Pfu* polymerase is crucial for detection of this problem, and will save the researcher hours of tedious checking of wild-type transformants.

Acknowledgments

Jane Nøhr was supported by grant no. 9502914 from the Danish Research Councils Committee on Biotechnology.

References

1. Botstein, D., and Shortle, D. (1985) Strategies and applications of in vitro mutagenesis. *Science* **229,** 1193–1201.
2. Papworth, C., Bauer, J., Braman, J., and Wright, D. (1996) Site-directed mutagenesis in one day with >80% efficiency. *Strategies* **9,** 3–4.
3. Barik, S. (1996) Site-directed mutagenesis in vitro by megaprimer PCR. *Methods Mol. Biol.* **57,** 203–215.
4. Ho, S. N., Hunt, H. D., Morton, R. M., Pullen, J. K., and Pease, L. R. (1989) Site-directed mutagenesis by overlap extension using the polymerase chain reaction. *Gene* **77,** 51–59.
5. Sambrook, J., Fritsch, E. F., and Maniatis, T. (1989) *Molecular Cloning: A Laboratory Manual*. Cold Spring Harbor Laboratory Press, Cold Spring Harbor, New York.
6. Makarova, O., Kamberov, E., and Margolis, B. (2000) Generation of deletion and point mutations with one primer in a single cloning step. *BioTechniques* **29,** 970–972.

12

Pulse-Chase Labeling Techniques for the Analysis of Protein Maturation and Degradation

Annemieke Jansens and Ineke Braakman

1. Introduction

Pulse-chase experiments have proved to be a powerful tool to study protein folding, maturation, and degradation in mammalian cells. When short pulses are applied, a fraction of the total protein pool can be followed from synthesis to degradation in its natural environment.

The technique was successfully used with a number of endogenous and viral proteins: IgA ***(1)***, thyroglobulin ***(2)***, Influenza hemagglutinin ***(3)***, vesicular stomatitis virus G protein ***(4)***, and HIV-1 Envelope glycoprotein ***(5)***.

This protocol describes a basic pulse-chase assay for adherent cells and cells in suspension. With minor modifications, described in the Notes section, this protocol can be adapted to study disulfide-bond formation, folding, oligomerization, maturation and other processes as well as degradation of proteins, in both adherent and suspension cells.

Pulse chase experiments can be divided into three stages: 1) the actual pulse chase, 2) immunoprecipitation of the protein of interest, and 3) sodium dodecyl sulfate polyacrylamide gel electrophoresis (SDS-PAGE) analysis (**Fig. 1**). At the end of each stage, samples in principle can be snap-frozen in liquid nitrogen and stored at –80°C.

2. Materials

2.1. Pulse-Chase

1. Adherent cell line expressing protein of interest grown in sterile 60-mm tissue-culture dishes (*see* **Note 1**).
2. 37°C humidified 5% CO_2 incubator.

From: *Methods in Molecular Biology, vol. 232: Protein Misfolding and Disease: Principles and Protocols*
Edited by: P. Bross and N. Gregersen © Humana Press Inc., Totowa, NJ

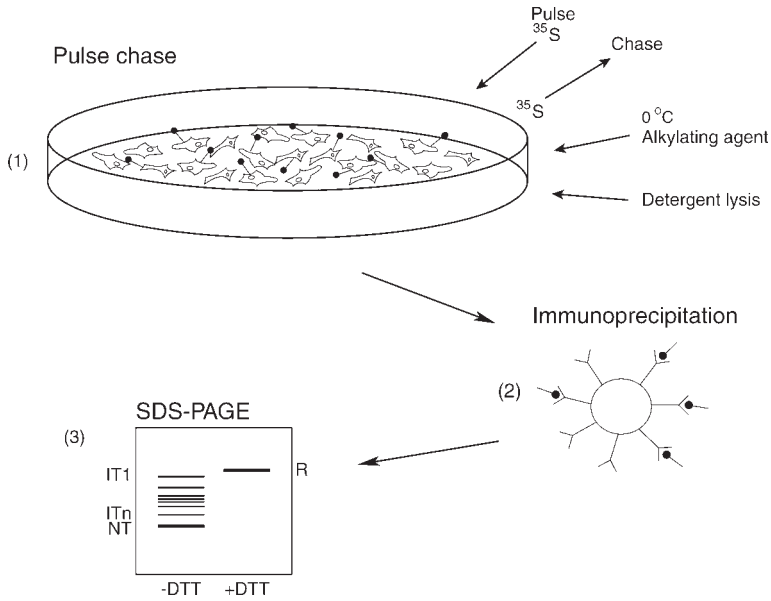

Fig. 1. Pulse-chase experiments can be divided into three stages: *(1)* the actual pulse chase, *(2)* immunoprecipitation of the protein of interest, and *(3)* SDS-PAGE analysis.

3. 37°C waterbath with nonfloating racks to hold tissue-culture dishes.
4. Aspiration flask suitable to collect liquid radioactive waste in a safe manner.
5. Flat, wide ice pan with fitted aluminium plate (e.g., VWR Scientific), covered with wet tissue paper to increase cooling of dishes.
6. HEPES (*N*-2-hydroxyethylpiperidine-*N'*-ethanesulfonic acid): 1 *M* in H_2O, pH 7.4, store at 4°C.
7. Methionine: 250 m*M* in H_2O, store at –20°C.
8. Cysteine: 500 m*M* in H_2O, store at –20°C.
9. *N*-ethylmaleimide (NEM): 1 *M* in ethanol, store at –20°C.
10. Ethylenediaminetetraacetic acid (EDTA): 200 m*M* in H_2O, pH 6.8.
11. Phenylmethylsulfonyl fluoride (PMSF): 1 *M* in dry isopropanol; store at –20°C.
12. Protease inhibitors: 10 mg/mL each of chymostatin, leupeptin, antipain, and pepstatin in dimethyl sulfoxide (DMSO), store at –20°C.
13. Wash buffer: Hank's balanced salt solution (HBSS; Invitrogen) at 37°C.
14. Depletion medium: cysteine and methionine-free tissue-culture medium (ICN) containing 10 m*M* HEPES, pH 7.4 at 37°C.
15. Labeling medium: cysteine and methionine-free tissue-culture medium containing 10 m*M* HEPES, pH 7.4, 125–250 μCi [^{35}S]-cysteine and/or methionine/mL; at 37°C; prepare fresh from stocks (*see* **Notes 2** and **3**).

16. Chase medium: complete tissue-culture medium appropriate for the cell line used, containing 10 m*M* HEPES, 5 m*M* cysteine, 5 m*M* methionine; at 37°C; prepare fresh from stocks (*see* **Notes 4** and **5**).
17. Stop buffer: HBSS containing 20 m*M* NEM; at 4°C (*see* **Notes 5** and **6**).
18. Iodoacetamide: 500 m*M* in H_2O, store at -20°C.
19. Iodoacetic acid: 500 m*M* in H_2O, store at -20°C.
20. Lysis buffer: phosphate-buffered saline (PBS), pH 7.4, or similar salt-containing buffer, containing 0.5% (v/v) Triton X-100, 1 m*M* EDTA, 20 m*M* NEM, 1 m*M* PMSF, protease inhibitors: 10 μg/mL each of chymostatin, leupeptin, antipain, and pepstatin (*see* **Notes 5–7**).
21. Cycloheximide: 50 m*M* in H_2O, store at –20°C.
22. 5 mL disposable pipet.
23. 1–10 mL dispenser.
24. Timer with seconds indication.
25. Cell scraper.
26. Liquid nitrogen.

2.2. Immunoprecipitation

1. 10% Protein A-Sepharose beads in PBS or similar buffer containing one-tenth of the concentration of same detergent used in lysis buffer and 0.1% bovine serum albumin (BSA) (*see* **Notes 8** and **9**).
2. Antibody against protein of interest.
3. Head over head rotator.
4. Eppendorf tube shakers.
5. Immunoprecipitation wash buffer: PBS, pH 7.4, containing 0.5% (v/v) Triton X-100 or 150 m*M* NaCl (*see* **Note 9**).
6. TE buffer: 10 m*M* Tris-HCl, pH 6.8, 1 m*M* EDTA.
7. Heat block at 95°C.
8. 200 m*M* DTT in H_2O stock; store at –20°C.
9. 2X concentrated nonreducing sample buffer: 400 m*M* Tris-HCl, pH 6.8, 6% (w/v) SDS, 20% glycerol, 2 m*M* EDTA, 0.01% (w/v) bromophenol blue.
10. 5X concentrated sample buffer: 1 *M* Tris-HCl, 7.5% (w/v) SDS, 50% glycerol, 5 m*M* EDTA, 0.02% (w/v) bromophenol blue; store at –20°C.

2.3. SDS-PAGE Analysis

1. SDS-PAGE equipment, preferably minigel systems (BioRad or Amersham-Pharmacia).
2. Coommassie stain: 0.25% (w/v) Coommassie brilliant blue in destain.
3. Destain: 30% (v/v) methanol and 10% (v/v) acetic acid in H_2O.
4. Neutralizer: 30% (v/v) methanol in PBS (*see* **Note 10**).
5. Enhancer: 1.5 *M* sodium salicylate in 30% (v/v) methanol in H_2O.
6. Schleicher & Schuell filter paper 0.4 mm.
7. Gel drying equipment.

3. Methods

3.1. Pulse-Chase (Basic Protocol)

Two alternative pulse-chase procedures, one for adherent cells (**Subheading 3.1.1.**) and one for suspension cells (**Subheading 3.1.2.**) are given.

3.1.1. Pulse-Chase for Adherent Cells

The volumes described here are based on 60 mm tissue culture dishes. When other sizes are used, volumes must be adjusted based on surface area of the dish.

1. Seed cells expressing the protein of interest in 60 mm dishes (*see* **Note 1**). On the day of the experiment the cells need to be subconfluent (90%). At least one dish per time point is needed.
2. Prepare the pulse chase set up (**Fig. 2**).
3. Wash cells with 2 mL wash buffer and add 2 mL depletion medium. Incubate cells for 15 min at 37°C in an humidified 5% CO_2 incubator (*see* **Note 11**).
4. Place the cells on the racks in the waterbath (37°C), make sure the water level is just above the racks and air bubbles do not accumulate under the dishes.
5. Pulse-label the cells, one dish at a time, by quickly aspirating the depletion medium and adding 400 µL labeling medium to the centre of the dish (for pulse times longer than 15 min a larger volume and incubation on a rocker in a 37°C humidified 5% CO_2 incubator is recommended). Swirl gently to equally divide the labeling medium over the cells, make sure no air bubbles accumulate under the dish. Incubate for the pulse period (*see* **Notes 2**, **3** and **11**).
6. For 0-min chase interval:
   a. Add 2 mL chase medium at precisely the end of the labeling interval to stop labeling instantly. Swirl gently to mix.
   b. Aspirate the chase medium as quickly as possible. Place the dish on the aluminium plate on the ice pan and immediately add 2 mL ice cold stop buffer.
7. For all other chase intervals:
   a. Add 2 mL chase medium at precisely the end of the pulse interval to stop labeling instantly. Swirl gently to mix. Aspirate chase medium and again add 2 mL chase medium. Incubate for the desired chase intervals on the 37°C waterbath for short intervals or in a 37°C humidified 5% CO_2 incubator for chase intervals over 30 min.
   b. At precisely the end of the chase interval, aspirate the chase medium. Place the dish on the aluminium plate on the ice pan and add 2 mL of ice-cold stop buffer.
8. Just before lysis, wash the cells again with 2 mL ice-cold stop buffer.
9. Aspirate dish as dry as possible and add 600 µL ice-cold lysis buffer.
10. Scrape cell remains off the dish with a cell scraper and transfer the lysate to an Eppendorf tube.

Fig. 2. Pulse-chase setup. 1) Tissue-culture dishes with adherent cells expressing the protein of interest, 2) waterbath with racks, 3) aspirating device, 4) aspiration flask with liquid radioactive waste, 5) flat ice pan with aluminium plate covered with pre-wetted tissues, 6) labeling medium, 7) chase medium, 8) stop buffer, 9) lysis buffer, 10) 5-mL pipet, 11) 1–10 mL dispenser, 12) timer, 13) cell scraper, 14) monitor for radioactivity, 15) solid radioactive waste.

11. Centrifuge the cell lysates at 16,000*g* for 10 min at 4°C to pellet the nuclei. At this point the postnuclear cell lysates can be snap-frozen in liquid nitrogen and stored at –80°C.

3.1.2. Pulse-Chase for Suspension Cells

The samples of the different chase intervals are taken from a single tube of labeled cells. Wash steps after the pulse and chase are not included because the centrifugation steps necessary for this procedure take too much time. Prior to starting the experiment it is necessary to determine: 1) the minimum volume for incubating the cells during the pulse (x µL), 2) the number of chase time points (y), and 3) the desired sample volume (z). For instance, we used per chase time point: $x = 100$ µL, $y = 1$, and $z = 500$ µL.

1. Transfer suspension cells to a sterile 50-mL tube with cap. Use approx 10^6 cells per time point.
2. Pellet cells at 500*g* for 4 min at 20–37°C. Resuspend cells in 2y mL depletion medium and pellet cells again. Resuspend cells in 2y mL depletion medium. Incubate cells for 15 min at 37°C in an CO_2 incubator.

3. Pellet cells at 500*g* for 4 min at 20–37°C. Resuspend cells in *x* µL depletion medium, change to appropriate tube if necessary, and place in waterbath (37°C).
4. Add 50–100 µCi ^{35}S labeled methionine and cysteine per time point and mix gently to start the pulse. Incubate for the pulse period.
5. Add ≥ 4 times *x* µL chase medium. The total volume should be slightly more than *y* times *z* µL to allow for fluid loss owing to evaporation during the experiment. Mix by gently pipetting up and down.
6. Immediately take the first sample of *z* µL. Transfer to eppendorf tube with pre-prepared *z* µL 2X concentrated lysis buffer on ice; mix well, and keep on ice.
7. After every chase interval, collect a *z* µL sample and add to *z* µL 2X concentrated lysis buffer; mix well, and keep on ice.
8. Centrifuge the cell lysates at 16,000*g* for 10 min at 4°C to pellet the nuclei. At this point the postnuclear cell lysates can be analyzed by immunoprecipitation and SDS-PAGE or snap-frozen in liquid nitrogen and stored at –80°C.

3.2. Immunoprecipitation

1. Mix 50 µL 10% Protein A-Sepharose beads and the antibody, shake or rotate head over head 1 h in an eppendorf tube shaker at 4°C (*see* **Note 8**).
2. Add 100–600 µL postnuclear cell lysate. Rotate head over head 1 h at 4°C (*see* **Note 8**).
3. Pellet Protein A-Sepharose beads by microcentrifuging 1 min at 16,000*g* at room temperature. Aspirate supernatant and resuspend beads in 1 mL immunoprecipitation wash buffer. Shake a minimum of 5 min in eppendorf tube shaker at room temperature (*see* **Note 9**). Repeat **step 3**.
4. Pellet beads and aspirate supernatant. Add 20 µL TE buffer, vortex, add 20 µL 2X sample buffer without reducing agent, vortex again.
5. Heat samples for 5 min at 95°C, vortex, and pellet Protein A-Sepharose beads. The supernatant is the nonreduced sample.
6. Transfer 18 µL supernatant to a tube containing 2 µL of 200 m*M* dithiothreitol (DTT) and vortex. Heat samples for 5 min at 95°C. Centrifuge shortly at 16,000*g* to give reduced sample (*see* **Note 12**).

3.3. SDS-PAGE

1. Prepare 1- or 0.75-mm thick polyacrylamide separating and stacking minigels (*see* **Note 13**).
2. Load 8 µL of each sample. Do not use the outer lanes of the gel and load 1X nonreducing sample buffer in empty lanes to prevent "smiling" of the bands.
3. Run each gel at 25 mA constant current until the dye front is at the bottom of the gel (approx 1 h).
4. Stain the gel with coomassie stain for 5 min and destain for at least 30 min.
5. Neutralize the gel in neutralizer for at least 5 min (0.75 mm) or 10 min (1 mm) (*see* **Note 10**).
6. Treat gel 15 min (0.75 mm) or 20 min (1 mm) with enhancer.

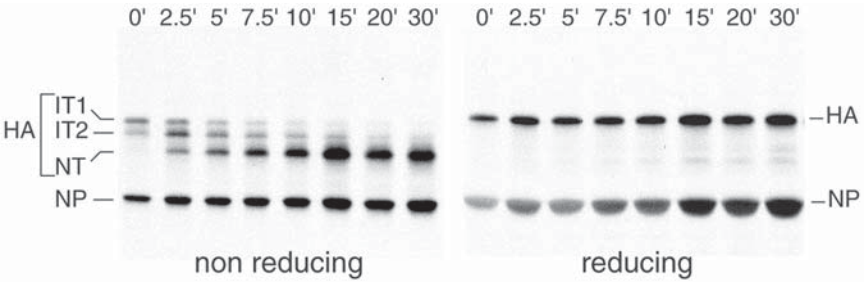

Fig. 3. Folding of influenza hemagglutinin (HA) in HeLa cells at 27°C. Cells were pulse labeled for 2 min with 50 μCi ^{35}S-labeled cysteine and 50 μCi tran[^{35}S] label. Chase medium contained 0.5 m*M* cycloheximide. Stop buffer and lysis buffer contained 20 m*M* NEM. HA was immunoprecipitated with a polyclonal antiserum directed against influenza virus and 10% heat-killed, fixed *Staphylococcus aureus* cells. HA folds into its native form (NT) via two less compact folding intermediates, IT1 and IT2 (nonreducing SDS-PAGE). When the same samples are reduced, one HA band is detected (reducing SDS-PAGE). In addition to HA, the polyclonal antiserum immunoprecipitates nucleoprotein (NP).

7. Dry gel on 0.4 mm Schleicher & Schuell filter paper. Expose to film (for example, Kodak BioMax MR-1) at –80°C or to a Phosphor imaging screen.

With minor modifications, the basic protocol can be extended to study conformational changes (*see* **Note 14**); aggregation and oligomerization of proteins (*see* **Note 15**); degradation (*see* **Note 16**); protein localization (*see* **Note 17**); or the effect of various conditions on folding, maturation, and degradation (*see* **Note 18**). **Figure 3** illustrates a typical folding assay for influenza hemagglutinin.

4. Notes

1. When (endogenous) protein expression is very low, cells can be transiently transfected with a lipid mixture and a plasmid encoding the protein of interest behind an appropriate promotor (*see* Chapter 16). Alternatively, virus-based expression systems can be used, such as Vaccinia T7 ***(6)*** or adenovirus ***(7)***.
2. Labeling medium should contain 50–100 μCi [^{35}]S-methionine and/or cysteine per 60-mm tissue-culture dish with subconfluent cells (1×10^6 cells). This amount is sufficient to visualize a highly expressed average protein in a 1- to 2-min pulse. Depending on the number of cysteines and methionines in the protein, ^{35}S-labeled methionine or a mixture of the two can be used. The stabilized form of methionine and cysteine (e.g., Redivue Promix ^{35}S cell labeling mix, Amersham Pharmacia) is less volatile and is preferred to minimize radioactive contamination of air, pipets, and equipment.

3. When the effects of certain conditions, such as ATP depletion, are tested it may be necessary to separate the folding process from translation. Disulfide-bond formation, and thereby folding of disulfide-bonded proteins, can be prevented by incubating the cells in a reducing agent. When the reducing agent is removed after pulse-labeling, disulfide bond formation and folding may proceed ***(8)***. At **step 5** of **Subheading 3.1.1.**, use pulse-labeling medium with 5–10 m*M* DTT, then proceed as described.
   Labeling efficiency may be slightly diminished by the presence of DTT; the duration of the pulse labeling therefore may be increased. During long incubations, DTT may affect cellular ATP levels, depending on the cell line. The efficiency, rate, and outcome of completely posttranslational folding should be compared to the regular folding assay before the effects of different conditions are tested.
4. When the kinetics of a process, e.g., disulfide-bond formation or degradation, are studied, cycloheximide (final concentration 1 m*M*) should be added to the chase medium. Cycloheximide will stop elongation of unfinished nascent polypeptide chains and will prevent incorporation of label in full-length protein after the pulse period.
5. Prepare pulse-chase media freshly before use. With a half-life of approx 30 min at 37°C and a few hours on ice, PMSF is highly unstable in water. Add just before use or as an alternative use the more stable Pefabloc (Boehringer).
6. The basic protocol can be used to study folding and disulfide-bond formation in proteins. An alkylating agent, (e.g., NEM) iodoacetamide, or iodoacetic acid) to block free SH-groups of cysteines must be included in the stop buffer and lysis buffer to prevent disulfide-bond formation to occur after the chase interval. In theory, alkylating agents can be omitted when only reduced samples are analyzed. Free SH-groups of cysteines, however, can promote aggregation, which may diminish detection of the protein of interest. Add NEM, iodoacetamide, or iodoacetic acid to a final concentration of 20 m*M*. In principle, these alkylating agents should give similar results except that electrophoretic mobilities may change ***(9)***.
7. During lysis it is crucial to keep the nuclei intact. A lysis buffer should contain a buffer with buffering capacity of approx pH 7.4 such as PBS, HEPES, or MES. Salt concentration should be chosen such that the nuclei are not disrupted owing to osmosis, preferably iso-osmotic. The amount and choice of detergent depends on the protein analyzed and the purpose of the experiments. When noncovalent interactions are studied, Triton X-100 often is not preferred. Instead, detergents with different characteristics can be tested, such as CHAPS ((3-[3-cholamidopropyl)dimethylammonio]-1-propanesulfonate), deoxycholate, octylglucoside, digitonin, or a mixture of detergent and lipid.
8. The amount of antibody needed is dependent on the antigen, the antibody, and its concentration. For each antibody-protein combination, the optimal coupling time and conditions need to be determined. During coupling, head over head rotation is preferred over shaking to minimize damage to Protein A-Sepharose beads.

When small volumes are used, however, shaking may give better results. Coupling times can vary between 30 min and overnight incubations. For some antibodies, the preincubation of antibody and sepharose beads can be omitted. Instead of Protein A-Sepharose beads, a solution of 10% heat-killed, fixed *Staphylococcus aureus* cells can be used. Some antibodies only bind protein G-sepharose beads. If coupling of the antibody to sepharose beads or *S. aureus* cells is poor, a linker of an anti-mouse IgG can be used.

9. The optimal wash buffer needs to be determined for every antibody-antigen combination. The wash buffers mentioned in the protocol are extremely mild and will maintain most of the antibody-antigen interaction but may lead to high background. To decrease background many variables can be changed. Detergents with different characteristics such as Triton X-100, CHAPS, deoxycholate, octylglucoside, digitonin, or a mixture of detergent and lipid can be used with increasing concentrations. The addition of SDS at a concentration ≥ 0.05% (w/v) may be especially helpful to reduce background. Also, salt concentration may be increased. In addition, the time of shaking during the washes can be increased, rather than the number of washes. The temperature of the wash can also affect the level of background: the higher the temperature, the lower the background. Wash temperatures may range from 4°C to room temperature. Different buffers may be tested, but their pH optimally should be above 7.0. Another method to reduce background is to preclear the antibody with nonlabeled lysates of cells lacking the protein of interest, or to preclear the lysate by a 1-h incubation with *S. aureus* cells. Protein A-sepharose beads should be washed and taken up in a buffer containing of 0.1% BSA to reduce nonspecific binding to the beads.
10. The incubation period with neutralizer should be minimally 5 min to ensure the pH > 6 (pH can be checked with pH paper) to prevent precipitation of salicylate in the enhancer solution. Prolonged incubations should be avoided to prevent diffusion of bands.
11. Variation in labeling between different dishes is a problem often encountered during pulse-chase experiments. The reason usually is insufficient accuracy during the pulse labeling. In this case, a digital timer with seconds indication is indispensable. The starvation incubation should be 15 min for the first pulsed sample and not exceed 30 min for later pulsed samples, to ensure optimal labeling. Starvation periods outside this time frame may lead to less labeling of proteins. As a control for variation in labeling, 5 µL total lysate of each sample can be analyzed by SDS-PAGE.
12. In reducing SDS-PAGE the protein ideally forms one band, although modifications of oligosaccharides can change the electrophoretic mobility, resulting in a fuzzy smear. In gel re-oxidation can also occur and is prevented by adding at least 2 times the molar DTT concentration of NEM to the samples prior to loading samples on gel. Samples containing excess NEM or another alkylating agent should not be heated to 95°C, to prevent nonspecific NEM binding to other amino acids than cysteine.

13. Adjust the acrylamide percentage to your protein. For instance, influenza HA (84 kD) folding is analyzed on 7.5% SDS-PAGE.
14. Because disulfide-bond formation is not identical to folding, it can be necessary to monitor conformational changes during folding of the protein. Combinations of the following modifications on the basic pulse-chase protocol are especially informative:
    a. By using an array of conformation-specific antibodies for immunoprecipitation, conformational changes can be monitored during folding and maturation ***(10)***.
    b. In general, a protein will become more compact during the folding process; this can lead to DTT resistance of particular disulfide bonds in a protein in the intact cell ***(11)***. DTT resistance can be analyzed by performing an additional 10 min chase in the presence of 10 m*M* DTT after the normal chase interval (**Subheading 3.1.**, **steps 6a**, and **7a**) of the basic pulse chase protocol.
    c. Changes in conformational compactness can also lead to protease resistance of certain parts of the protein ***(12)***. Follow the basic protocol until **Subheading 3.1.**, **step 11**. Omit EDTA, PMSF, and other protease inhibitors in the lysis buffer, and incubate part of the postnuclear lysate with the desired protease on ice. Optimal concentration and incubation time should be determined for each protease. Add PMSF and (specific) protease inhibitors and proceed with immunoprecipitation as in **Subheading 3.2.**, **step 1** of the basic protocol. With time, one or more protease resistant bands can appear. With the use of conformation-specific antibodies, specific resistant domains can be identified.
15. Aggregation and oligomerization can be detected by the appearance of large molecular complexes in the gel. Noncovalent complexes need to be detected by velocity sucrose gradients ***(13)*** or can be stabilized by chemical cross linking ***(14,15)***.
16. To study protein degradation, proteasome inhibitors and inhibitors of lysomal and autophagic pathways ***(16,17)*** can be used in the pulse-chase protocol.
17. Protein localization can be indicative for the maturation state of proteins. The following adaptations on the basic protocol allow the detection of different maturation states:
    a. Endo H sensitivity. Because Endo H specifically cleaves *N*-linked glycans in their pre-Golgi-state, Endo H sensitivity is a measure for pre-Golgi localization of an *N*-glycosylated protein ***(18)***. Follow the basic protocol until **step 2** in **Subheading 3.2.**, then pellet beads and aspirate supernatant. Resuspend beads in 15 µL 0.2% SDS in 100 m*M* sodium acetate, pH 5.5, and heat at 95°C for 5 min. Cool, add 15 µL 100 m*M* sodium acetate, pH 5.5, containing 0.025 U EndoH (Boehringer) and protease inhibitors: 10 µg/mL each of chymostatin, leupeptin, antipain, and pepstatin, and incubate 1.5 h at 37°C. Add 7.5 µL 5X sample buffer and mix. Continue basic protocol with **step 5** in **Subheading 3.2.**
    b. Surface expression. Surface expression can be monitored by protease digestion on intact cells ***(19)***. Follow the basic protocol until **Subheading 3.1.1.**, **step 7b**, wash the cells two times with 2 mL stop buffer. Add 0.5 mL PBS

containing 100 μg/mL trypsin or another protease and 2 m*M* $CaCl_2$ at 4°C to the cells. Incubate 30 min on ice. Collect fluid from cells and add (in final concentration) 100 μg/mL soy bean trypsin inhibitor, 1 m*M* PMSF, and other protease inhibitors: 10 μg/mL each of chymostatin, leupeptin, antipain, and pepstatin. Use for immunoprecipitation. Add to the cells 0.5 mL PBS containing 100 μg/mL soy bean trypsin inhibitor or other protease inhibitors and incubate 5 min on ice and repeat. Lyse the cells in 600 μL lysis buffer and continue with the basic protocol **step 11** in **Subheading 3.1.1.** When the protein of interest is on the cell surface, the protein (fragments) can be found in the fluid taken off the cells after digestion and a decrease in signal should be observed in the cell fraction. However, if the protein cannot be detected in the fluid collected from the cells, the protein might be totally degraded by the trypsin. Protein fragments might be present on the cell surface. For instance, Influenza hemagglutinin trimers are digested into two subunits that stay associated with the plasma membrane and can be detected by 12% SDS-PAGE ***(12)***.

Other methods to monitor surface expression include biotinylation and antibody recognition of surface proteins ***(20)***.

In accordance, secretion of the protein in the medium can be monitored by collecting the chase medium after the chase interval and using this for immunoprecipitation.

18. The effect of various conditions, such as the influence of *N*-glycosylation ***(21)***, ATP ***(22)***, calcium ***(23,24)*** and temperature (**Fig. 3**), can be tested on folding, maturation, and degradation.

Acknowledgments

We thank A. I. Azuaga-Fortes, I. M. Liscaljet, and C. M. Maggioni for useful discussions and critical reading of the manuscript, and J. den Boesterd for assistance with the figures.

A version of this chapter has been printed previously as part of the PhD thesis of Annemieke Jansens "Folding of the LDL receptor in the endoplasmatic reticulum" (University of Utrecht, Netherlands).

References

1. Solari, R. and Kraehenbuhl, J. P. (1984) Biosynthesis of the IgA antibody receptor: a model for the transepithelial sorting of a membrane glycoprotein. *Cell* **36,** 61–71.
2. Kim, P. S. and Arvan, P. (1991) Folding and assembly of newly synthesized thyroglobulin occurs in a pre-Golgi compartment. *J. Biol. Chem.* **266,** 12,412–12,418.
3. Braakman, I., Hoover-Litty, H., Wagner, K. R., and Helenius, A. (1991) Folding of influenza hemagglutinin in the endoplasmic reticulum. *J. Cell Biol.* **114,** 401–411.
4. Doms, R. W., Ruusala, A., Machamer, C., Helenius, J., Helenius, A., and Rose, J. K. (1988) Differential effects of mutations in three domains on folding, quaternary structure, and intracellular transport of vesicular stomatitis virus G protein. *J. Cell Biol.* **107,** 89–99.

5. Earl, P. L., Moss, B., and Doms, R. W. (1991) Folding, interaction with GRP78-BiP, assembly, and transport of the human immunodeficiency virus type 1 envelope protein. *J. Virol.* **65,** 2047–2055.
6. Fuerst, T. R., Niles, E. G., Studier, F. W., and Moss, B. (1986) Eukaryotic transient-expression system based on recombinant vaccinia virus that synthesizes bacteriophage T7 RNA polymerase. *Proc. Natl. Acad. Sci. USA* **83,** 8122–8126.
7. Bastaki, M., Braiterman, L. T., Johns, D. C., Chen, Y. H., and Hubbard, A. L. (2002) Absence of direct delivery for single transmembrane apical proteins or their "Secretory" forms in polarized hepatic cells. *Mol. Biol. Cell* **13,** 225–237.
8. Braakman, I., Helenius, J., and Helenius, A. (1992) Manipulating disulfide bond formation and protein folding in the endoplasmic reticulum. *EMBO J.* **11,** 1717–1722.
9. Hollecker, M. (1989) Counting integral numbers of residues by chemical modification, in *Protein Structure, A Practical Approach* (Creighton, T. E., ed.), IRL Press, Oxford University Press, Oxford, pp. 145–153.
10. Hurtley, S. M., Bole, D. G., Hoover-Litty, H., Helenius, A., and Copeland, C. S. (1989) Interactions of misfolded influenza virus hemagglutinin with binding protein (BiP). *J. Cell Biol.* **108,** 2117–2126.
11. Tatu, U., Braakman, I., and Helenius, A. (1993) Membrane glycoprotein folding, oligomerisation and intracellular transport: effects of dithiothreitol in living cells. *EMBO J.* **12,** 2151–2157.
12. Copeland, C. S., Doms, R. W., Bolzau, E. M., Webster, R. G., and Helenius, A. (1986) Assembly of influenza hemagglutinin trimers and its role in intracellular transport. *J. Cell Biol.* **103,** 1179–1191.
13. Doms, R. W., Keller, D. S., Helenius, A., and Balch, W. E. (1987) Role for adenosine triphosphate in regulating the assembly and transport of vesicular stomatitis virus G protein trimers. *J. Cell Biol.* **105,** 1957–1969.
14. Wong, S. S. and Wong, L. J. (1992) Chemical crosslinking and the stabilisation of proteins and enzymes. *Enzyme Microb. Technol.* **14(11),** 866–874.
15. Tatu, U. and Helenius, A. (1997) Interactions between newly synthesized glycoproteins, calnexin and a network of resident chaperones in the endoplasmic reticulum. *J. Cell Biol.* **136,** 555–565.
16. Gelman, M. S., Kannegaard, E. S., and Kopito, R. R. (2002) A principal role for the proteasome in ER-associated degradation of misfolded intracellular Cystic Fibrosis Transmembrane Conductance Regulator. *J. Biol. Chem.* **277,** 11,709–11,714.
17. Thevenod, F. and Friedmann, J. M. (1999) Cadmium-mediated oxidative stress in kidney proximal tubule cells induces degradation of Na+/K(+)-ATPase through proteasomal and endo-/lysosomal proteolytic pathways. *FASEB J.* **13,** 1751–1761.
18. Tarentino, A. L., Trimble, R. B., and Maley, F. (1978) Endo-beta-*N*-Acetylglucosaminidase from Streptomyces plicatus. *Methods Enzymol.* **50,** 574–580.
19. de Silva, A. M., Balch, W. E., and Helenius, A. (1990) Quality control in the endoplasmic reticulum: folding and misfolding of vesicular stomatitis virus G protein in cells and in vitro. *J. Cell Biol.* **111,** 857–866.

20. Harter, C. and Mellman, I. (1992) Transport of the lysosomal membrane glycoprotein lgp120 (lgp-A) to lysosomes does not require appearance on the plasma membrane. *J. Cell Biol.* **117,** 311–325.
21. Hammond, C., Braakman, I., and Helenius, A. (1994) Role of *N*-linked oligosaccharide recognition, glucose trimming, and calnexin in glycoprotein folding and quality control. *Proc. Natl. Acad. Sci. USA* **91,** 913–917.
22. Podbilewicz, B. and Mellman, I. (1990) ATP and cytosol requirements for transferrin recycling in intact and disrupted MDCK cells. *EMBO J.* **9,** 3477–3487.
23. Guest, P. C., Bailyes, E. M., and Hutton, J. C. (1997) Endoplasmic reticulum Ca2+ is important for the proteolytic processing and intracellular transport of proinsulin in the pancreatic beta-cell. *Biochem. J.* **323(Pt 2),** 445–450.
24. Lodish, H. F. and Kong, N. (1990) Perturbation of cellular calcium blocks exit of secretory proteins from the rough endoplasmic reticulum. *J. Biol. Chem.* **265,** 10,893–10,899.

13

Detection of Aggregates and Protein Inclusions by Staining of Tissues

James E. Galvin

1. Introduction

Immunohistochemistry (IHC) and similar techniques are the cornerstone of pathologic investigation to visualize and localize protein aggregates and inclusions found in the brains of individuals with neurodegenerative diseases. The principle of IHC is: use an antibody against a specific protein or sequence contained within a protein to demonstrate its presence within a section of tissue. IHC complements nicely traditional histopathologic staining such as Hematoxylin/Eosin and Silver stains and adds specificity to the identification of protein misfolding in neuromorphometric analysis.

Monoclonal and polyclonal antibodies (MAbs/PAbs) are now available from a wide variety of commercial sources directed against most, if not all, of the major components of inclusions. Because of their ready availability, IHC has become an essential diagnostic tool for the detection and evaluation of aggregates and protein inclusions.

1.1. Inclusions in Neurodegenerative Diseases

The presence of "disease-specific" pathologic changes in the brains of patients with neurodegenerative diseases assist pathologists in the diagnosis and characterization of dementing illnesses. Intraneuronal inclusions owing to abnormalities in protein folding are common features in many neurodegenerative disorders (**Table 1**) ***(1,2)***. It is now clear however, that inclusions are not specific for any one disease. For example neurofibrillary tangles (NFTs) are found in Alzheimer's disease (AD); frontotemporal dementia (FTD); progressive supranuclear palsy (PSP); corticobasal degeneration (CBD); dementia with

From: *Methods in Molecular Biology, vol. 232: Protein Misfolding and Disease: Principles and Protocols*
Edited by: P. Bross and N. Gregersen © Humana Press Inc., Totowa, NJ

Table 1
Abnormal Protein Folding and Inclusions in Neurodegenerative Disease

Disease	Inclusions	Protein
Alzheimer's disease	Senile plaque	Amyloid β-protein
	Neurofibrillary tangle	Tau
	Neuropil thread	
	Hirano body	Actin-binding protein
Parkinson's disease	Lewy body	α-Synuclein
	Dystrophic neurite	
Dementia with Lewy bodies	Lewy body	α-Synuclein
	Dystrophic neurite	
ALS-Parkinson-dementia complex	Senile plaque	β-Amyloid
	Neurofibrillary tangle	Tau
	Lewy body	α-Synuclein
Frontotemporal dementia	Neurofibrillary tangle	Tau
Pick's disease	Pick body	Tau
Corticobasal degeneration	Neurofibrillary tangle	Tau
	Coil body	
	Astrocytic plaque	
Progressive supranuclear palsy	Neurofibrillary tangle	Tau
	Tufted astrocyte	
Amyotrophic lateral sclerosis	Skein body	Ubiquitin
	Hyaline conglomerate	Neurofilament
Neurodegeneration with brain iron accumulation	Axonal spheroid	α-Synuclein
	Lewy body	
Multiple system atrophy	Glial cytoplasmic inclusion	α-Synuclein
Huntington's disease	Intraneuronal inclusions	Polyglutamine
Creutzfeld-Jacob disease	Plaque	Prion protein

150

Lewy bodies (DLB); as well as several rare disorders such as Niemann-Pick disease, Dementia pugilistica, and Subacute sclerosing panencephalitis ***(2–7)***.

The finding that insoluble lesions owing to protein misfolding across different cell types and across different disorders suggests that many of the neurodegenerative disorders share common pathologic roots ***(2)***. Despite the fact that the disorders themselves express different clinical phenotypes and pathologic lesions, the mechanisms underlying protein misfolding and subsequent filament formation may be similar. A common theme emerging in the study of neurodegenerative disease is to consider these disorders as abnormalities in protein metabolism (i.e., proteinopathy) ***(2)***. The posttranslational modification of soluble proteins alters in some way their biophysical properties and leads to the formation of insoluble filamentous aggregates ***(1,2)***.

These biochemical changes likely lead to the initiation of a cascade of intracellular events, ultimately resulting in neuronal dysfunction and death. This dysfunction produces the characteristic clinical phenotype for each disorder. It is reasonable therefore to propose that understanding shared abnormalities in protein folding across disorders (e.g., synucleinopathies, tauopathies, amyloidopathies) will provide insights into disease mechanisms underlying neurodegenerative disorders characterized by abundant filamentous lesions ***(1,2,4)***.

1.2. Amyloid β-Protein

Amyloid β-protein (Aβ) is a 39–43 amino acid peptide cleaved from a larger precusor protein (amyloid precursor protein or APP) found on chromosome 21 ***(8–10)***. Aβ deposits extracellularly as senile plaques either as a loose, nonfibrillar form (diffuse plaques) or a more compacted, fibrillar form, often with dystrophic neurites coursing through the plaque (neuritic plaque).

1.2.1. Alzheimer's Disease

AD, the most common form of dementia, is characterized by abundant diffuse and neuritic plaques throughout nearly all cortical regions ***(8,10)***. Mutations in three proteins have been described leading to early onset inherited forms of AD: APP protein on chromosome 21, presenilin-1 on chromosome 14, and presenilin-2 on chromosome 1 ***(11)***. All mutations lead to an increased production of the 42-amino acid isoform of Aβ (the predominant form in neuritic plaques).

1.2.2. Down's Syndrome

Individuals with Down's syndrome (DS) who reach the age 40–45 will develop cognitive decline, and their brains are characterized by senile plaques (SPs) identical to those seen in AD ***(8,12)***. The chromosomal abnormality in the

vast majority of DS patients is a triplication of chromosome 21, the site of the APP gene; hence, it is not surprising to find SPs as a major pathologic lesion.

1.3. Tau Protein

Tau protein is a microtubule-associated protein encoded on chromosome 17 ***(3)***. Its normal function is to stabilize microtubules and it has numerous sites available for phosphorylation. When hyperphosphorylated, tau forms insoluble filaments that deposit in the cell body of the neuron as an NFT and in the axons and dendrites as neuropil threads (NTs) ***(3,4)***.

1.3.1. Alzheimer's Disease

NFTs in AD are composed primarily of paired helical filaments (two strands of 10 nm-in diameter filaments that twist around each other like a helix) ***(3)***. NFTs first appear in the hippocampus and entorhinal cortex in the AD brain and later involve the limbic and neocortex as the dementia severity worsens.

1.3.2. Frontotemporal Dementias

These dementias are characterized by wide range of behavioral, social, cognitive, and motor disturbances ***(5)***. Unlike AD, Aβ often is not found in the brains of patients with FTD. Inherited forms of FTD have been linked to chromosome 17 and are often associated with features of parkinsonism ***(6)***. The NFTs in FTD and AD are similar in appearance.

1.3.3. Corticobasal Degeneration

This rare disorder is characterized by asymmetric parkinsonism, cortical sensory abnormalities, and dementia ***(7)***. Pathologically, neuronal tau inclusions are seen in swollen neurons. Additionally, there are glial tau inclusions in oligodendrocytes (coiled bodies) and the processes of astrocytes (astrocytic plaques).

1.3.4. Progressive Supranuclear Palsy

This disorder is characterized by parkinsonism, axial rigidity, and a supranuclear vertical gaze palsy ***(7)***. Pathologically, neuronal tangles are seen in cortical and subcortical neurons and glial tau inclusions are found in astrocytes (tufted astrocytes).

1.4. α-Synuclein Protein

α-synuclein (AS) is a 141-amino acid presynaptic protein of unknown function found on chromosome 4q21.3-q22 ***(2,13–15)***. AS is the major building of filaments found in neuronal (Lewy bodies) ***(2,13)*** and oligodendrocyte (Glial cytoplasmic) inclusions ***(2,16)***.

1.4.1. Parkinson's Disease and Dementia with Lewy Bodies

In 1997, investigators linked mutations in the AS gene with autosomal dominant Parkinson's disease (PD) in several Mediterranean families (A53T mutation) ***(14)*** and one large German family (A30P mutation) ***(15)***. Subsequently, AS was found to be the major structural component of the filaments found in substantia nigra (SN) Lewy bodies of PD and the neocortical Lewy bodies seen in Dementia with Lewy bodies (DLB) ***(13)***. Other components of Lewy bodies include ubiquitin and neurofilaments ***(2,17,18)***.

1.4.2. Multiple Systems Atrophy

AS has also been found to be the major filamentous component of the glial cytoplasmic inclusion seen in multiple system atrophy (MSA) ***(16)***, a syndrome complex with parkinsonism; cognitive decline; and abnormalities in autonomic control of blood pressure, cerebellum, and gait.

1.4.3. Other Disorders With Synuclein Inclusions

Approximately 25% of AD patients will have cortical Lewy bodies on autopsy, even in the absence of parkinsonism ***(2,17)***. A significant proportion of individuals with DS also will have Lewy bodies, predominantly found in the amygdala ***(12)***. Neurodegeneration with brain iron accumulation (formerly referred to as Hallervorden-Spatz syndrome) is characterized by axonal spheroid, dystrophic neurites and Lewy body-like inclusions that are all immunoreactive for α-synuclein ***(19)***.

2. Materials

2.1. Detection of Protein Aggregates by Immunohistochemistry (9,12,13,16–23)

1. Tris-buffered saline (TBS): 100 m*M* Tris-HCl, pH 7.5, 0.9% (w/v) NaCl; use fresh buffer for each step.
2. Phosphate-buffered saline (PBS): 0.13 *M* NaCl, 7 m*M* Na_2HPO_4, 7 m*M* NaH_2PO_4; use fresh buffer for each step.
3. Tissue processing and fixation: Fixed tissue may be embedded and stored indefinitely. Previously frozen tissue may be used (*see* **Note 1**). All of these procedures may also be performed on free-floating sections.

The most common fixative agents used in archived neuronal tissue are:

a. 10% Neutral-buffered formalin (available commercially).
b. 4% Paraformaldehyde: 4 g paraformaldehyde are added to 100 mL PBS under a hood. Solution is stirred and heated to 50°C for 15 min. Add a few drops of 2 *M* NaOH to clear solution and filter. Always prepare fresh.
c. 70% Ethanol (EtOH), 150 m*M* NaCl.

Whole brain must be submerged in fixative for a minimum of 3–4 wk to fix the tissue but this does not give optimum histopathologic preservation of structure and antigens for immunohistochemistry. Fresh dissection of brain regions in 1–2-cm thick sections and overnight fixation gives excellent preservation of antigen for histopathologic and neuromorphometric analysis.

4. Mounting tissue: Tissue section should be no thicker than 10 μm to permit adequate penetration of antibodies and reagents. To assure that sections adhere to glass slides, the slides should be pretreated with a polymer such as poly-L-lysine or kits such as Vectorbond reagent (Vector Labs, Burlingame, CA). Although slightly more expensive, Fisher SuperFrost Plus (Fisher Scientific, Cat. no. 12-550-15) slides provide superior adherence owing to electrostatic charges with minimal effort.
5. Controls for IHC are essential for interpretation of staining. Controls should include both tissue and antibody controls. To assure that the procedure worked, tissue with known immunoreactivity (i.e., AD temporal cortex for Aβ staining) should be used as a positive control, and known normal tissue with immunoreactivity should be used as a negative control. A section should also be incubated with normal serum without primary antibody to account for any nonspecific binding that may occur.
6. Blocking agents: Blocking solutions are critical to diminish nonspecific binding. Nonspecific binding reduces the signal and will make it much harder to discern small or weakly staining intraneuronal inclusions. There are several different agents used for blocking. Blockers typically used for Western blots such as 2% milk are not recommended. Recommended blockers include bovine serum albumin (BSA; 1–2%) added to buffer, detergents (0.1–0.2% Triton X-100), or 2% IgG-free serum (e.g., horse, goat) added to buffer. Neural tissue is rich in peroxidase and alkaline phosphatase that may interfere with IHC chromogen development (*see* **Note 2**). For peroxidase-based reactions, pretreatment with methanol/hydrogen peroxide (*see* **Subheading 3.1.2.1., step 6**) will eliminate endogenous activity. For alkaline phosphatase reactions, 1 m*M* levimisole may be added. Blocking agents can be kept refrigerated at 4°C for up to 2 wk. Discard if solution becomes cloudy or precipitates.
7. Antibodies: A wide variety of antibodies against major components of protein inclusions are commercially available, although many of these can be quite expensive. **Table 2** summarizes some of the antibodies used in IHC evaluation of neural tissue as well as providing vendor names. Directories of antibodies are also available on the Internet (www.alzforum.org).
8. Uneven labeling: Poor tissue fixation, poor sections, uneven thickness of sections, sections drying out or not covering the entire section with antibody, and air bubbles over the section during procedures are common reasons for uneven labeling. Be sure to incubate sections in a humidified or moist chamber.
9. Counterstaining: Counterstaining techniques (*see* **Note 3**) are useful to allow for detection of nuclei and morphology. These techniques are to be used after completion of immunohistochemical reactions. The choice of color should be

Table 2
Commercially Available Antibodies Against Major Protein Constituents of Neuronal Inclusions

Antigen	Vendor	Epitope	Specificity	Host
α-Synuclein	Abcam	aa 116-131	Human, rat	Sheep
α-Synuclein	Alexis	aa 116-131	Human, mouse	Mouse
α-Synuclein	Biosource		Human	Rabbit
α-Synuclein	Chemicon	aa 111-131	Human, rat	Rabbit
α-Synuclein	Chemicon	aa 111-131	Human	Goat
α-Synuclein	Chemicon	aa 108-121	Human, rat, mouse	Sheep
α-Synuclein	Novo-Castra	Full length		Mouse
α-Synuclein (4B12)	Signet	Full length	Human	Mouse
α-Synuclein (LB509)	Zymed	aa 117-124	Human-specific	Mouse
Amyloid precursor protein (APP) (3G12)	Accurate		Human	Mouse
APP	Alexis	aa 653-662	Human, rat mouse	Rabbit
APP	Biosource	aa 1-100	Human-specific	Mouse
APP	Chemicon	aa 99-126	Human, mouse	Rabbit
APP	Zymed	APP 695	Human	Mouse
β-Amyloid (6F/3D)	Accurate	aa 8-17	Human	Mouse
β-Amyloid	Biosource	Aβ 1-40	Human	Mouse
β-Amyloid	Biosource	Aβ 1-42	Human	Mouse
β-Amyloid (AB10)	Chemicon	aa 1-16	Human	Mouse
β-Amyloid (4G8)	Signet	aa 17-24	Human, mouse	Mouse
β-Amyloid (6E10)	Signet	aa 1-17	Human, mouse	Mouse
Tau (Alz50)	Peter Davies	PHF-tau	Human	Mouse
Tau (PHF-1)	Peter Davies	Ser396, Ser404	Human	Mouse
Tau (Tau-5)	Chemicon		Human, rat	Mouse
Tau	DAKO		Human	Rabbit
Tau (AT8)	Endogen	Ser202	Human	Mouse
Tau (AT180)	Endogen	Thr231	Human	Mouse
Tau (T14)	Zymed	aa 83-120	Human	Mouse
Tau (T46)	Zymed	aa 404-441	Human	Mouse
Ubiquitin (1510)	Chemicon		Human	Mouse
Ubiquitin (1680)	Chemicon		Human	Rabbit

Key: aa, amino acid; PHF, paired helical filament; Ser, serine; Thr, threonine.

based on personal preference and compatibility with the choice of chromogen during immunohistochemistry. The three most commonly used counterstains are hematoxylin (blue), methyl green (green), and nuclear fast red (pink). Many vendors (i.e., Vector Laboratories) sell these counterstains in stock solution concentration. The brown chromogen (DAB) works well with most counterstains. Some colors may be incompatible (e.g., vector red with nuclear fast red). The package insert should be consulted.

10. Coverslipping: Most chromogens are stable in solvents and can be cleared in xylene (check package insert). Dehydration of sections prior to light microscopy will improve resolution.
11. Staining in animal tissue: With the advent of transgenic animal models, the use of immunohistochemical techniques has become a powerful investigative tool in the neuromorphometric analysis of mouse brain ***(22)***. Most MAbs are derived from murine tissue and thus may increase the nonspecific binding of the antibodies and the background staining. One way to optimize staining of mouse brain with murine MAbs is the M.O.M. immunodetection kit (Mouse on Mouse, Vector labs).

2.2. Detection of Protein Aggregates by Immunofluourescence (16,18,23)

1. Antibodies: A variety of fluorochrome antibodies are available commercially. Common fluorochromes include antibodies that fluoresce green (fluorescein, FITC), red (rhodamine, Texas red and TRITC) and blue (AMCA). Commercial vendors that we have had good results with include Jackson ImmunoResearch Laboratories, Molecular Probes, Sigma, and Vector Labs.
2. Thioflavin S ***(23)*** stock solutions:

   a. 0.05% $KMnO_4$/PBS.
   b. 0.2% $K_2S_2O_5$/0.2% oxalic acid/PBS.
   c. 50% EtOH/50% PBS.
   d. 0.0125% Thioflavin S/40% EtOH/60% PBS (make fresh for each use; *see* **Note 4**).

3. Congo red ***(23)*** stock solutions:

   a. NaCl saturated 80% EtOH: Add NaCl in excess to 80% EtOH, stir well, and allow undissolved NaCl to settle out of solution overnight.
   b. Congo red/NaCl saturated 80% EtOH: Prepare as in **step a** and add Congo red in excess, stir well and allow undissolved Congo red and NaCl to settle out of solution overnight.
   c. 1% NaOH.

4. Counterstaining and coverslipping: Counterstaining can be beneficial in examining neural tissue by fluorescence for orientation and localization of inclusions near nuclei. Two principle counterstains are used: DAPI and Propidium Iodide (PI). DAPI produces a blue fluorescence with excitation at 360 nm and emission at 460 nm. PI fluoresces red at excitation of 535 nm and emission of 615 nm.

Sections should be coverslipped with a nonfading mounting media to prevent rapid loss of fluorescence during microscopic examination. An excellent choice is Vectashield (Vector Labs). Vectashield with DAPI or PI counterstain already added are also available.

3. Methods

3.1. Immunohistochemistry (9,12,13,16–23)

Antibodies should be diluted prior to use in serum/buffer solution used for blocking. Optimal working dilutions need to be assessed for each new antibody tested and for every fixative.

3.1.1. Single-Labeling Studies: Overnight ABC Procedure for Paraffin Sections

3.1.1.1. Day 1 (*see* **Note 5**)

1. Immerse sections twice in xylene 5 min each.
2. Immerse sections twice in 100% EtOH 1 min each.
3. Immerse sections in descending EtOH series (95, 80, 70%) 1 min each.
4. Immerse in distilled H_2O 5 min.
5. Antigen-retrieval step if necessary (*see* **Subheadings 3.3.1.** to **3.3.3.** and **Note 6**).
6. Immerse sections in freshly prepared methanol/H_2O_2 (150 mL methanol + 30 mL 30% H_2O_2) for 30 min.
7. Rinse in running H_2O 10 min.
8. Immerse in 0.1 *M* TBS, pH 7.6, for 5 min.
9. Immerse in 0.1 *M* TBS/2% serum for 5 min.
10. Wipe excess fluid from sections and apply 100 µL 1° antibody (Ab).
11. Incubate in humidified chamber (*see* **Note 6**) overnight at 4°C.

3.1.1.2. Day 2

1. Rinse off 1° Ab from tissue with TBS wash bottle (be careful to spray around tissue, not directly on tissue).
2. Immerse in 0.1 *M* TBS 5 min.
3. Immerse in 0.1 *M* TBS/2% serum 5 min.
4. Wipe excess tissue from sections.
5. Apply 100 µL 2° Ab (Vector Labs species-specific IgG at 1/1000).
6. Incubate for 1 h at room temperature.
7. Rinse off 2° Ab with TBS.
8. Immerse in 0.1 *M* TBS 5 min.
9. Immerse in 0.1 *M* TBS/2% serum 5 min.
10. Wipe excess tissue from sections.
11. Prepare ABC reagent from Vector 15 min prior to use.
12. Apply 100 µL ABC reagent.
13. Incubate for 1 h at room temperature.
14. Rinse off ABC reagent with TBS.

15. Immerse in 0.1 *M* TBS 5 min.
16. Prepare chromogen (DAB, DAB-Co, VIP, VectorRed) according to directions.
17. Apply chromogen and develop (watch closely for color change).
18. Wash section in TBS.
19. Lightly counterstain (*see* **Subheading 2.1., item 9**).
20. Dehydrate in ascending series of EtOH (70, 80, 95, 100, 100%) 1 min each.
21. Clear in two changes of xylene 5 min each.
22. Coverslip.

3.1.2. Double-Labeling Studies: Double Stain Procedure for Paraffin Sections

3.1.2.1. Day 1

1. Immerse sections twice in xylene 5 min each.
2. Immerse sections twice in 100% EtOH 1 min each.
3. Immerse sections in descending EtOH series (95, 80, 70%) 1 min each.
4. Immerse sections in distilled H_2O 1 min.
5. Antigen-retrieval step, if necessary.
6. Immerse sections in freshly prepared Methanol/H_2O_2 (150 mL Methanol + 30 mL 30% H_2O_2) for 30 min.
7. Rinse in running H_2O 10 min.
8. Immerse in 0.1 *M* TBS, pH 7.6, for 5 min.
9. Immerse in 0.1 *M* TBS/2% serum for 5 min.
10. Wipe excess fluid from sections and apply 100 µL 1° antibody (Ab).
11. Incubate in humidified chamber (*see* **Note 7**) overnight at 4°C.

3.1.2.2. Day 2

1. Rinse off 1° Ab from tissue with TBS wash bottle (careful to spray around tissue not directly on tissue).
2. Immerse in 0.1 *M* TBS 5 min.
3. Immerse in 0.1 *M* TBS/2% serum 5 min.
4. Wipe excess tissue from sections.
5. Apply 100 µL 2° Ab (Vector Labs species specific IgG at 1/1000).
6. Incubate for 1 h at room temperature.
7. Rinse off 2° Ab with TBS.
8. Immerse in 0.1 *M* TBS 5 min.
9. Immerse in 0.1 *M* TBS/2% serum 5 min.
10. Wipe excess tissue from sections.
11. Prepare ABC reagent from Vector 15 min prior to use.
12. Apply 100 µL ABC reagent.
13. Incubate for 1 h at room temperature.
14. Rinse off ABC reagent with TBS.
15. Immerse in 0.1 *M* TBS 5 min.
16. Prepare chromogen (DAB, DAB-Co, VIP, vector red) according to directions.

17. Apply chromogen and develop (watch closely for color change).
18. Wash section in TBS.
19. Immerse sections in freshly prepared methanol/H_2O_2 (150 mL methanol + 30 mL 30% H_2O_2) for 30 min.
20. Immerse in 0.1 *M* TBS, pH 7.6, for 5 min.
21. Immerse in 0.1 *M* TBS/2% serum for 5 min.
22. Wipe excess fluid from sections and apply 100 µL of second 1° Ab.
23. Incubate in humidified chamber (*see* **Note 7**) overnight at 4°C.

3.1.2.3. Day 3

1. Rinse off 1° Ab from tissue with TBS wash bottle (be careful to spray around tissue, not directly on tissue).
2. Immerse in 0.1 *M* TBS 5 min.
3. Immerse in 0.1 *M* TBS/2% serum 5 min.
4. Wipe excess tissue from sections.
5. Apply 100 µL 2° Ab (Vector Labs species-specific IgG at 1:1000).
6. Incubate for 1 h at room temperature.
7. Rinse off 2° Ab with TBS.
8. Immerse in 0.1 *M* TBS 5 min.
9. Immerse in 0.1 *M* TBS/2% serum 5 min.
10. Wipe excess tissue from sections.
11. Prepare ABC reagent from Vector 15 min prior to use.
12. Apply 100 µL ABC reagent.
13. Incubate for 1 h at room temperature.
14. Rinse off ABC reagent with TBS.
15. Immerse in 0.1 *M* TBS 5 min.
16. Prepare chromogen (DAB, DAB-Co, VIP, VectorRed) according to directions.
17. Apply chromogen and develop (watch closely for color change).
18. Wash section in TBS.
19. Lightly counterstain.
20. Dehydrate in ascending series of EtOH (70, 80, 95, 100, 100%) 1 min each.
21. Clear in two changes of xylene 5 min each.
22. Coverslip.

3.2 Immunofluorescence (16,18,23)

Antibodies should be prepared fresh and diluted with serum/buffer solution used for blocking. Once prepared, fluorescent antibodies should be kept in the dark.

3.2.1. Double-Labeling Studies

3.2.1.1. Day 1

1. Immerse sections twice in xylene 5 min each.
2. Immerse sections twice in 100% EtOH 1 min each.

3. Immerse sections in descending EtOH series (95, 80, 70%) 1 min each.
4. Immerse in 0.1 *M* TBS, pH 7.6, 5 min.
5. Immerse in 0.1 *M* TBS/2% serum for 5 min.
6. Wipe excess fluid from sections and apply 100 µL 1° antibody (Ab).
7. Incubate in humidified chamber (*see* **Note 7**) overnight at 4°C.

3.2.1.2. Day 2

1. Rinse off 1° Ab from tissue with TBS wash bottle (careful to spray around tissue, not directly on tissue).
2. Immerse in 0.1 *M* TBS 5 min.
3. Immerse in 0.1 *M* TBS/2% serum 5 min.
4. Wipe excess tissue from sections.
5. Apply 2° Ab (fluorochrome) 100 µL to section.
6. Incubate in covered tray (**in the dark**) for 2 h at room temperature.
7. Rinse off 2° Ab.
8. Immerse in 0.1 TBS, place on shaker 2 × 20 min each.
9. Immerse in water 5 min.
10. Post fix in neutral-buffered formalin for 30 min.
11. Wash in water twice, 10 min each time.
12. Coverslip with Vectorshield or other nonfading medium (*see* **step 4** in **Subheading 2.2.**).
13. Store at 4°C in dark.

*3.2.2. Thioflavin S Staining **(23)***

1. Deparaffinize sections as in **Subheading 3.1.** and hydrate to distilled H_2O.
2. Immerse sections in neutral-buffered formalin for 1 h.
3. Rinse in tap water for 10 min.
4. Immerse in PBS 5 min.
5. Immerse in 0.05%$KMnO_4$/PBS 20 min.
6. Rinse in PBS twice for 2 min each.
7. Destaining step: immerse in 0.2%$K_2S_2O_5$/0.2% oxalic acid/PBS 1–3 min. Incubation should extend until brown color has been removed completely from sections.
8. Rinse in PBS three times for 2 min each.
9. Immerse sections in 0.0125% thioflavin S/40% EtOH/60% PBS for 3 min in dark (cover staining dish with aluminum foil).
10. Differentiate sections: Immerse in 50% EtOH/50% PBS twice 10 s.
11. Rinse in PBS three times 5 min each.
12. Coverslip with Vectashield and seal edges with nail polish.

*3.2.3. Congo Red Staining **(23)***

1. Deparaffinize sections as above and hydrate to distilled H_2O if a hematoxylin counterstain is desired. If not, hydrate sections through 80% EtOH and continue to **step 3**.

2. Counterstain in filtered Hematoxylin for 1 min; rinse in several changes of H_2O.
3. Decant NaCl saturated 80% EtOH into staining container (do not agitate sedimented NaCl); add 1 mL 1% NaOH/100 mL NaCl saturated 80% EtOH.
4. Immerse sections for 10 min.
5. Decant Congo red solution; add 1 mL 1% NaOH/100 ml Congo red solution.
6. Blot section and immerse in Congo red solution for 10 min.
7. Blot sections and differentiate in 80% EtOH until pink stain is barely visible macroscopically; check fluorescence for desired background.
8. Dehydrate in ascending series of EtOH (70, 80, 95, 100, 100%) 1 min each.
9. Clear in 2 changes of xylene 5 min each.
10. Coverslip.

Results:

Amyloid:	Pink to red
Elastic fibers:	Lighter red
Nuclei:	Blue (if counterstained)
Background:	Unstained
Polarized light:	Apple-green
Fluorescence:	Yellow to green

3.3. Antigen Retrieval

All steps here take place after the slides are deparaffinized and before placement in the methanol/H_2O_2 solution in IHC protocols and before TBS in the immunofluoresence protocol (*see* **Note 6**.)

3.3.1. Triton X-100(0.2%)/0.1 mM TBS ***(18–20)***

1. Place slides in solution for 5 min at room temperature.
2. Rinse in running water 2 min.
3. Place sections in buffer to be used for immunostaining 5 min.

3.3.2. Formic Acid (88%) ***(9,19,20)***

1. Place section in 88% formic acid for 1–5 min. (The longer the sections remain in formic acid, the more likely that neuronal morphology will be disrupted.)
2. Wash in running water for 5 min.
3. Place sections in buffer to be used for immunostaining 5 min.

3.3.3. Microwave ***(24)***

1. Place slides in metal-free staining rack containing distilled H_2O into microwave.
2. Heat at highest setting for approx 3.5 min OR until boiling.
3. If slides do not boil after 3.5 min, heat for 20-s increments until solution reaches 95°C.
4. Maintain temperature at 95°C for 5 min, heating additional 20 s increments as necessary.

5. Let stand to equilibrate to room temperature 15–20 min.
6. Place in buffer to be used for subsequent immunostaining 5 min.

3.3.4. Antigen Amplification

For improved signal, tyramine amplification systems (e.g., Perkin Elmer, Life Sciences, Boston MA) may be used. This method will enable weaker IHC signals to be detected more readily.

4. Notes

1. Previously frozen tissue can be processed by EtOH fixation. Tissue of interest is removed via mallet and chisel. Do not allow tissue to thaw. Immediately place tissue into 70% EtOH/150 m*M* NaCl. Trim tissue to no thicker than 5 mm and allow section to fix overnight at room temperature on a shaker. Process the tissue for paraffin embedding as per protocol.
2. Endogenous peroxidase or alkaline phosphatase will increase the background and diminish specific signaling. Pretreating the sections with hydrogen peroxide or levimisole (*see* **Subheading 2.1.4.**) will significantly diminish the background in this case. Avoid allowing sections to dry out because this can either increase the background or prevent adequate staining. Leaving the secondary antibodies on for longer periods of time (> 1 h) also will increase the background. An important point to remember: not all antibodies are created equal. PAbs may be more sensitive but also produce higher background. Blocking for longer periods of time (up to 1 h) or increasing the concentration of serum in the blocking agent (up to 50%) should diminish the interference.
3. Counterstains should be optimized for each tissue type, antigen-unmasking protocol, and IHC staining intensity desired. Slight changes in color of chromogens may occur owing to counterstaining (i.e., Vector NovaRed becomes slightly brownish with Methyl Green counterstaining).
4. In the thioflavin protocol, tissue tends to disintegrate at higher concentrations of $KMnO_4$/PBS and $K_2S_2O_5$/oxalic acid/PBS stock solutions (be careful with free-floating sections). Make minimal amounts of the Thioflavin stock solution; it really should be used fresh but can be reused up to 1 wk if stored in dark container at 4°C.
5. Overnight staining can be completed in a single day. After application of primary antibody, sections can be incubated at room temperature for 4 h. The Day 2 protocol can then be begun.
6. Commercial Antigen Recovery kits. There are several commercially available kits (e.g., Vector Labs, Signet Labs) that typically combine citric acid and heat to improve antigen recovery and antibody binding. If purchased, follow package insert.
7. A simple method for making a humidified chamber is to place damp Kimwipes in the staining tray with the sections and cover.

Acknowledgments

This work was supported in part by a pilot grant from the State of Missouri Alzheimer's Disease and Related Disorders Program and by generous support of Alan A. and Edith L. Wolff.

References

1. Trojanowski, J. Q., Goedert, M., Iwatsubo, T., and Lee, V. M.-Y. (1998) Fatal attraction: abnormal protein aggregation and neuron death in Parkinson's disease and Lewy body dementia. *Cell Death Differ.* **5,** 832–837.
2. Galvin, J. E., Lee, V. M. Y., and Trojanowski, J. Q. (2000) Synucleinopathies: Clinical and pathological implications. *Arch. Neurol.* **58,** 186–190.
3. Vogelsberg-Ragaglia, V., Trojanowski, J. Q., and Lee, V. M.-Y. (1999) Cell biology of tau and cytoskeletal pathology of Alzheimer's disease, in *Alzheimer's Disease*, 2nd ed. (Terry, R. D., Katzman, R., Bick, K. L., and Sisodia, S. S., eds.), Lippincott Williams & Wilkins, Philadelphia, PA, pp. 359–372.
4. Spillantini, M. G., Tolnay, M., Love, S., and Goedert, M. (1999) Microtubule-associated protein tau, heparan sulphate and α-synuclein in several neurodegenerative diseases with dementia. *Acta Neuropathol.* **97,** 585–594.
5. Neary, D., Snowden, J. S., Gustafson, L., Passant, U., Stuss, D., Black, S., et al. (1998) Frontotemporal lobar degneration: a consensus on clinical diagnostic criteria. *Neurology* **51,** 1546–1554.
6. Foster, N. L., Wilhelmsen, K., Sima, A. A., Jones, M. Z., D'Amato, C. J., and Gilman, S. (1997) Frontotemoral dementia and parkinsonism linked to chromosome 17: a consensus conference. *Ann. Neurol.* **41,** 706–715.
7. Dubinsky, R. M. (2000) Parkinsonism syndromes: clinical features, in *Neurodegenerative Dementias* (Clark, C. M., and Trojanowski, J. Q., eds.), McGraw-Hill, New York, NY, pp. 241–246.
8. Dickson, D. W. (1997) The pathogenesis of senile plaques. *J. Neuropathol. Exp. Neurol.* **56,** 321–339.
9. Ginsberg, S. D., Galvin, J. E., Lee, V. M., Rorke, L. B., Dickson, D. W., Wolfe, J.H., et al. (1999) Accumulation of intracellular amyloid β-peptide ($A\beta_{1\text{-}40}$) in mucopolysaccharidosis brains. *J. Neuropathol. Exp. Neurol.* **58,** 815–824.
10. Mirra, S. S., Gearing, M., McKeel, D. W. Jr., Crain, B. J., Hughes, J. P., van Belle, G., and Heyman, A. (1994) Interlaboratory comparison of neuropathology assessments in Alzheimer's disease: a study of the Consortium to Establish a Registry for Alzheimer's Disease (CERAD). *J. Neuropathol. Exp. Neurol.* **53,** 303–315.
11. Lippa, C.F., Swearer, J.M., Kane, K.J., Nochlin, D., Bird, T.D., Ghetti, B., et al. (2000) Familial Alzheimer's disease: site of mutation inlfluences clinical phenotype. *Ann. Neurol.* **48,** 376–379.
12. Lippa, C. F., Schmidt, M. L., Lee, V. M.-Y., and Trojanowski, J. Q. (1999) Antibodies to alpha-synuclein detect Lewy bodies in many Down's syndrome brains with Alzheimer's disease. *Ann. Neurol.* **45,** 353–357.

13. Baba, M., Nakajo, S., Tu, P. H., Tomita, T., Nakaya, K., Lee, V. M.-Y., et al. (1998) Aggregation of α-synuclein in Lewy bodies of sporadic Parkinson's disease and dementia with Lewy bodies. *Am. J. Pathol.* **152,** 879–884.
14. Polymeropoulos, M. H., Lavedan, C., Leroy, E., Ide, S. E., Dehejia, A., Dutra, A., et al. (1997) Mutation in the α-synuclein gene identified in families with Parkinson's disease. *Science* **276,** 2045–2047.
15. Kruger, R., Kuhn, W., Muller, T., Woitalla, D., Graeber, M., Kosel, S., et al. (1998) Ala30Pro mutation in the gene encoding α-synuclein in Parkinson's disease. *Nature Genet.* **18,** 106–108.
16. Tu, P. H., Galvin, J. E., Baba, M., Giasson, B., Leight, S., Nakajo, S., et al. (1998) Glial cytoplasmic inclusions in white matter oligodendrocytes of multiple systems atrophy brains contain insoluble α-synuclein. *Ann. Neurol.* **44,** 415–422.
17. Galvin, J. E., Lee, V. M. Y., Schmidt, M. L., Tu, P. H., Iwatsubo, T., and Trojanowski, J. Q. (1999) Pathobiology of the Lewy body. *Adv. Neurol.* **80,** 313–324.
18. Galvin, J. E., Lee, V. M. Y., Baba, M., Mann, D. M. A., Dickson, D. W., Yamaguchi, H., et al. (1997) Monoclonal antibodies to purified cortical Lewy bodies recognize the midsize neurofilament subunit. *Ann. Neurol.* **42,** 595–603.
19. Galvin, J. E., Giasson, B. I., Hurtig, H. I., Lee, V. M.-Y., and Trojanowski, J. Q. (2000) Neurodegeneration with brain iron accumulation, type 1 (NBIA 1) is characterized by α-, β and γ-synuclein neuropathology. *Am. J. Pathol.* **157,** 361–368.
20. Galvin, J. E., Schuck, T. M., Lee, V. M.-Y., and Trojanowski, J.Q. (2001) Differential expression and distribution of α-, β and γ-synuclein in the developing human substantia nigra. *Exp. Neurol.* **168,** 347–355.
21. Galvin, J. E., Uryu, K., Lee, V. M. Y., and Trojanowski, J. Q. (1999) Axon pathology in Parkinson's disease and Lewy body dementia hippocampus contains α-, β- and γ-synuclein. *Proc. Natl. Acad. Sci. USA* **96,** 13,450–13,455.
22. Galvin, J. E., Nakamura, M., McIntosh, T. K., Saatman, K. E., Sampathu, D., Raghupathi, R., et al. (2000) Neurofilament-rich intraneuronal inclusions exacerbate neurodegenerative sequelae of brain trauma in NFH/LacZ transgenic mice. *Exp. Neurol.* **165,** 77–89.
23. Ginsberg, S. D., Galvin, J. E., Chiu, T. S., Masliah, E., Lee, V. M.-Y., and Trojanowski, J. Q. (1998) RNA sequestration to pathological lesions of neurodegenerative disorders. *Acta Neuropathol.* **96,** 487–494.
24. Yachnis, A. T., Rorke, L. B., Lee, V. M.-Y., and Trojanowski, J. Q. (1993) Expression of neuronal and glial polypeptide during histogenesis of the human cerebellar cortex including observations on the dentate nucleus. *J. Comp. Neurol.* **334,** 356–369.

14

Study of Mutant Proteins With Folding Defects in Cultured Patient Cells

Gabriele Dodt and Claudia Walter

1. Introduction

The example used in this chapter concerns the group of autosomal recessive inherited peroxisome biogenesis disorders (PBDs). These disorders are genetically heterogeneous with at least 12 different complementation groups (CGs). CG 1 is the largest characterized by mutations in *HsPEX1*, a gene encoding a 143 kD AAA protein (ATPases associated with diverse cellular activities) ***(1–3)***. About 65% of the PBD patients suffering from peroxisome biogenesis disorders harbor mutations in *PEX1* ***(4–6)***. Although the function of *PEX1* is not defined yet, it is likely that *PEX1* plays a significant role in the import of peroxisomal matrix proteins from the cytosol—where they are translated —into the peroxisomes ***(1,2,7,8)***.

One of the two relatively common alleles in the *HsPEX1* gene that have been identified carries a missense mutation (G843D) and is associated with the milder forms of the PBDs like neonatal adrenoleukodysthrophy (NALD) and infantile Refsum disease (IRD) ***(1,2,6,9–11)***. A second allele with a 1bp insertion (c.2097-2098insT) resulting in a premature stop at amino acid 740 is often present in patients with the severe classical Zellweger syndrome (ZS) ***(6,11)***. Residual amounts of *PEX1* protein were found in the fibroblasts of patients with milder phenotypes, whereas a complete lack of *PEX1* was associated with ZS.

Fibroblasts harboring the G843D allele are characterized by a temperature-dependent phenotype with restoration of import of the matrix enzyme catalase and peroxisomal functions at 30°C ***(9)*** compared to 37°C, where almost no catalase import and peroxisomal functions are detected.

From: *Methods in Molecular Biology, vol. 232: Protein Misfolding and Disease: Principles and Protocols*
Edited by: P. Bross and N. Gregersen © Humana Press Inc., Totowa, NJ

When we examined the *PEX1* protein levels in all patient fibroblasts with the G843D allele, the steady-state level was reduced to 5–10% of that in control fibroblasts. Because the mRNA level in these patients seemed to be normal ***(6)***, a likely possibility is that the mutant *PEX1* protein is degraded immediately. It has been reported that missense mutations often result in partially misfolded proteins that undergo rapid degradation ***(12–14)***. The temperature effect described earlier is a rather common feature of proteins that arise from alleles with missense mutations, because misfolding is reduced at the lower temperature ***(14)***. This results in higher protein levels, leading to an almost normal cellular phenotype.

Here we describe how the determination of the protein level of the respective protein and the test for a temperature effect on the steady-state level of protein and for the function of the protein can help to identify mutant proteins with folding problems. Particularly, we investigated the *PEX1* function by monitoring the import of catalase and by analyzing the *PEX1* protein level under different culturing temperatures.

2. Materials

1. Dulbecco's modified Eagle's medium (DMEM) (PAA, Linz, Austria).
2. Trypsin-EDTA solution: 0.5 g/L trypsin 1/250 (Life Technologies, Eggenstein, Germany), 0.2 g/L ethylenediamine tetraacetic acid (EDTA) • 4Na in Hank's solution without Ca^{2+} and Mg^{2+} (PAA). Filter-sterilize, freeze in aliquots, and store an opened aliquot at 4°C.
3. Hanks' solution without Ca^{2+} and Mg^{2+} (PAA).
4. 5X Sodium dodecyl sulfate (SDS) sample buffer: 10% (w/v) (SDS), 50% (v/v) glycerol, 25% (v/v) β-mercaptoethanol, 0.01% (w/v) bromophenol blue, and 312.5 m*M* Tris-HCl, pH 6.8.
5. SDS running buffer: 26 m*M* Tris-base, 190 m*M* glycine, 0.1% (w/v) SDS. pH should be 8.3; if not discard and make up fresh; do not adjust pH.
6. Coomassie Protein Assay Reagent (Pierce, Rockford, IL).
7. BioRad mini gel apparatus, or equivalent.
8. BioRad mini blot apparatus (BioRad, Munich, Germany) with one cool element, or equivalent.
9. Blotting buffer: 200 mL methanol, 100 mL 10X Tris-glycine buffer (250 m*M* Tris-base, 1.9 *M* glycine) and 0.5 mL 20% (w/v) SDS; add H_2O to 1 L total volume; pH should be 8.3. See comments to **step 5**.
10. Ponceau S solution: 2% Ponceau S in 30% trichloracetic acid (TCA), 30% sulfosalicylic acid, dilute this stock solution 1:10 with water before use.
11. Blocking solution: phosphate-buffered saline (PBS) containing 0.05% (w/v) Tween 20 and 5% (w/v) nonfat dry milk (NFDM).
12. Wash solution: PBS containing 0.1% (w/v) Triton X-100, and 0.02% (w/v) SDS.
13. Primary antibodies: anti-*PEX1* polyclonal rabbit antibodies ***(15)***, diluted 1/15,000 in PBS, 0.1% (w/v) Triton, 2% NFDM.

14. Secondary antibodies: anti-rabbit IgG coupled to horseradish peroxidase (Amersham Biosciences, Freiburg Germany; 1/15,000 in PBS with 0.1% Triton X-100 and 2% NFDM).
15. ECL Western blotting detection reagent (Amersham).
16. Hyperfilm ECL (Amersham).
17. DPBS (Life Technologies), $CaCl_2$ is provided separately and can be omitted.
18. 3% formaldehyde solution in DPBS: 0.41 mL 37% formaldehyde in 5 mL DPBS. Prepare fresh.
19. 1% TritonX-100 in DPBS. Prepare fresh.
20. Primary antibodies: anti human catalase IgG sheep (The Binding Site) diluted 1/100 in DPBS. Prepare fresh.
21. Secondary fluorescent-labeled antibodies: for example, anti-sheep Alexa 488 or Alexa 594 (Molecular Probes) diluted 1/300 in DPBS. Prepare fresh and keep dark.
22. Mounting solution: Preparation: 2.4 g Mowiol 4-88 (Calbiochem), 6 g glycerin, and 6 mL H_2O are mixed overnight at room temperature. Add 12 mL 0.2 *M* Tris-HCl, pH 8.5 and heat for 5–10 min at 50°C. Mix and let it cool down. Add 1.2 mL of an n-propylgallate solution (50 mg/mL) in glycerin (freshly prepared). Keep dark. Spin down for 15 min at 3500*g* at room temperature and aliquot the clear supernatant. Store aliquots at –80°C. Discard when the solution gets yellow or brown.

3. Methods

To identify mutant proteins with possible folding defects leading to faster degradation of the proteins, we investigated several aspects of PEX1 expression. If a mutation analysis has already been done, all alleles with missense mutations or mutations that probably do not lead to mRNA decay are good candidates to investigate. If antibodies against the protein are available, the first step would be to examine the steady-state level of the protein in cultured fibroblast cells from the patients (*see* **Subheading 3.2.**). All candidates with reduced protein levels can then be tested for a temperature-dependent phenotype. In this regard an assay for the function of the protein should be available. In our case the import capacity for the peroxisomal matrix protein catalase was chosen. In this respect it is important to note that catalase seems to be the protein with by far the lowest import rate even under normal conditions ***(16,17)***. This makes it a good candidate to detect slight reductions in peroxisomal import. For other possible parameters that can be tested, see the publication of Tamura and colleagues ***(18)***.

The respective cultures are grown in parallel at 37°C and at 30°C and the peroxisomal import is monitored by indirect immunofluorescence microcopy using catalase antibodies and examining the peroxisomal localization (*see* **Subheading 3.3.**). At the same time, the steady-state level of PEX1 protein is determined at both temperatures under the same conditions by Western-blot

analysis (*see* **Subheading 3.2.**). If the recovery of function is achieved at the lower temperature and if this is accompanied by an increase of PEX1 protein, this will be a good hint for a folding defect.

3.1. Evaluation of Temperature Dependency (as Indicator of Protein Stability)

1. Primary fibroblast cell lines are cultured in DMEM (*see* **Note 1**) supplemented with 10% (v/v) fetal calf serum (FCS), 2 m*M* L-glutamine, 10,0000 U/L penicillin, and 100 mg/L streptomycin at 8.5% CO_2. To investigate possible temperature effects on the amount of PEX1 protein and on the function of the protein, we cultured human fibroblasts with the G843D mutation (patients assigned to CG1 by complementation analysis ***(5)*** at the Amsterdam Medical Center) and a control for 3 d (to near confluency) at 37°C and at 30°C. For determination of the protein level, the cells are seeded in 75 cm^2 flasks (*see* **Note 2**). Cells destined for immunofluorescence microscopy are seeded directly onto coverslips.
2. To a 75-cm^2 flask, add 1.5 mL trypsin solution. When cells start rounding up, aspirate all trypsin, put the flask at 37°C, wait till the cells start losing contact from the surface, shake off the cells from the surface, and use 7 mL DMEM plus supplements to transfer the cells to a 15-mL centrifugation tube. Spin down cells for 7 min at approx 200*g* and aspirate supernatant. The pellet is resolved in 7 mL Hanks solution with Ca^{2+} and Mg^{2+} and the cells are spun down again. Repeat this washing step.
3. Resuspend the final pellet in 150 µL H_2O and transfer to a microcentrifuge tube. Put on ice. Immediately take an aliquot for protein estimation (10 µL) and add one-fourth the volume of 5-times concentrated SDS sample buffer to the remaining sample. Boil immediately for 5 min and freeze at –80°C.
4. Dilute the aliquot of the cell extract taken for protein estimation 1:10 with H_2O. Take 5–10 µL of your diluted sample and make up to 500 µL with H_2O. Add 500 µL Coomassie Protein Assay Reagent (Pierce) and incubate for 5 min at room temperature. Measure absorbance at 595 nm against blank. Correlate to a standard curve (for example from 0.5–4 µg BSA per sample). Compare mutant cells to wild-type cells.

3.2. Western Blot Analysis of PEX1

1. The cell lysates are thawed and boiled for 3 min and then centrifuged at 12,000*g* for 5 min. The supernatants are separated by sodium dodecylsulfate polyacrylamide gel electrophoresis (SDS-PAGE) on 8% gels (25 µg total protein/slot) with a BioRad mini gel apparatus in running buffer. The conditions are 60 V (or 10 mA per gel) throughout the collection gel and 180 V (or 30 mA per gel) for the separation gel. The run is continued for additional 15 min when the dye front reached the end of the glass plates.
2. Transfer the separated proteins onto nitrocellulose membrane for 5 h at 30 V using a BioRad mini blot apparatus (BioRad) with one cool element (frozen at –80°C) in blotting buffer (*see* **Note 3**).

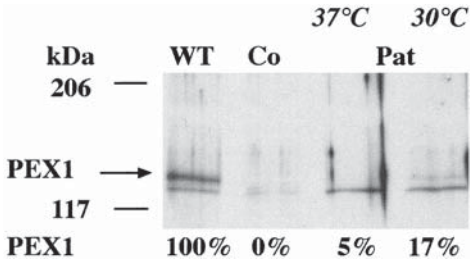

Fig. 1. Increase in the PEX1 protein level of patient fibroblasts harboring the G843D allele at 30°C. Cells were cultured for 3 d at 37°C or 30°C. Cell lysates were subjected to SDS-PAGE and transferred onto nitrocellulose. Immunoblot analysis was performed using polyclonal antibodies (PAbs) against PEX1 protein. In comparison to wild-type, we could detect about 5% PEX1 in lysates of cells incubated at 37°C and about 17% PEX1 in lysates of fibroblasts incubated at 30°C. This increase of protein amount may be explained by an improved stability of PEX1 at the lower temperature. WT, wild-type; Co, control patient fibroblasts without detectable PEX1 mRNA; Pat, patient fibroblasts. The position of the PEX1 protein is indicated by an arrow, the lower band is an unspecific protein recognized by anti-PEX1 antibodies. The molecular weight marker is indicated on the left.

3. To control transfer, stain the membranes with Ponceau S solution for 5–10 min and destain in PBS until the bands appear.
4. Transfer the membrane into blocking solution and incubate for 1 h at 30°C.
5. Incubate the blot with the primary antibodies (anti-PEX1 1:15000 in PBS, 0.1% Triton, 2% NFDM) overnight at 4°C.
6. Wash five times 10 min with wash solution at room temperature.
7. Incubate with the secondary antibodies (anti-rabbit IgG coupled to horseradish peroxidase, diluted 1:15,000 in PBS with 0.1% Triton X-100 and 2% NFDM) for 1 h at room temperature.
8. Wash as described in **step 6**. Omit SDS in the last wash.
9. Develop the blot with the ECL Western-blotting detection reagent and expose to Hyperfilm ECL for 2–40 min. The PEX1 band should be easily visible in normal fibroblasts.
10. Digitize the exposed film with a flatbed scanner (Arcus II, Agfa) and quantify the PEX1 protein compared to wild type fibroblasts using for example MacBas software (Fuji) (*see* **Note 4**).
11. An example for a PEX1 blot from cells bearing the G843D mutation and grown at different temperatures is shown in **Fig. 1**.

3.3. Immunofluorescence Analysis to Evaluate Catalase Import

1. One day before the actual experiment, seed well growing fibroblasts onto coverslips (18 mm) in 6-cm dishes (five per dish). For the experiment evaluating the temperature dependency, seed the cells directly onto coverslips, incubate at the

indicated temperature for 3 d, and then proceed with the immunofluorescence. The density of the cells should be approx 50–70% at the time of immunofluorescence (*see* **Note 5**).
2. Suck off the medium and quickly wash the cells three times with DPBS. A squeezing bottle can be used, but do not squeeze directly on the cells.
3. Fix the cells for 20 min in 5 mL of freshly prepared 3% formaldehyde solution in DPBS.
4. Wash two times in DPBS.
5. Permeabilize the cells for exactly 5 min with 1% TritonX-100 in DPBS.
6. Wash twice with DPBS.
7. Dilute the primary antibodies (anti-human catalase IgG sheep) in DPBS, spin down for 5 min at 12,000*g*, and take the supernatant. Spread out parafilm on the bench and for each coverslip add a drop of 30 μL antibodies. Drain the coverslip by placing the edge on a paper tissue and put it upside down onto this drop. Incubate for 30 min. Try to keep the coverslips moist (for example, place lids of the 3-cm dishes over the coverslips).
8. After incubation, place a drop of buffer at the side of the coverslips so that they swim up, then place the coverslips sunny side up in a 3-cm dish and wash 10 times with DPBS.
9. Repeat this procedure for the secondary fluorescent-labeled antibodies (anti-sheep Alexa 488 or 594) and incubate for 10 min in the dark (cover with aluminum foil).
10. Wash 10 times with DPBS.
11. Place a drop (10 μL) of mounting solution onto a clean glass slide and place the coverslip, after draining of the washing solution, upside down on this drop; do so carefully, to avoid trapping air bubbles. Carefully press the coverslips onto the slide and take away excess mounting solution.
12. Leave the slides for some hours or overnight at room temperature in the dark so that they can harden. Afterwards the coverslips can be sealed with nail polish. If the slides should be investigated immediately, set the coverslips with some drops of nail polish, but do not seal them completely.
13. View the samples with a fluorescence microscope using a 63X oil objective.

Figure 2 gives an example for catalase staining of patient fibroblasts with the G843D mutation that were grown at 37°C and 30°C, respectively.

4. Notes

1. Other media besides DMEM may be used to grow the fibroblasts. Match the bicarbonate content of the media and the CO_2 level.
2. The cells will have very different growth rates at the different temperatures. Try to adjust the amount of cells being seeded, so that both cultures reach a nearly confluent state at the time of harvest. In case there are still less cells at 30°C, try to adjust the volume for preparation of the cells pellets, so that the protein contents of the sample are not too different.

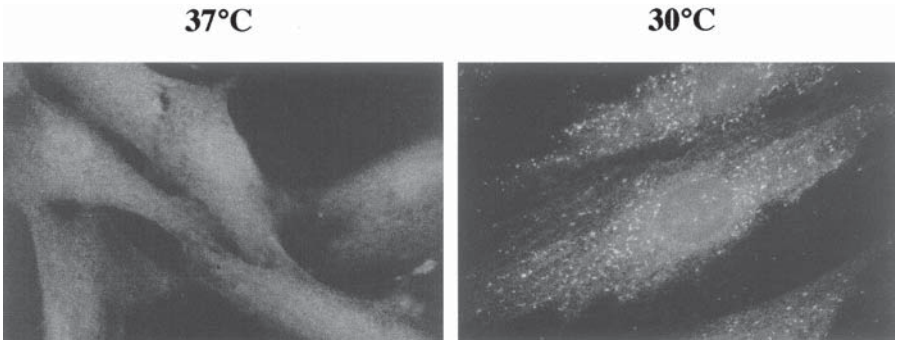

Fig. 2. Catalase import in peroxisomes of patient fibroblasts harboring the PEX1 G843D allele. Fibroblasts were cultured for 3 d at either 30°C or 37°C and then treated for indirect immunofluorescence. Catalase staining was diffuse, indicating a cytoplasmic localization at 37°C and no import into the peroxisomes. At 30°C, catalase was imported into peroxisomes in most of the cells, indicated by the punctuate staining pattern. The punctuate structures colocalized with the peroxisomal membrane protein PMP70 (data not shown).

3. The conditions shown here work well for the PEX1 antibodies. Other proteins probably need different conditions that need to be tested. In our case, it was necessary to blot for a longer time at a lower voltage to get a sufficient amount of the larger PEX1 protein transferred to the membrane. The composition of the blocking solution and washing solutions was also critical.
4. Any other scanners or software programs can be used equally well. The NIH imager, for example, is freely available.
5. The immunofluorescence works best when the cells are 50–75% confluent. This density also makes it easier to take pictures of single cells.
6. Any other mounting solution or anti-fading solutions (some are commercially available) can be tried.

Acknowledgments

We are grateful to R.J.A. Wanders and his group for their collaboration and for the patient cell lines, and to C. Klein and E. Becker for technical assistance.

References

1. Reuber, B. E., Germain-Lee, E., Collins, C. S., Morrell, J. C., Ameritunga, R., Moser, H. W., et al. (1997) Mutations in *PEX1* are the most common cause of peroxisome biogenesis disorders. *Nat. Genet.* **17,** 445–448.
2. Portsteffen, H., Beyer, A., Becker, E., Epplen, C., Pawlak, A., Kunau, W.-H., and Dodt, G. (1997) Human *PEX1* is mutated in complementation group 1 of the peroxisome biogenesis disorders. *Nat. Genet.* **17,** 449–452.

3. Tamura, S., Okumoto, K., Toyama, R., Shimozawa, N., Tsukamoto, T., Suzuki, Y., et al. (1998) Human *PEX1* cloned by functional complementation on a CHO cell mutant is responsible for peroxisome-deficient Zellweger syndrome of complementation group I. *Proc. Natl. Acad. Sci. USA* **95,** 4350–4355.
4. Moser, A. B., Rasmussen, M., Naidu, S., Watkins, P. A., McGuinness, M., Hajra, A. K., et al. (1995) Phenotype of patients with peroxisomal disorders subdivided into sixteen complementation groups. *J. Pediatr.* **127,** 13–22.
5. Wanders, R. J., Mooijer, P. A., Dekker, C., Suzuki, Y., and Shimozawa, N. (1999) Disorders of peroxisome biogenesis: complementation analysis shows genetic heterogeneity with strong overrepresentation of one group (*PEX1* deficiency). *J. Inherit. Metab. Dis.* **22,** 314–318.
6. Maxwell, M. A., Nelson, P. V., Chin, S. J., Paton, B. C., Carey, W. F., and Crane, D. I. (1999) A common *PEX1* frameshift mutation in patients with disorders of peroxisome biogenesis correlates with the severe Zellweger syndrome phenotype. *Hum. Genet.* **105,** 38–44.
7. Collins, C. S., Kalish, J. E., Morrell, J. C., McCaffery, J. M., and Gould, S. J. (2000) The peroxisome biogenesis factors pex4p, pex22p, pex1p, and pex6p act in the terminal steps of peroxisomal matrix protein import. *Mol. Cell Biol.* **20,** 7516–7526.
8. Sacksteder, K. A. and Gould, S. J. (2000) The genetics of peroxisome biogenesis. *Annu. Rev. Genet.* **34,** 623–652.
9. Imamura, A., Tamura, S., Shimozawa, N., Suzuki, Y., Zhang, Z., Tsukamoto, T., et al. (1998) Temperature-sensitive mutation in *PEX1* moderates the phenotypes of peroxisome deficiency disorders. *Hum. Mol. Genet.* **7,** 2089–2094.
10. Gärtner, J., Preuss, N., Brosius, U., and Biermanns, M. (1999) Mutations in *PEX1* in peroxisome biogenesis disorders: G843D and a mild clinical phenotype. *J. Inherit. Metab. Dis.* **22,** 311–313.
11. Collins, C. S. and Gould, S. J. (1999) Identification of a common *PEX1* mutation in Zellweger syndrome. *Hum. Mutat.* **14,** 45–53.
12. Waters, P. J., Parniak, M. A., Akerman, B. R., and Scriver, C. R. (2000) Characterization of phenylketonuria missense substitutions, distant from the phenylalanine hydroxylase active site, illustrates a paradigm for mechanism and potential modulation of phenotype. *Mol. Genet. Metab.* **69,** 101–110.
13. Waters, P. J., Parniak, M. A., Hewson, A. S., and Scriver, C. R. (1998) Alterations in protein aggregation and degradation due to mild and severe missense mutations (A104D, R157N) in the human phenylalanine hydroxylase gene (PAH). *Hum. Mutat.* **12,** 344–354.
14. Bross, P., Corydon, T. J., Andresen, B. S., Jorgensen, M. M., Bolund, L., and Gregersen, N. (1999) Protein misfolding and degradation in genetic diseases. *Hum. Mutat.* **14,** 186–198.
15. Walter, C., Gootjes, J., Mooijer, P. A., Portsteffen, H., Klein, C., Waterham, H. R., et al. (2001) Disorders of peroxisome biogenesis due to mutations in *PEX1*: phenotypes and *PEX1* protein levels. *Am. J. Hum. Genet.* **69,** 35–48.
16. Lazarow, P. B., Robbi, M., Fujiki, Y., and Wong, L. (1982) Biogenesis of peroxisomal proteins in vivo and in vitro. *Ann. NY Acad. Sci.* **386,** 285–300.

17. Warren, D. S., Morrell, J. C., Moser, H. W., Valle, D., and Gould, S. J. (1998) Identification of *PEX10*, the gene defective in complementation group 7 of the peroxisome-biogenesis disorders. *Am. J. Hum. Genet.* **63,** 347–359.
18. Tamura, S., Matsumoto, N., Imamura, A., Shimozawa, N., Suzuki, Y., Kondo, N., and Fujiki, Y. (2001) Phenotype-genotype relationships in peroxisome biogenesis disorders of *PEX1*-defective complementation group 1 are defined by Pex1p-Pex6p interaction. *Biochem. J.* **357,** 417–426.

15

E. coli Expression System for Identifying Folding Mutations of Human Adenosine Deaminase

Ines Santisteban, Francisco X. Arredondo-Vega, Shannon Daniels, and Michael S. Hershfield

1. Introduction

Adenosine deaminase (ADA), a soluble zinc-containing enzyme of the purine nucleoside inter-conversion pathway, plays an essential role in the development of immune function. Most patients with inherited deficiency of ADA have severe combined immunodeficiency (SCID). This is a fatal syndrome with onset in infancy that results from a depletion of all lymphocyte lineages owing to toxic effects of ADA substrates adenosine (Ado) and 2'-deoxyadenosine (dAdo). A milder immune deficiency ("delayed" or "late/adult" onset) also occurs, and some healthy children and adults have been identified through screening as lacking ADA in erythrocytes, while having variable ADA activity in their nucleated cells and cell lines ("partial ADA deficiency"). Although erythrocyte ADA activity is low in all patients, clinical severity correlates well with the level of erythrocyte dAdo nucleotides (dAXP, mainly dATP).

More than 70 ADA mutations, the majority missense, have been identified. About half of these mutations have been identified in single patients and most patients are compound heterozygotes, possessing two different mutant ADA alleles. It is difficult to precisely quantify residual ADA activity in nonerythroid cells of patients owing to the wide range of activity among normal individuals. To overcome these limitations, we have established a convenient, robust system for quantifying the catalytic activity of recombinant ADA proteins expressed constitutively in *Escherichia coli* ***(1)***. ADA is well-suited for expression in *E. coli* because human ADA is active as a monomer of 41 kDa, and it does not undergo glycosylation or other modification in human cells. For

From: *Methods in Molecular Biology, vol. 232: Protein Misfolding and Disease: Principles and Protocols*
Edited by: P. Bross and N. Gregersen © Humana Press Inc., Totowa, NJ

our studies, we used a strain of *E. coli* (SØ3834) that has a deletion in the gene for the homologous bacterial ADA ***(2)***.

We first used the SØ3834 expression system to study 28 cDNAs with different single amino acid mutations derived from 52 patients spanning the phenotypic range associated with ADA deficiency ***(1)***. The ADA activity expressed by these cDNAs ranged over five orders of magnitude, from 0.001% to 28% of the activity obtained with wild-type human ADA cDNA. We were able to demonstrate a good correlation between genotype ranked by level of ADA activity expressed by both alleles, clinical severity, and level of erythrocyte dAdo nucleotides. This classification has since been validated by application to several novel mutations found in families with discordant and unusual phenotypes, helping to more precisely define the threshold level of ADA expression associated with adequate immune function ***(3,4)***. In addition to genotype-phenotype analysis, we have used the *E. coli* SØ3834 expression system for "homolog scanning" studies to localize the binding site of human ADA for the cell membrane "ADA complexing protein" CD26/dipeptidyl peptidase IV ***(5)***.

In ongoing studies (unpublished) we have adapted the SØ3834 expression system for identifying and mapping ADA mutations that have large effects on folding. For this purpose, we have co-expressed mutant ADA cDNAs along with the *E. coli* chaperonins GroEL and GroES. Together these proteins, encoded by the *groE* operon, have been shown to assist in the folding of a variety of proteins of *E. coli* and non-*E. coli* origin ***(6–8)***, including proteins involved in metabolic pathways ***(9,10)***. This chapter summarizes the basic SØ3834 expression system and its adaptation for investigating folding mutations of human ADA.

1.1. General Strategy

For the basic expression studies, ADA cDNAs were cloned into the NcoI site of the TAC promoted plasmid vector pZ, a pEMBL derivative that contains the Amp^r marker ***(1,2)***. Initial cloning was done in *E. coli* XLI-Blue (recA1, endA1, gyrA96, thi-1, hdsR17, supE44, relA1, lac[F' proAB lacIqZΔM15 Tn10 Tet^r]. Confirmed recombinant clones were then expressed in *E. coli* SØ3834, a multiple auxotroph (rpsL, Δadd-uid-man, metB, guaA, ura::Tn10) with a deletion of the bacterial ADA gene ***(11,12)***. For the studies involving GroEL/GroES, ADA cDNA/pZ were co-transformed with pGroESL (kindly provided by A. Gatenby, DuPont) containing the *E. coli groE* operon with transcription driven by pLac and a natural heat-shock promoter in the *groE* operon ***(13)***. This plasmid provides chloramphenicol resistance to its host cells. Removal of the GroESL cDNA yielded the vector pTG10, which is used in control co-transformations. pZ-derived constructs and pGroESL are compatible plasmids by virtue of having different origins of replication.

2. Materials

1. Luria broth (LB) from Gibco-BRL. Prepare in distilled water, 25 g/L. Autoclave 15 min/121°C.
2. LB/agar.
3. Carbenicillin: 50 mg/mL stock solution in distilled water. Sterilize by filtration (0.22 μm filter) (*see* **Note 1**).
4. Tetracycline: 12.5 mg/mL in 70% ethanol (1000X Tet stock).
5. Chloramphenicol: 34 mg/mL in ethanol (1000X chloramphenicol stock).
6. AEBSF hydrochloride (protease inhibitor, Calbiochem). Dissolve 50 mg in 2.1 mL sterile distilled water to obtain 100 m*M* solution.
7. Lysis buffer/AEBSF: 10 m*M* Tris-HCl, pH 7.5, 75 m*M* KCl, 10 m*M* $MgCl_2$, 1 m*M* dithiothreitol (DTT). Filter-sterilize. Before use add 10 μL of 100 m*M* AEBSF per 1 mL lysis buffer.
8. Lysis buffer/AEBSF/BSA: Lysis buffer/AEBSF containing 1 mg/mL bovine serum albumin (BSA).
9. IPTG, 100 m*M*, sterilize by filtration.
10. [8-^{14}C] Adenosine 45–60 mCi/mmol, from Moravek Biochemicals (Brea, CA). Adjust by addition of unlabeled adenosine to give a solution of approx 1 m*M* total adenosine and 10,000–30,000 cpm/nmol. The exact concentration is calculated from the absorbance at 257 nm of a dilution in 10 m*M* HCl using the extinction coefficient of 14.6.
11. Cellulose thin-layer chromatography (TLC) plates with fluorescent indicator (Baker-flex, J.T. Baker, NJ).

3. Methods

3.1. Transformation (SØ3834)

1. Place 1–2 μL (10 ng) of each plasmid DNA in a sterile polypropylene, round-bottom tube (*see* **Note 2**).
2. Add 30–50 μL competent cells. Place on ice for 30 min.
3. Heat shock for 90 s at 42°C. Place tube on ice 2 min.
4. Add 250 μL LB. Incubate 1 h/37°C/150–200 rpm.
5. Plate 25 μL and 50 μL onto LB/agar plates containing the appropriate antibiotics: for pZ, carbenicillin; for pZ and pGroESL, carbenicillin plus chloramphenicol. Tetracycline should also be included whenever *E. coli* SØ3834 is grown.
6. Incubate at 37°C overnight.

3.2. Growth and Harvesting

3.2.1. Constitutive Expression of pZ/ADA Constructs

1. Using individual SØ3834 colonies, start three 3-mL cultures (LB + antibiotics: carbenicillin, tetracycline).
2. After 6–8 h in a shaking incubator (37°C, 225 rpm) remove 10–20 μL from each culture to seed three 10-mL subcultures (LB + antibiotics).

3. Grow overnight; OD600 should be 0.8–1.
4. From each of the 10-mL overnight cultures harvest two cell pellets from 3-mL aliquots by centrifugation.
5. Store pellets at –80°C.

3.2.2. Induced Expression of pZ/ADA Plus pTG/GroESL Co-transformed Cultures

1. From 3 individual SØ3834 colonies, start three 3-mL cultures (LB+ antibiotics: carbenicillin, tetracycline, chloramphenicol).
2. After 6–8 h in a shaking incubator (37°C, 225 rpm) remove 10–20 μL from each culture to seed three 10-mL subcultures (LB+ antibiotics).
3. Grow 16–18 h at 37°C until OD600 reaches >0.6. At this point a 1.5 mL aliquot of each culture is removed to prepare DNA to ascertain the presence of both plasmids by restriction enzyme digestion (**Fig. 1**).
4. After adjusting the culture volume to 10 mL (to compensate for volume removed to check OD600), induce with 50 μL of 100 m*M* IPTG.
5. Grow for additional 1 h at 37°C/225 rpm. Harvest pellets as in **Subheading 3.2.1.** and store at –80°C.

3.3. Characterization of ADA

3.3.1. Lysate Preparation

1. Resuspend each cell pellet in 100 μL lysis buffer/AEBSF. Vortex.
2. Sonicate on ice 2 × 15 sec at 100% output.
3. Centrifuge 15 min/4°C/15,000*g* in microcentrifuge. Transfer supernatant (cell lysate) to a new microcentrifuge tube and place on ice (*see* Note 3).

3.3.2. ADA Assay

1. To achieve the linear range, serial 1:10 dilutions (5–50 μL) of lysates are prepared in lysis buffer/AEBSF/BSA (1 mg/mL), changing pipet tips between every dilution step (*see* **Note 4**).
2. ADA activity is measured by monitoring the conversion of adenosine (Ado) to inosine (Ino) using as substrate 150 μ*M* [8-^{14}C] Adenosine (Moravek Biochemicals, CA) ***(14)***. Each 50 μL reaction consists of 10 μL sample to be assayed and 40 μL of a master mix. The latter contains, per assay, 7.5 μL 1 m*M* ^{14}C-Ado (specific activity 5–20 μci/μmol), 2.5 μL 1 *M* Tris-HCl, pH 7.4, and 30 μL water. The reaction is started at 37°C by addition of the master mix.
3. After incubation for 15 min, 5 μL of reactions are spotted onto the origin of a lane on a cellulose TLC plate with fluorescent indicator, onto which 5 μL of a UV marker solution (2 mg/mL each of unlabeled Ado and Ino) had previously been applied and allowed to dry. Eight (and with experience up to 12) samples can be applied along the origin; also, the 20-cm plate may be cut in half so that samples can be run on each 10-cm half plate.

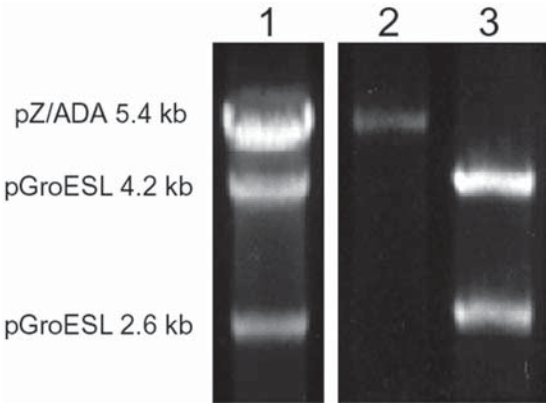

Fig. 1. *Eco*RI digest of miniprep DNA from overnight cultures of SØ3834 transformants. Lane 1, cotransformed with pZ/ADA and pGroESL. Lane 2, transformed with pZ/ADA. Lane 3, transformed with pGroESL.

4. The TLC plates are developed in 1% Tris base and air-dried. Using a handheld UV lamp, the Ino spot (closest to the solvent front) for each sample is outlined, cut out, placed in scintillation fluid, and counted. For the blank lane, in which 10 µL of lysis buffer substitutes for the sample, both the Ino and Ado spots are counted; the dpm in the Ino spot is used as the blank value, and the dpm in the Ado spot is used as the "max" value to calculate the substrate specific radioactivity (dpm/nmol Ado). Typically, the blank is <70 dpm and the "max" is 10,000–12,000 dpm. Incorporation of 200–5000 dpm into Ino during the assay is acceptable for quantitation.

Calculation of ADA activity:

a. Ado Specific activity (SA):

$$\text{SA (dpm / nmol)} = \frac{(\text{max dpm} - \text{blank})}{7.5 \text{ nmol } ^{14}\text{C Ado per assay}} \times \frac{50}{5}$$

b. ADA activity (nmol/h/mL lysate):

$$(\text{lysate dpm} - \text{blank}) \times \frac{50}{5} \times \frac{1}{\text{SA}} \times \frac{60}{15} \times \text{dil. factor} \times \frac{1}{0.005} \text{ mL}$$

where $\frac{50}{5}$ is owing to the 5/50 µL volume spotted

$\frac{60}{15}$ = conversion to h units

ADA activity is expressed as nmol Ino formed per h per mg lysate protein. Total lysate protein is quantitated with the BCA kit (Pierce).

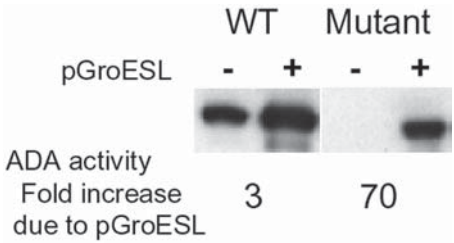

Fig. 2. Western Blot with anti-human ADA MAb 1C5 of lysates of WT ADA and a mutant ADA cDNA coexpressed with pGroESL in *E. coli* SØ3834. The ADA activity (nmol/h/mg extract protein) of the mutant coexpressed with pGroESL was 0.24% of wild-type activity.

3.3.3 ADA Protein Analysis

Aliquots of lysates containing 30–50 μg total protein are resolved by 12% SDS-PAGE. Duplicate gels are run, one of which is stained for protein with coomassie blue, and the other transferred to nitrocellulose for Western blotting. For the latter, we have used either a polyclonal antibody (PAb) to ADA (such as goat antibody, kindly provided to us by Dr. Dan Wiginton, University of Cincinatti) ***(1)***, or mouse monoclonal antibody (MAb) 1C5, developed in this laboratory ***(5)*** (**Fig. 2**) (*see* **Notes 5** and **6**).

4. Notes

1. Carbenicillin is the antibiotic of choice rather than ampicillin because it is more stable in the low pH conditions that develop during bacterial fermentation. It is used at a 4X concentration in the culture medium to further prevent loss of the pZ plasmid (4 μL per mL LB of a 50 mg/mL 1000X stock solution).
2. It is important when doing a double transformation (pZ construct and pGroESL) to have the DNA from both plasmids in the transformation tube before adding the competent cells.
3. The assay for ADA activity should be performed on freshly prepared cell lysates that have not been frozen. However, the Western-blot analysis can be performed later with lysates that have been frozen.
4. Each lysate should be assayed at two dilution levels (or more, as may be necessary), with each dilution level assayed in duplicate. Lysates resulting from at least three independent colonies from each transformation should be assayed in this manner in order to be able to calculate the mean ADA activity and standard deviation (SD).
5. Although the difference in level of expression of mutant ADA cDNAs owing to the presence or absence of pGroESL coexpression can be dramatic, as detected by Western blot and in some cases assay for ADA activity, these differences cannot be appreciated on the coomassie blue-stained gels.

6. The ADA bands on Western blots can be detected by any of several methods. We currently prefer to use the ECL Plus reagents (Amersham Pharmacia Biotech).

Acknowledgments

This work was supported by NIH Grant DK20902 and by a grant from Enzon, Inc.

References

1. Arredondo-Vega, F. X., Santisteban, I., Daniels, S., Toutain, S., and Hershfield, M. S. (1998) Adenosine deaminase deficiency: genotype-phenotype correlations based on expressed activity of 29 mutant alleles. *Am. J. Hum. Genet.* **63,** 1049–1059.
2. Chang, Z. Y., Nygaard, P., Chinault, A. C., and Kellems, R. E. (1991) Deduced amino acid sequence of Escherichia coli adenosine deaminase reveals evolutionarily conserved amino acid residues: implications for catalytic function. *Biochemistry* **30,** 2273–2280.
3. Ariga, T., Oda, N., Santisteban, I., Arredondo-Vega, F. X., Shioda, M., Ueno, H., et al. (2001) Molecular basis for paradoxical carriers of adenosine deaminase (ADA) deficiency that show extremely low levels of ADA activity in peripheral blood cells without immunodeficiency. *J. Immunol.* **166,** 1698–1702.
4. Arredondo-Vega, F. X., Santisteban, I., Richard, E., Bali, P., Koleilat, M., Loubser, M., et al. (2002) Adenosine deaminase deficiency with mosaicism for a "second-site suppressor" of a splicing mutation: decline in revertant T lymphocytes during enzyme replacement therapy. *Blood* **99,** 1005–1013.
5. Richard, E., Arredondo-Vega, F. X., Santisteban, I., Kelly, S. J., Patel, D. D., and Hershfield, M. S. (2000) The binding site of human adenosine deaminase for CD26/Dipeptidyl peptidase IV: the Arg142Gln mutation impairs binding to cd26 but does not cause immune deficiency. *J. Exp. Med.* **192,** 1223–1236.
6. Hartl, F. U. (1996) Molecular chaperones in cellular protein folding. *Nature* **381,** 571–579.
7. Sigler, P. B., Xu, Z., Rye, H. S., Burston, S. G., Fenton, W. A., and Horwich, A. L. (1998) Structure and function in GroEL-mediated protein folding. *Annu. Rev. Biochem.* **67,** 581–608.
8. Houry, W. A., Frishman, D., Eckerskorn, C., Lottspeich, F., and Hartl, F. U. (1999) Identification of in vivo substrates of the chaperonin GroEL. *Nature* **402,** 147–154.
9. Andresen, B. S., Bross, P., Udvari, S., Kirk, J., Gray, G., Kmoch, S., et al. (1997) The molecular basis of medium-chain acyl-CoA dehydrogenase (MCAD) deficiency in compound heterozygous patients: is there correlation between genotype and phenotype? *Hum. Mol. Genet.* **6,** 695–707.
10. Gamez, A., Perez, B., Ugarte, M., and Desviat, L. R. (2000) Expression analysis of phenylketonuria mutations. Effect on folding and stability of the phenylalanine hydroxylase protein. *J. Biol. Chem.* **275,** 29,737–29,742.

11. Jochimsen, B., Nygaard, P., and Vestergaard, T. (1975) Location on the chromosome of Escherichia coli of genes governing purine metabolism. Adenosine deaminase (add), guanosine kinase (gsk) and hypoxanthine phosphoribosyltransferase (hpt). *Mol. Gen. Genet.* **143,** 85–91.
12. Hove-Jensen, B., and Nygaard, P. (1989) Role of guanosine kinase in the utilization of guanosine for nucleotide synthesis in *Escherichia coli*. *J. Gen. Microbiol.* **135,** 1263–1273.
13. Goloubinoff, P., Gatenby, A. A., and Lorimer, G. H. (1989) GroE heat-shock proteins promote assembly of foreign prokaryotic ribulose bisphosphate carboxylase oligomers in *Escherichia coli*. *Nature* **337,** 44–47.
14. Arredondo-Vega, F. X., Kurtzberg, J., Chaffee, S., Santisteban, I., Reisner, E., Povey, M. S., and Hershfield, M. S. (1990) Paradoxical expression of adenosine deaminase in T cells cultured from a patient with adenosine deaminase deficiency and combine immunodeficiency. *J. Clin. Invest.* **86,** 444–452.

16

Characterization of Overexpressed Mutant Proteins in Mammalian Cells

Thomas Juhl Corydon

1. Introduction

Overexpression and characterization of mutant proteins in mammalian cells is of crucial importance in order to understand the disease-causing nature of mutant proteins in human diseases. Much of the present knowledge of the mechanisms behind disease-causing proteins comes from cellular analysis of the plethora of naturally occurring mutations. Functional testing of these gene variants depends on efficient gene transfer to mammalian cells. A wide variety of methods for transfection of tissue-culture cells has been applied. The two common methods for transient transfection of adherent cells, chemical treatment with calcium-phosphate and lipid-based procedures, have all been used and will be described here. For a detailed treatment of the subject, including stable transfection and viral-mediated gene transfer, the reader is referred to **refs. *1–6*.**

Next, it is important to design sensitive methods for thorough characterization of wild-type (WT) and mutant proteins from transfected cells. Two of the most commonly used methods are Western blotting and pulse-chase followed by immunoprecipitation (*see also* Chapter 12). The former is used for investigation of the steady-state level of a given protein, whereas the latter is used for analysis of protein synthesis, kinetics of processing, and turnover of proteins. If the given protein is an enzyme, functional analysis such as activity measurements can be performed as well. This kind of experiment is often very useful because only fully folded native proteins are catalytically active. *In situ* immunostaining of transfected cells have also proven to be very useful for the characterization of expressed WT and mutant proteins. Like immunoprecipita-

From: *Methods in Molecular Biology, vol. 232: Protein Misfolding and Disease: Principles and Protocols*
Edited by: P. Bross and N. Gregersen © Humana Press Inc., Totowa, NJ

tion, this procedure demands a specific antibody for the labeling of the overexpressed protein. However, if there are no suitable antibodies available, fusion-proteins between the protein in question and different tags can be designed. The 238-amino acid green fluorescent protein (GFP) of the jellyfish *Aequorea victoria*, c-myc, or FLAG epitopes have been utilized as excellent reporters in cellular protein localization studies ***(7–13)***. Apart from the ease of detection compared to nonfluorescent tags, GFP can be used in the study of protein dynamics in living cells ***(14,15)***. However, proteins labeled with tags might cause disturbances in the assembly and/or cellular trafficking of the fusion protein compared to the untagged protein. The presence of a flexible region between GFP and the fusion partner has previously been shown to improve the cellular transport and function of fusion proteins ***(8)***. Short-chain acyl-CoA dehydrogenase (SCAD) ***(16)*** and the ClpX chaperone ***(17)*** together with the low density lipoprotein (LDL) receptor ***(18–20)*** will be used to exemplify the methods utilized for the expression and characterization of mutant variant proteins in mammalian cells.

2. Materials

1. Cell cultures: We routinely use Chang cells (a human hepatoma cell line [American Type Culture Collection, CCL-13]) and COS-7 cells (a monkey kidney cell line [American Type Culture Collection, CRL-1651]) for transient expression experiments (*see* **Note 1**). Chang and COS-7 cells are maintained in complete RPMI 1640 in a 5% CO_2 and 95% air atmosphere at 37°C.
2. Phosphate-buffered saline (PBS): 8 g NaCl, 0.2 g KCl, 1.15g $Na_2HPO_4(2H_2O)$, 0.2 g KH_2PO_4. Add H_2O to 1000 mL, pH 7.2 (autoclaved).
3. Buffer A: 150 m*M* NaCl, 1 m*M* ethylenediamine tetraacetic acid (EDTA), pH 8.0, 10 m*M* Tris-HCl, pH 7.5 (sterile filtrated).
4. $CaCl_2$: 2.5 *M* in H_2O.
5. Transfection buffer (Tx): 50 m*M* *N*-2-Hydroxyethylpiperazine-*N*'-2-Ethene Sulphonic Acid (HEPES)-NaOH, pH 7.1, 250 m*M* NaCl, 1.5 m*M* sodium phosphate, pH 7.0. Mix the following of sterile stock solutions: 500 µL 500 m*M* HEPES, pH 7.1, 625 µL 2 *M* NaCl, 7.5 µL 1 *M* sodium phosphate, pH 7.0, 3.9 mL H_2O (total volume 5 mL).
6. Complete RPMI 1640 or DMEM (Gibco-BRL Life Technologies) plus 10% fetal calf serum (FCS) (Gibco-BRL), 100 U/mL penicillin, 0.1 mg/mL streptomycin (both Leo Pharmaceutical Products Ltd.) and 0.29 mg/mL glutamine.
7. HBS: 0.9% NaCl, 20 m*M* HEPES, pH 7.4 (higher pH will reduce transfection efficiency).
8. HEPES: Suspended in H_2O, pH 7.1 (autoclaved).
9. Hanks' Balanced Salt Solution (HBSS): 400 mg KCl, 60 mg KH_2PO_4, 8000 mg NaCl, 57.9 mg $Na_2HPO_4{\cdot}2H_2O$, 10 mg Phenol red. Add H_2O to 1000 mL (autoclaved).

10. RPMI labeling medium: RPMI (without cysteine, methionine, inositol, glutamine, arginine, leucine, glucose) (Gibco-BRL). Add 100 µL inositol, arginine, leucine, and glucose (all ×100, Gibco-BRL), 0.29 mg/mL glutamine, 100 U/mL penicillin, 0.1 mg/mL streptomycin, 400 µL HEPES and 5% (v/v) dialyzed serum (Sigma). Final volume 10 mL.
11. Chase medium: Complete RPMI 1640 plus 0.1% (w/v) L-methionine, 0.1% (w/v) L-cysteine, and 20 m*M* HEPES, pH 7.1.
12. PRO-MIX (a defined cell-labeling mixture of L-[^{35}S]-methionine and L-[^{35}S]-cysteine) (Amersham Pharmacia Biotech).
13. Protein A-Sepharose (Amersham Pharmacia Biotech).
14. Cell lysis buffer: 50 m*M* Tris-HCl, pH 7.8, 5 m*M* EDTA, pH 8.0, 1 m*M* DTE, 10 µg/mL aprotinin, 1 mg/mL trypsin inhibitor. Before use add Pefabloc SC (Roche) to a final concentration of 1 m*M*.
15. Dilution buffer high: 50 m*M* Tris-HCl, pH 8.5, 150 m*M* NaCl, 1% (v/v) Triton X-100, 0.5% sodium dodecyl sulphate (SDS) (v/v).
16. TE: 10 m*M* Tris-HCl, 0.1 m*M* EDTA, pH 8.0 (autoclaved).
17. FuGENE 6 (Roche).
18. DC-Chol is prepared essential as described by Gao and Hunag ***(21)***. Fill a 10-mL glass syringe (baked at 150°C in vacuum, overnight) with 2.25 g of cholesteryl chloroformat (Sigma C6633). Aspirate 5 mL dry chloroform into the syringe and let the cholesteryl chloroformat dissolve. Add drop-wise to a solution of dimethylethylenediamine (Sigma D1894, asymmetric) (2 mL in 3 mL dry chloroform, Bake Fisher Molecular Sieve 4Å at 150°C, in vacuum, overnight, add 1/3 vol to the chloroform, shake well, and use next day) at 0°C with magnetic stirring. The resulting solution is viscous. Do not leave the solution on ice for too long. Remove the chloroform by evaporation. Dissolve the residue (which is still liquid) by adding a few mL of ethanol. After having dissolved the residues, which may be improved by heating to 45°C, allow the species to crystallize at 4°C. Remove as much as possible of the liquid by a pre-cooled sintered glass filter with vacuum applied. Repeat crystallization step twice, but use ethyl-acetat instead of ethanol. Dry crystals completely in vacuum overnight. The resulting powder is white.
19. The making of DC-Chol/DOPE liposomes. DC-Chol/DOPE, molar ratio: 1.2/0.8, weight ratio: 1/1. Dissolve 10 mg DC-Chol in 1 mL DOPE (supplied as 10 mg/mL in chloroform). Dispense as 50 µL aliquots into 2-mL glass vials. Evaporate to dryness and store at –20°C. Before use, hydrate in 1 mL pyrogen-free double-distilled water overnight. Vortex for 2–3 min until the lipid film is completely resuspended. Stable at 4°C for at least 6 wk. Do not freeze.
20. PBS-T: PBS including 0.1% (v/v) Tween 20.
21. Cycloheximide (Sigma).
22. Rhodamine 6G (Sigma).
23. Rabbit anti-Hsp60 antibody (Sigma).
24. Rhodamine-conjugated goat anti-mouse antibody (Sigma).
25. 9E10 Anti-Myc monoclonal antibody (MAb) against the c-myc tag (RDI).

26. Conjugated antibodies and MitoTracker Red CMXRos (all from Molecular Probes).
27. Monoclonal anti-LDL receptor antibody immunoglobulin IgG-C7 (Amersham Pharmacia Biotech).
28. Paraformaldehyde (Merck).
29. Antifade solution: Add 4.8 g Mowiol 4-88 (Hoechst) to 12 g glycerol. Mix. Add 12 mL double-distilled water and incubate overnight at 65°C. Add 24 mL 0.2 *M* Tris-HCl, pH 8.3, and incubate overnight at 65°C. Most of the Mowiol should now be dissolved. Clarify by centrifugation at 5000*g* for 15 min.
30. Bio-Safe Coomassie stain (BioRad).

3. Methods

3.1. Plasmids

Mutagenesis of cDNA can be performed in a variety of ways (*see* Chapter 11, this volume). After having verified that the cDNA in question has the correct sequence subcloning into an appropriate expression vector for mammalian cells is often acquired. For this purpose several commercial vectors are available with different promoters, processing signals, purification tags, labeling tags, and selection markers. For further information, *see* Chapter 8, this volume. Having constructed an expression vector supercoiled plasmid DNA should be purified and dissolved in TE (*see* **Note 2**).

3.1.1. pMP6 Expression Vectors

SCAD is a nuclear-encoded enzyme involved in the mitochondrial β-oxidation of straight-chain fatty acids ***(22,23)***. A number of mutations have been identified in human inborn errors of SCAD ***(24–27)***. The SCAD R22W mutation is disease-causing and cells from a patient had previously been shown to synthesize a labile variant SCAD protein ***(24)***.

SCAD WT, R22W, and R22C (artificially constructed) cDNA fragments were isolated and ligated into the expression plasmid pMP6 (an AAV-based vector) between the cytomegalovirus (CMV) promoter and the SV40 processing signal by standard recombinant DNA methods ***(1,16)***.

3.1.2. GFP Fusion Proteins

Like other membrane proteins the LDL receptor is translocated into the endoplasmic reticulum (ER) followed by *N*-glycosylation and transport to the cell membrane where it binds LDL-particles. After endocytosis and release of the ligand, receptors are recycled to the cell membrane. Familial Hypercholesterolemia is caused by mutations in the LDL receptor gene ***(28)***.

Fusions between coding sequences encoding WT LDL receptor and enhanced green fluorescent protein (EGFP) driven by the CMV promoter were

generated in the pEGFP-N1 vector (Clontech) by standard cloning procedures ***(1)***. Different linkers between the LDL receptor and GFP were tested. Cellular studies showed that the construct with two copies of the sequence 5'-AAGCTGCAGCAGCTGCGGCCG-3' inserted in the unique restriction site between the LDL receptor and GFP sequences (LDLR-20-GFP) produced normally localized WT LDL receptor GFP protein with activity comparable to WT LDL receptor protein. Fusions containing W556S or C660X (both disease-causing ***[18,19]***) mutant LDL receptor sequences were generated by replacing the 1275 bp *Acc*B7I-fragment of the LDL receptor cDNA sequence with the corresponding mutant LDL receptor cDNAs. For a detailed description, *see* **ref. *20***.

3.1.3. Construction of c-myc Fusion Proteins

Human ClpX is an orthologue of the *E. coli* ClpX chaperone and protease subunit. The *E. coli* ClpX chaperone functions as gatekeeper that selects substrates and presents them in an adequate—unfolded—conformation to the ClpP protease ***(29)***. Human ClpX cDNA sequence was cloned between the *Kpn*I and *Xho*I sites of pcDNA3.1/Myc-His B (Invitrogen). The resulting construct, containing the ClpX cDNA COOH-terminally fused to the C-Myc-His tag, was used to transfect mammalian cells as previously described ***(17)***.

3.2. Transient Expression in Mammalian Cells

The next step in the procedure involves transfection of mammalian cells. In the following calcium-phosphate co-precipitation, liposome-mediated gene transfer is outlined. In order to increase the transfection efficiency cells are subcultivated the day before transfection. Upon transfection cells should be semi-confluent. Cells are either analyzed for transgene expression or harvested 24–72 h post transfection. For scale-up proportionally increase the quantity of all components.

3.2.1.Calcium-Phosphate Mediated Transfection

1. For transfection of cells cultured in a 10 cm^2 dish add 6 μg super-coiled DNA to a polystyrene vial containing 12 μL $CaCl_2$ and buffer A to a final volume of 112 μL. (*see* **Note 3**).
2. Add 112 μL Tx buffer to another polystyrene vial.
3. Transfer the DNA, buffer A, $CaCl_2$ mixture to the vial containing Tx buffer. Leave for 30 min at room temperature. The solution should become turbid as the complexes are generated.
4. Substitute the cultivation medium with DMEM (*see* **Note 4**).
5. Transfer 224 μL Tx-DNA complex to the cells (now maintained in DMEM).
6. Incubate 16 h at 37°C.

7. Wash the cells three times in PBS and add normal cultivation medium. Alternatively, subcultivate cells (*see* **Note 5**).

3.2.2. Transfection With Lipid-Based Reagent (FuGENE 6)

1. For transfection of cells cultured in a 10 cm^2 flask add 4.5 µL FuGENE 6 (warmed to ambient temperature) to a vial containing serum-free medium (e.g., RPMI 1640). The final volume should be 100 µL. Incubate at room temperature for 5 min (*see* **Note 6**).
2. 1.5 µg super-coiled DNA is added to a new vial.
3. 100 µL of the pre-incubated FuGENE 6-medium mixture is added to the vial containing DNA. Incubate 15 min at room temperature.
4. Transfer the DNA-FuGENE 6 mixture to the cells (*see* **Note 7**).

3.2.3. Transfection of Mammalian Cells Using Cationic Lipids (DOPE/DC-COL)

1. Hydrate DOPE/DC-Chol 50:50 (w/w) with 1 mL pyrogen-free double-distilled water overnight. Alternatively, the vial can be sonicated in a water bath for 5 min.
2. Vortex for 2–3 min (feels like a very long time, if you do not use a vibrax) or until the lipids are completely re-suspended. Bilaminar liposomes are formed. The transfection reagent is stable at 4°C for at least 4 mo. Do not freeze.
3. For transfection of cells cultured in a 10 cm^2 flask transfer 12.5 µL transfection reagent to a polystyrene vial containing 40 µL HBS.
4. 2.5 µg super-coiled DNA is mixed with HBS in a new polystyrene vial. The total volume should be 50 µL (*see* **Note 8**).
5. Add slowly the DNA-HBS solution to the transfection reagent. Incubate for 10 min. The mixture should become turbid as the complexes are generated.
6. Wash the cells in serum-free medium.
7. Add 1 mL serum-free medium to the transfection mixture and apply to cells for 3–4 hours at 37°C (*see* **Note 9**).
8. Replace serum-free medium with normal growth medium.

In our hands, the calcium-phosphate co-precipitation and DC-Chol/DOPE procedures are not as efficient and cannot be used on the same wide spectrum of cells as the FuGENE 6 transfection reagent. However, they are both inexpensive compared to FuGENE 6. All three methods have been used for co-transfection experiments. Novel tools for gene delivery to mice by intravenous injection of cDNA using a hydrodynamic-based procedure are being developed ***(30,31)***. This method may be generally applicable in the characterization of mutant proteins in animals liver cells in vivo ***(20)***.

3.2.4. Harvest

1. After 24–72 h of expression remove the cultivation medium and wash the cells twice in ice-cold PBS.
2. Displace the cells with a cell plastic scraper in a small volume of ice-cold PBS and collect the cells by centrifugation (370*g*; 3 min).

3. The cell pellet can either be used directly or stored at –20°C (^{35}S-labeled samples should be frozen at –70°C).

3.3. Cell Disruption

Described below are the steps that can be utilized for disruption of mammalian cells in a manner that ensures release of significant quantities of overexpressed proteins.

3.3.1. Cell Lysis

1. Resuspend cell pellet in 100 µL lysis buffer.
2. Freeze the cell suspension on dry ice for 2 min and thaw again in a water bath (room temperature or 37°C) for 2 min. Repeat this step twice.
3. Spin samples at 10,000*g* at 4°C for 30 min.
4. Transfer supernatant to a new pre-cooled tube and measure the protein concentration.
5. Leave the tube on ice for further analysis or store supernatant at –20/–70°C.

3.4. Characterization of Overexpressed Proteins at Steady-State

Following transfection, harvest and disruption of cells, the next step is characterization of the overexpressed protein. **Subheadings 3.4.1.** and **3.4.2.** define the procedure for steady-state analysis, including methods for quantitating the total amount and the enzymatic activity of a given protein. **Subheading 3.4.3.** describes analysis of intact cells by immunofluorescence based methods. The advantages of each of these methods are exemplified in **Figs. 1–5**. Because the cultivation temperature in itself might have a positive effect on the folding of proteins the effect of cultivation temperature on the biogenesis of protein/active enzyme should be evaluated.

3.4.1.Western Blotting Analysis

1. Load between 1–10 µg total protein on a gel and perform electrophoresis and blotting according to usual techniques (*see* **Note 10**).
2. Block nonspecific binding sites by incubating the membrane in 5% nonfat dried milk in PBS-T for 1 h at room temperature on an orbital shaker. Alternatively, leave the membranes in the blocking solution overnight at 4°C without shaking.
3. Discard blocking solution and rinse the membrane twice for 2 min in PBS-T (>4 mL/cm^2).
4. Incubate with primary antibody diluted in PBS-T for 1 h at room temperature on an orbital shaker (*see* **Note 11**).
5. Discard the antibody solution and rinse the membrane twice in PBS-T for 1 min, followed by a third washing step in PBS-T for 15 min at room temperature on an orbital shaker.
6. Wash the membrane three times in PBS-T for 5 min at room temperature on an orbital shaker.

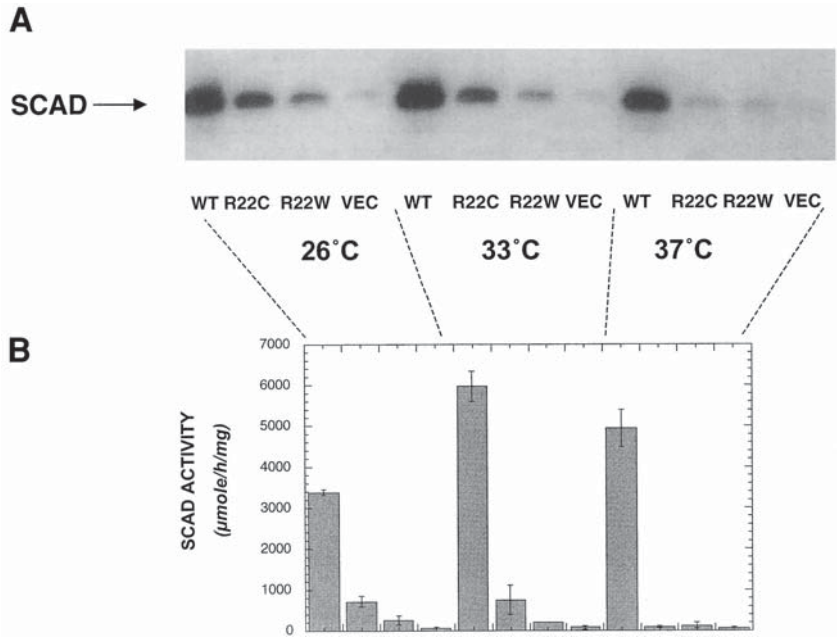

Fig. 1. Western blot and activity measurements of SCAD variant proteins expressed at steady state in transfected COS-7 cells cultivated at different temperatures. As a negative control vector without SCAD cDNA insert was used (Vec). (**A**) Identical amounts (10 µg) of total soluble protein from the cell extracts were subjected to SDS-PAGE and transferred to nitrocellulose for Western blotting as described in **ref. *16***. (**B**) SCAD enzyme activity was measured in the cell extracts used in the Western blot with the ferricenium ion assay as previously described ***(16)***. Note that reduced cultivation temperature in itself has a positive effect on the expressed amount and enzyme activity of the two SCAD mutants. Reproduced from **ref. *16*** with permission from the American Society for Biochemistry and Molecular Biology.

7. Incubate with secondary antibody diluted in PBS-T for 1 h at room temperature on an orbital shaker (*see* **Note 12**).
8. Discard the antibody solution and rinse the membrane twice in PBS-T for 1 min, followed by a third washing step in PBS-T for 15 min at room temperature on an orbital shaker.
9. Wash the membrane three times in PBS-T for 5 min at room temperature on an orbital shaker.
10. Perform detection according to usual techniques.

3.4.2. Enzyme Activity and Turnover Analysis of SCAD Proteins

The activity of SCAD enzymes is determined with the ferricenium ion-based colorimetric assay essentially as described in **ref. *16*,*32*** using n-butyryl-CoA

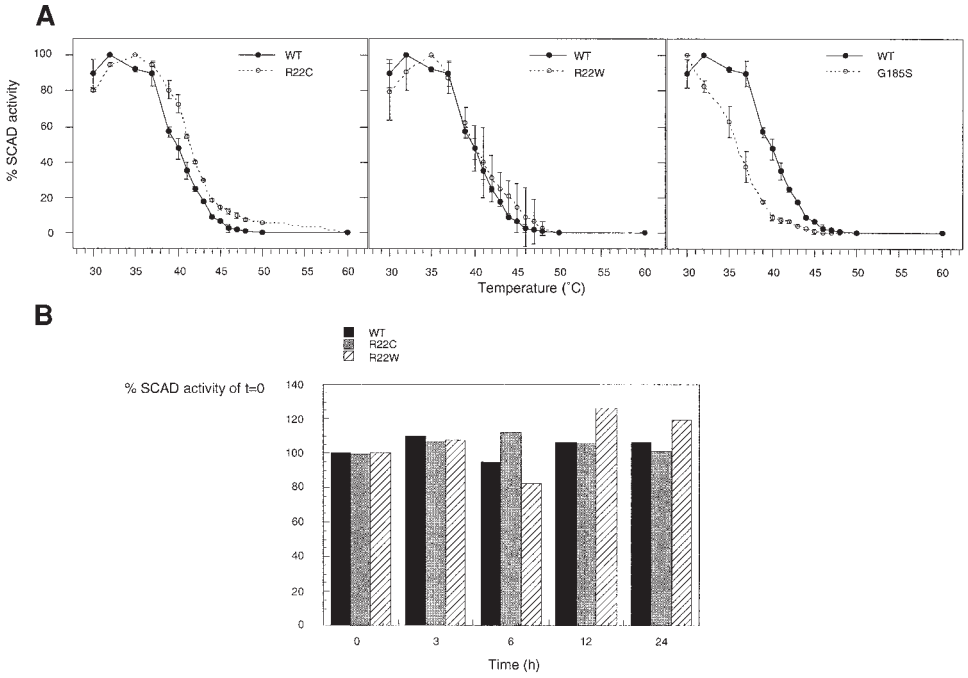

Fig. 2. Thermal stability profiles and kinetic stability in intact cells. Transiently transfected COS-7 cells overexpressing variant SCAD proteins were cultivated at the permissive temperature (26°C). (**A**) Aliquots from cell extracts were incubated at different temperatures for 10 min and the SCAD enzyme activity was measured and plotted vs the incubation temperature (percentage of activity measured at 32°C). For comparison, the profile obtained with extracts from cells over-expressing SCAD G185S ***(37)*** enzyme is shown. The data clearly demonstrate that the R22W and R22C mutant enzymes are as resistant to thermal inactivation as the WT, whereas the curve of the G185S mutant enzyme is shifted to lower temperatures, showing that this mutation displays a lower resistance to thermal inactivation of the tetramer once it is formed. (**B**) Forty-eight h after transfection protein synthesis was arrested by adding 10 μ*M* cycloheximide and the turnover of enzymes was followed by analysing the SCAD activity at different times. The unaltered resistance to thermal inactivation of SCAD variant enzymes shown in (**A**) correlates with an unchanged kinetic stability of the variant enzymes in intact transfected cells ***(16)***. Reproduced from **ref. *16*** with permission from the American Society for Biochemistry and Molecular Biology.

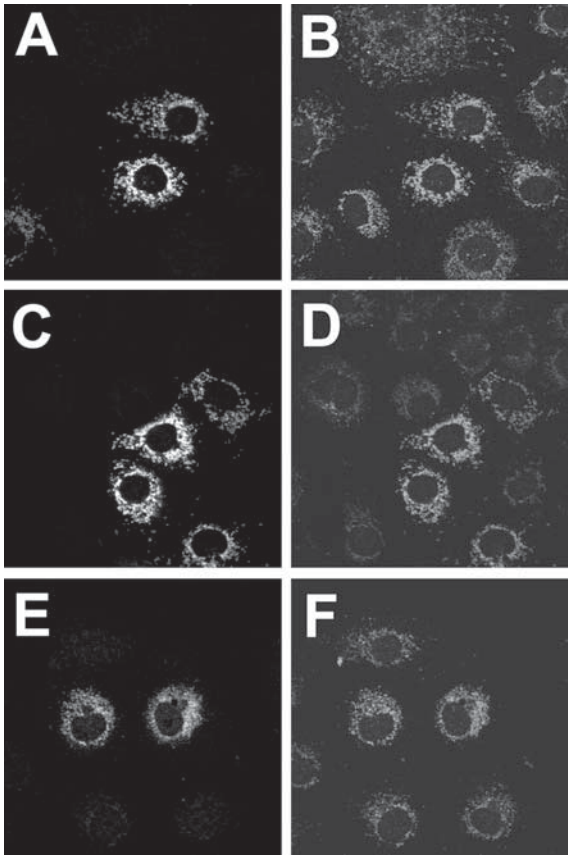

Fig. 3. Co-localization analysis of SCAD mutant and Hsp60 proteins. COS-7 cells were maintained at 26°C and transfected with SCAD WT (**A**,**B**), SCAD R22C (**C**,**D**) and SCAD R22C (**E**,**F**) expression vectors and analysed by CLSM. Overexpressed SCAD proteins were visualized using the rabbit anti-rat SCAD antibody followed by fluorescein-conjugated porcine anti-rabbit antibodies (left panel). Endogenously expressed Hsp60 was stained with mouse anti-human Hsp60 antibody followed by rhodamine-conjugated goat anti-mouse antibody (right panel). The fact that identical mitochondrial patterns are observed for SCAD WT and mutant proteins in combination with the data shown in **Figs. 1** and **2**, shows, that mutant proteins are imported an processed in the mitochondria ***(16)***. Reproduced from **ref.** ***16*** with permission from the American Society for Biochemistry and Molecular Biology.

as substrate (*see* **Fig. 1B**). This assay is not described in detail here because it is only applicable for this specific enzyme.

The growth temperature might have an influence on the kinetic stability of the synthesis of a given protein. As a measure of this parameter, thermal stabil-

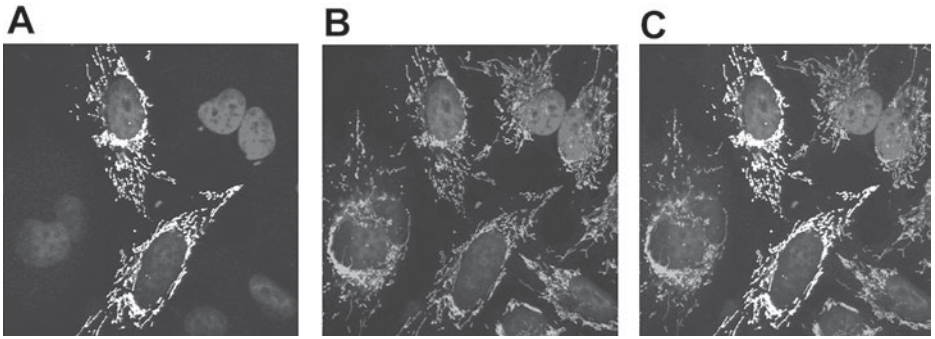

Fig. 4. Co-localization of ClpX by using c-myc tag and a mitochondrial selective dye. ClpX was overexpressed as a chimera of ClpX and the c-myc tag in transfected Chang cells cultured in slide flasks ***(17)***. Cells were labeled 36 h post-transfection with the mitochondrial probe (MitoTracker Red CMXRos), fixed and permeabilized. The subcellular localization was examined using *in situ* immunostaining and CLSM. (**A**) ClpX visualized by anti-myc and fluorescein labeled antibodies that indirectly immunostain human ClpX. (**B**) Mitochondria from the same section as shown in (A) stained with the rhodamine labeled MitoTracker. (**C**) Merging of the two pictures (A) and (B) illustrates that the ClpX and the MitoTracker dye co-localize, showing that ClpX is imported and processed in mitochondria. Nuclear DNA is counterstained with Hoechst 33258. Reproduced from **ref. *17*** with permission ©Springer-Verley GmBH & Co. KG.

ity profiles of residual active mutant enzymes can be determined in extracts from transfected cells. Samples are incubated at different temperatures ranging from 4–60°C for 10 min prior to activity measurement (*see* **Fig. 2A** and **ref. *16***). In order to investigate the fate of the fully folded protein inside the cell turnover analysis can be performed as previously described ***(16)***. For this purpose, SCAD activity was measured at different time points in transfected cells where the protein synthesis was arrested with cycloheximide (see below and **Fig. 2B**).

1. Transfect COS-7 cells and cultivate for 36–48 h.
2. Arrest protein synthesis by adding cycloheximide to a final concentration of 10 μ*M* (optimized in a control experiment).
3. Harvest aliquots of cells after various periods of incubation and analyze extracts by activity assay.

3.4.3. In situ *Immunostaining of Proteins*

Many biological studies of cells have been performed by immunofluorescent techniques using antibodies or tagged proteins. These kinds of experiments are important in order to investigate whether incorrect trafficking/

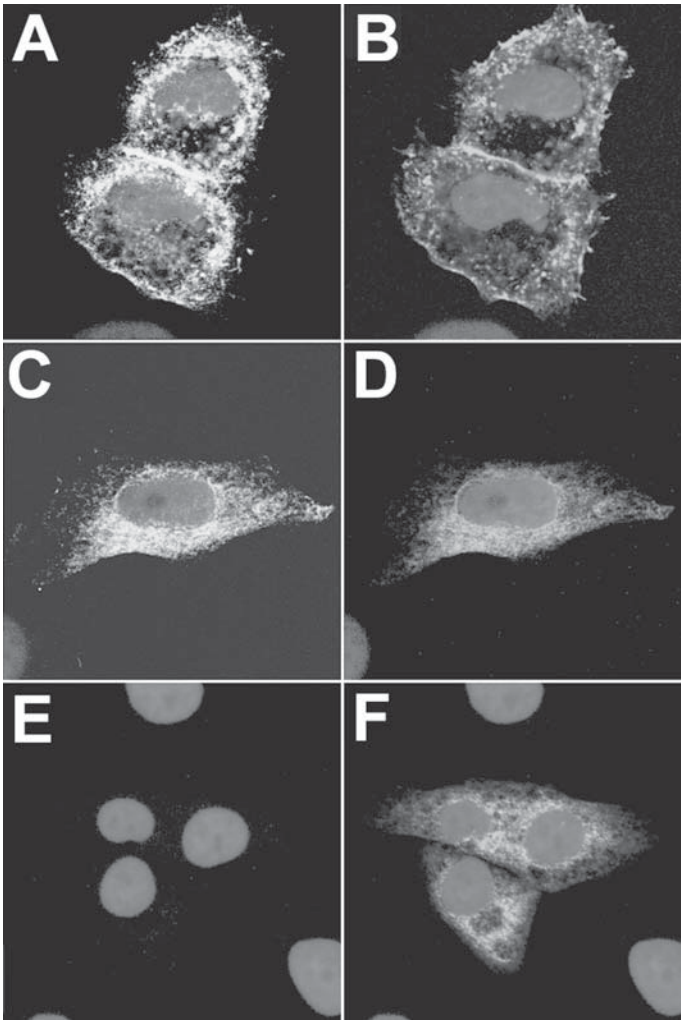

Fig. 5. Comparison of GFP fluorescent and LDL receptor immunostaining. Transfected Chang cells were analyzed by CLSM simultaneously for GFP fluorescence (left panel) and immunofluorescence staining using a mouse-anti LDL receptor antibody (C7), detected by rhodamine-conjugated secondary antibody (right panel). Nuclear DNA is counterstained with Hoechst 33258. (**A**,**B**), WT LDL receptor-20-GFP; (**C**,**D**) W556S LDL receptor-20-GFP; (**E**,**F**) C660X LDL receptor-20-GFP. The C7 immunostaining showed that the WT LDLR-20-GFP protein was localized on the cell surface, whereas the two mutant proteins were localized intracellularly. Using an ER probe, we have shown that the pattern of the two mutant proteins co-localize with ER ***(20)***. Similar to the C7 staining, GFP fluorescence from the WT LDLR-20-GFP protein was localized to the cell surface. *(Continued on facing page.)*

targeting of a mutant protein, caused by, e.g., improper folding, may explain the disease-causing nature of the mutation (*see* **Figs. 3–5**). The following procedure describes the localization of the ClpX chaperone by indirect immunostaining using the c-myc tag fused to the ClpX protein (**Fig. 4**). However, the procedure is generally applicable for c-myc-tagged proteins.

1. Transfect Chang cells with ClpX-c-myc cDNA constructs and cultivate for 24–48 h in tissue-culture slide flasks.
2. In order to detect both ClpX and mitochondria, incubate the cells with 50 n*M* MitoTracker Red CMXRos 48 h post-transfection for 30 min at 37°C prior to fixation (*see* **Note 13**).
3. Wash cells twice in ice-cold PBS.
4. Fix cells in ice-cold 4% paraformaldehyde for 5 min at 4°C.
5. Wash cells three times in PBS for 3 min.
6. Incubate 20 min in freshly made 70% ethanol. Store slides at –20°C or proceed with further analysis.
7. Add monoclonal anti-c-myc antibody to the slide and protect the cells with a cover glass. Incubate in a moisture chamber for 1 h at room temperature (*see* **Note 11**)
8. Wash cells three times for 5 min in PBS.
9. Add fluorescein-conjugated goat anti-mouse antibody to the slide and protect the cells with a cover glass. Incubate in a moisture chamber for 1 h at room temperature (*see* **Note 11**).
10. Wash cells three times for 5 min in PBS.
11. Counterstain DNA with Hoechst 33258 (1 μg/mL) for 1 min and wash cells in PBS.
12. Evaluate the experiment by UV-fluorescent microscopy and confocal laser scanning microscopy (CLSM) in antifade solution.

3.5. Characterization of Overexpressed Proteins: Pulse-chase Analysis

Pulse-chase experiments combined with immunoprecipitation is a very powerful technique allowing analysis of protein synthesis, kinetics of processing, and turnover of proteins. This procedure has been applied in the characterization of mutant SCAD proteins overexpressed in cells cultivated at different cultivation temperature using anti-SCAD antibodies as shown in **Fig. 6**.

Fig. 5 *(Continued from page194)* Correspondingly GFP fluorescence from cells expressing the W556S fusion protein resembled the intracellular, ER like, C7 staining. No GFP fluorescence could be observed with C660X LDLR-20-GFP containing a stop codon before GFP in the normal reading frame ***(20)***. Reproduced from **ref. *20*** with permission from Nture Publishing Group.

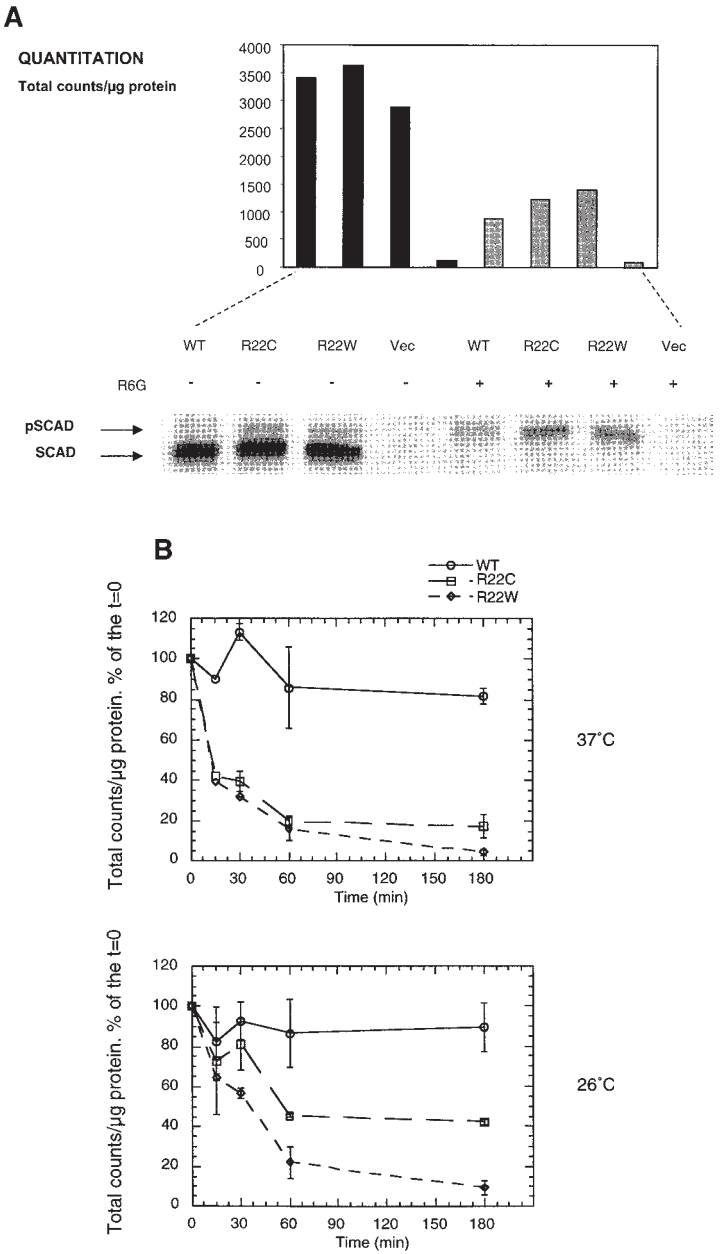

Fig. 6. *(Continued on next page)* Pulse-chase experiments with newly synthesized mitochondrial proteins. (**A**) Transfected COS-7 cells were cultivated in 10 cm^2 dishes at 37°C. The cells were metabolically labeled for 15 min in the presence or absence of rhodamine 6G (R6G) and then harvested. Upper part, bands in dried gels were quan-

3.5.1. Pulse-Labeling of Transfected Cells With [^{35}S]-Methionine/[^{35}S]-Cysteine and Pulse-C hase

1. Transfect cells in small dishes (10 cm^2) over night (*see* **Note 14**).
2. Next morning: Wash cells twice in pre-warmed HBSS (37°C).
3. In order to deplete unlabeled methionine and cysteine add 500 µL of pre-warmed (37°C) RPMI labeling medium. Incubate 30 min at 37°C.
4. Discard medium.
5. Add 500 µL pre-warmed (37°C) labeling medium containing 0.1 mCi PRO-MIX per well.
6. Inc. 30 min at 37°C under normal cultivation conditions (*see* **Note 15**).

7a. "Pulse-analysis": Wash cells twice in 1000 µL ice-cold PBS. Add 1000 µL ice-cold PBS and harvest the cells with a cell scraper. Radioactive samples are stored at –70°C.

7b. "Chase-analysis": Wash cells twice in 1000 µL ice-cold PBS and add 1500 µL chase medium. Cells are harvested after different chase periods and stored as described in the previous step.

3.5.2. Immunoprecipitation of Radiolabeled Proteins

1a. Incubate the labeled cells in lysis buffer for 1 h at 4°C. Use 100 µL lysis buffer. Centrifuge the lysate at 4°C (10,000*g*; 30 min) and save the supernatant. Save 1 µL of the supernatant for SDS-polyacrylamide gel electrophoresis (PAGE) analysis (*see* **Note 16**).

1b. Incubate antibodies with 30 µL of a 1:1 slurry of protein A-Sepharose dilution per 100 µL supernatant. Shake 1.5 h at 4°C. (*see* **Note 11** and **17**).

2. Transfer 30 µL of the mixture from **step 1b** to each of the supernatant samples in **step 1a**. Shake overnight at 4°C.
3. Collect the pellet by centrifugation at 4°C (2000*g*; 3 min).
4. Wash the protein A-Sepharose with 1000 µL of dilution buffer high. Shake 30 s at 4°C and centrifuge 3 min at 2000*g* (4°C). Carefully remove the supernatant and leave about 10 µL of fluid above the pellet.
5. Repeat **step 4**.

Fig. 6 *(continued from page 14)* titated with a phosphor imager. Black columns represents mature SCAD and gray columns represents precursor (pSCAD). Lower part, fluorogram, the positions of pSCAD and mature SCAD are indicated. (**B**) COS-7 cells were cultivated and transfected in 10 cm^2 dishes at 37°C and 26°C, respectively. After a 15 min pulse-labeling, the labeling medium with [^{35}S]-methionine and [^{35}S]-cysteine was replaced with growth medium and the cells were chased as indicated. Dried gels were analyzed with a phosphor imager. As discussed in Figs. 1–3 and **ref. *16***, the effect of two mutations results in rapid intramitochondrial degradation owing to elimination of partly folded or misfolded proteins. This effect is to some extent compensated by reduced cultivation temperature. Reproduced from **ref. *16*** with permission from the American Society for Biochemistry and Molecular Biology.

6. Collect the pellet by centrifugation at 4°C (2000*g*; 3 min).
7. Add dilution buffer high to a total volume of 20 μL.
8. Add 20 μL 2X sample buffer with DTT. Incubate 5 min at 100°C. Vortex and centrifuge at room temperature (10,000*g*; 5 min). Transfer supernatant to new tubes and measure total volume.
9. Half of each sample (approx 20 μL) is subjected to SDS-PAGE.
10. The gels are dried and protein bands quantitated using a phosphor imager (*see* **Note 16**).

4. Notes

1. Different mammalian cells should be tested in order to evaluate which cell-line is the most suitable. We have experienced that some proteins are expressed and/or processed differently in different cells, e.g., the mitochondrial localized caseinolytic protease (ClpP) are poorly processed in COS-7 cells as compared to Chang cells ***(33)***. This phenomenon has also been observed in the analysis of the LDL receptor ***(34)***.
2. For purification of supercoiled (very important for transient expression) plasmid DNA standard purification methods, such as gravity-flow anion-exchange based plasmid kits, are used. For further reading, *see* **ref. *1***.
3. The described transfection protocol is based on the procedure described by Graham and van der Eb ***(35)***. Commercial alternatives are available. Polystyrene tubes should be used in all steps.
4. DMEM is used because of the high concentration of calcium.
5. DNA-calcium-phosphate complexes are easily observed using a normal light microscope. These complexes can obtain different sizes and properly reflect variable DNA quality and/or different precipitation conditions (such as pH). In order to test the quality of the DNA-calcium-phosphate precipitates, different batches of HEPES (pH range 6.9–7.15) can be tested. Not all cells can be transfected using the calcium-phosphate co-precipitation procedure. Some cells lose viability because of the high calcium concentration, so other transfection methods must be used with these species. We have used the procedure to transfect Chang and COS-7 cells. Some of the transfected cells may die upon subcultivation. Therefore, we usually wash the cells in PBS and supply with fresh growth medium.
6. This protocol is optimized for a 10 cm^2 flask. It is important that the transfection reagent is pipetted directly into the serum-free medium (drop-wise). Do not allow the undiluted transfection reagent to come into contact with any plastic surface. The transfection frequency is markedly reduced using serum-containing medium. We have used this protocol for efficient transfection (up to 40–50% positive cells) of adherent cells such as COS-7, Chang cells, human primary fibroblasts, Neuro2A (mouse neuroblastoma cells; ATCC), NT2 (Human teratocarcinoma cells; Stratagene), CHO (Chinese hamster ovary cells; ATCC), AML12 (mouse hepatocyte; ATCC), and C2C12 (mouse muscle myoblast; ATCC). Moreover, we have performed co-transfection experiments simulta-

neously with three different plasmids. To further optimize transfection conditions, use different amounts of FuGENE 6, while keeping the amount of supercoiled DNA constant. Otherwise follow the manufacture's recommendations. The protocol can also be used for nonadherent cells, but with reduced transfection efficiency.

7. Normally no toxic effects are seen after DNA-FuGENE 6 treatment. Therefore, the complex can be left on the cells until the protein expression assay. However, cells should be examined 12–24 h post-transfection and medium replaced if necessary.
8. The lipid:DNA ratio should be kept at 5:1 during initial optimizing experiments, because the complexes formed under these conditions are very stable. For further optimization, alter the total amount of added DNA/lipid and/or time of transfection.
9. This cationic liposome reagent facilitates efficient DNA-mediated transfection of mouse fibroblast cells and human keratinocytes.
10. We normally use pre-cast gels for native and SDS gel electrophoresis. Proteins should be transferred to nitrocellulose membranes or similar for optimal results. Blots may be used immediately or stored dry at 4°C for 2–3 mo.
11. Dilution factor, incubation times, and temperatures should be determined empirically for each antibody.
12. We usually use a horseradish peroxidase (HRP) labeled secondary antibody. Dilution factor, incubation times, and temperatures should be determined empirically for each antibody.
13. The probe-containing medium should be pre-warmed to the appropriate cultivation temperature. If the cell does not appear to be sufficiently stained, either increase the labeling concentration or the time allowed for the dye to accumulate. All kinds of organel markers are commercially available, including probes that are well-retained after fixation and permeabilization. Alternatively, use endogenously expressed proteins that co-localize with the protein of interest. For mitochondria, we have used anti-Hsp60 antibodies.
14. We routinely use small dishes with an area of 10 cm^2 for pulse-chase experiments of transfected cells. Therefore, only 500 μL labeling medium is needed to cover the cells in a dish, leading to reduced consumption of label. In order to obtain efficient labeling, it is important that all solutions added to the cells during the pulse experiment are pre-warmed to 37°C. Moreover, cells should be kept at 37°C at all steps (except harvest). This includes steps in which the cells are outside the CO_2 incubator. To overcome this problem we have used a heating table with thermostatic control (Medite, Germany).
15. The extent of the labeling experiment depends on many parameters, including transfection frequency, expression level, cellular handling of the labeled proteins, purification (immunoprecipitation) of labeled proteins, and detection system. Optimization is normally acquired in each case. For extended pulse-labeling (more than 2 h), unlabeled methionine (1 mg/L) and cysteine (4 mg/L) should be

added to the labeling medium (containing ^{35}S labeled methionine and cysteine) to avoid shortage of methionine and cysteine.

16. In order to test whether cells in different dishes are labeled equally, 1 µL sample from **step 1a** is subjected to SDS-PAGE. The intensity from the different samples should be comparable. Another factor that might influence the overall result of the immunoprecipitation protocol is the amount of antibody added to each sample. To analyze this, the SDS-gel is incubated with Bio-Safe coomassie stain after electrophoresis. Equal amounts of immunoglobulin should be expected. Finally, quantitation and analysis of radioactive bands should be performed in an accurate and reproducible way. For further reading of the subject, the reader is referred to ***(36)***.
17. In order to ensure optimal conditions for the interaction between antibodies and beads, the reaction should be vortexed at revolutions allowing the beads to be in suspension constantly.

Acknowledgments

The author thanks Dr. Ramila Phillip, Applied Immune Sciences Inc., Santa Clara, CA, USA, for providing the pMP6-vector. Dr. Kay Tanaka, Department of Genetics, Yale University School of Medicine, New Haven, CT, USA, is acknowledged for providing the SCAD immunoglobulins. Dr. Thomas G. Jensen, Department of Human Genetics, Aarhus University, Denmark, is thanked for critical reading of the manuscript. This work was supported by the Karen Elise Jensens Fund, the Danish Medical Research Council, the Institute of Experimental Clinical Research, the Aarhus County Research Initiative, and the Danish Centre for Human Genome Research. **Figures 1–3** and **6**, **4**, **5** are reproduced from ***(16,17,20)***, respectively, with permission from the publishers.

References

1. Sambrook, J. and Russell, D. W. (2001) *Molecular Cloning, A Laboratory Manual*, 3rd ed. Cold Spring Harbor Laboratory Press, Cold Spring Harbor, New York.
2. Kay, M. A., Glorioso, J. C., and Naldini, L. (2001) Viral vectors for gene therapy: the art of turning infectious agents into vehicles of therapeutics. *Nat. Med.* **7,** 33–40.
3. Boussif, O., Lezoualc'h, F., Zanta, M. A., Mergny, M. D., Scherman, D., Demeneix, B., and Behr, J. P. (1995) A versatile vector for gene and oligonucleotide transfer into cells in culture and in vivo: polyethylenimine. *Proc. Natl. Acad. Sci. USA* **92,** 7297–7301.
4. Yanez, R. J. and Porter, A. C. (1998) Therapeutic gene targeting. *Gene Ther.* **5,** 149–159.
5. Rubanyi, G. M. (2001) The future of human gene therapy. *Mol. Aspects Med.* **22,** 113–142.
6. Crystal, R. G. (1995) Transfer of genes to humans: early lessons and obstacles to success. *Science* **270,** 404–410.
7. Kain, S. R., Adams, M., Kondepudi, A., Yang, T. T., Ward, W. W., and Kitts, P. (1995) Green fluorescent protein as a reporter of gene expression and protein localization. *BioTechniques* **19,** 650–655.

8. Cubitt, A. B., Heim, R., Adams, S. R., Boyd, A. E., Gross, L. A., and Tsien, R. Y. (1995) Understanding, improving and using green fluorescent proteins. *Trends Biochem. Sci.* **20,** 448–455.
9. Hampton, R. Y., Koning, A., Wright, R., and Rine, J. (1996) In vivo examination of membrane protein localization and degradation with green fluorescent protein. *Proc. Natl. Acad. Sci. USA* **93,** 828–833.
10. Loimas, S., Wahlfors, J., and Janne, J. (1998) Herpes simplex virus thymidine kinase-green fluorescent protein fusion gene: new tool for gene transfer studies and gene therapy. *BioTechniques* **24,** 614–618.
11. Scholz, G. M., Cartledge, K., and Hall, N. E. (2001) Identification and characterization of Harc, a novel Hsp90-associating relative of Cdc37. *J. Biol. Chem.* **276,** 30,971–30,979.
12. Perrin, M. H., Fischer, W. H., Kunitake, K. S., Craig, A. G., Koerber, S. C., Cervini, L. A., et al. (2001) Expression, purification, and characterization of a soluble form of the first extracellular domain of the human type 1 corticotropin releasing factor receptor. *J. Biol. Chem.* **276,** 31,528–31,534.
13. Crawford, B. E., Olson, S. K., Esko, J. D., and Pinhal, M. A. (2001) Cloning, Golgi localization, and enzyme activity of the full-length heparin/heparan sulfate-glucuronic acid C5-epimerase. *J. Biol. Chem.* **276,** 21,538–21,543.
14. Lippincott-Schwartz, J. and Zaal, K. J. (2000) Cell cycle maintenance and biogenesis of the Golgi complex. *Histochem. Cell Biol.* **114,** 93–103.
15. Wahlfors, J., Loimas, S., Pasanen, T., and Hakkarainen, T. (2001) Green fluorescent protein (GFP) fusion constructs in gene therapy research. *Histochem. Cell Biol.* **115,** 59–65.
16. Corydon, T. J., Bross, P., Jensen, T. G., Corydon, M. J., Lund, T. B., Jensen, U. B., et al. (1998) Rapid degradation of short-chain acyl-CoA dehydrogenase (SCAD) with temperature-sensitive folding defects occurs after import into mitochondria. *J. Biol. Chem.* **273,** 13,065–13,071.
17. Corydon, T. J., Wilsbech, M., Jespersgaard, C., Andresen, B. S., Borglum, A. D., Pedersen, S., et al. (2000) Human and mouse mitochondrial orthologs of bacterial ClpX. *Mamm. Genome* **11,** 899–905.
18. Jensen, H. K., Holst, H., Jensen, L. G., Jorgensen, M. M., Andreasen, P. H., Jensen, T. G., et al. (1997) A common W556S mutation in the LDL receptor gene of Danish patients with familial hypercholesterolemia encodes a transport-defective protein. *Atherosclerosis* **131,** 67–72.
19. Lehrman, M. A., Schneider, W. J., Brown, M. S., Davis, C. G., Elhammer, A., Russell, D. W., and Goldstein, J. L. (1987) The Lebanese allele at the low density lipoprotein receptor locus. Nonsense mutation produces truncated receptor that is retained in endoplasmic reticulum. *J. Biol. Chem.* **262,** 401–410.
20. Holst, H., Dagnæs-Hansen, F., Corydon, T. J., Andresen, P. H., Jorgensen, M. M., Kolvraa, S., et al. (2001) Hydrodynamic gene transfer of LDL-receptor GFP fusion proteins to mouse liver for the characterization of LDL-receptor mutations. *Eur. J. Hum. Genet.* **9,** 815–822.
21. Gao, X., and Huang, L. (1991) A novel cationic liposome reagent for efficient transfection of mammalian cells. *Biochem. Biophys. Res. Commun.* **179,** 280–285.

22. Beinert, H. (1963) Acyl-CoA dehydrogenases. *Enzymes* **7,** 447–476.
23. Matsubara, Y., Indo, Y., Naito, E., Ozasa, H., Glassberg, R., Vockley, J., et al. (1989) Molecular cloning and nucleotide sequence of cDNAs encoding the precursors of rat long chain acyl-coenzyme A, short chain acyl-coenzyme A, and isovaleryl-coenzyme A dehydrogenases. Sequence homology of four enzymes of the acyl-CoA dehydrogenase family. *J. Biol. Chem.* **264,** 16,321–16,331.
24. Amendt, B. A., Greene, C., Sweetman, L., Cloherty, J., Shih, V., Moon, A., et al. (1987) Short-chain acyl-coenzyme A dehydrogenase deficiency. Clinical and biochemical studies in two patients. *J. Clin. Invest.* **79,** 1303–1309.
25. Gregersen, N., Winter, V. S., Corydon, M. J., Corydon, T. J., Rinaldo, P., Ribes, A., et al. (1998) Identification of four new mutations in the short-chain acyl-CoA dehydrogenase (SCAD) gene in two patients: one of the variant alleles, 511C—>T, is present at an unexpectedly high frequency in the general population, as was the case for 625G—>A, together conferring susceptibility to ethylmalonic aciduria. *Hum. Mol. Genet.* **7,** 619–627.
26. Corydon, M. J., Vockley, J., Rinaldo, P., Rhead, W. J., Kjeldsen, M., Winter, V., et al. (2001) Role of common gene variations in the molecular pathogenesis of short- chain acyl-CoA dehydrogenase deficiency. *Pediatr. Res.* **49,** 18–23.
27. Naito, E., Ozasa, H., Ikeda, Y., and Tanaka, K. (1989) Molecular cloning and nucleotide sequence of complementary DNAs encoding human short chain acyl-coenzyme A dehydrogenase and the study of the molecular basis of human short chain acyl-coenzyme A dehydrogenase deficiency. *J. Clin. Invest.* **83,** 1605–1613.
28. Goldstein, J. L., Hobbs, H. H., and Brown, M. S. (1995) Familial hypercholesterolemia, in *Metabolic and Molecular Basis of Inherited Diseases*, vol. 2, 7th ed. (Scriver, C. R., Beaudet, A. L., Sly, W. S., and Valle, D., eds.), McGraw-Hill, New York, pp. 1981–2030.
29. Gottesman, S., Clark, W. P., de Crecy Lagard, V., and Maurizi, M. R. (1993) ClpX, an alternative subunit for the ATP-dependent Clp protease of Escherichia coli. Sequence and in vivo activities. *J. Biol. Chem.* **268,** 22618–22626.
30. Zhang, G., Budker, V., and Wolff, J. A. (1999) High levels of foreign gene expression in hepatocytes after tail vein injections of naked plasmid DNA. *Hum. Gene Ther.* **10,** 1735–1737.
31. Liu, F., Song, Y., and Liu, D. (1999) Hydrodynamics-based transfection in animals by systemic administration of plasmid DNA. *Gene Ther.* **6,** 1258–1266.
32. Lehman, T. C., Hale, D. E., Bhala, A., and Thorpe, C. (1990) An acyl-coenzyme A dehydrogenase assay utilizing the ferricenium ion. *Anal. Biochem.* **186,** 280–284.
33. Corydon, T. J., Bross, P., Holst, H. U., Neve, S., Kristiansen, K., Gregersen, N., and Bolund, L. (1998) A human homologue of Escherichia coli ClpP caseinolytic protease: recombinant expression, intracellular processing and subcellular localization. *Biochem. J.* **331,** 309–316.
34. Jorgensen, M. M., Jensen, O. N., Holst, H. U., Hansen, J. J., Corydon, T. J., Bross, P., et al. (2000) Grp78 is involved in retention of mutant low density lipoprotein receptor protein in the endoplasmic reticulum. *J. Biol. Chem.* **275,** 33,861–33,868.
35. Graham, F. L. and van der Eb, A. J. (1973) A new technique for the assay of infectivity of human adenovirus 5 DNA. *Virology* **52,** 456–467.
36. Ritco-Vonsovici, M. and Willison, K. R. (2000) Defining the eukaryotic cytosolic chaperonin-binding sites in human tubulins. *J. Mol. Biol.* **304,** 81–98.
37. Corydon, M. J., Gregersen, N., Lehnert, W., Ribes, A., Rinaldo, P., Kmoch, S., et al. (1996) Ethylmalonic aciduria is associated with an amino acid variant of short-chain acyl-Coenzyme A dehydrogenase. *Pediatr. Res.* **39,** 1059–1066.

17

Investigation of Unfolded-Protein Response in Cells Expressing Familial Alzheimer's Disease-Linked Presenilin Variants

Gopal Thinakaran, James W. Bowen, Daisuke Ito, Jae-Yoon Leem, Margaret L. Veselits, and Naoyuki Sato

1. Introduction

Affected individuals in the vast majority of pedigrees with early-onset familial Alzheimer's disease (FAD) harbor mutations in *PSEN1*, the gene that encodes a polytopic membrane protein termed Presenilin 1 (PS1) ***(1)***. Recent genetic, biochemical, and pharmacological evidence indicate that PS1 plays a critical role in the proteolysis and trafficking of a selected set of transmembrane proteins including the amyloid precursor protein (APP) and Notch 1 ***(2)***. Intrigued by two recent reports, which suggested that loss of PS1 function, or expression of FAD-linked PS1 variants, compromised the mammalian unfolded-protein response (UPR), we sought to evaluate the potential role of PS1 in the mammalian unfolded-protein response.

The UPR, involving the coordinate transcriptional activation of a set of genes that encode endoplasmic reticulum (ER) chaperones and certain cell-death signals, occurs as a result of the accumulation of misfolded proteins in the ER ***(3,4)***. The UPR is activated by agents that affect ER homeostasis, including tunicamycin, thapsigargin, Ca^{2+} ionophores, and reducing agents. In yeast, the most proximal reactions necessary for promoting the UPR are the dimerization and trans-autophosphorylation of ER resident transmembrane kinase, termed IRE1p ***(3,5)***. In mammalian cells, two IRE1p homologues namely, IRE1α and IRE1β, have been identified; ER stress causes dissociation of BiP/GRP78 (IgG

From: *Methods in Molecular Biology, vol. 232: Protein Misfolding and Disease: Principles and Protocols*
Edited by: P. Bross and N. Gregersen © Humana Press Inc., Totowa, NJ

binding protein) from the lumenal, stress-sensing, domain of IRE1α and IRE1β and leads to their oligomerization, activating trans-autophosphorylation and downstream signaling to the UPR ***(5–8)***. The C-terminal effector domain of IREs may, under certain circumstances, be liberated from the full-length protein by proteolysis and translocated to the nucleus ***(9)***.

The prototypical inducers of the UPR are tunicamycin, a nucleoside antibiotic that inhibits *N*-glycosylation of target asparagine residues in the lumenal domains of proteins expressed in the ER; and thapsigargin, an inhibitor of the ER Ca^{2+} ATPase. The cellular response to these ER stressors is to transcriptionally activate genes that encode protein chaperones such as BiP, GRP94, protein disulfide isomerase, Erp72, and the transcription factor CHOP (C/EBP-homologous protein) ***(3,10,11)***. This chapter describes the details of the investigation wherein we evaluated the well-characterized aspects of the mammalian UPR. This includes analysis of BiP expression by Northern blotting, promoter assay, and steady-state protein levels. In addition, we examine two other UPR-related proteins, GRP94 and CHOP. Finally, we also detail our analysis of the activation of ER transmembrane kinases IRE1α and PERK. Our studies provide evidence that neither the ER stress-induced accumulation of *BiP* and *CHOP* mRNA/protein nor the activation of ER stress kinases IRE1 and PERK are compromised in cells expressing FAD-linked PS1 variants. Our findings provide compelling evidence that expression of FAD-linked PS1 variants has no discernible impact on ER stress-mediated induction of established "readouts" of the UPR pathway.

2. Materials

1. PS1 expression plasmids.
2. Antibodies raised against PS1, CHOP, KDEL, β-tubulin, IRE1α ***(12)***, and PERK ***(13)***.
3. Cell-culture medium.
4. Antibiotics for selection of stable transfectants: zeocin and hygromycin.
5. Trizol reagent (Life Technologies, Inc.).
6. 5 m*M* dNTPs.
7. RNasin (20–40 U/μL).
8. 100 m*M* dithiothreitol (DTT).
9. pd(N)6 (1 μg/μL) (Pharmacia).
10. SuperScriptII $RnaseH^-$ Reverse transcriptase (200 U/μL; Life Technologies).
11. Diethyl pyrocarbonate (DEPC) treated water (*see* **Note 1**).
12. Thermal cycler.
13. Primer pairs for PCR (*see* **Note 2**).
14. Taq DNA polymerase (2.5 U/μL).
15. Protein lysis buffer: 150 m*M* NaCl, 50 m*M* Tris-HCl, pH 7.4, 0.5% sodium deoxycholate, 0.25% sodium dodecyl sulfate (SDS), 5m*M* ethylenediamine

tetraacetic acid (EDTA), 0.2 *M* phenylmethylsulfonyl fluoride (PMSF), 1:200 dilution of protease inhibitor cocktail (Sigma; P8340) (*see* **Note 3**).
16. Protein A coupled to agarose (Roche).
17. Laemmli buffer: Phosphate-buffered saline (PBS) containing 1 m*M* $MgCl_2$ and 1 m*M* $CaCl_2$.
18. IP lysis buffer: 20 m*M* HEPES, pH 7.5, 150 m*M* NaCl, 1% Triton X-100, 10% glycerol, 1 m*M* EDTA, 10 m*M* tetrasodium pyrophosphate, 100 m*M* NaF, 17.5 m*M* β-glycerophosphate, 1 m*M* PMSF, 1/200 dilution of protease inhibitor cocktail.
19. IP wash buffer: 20 m*M* Tris-HCl, pH 7.4, 150 m*M* NaCl, 1 m*M* EDTA, 1% Nonidet P-40, 1% sodium deoxycholate, 0.1% SDS, 50 m*M* NaF, 1:200 dilution of protease inhibitor cocktail.
20. Alkaline phosphatase and digestion buffer (Roche).

3. Methods

3.1. Generation of Stable PS1 Cell Lines and Pooled Stables

A high-efficiency mammalian transfection method ***(14)*** was employed for transfection of cells. To generate stable PS1 lines (*see* **Subheading 3.1.1.**), a mouse N2a neuroblastoma cell line termed Swe.10 ***(15)*** that constitutively expresses human APP695 harboring the "Swedish" double mutation was used as parental cells. The PS1 expression plasmids used in our studies encode Wt PS1, PS1D385A mutant, or FAD-linked C410Y variant from a CMV promoter and harbor zeocin-resistance cassette. For certain experiments that are potentially confounded by protein expression levels or clonal variability, it is preferable to generate stably transfected pools that represent a wide range of transgene expression instead of undertaking tedious characterization of multiple stable cell lines with different degrees of transgene expression. Hence, we also generated stable N2a Swe.10 and human 293 pools, by transfecting them with an empty bicistronic vector (pIRE1hyg; CLONTECH), or pIRE1hyg containing Wt PS1 or the FAD-linked M146L, H163R, and ΔE9 mutant cDNA.

3.1.1. Generation of Independent Stable Transfectants

1. One day before initiating transfection, seed 0.5×10^6 cells in 60-mm dishes containing 5 ml of growth medium (50% OptiMEM, 45% Dulbecco's modified Eagle's medium [DMEM], 5% fetal calf serum [FCS]).
2. Prepare a transfection mixture containing 10 μg of plasmid expression vector in BES buffer as described ***(14)***.
3. Add the transfection mixture to the dishes and incubate at 3% CO_2. A fine precipitate develops during the overnight incubation.
4. After 12–16 h, wash the dishes with growth medium and transfer to 5% CO_2.
5. Trypsinize the cells and plate 1:50 dilution of transfected cells in five 100-mm dishes in growth medium.
6. The following day, replace growth medium with the appropriate selection medium (growth medium containing 400 μg/mL zeocin).

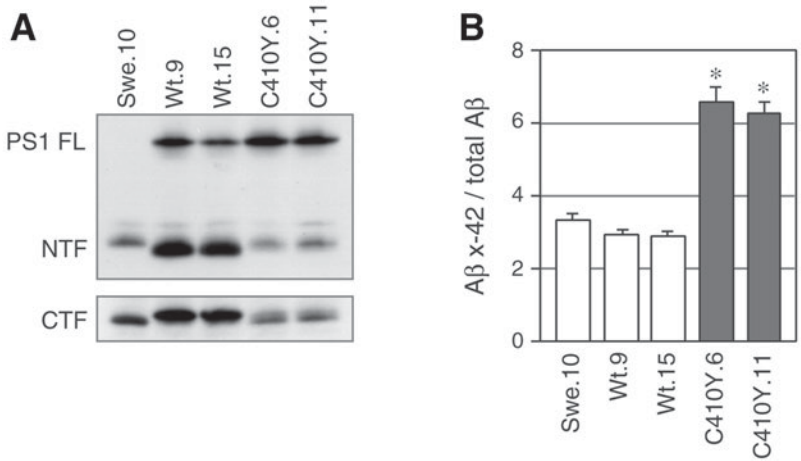

Fig. 1. Stable expression of PS1 in N2a cells. (**A**) PS1 expression was analyzed in detergent lysates prepared from parental N2a cell line Swe.10, or independent stable Swe.10 derivatives that express human Wt PS1 (Wt.9 and Wt.15), or the FAD-linked PS1 C410Y mutant (C410Y.6 and C410Y.11). Full-length PS1 (*PS1 FL*), and N- and C-terminal proteolytic derivatives (*NTF* and *CTF*, respectively) are indicated. (**B**) Quantitative analysis of secreted Ab x-40 and x-42 in the media conditioned by stable lines was performed using two-site ELISAs. The ratio of Abx-42/total Ab was calculated from two independent experiments (nine samples) and the mean (±S.E.) is plotted. Cells expressing C410Y mutant PS1 secrete approx twofold more Ab42 compared to Swe.10 or Wt PS1 lines; the total amount of Ab40 was not significantly different between control, Wt PS1 and mutant PS1 cells. *, $p < .0001$.

7. Remove and replace selection medium every 3–4 d. Colonies will be visible after 2–3 wk. Transfer individual colonies into 24-well dishes for expansion.
8. Analyze transgene expression by Western-blot analysis using PS1 antibodies ***(16)*** and choose individual clones with low-, medium- and high-expression levels for further studies.

Western-blot analysis using PS1 antibodies demonstrates the expression of human Wt PS1 and mutant PS1 polypeptides in these lines, and as described earlier ***(17,18)*** overexpression of the human PS1 polypeptides resulted in the "replacement" of the majority of the murine PS1 derivatives (**Fig. 1A**). Furthermore, as expected from earlier studies ***(19)***, two-site enzyme-linked immunosorbent assay (ELISA) assays confirmed that the levels of Aβ42 secreted by the PS1 C410Y cell lines are twofold higher than parental Swe.10 or Wt PS1 lines (Aβ42/total Aβ ratio Swe.10 and Wt PS1 lines is 3.01 ± 0.09 vs C410Y lines, 6.37 ± 0.24; $p < .0001$) (**Fig. 1B**). Thus these cell lines are appropriate for the present investigation on the influence of mutant PS1 expression on the induction of mammalian UPR.

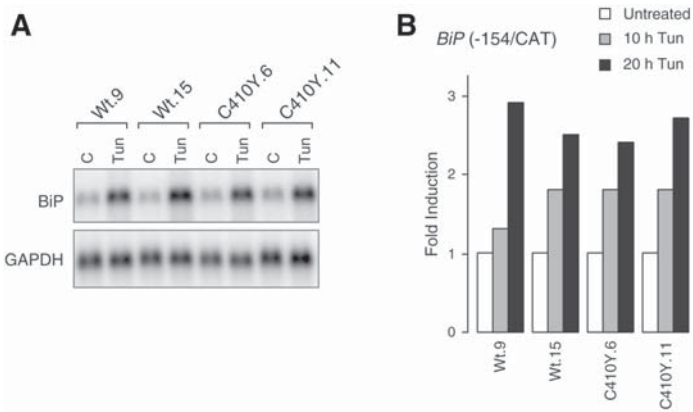

Fig. 2. Analysis of *BiP* expression in N2a cell lines. (**A**) Total RNA was isolated from stable N2a cell lines that express Wt PS1 or C410Y PS1 variant. ER stress was induced by exposing cells to tunicamycin (2 μg/mL) for 5 h. The levels of BiP and *GAPDH* mRNA were analyzed by Northern-blot hybridization. Signal intensities were quantified by Phosphorimage analysis and *BiP* mRNA levels were normalized to *GAPDH* levels. (**B**) Cells were co-transfected with the reporter plasmid *BiP* (-154CAT) and the control SV40 β-galactosidase plasmid. Cells were treated with 2 μg/mL tunicamycin (Tun) for 10 or 20 h (three dishes each) before harvest. Lysates were normalized for transfection efficiency by β-galactosidase activity. *BiP* promoter activity was determined by the percentage conversion of [^{14}C]chloramphenicol to its acetylated forms and quantified by Phosphorimaging. Fold-induction relative to untreated cultures for each line is plotted.

3.1.2. Generation of Pooled Stable Transfectants

1. Perform transfection as described in **Subheading 3.1.1.**, **steps 1–3**.
2. Trypsinize the cells 12–16 h after transfection and plate them in 100-mm dishes.
3. Begin selection in the appropriate medium the following day.
4. Approximately 200–300 colonies will be visible after 3 wk of growth in selection medium. Trypsinize and pool the stable colonies for further studies. Because pIRE is a bicistronic expression plasmid, all hygromycin-resistant cells will express PS1, albeit at different levels.

3.2 Analysis of mRNA Levels

Total RNA was prepared by guanidinium thiocyanate lysis and CsCl ultracentrifugation or using Trizol reagent ***(20)***. Northern-blot hybridization is the preferred method of choice for accurate evaluation of mRNA abundance. Standard methods were used for labeling probes and hybridization ***(21)***. Northern-blot analysis of *BiP* expression in PS1 cell lines is shown in (**Fig. 2A**). Tunicamycin treatment resulted in increased accumulation of *BiP* mRNA both in wt and mutant PS1 cell lines and no significant difference was observed in the hybridization intensity. Similarly, analysis of BiP mRNA in stable pools of

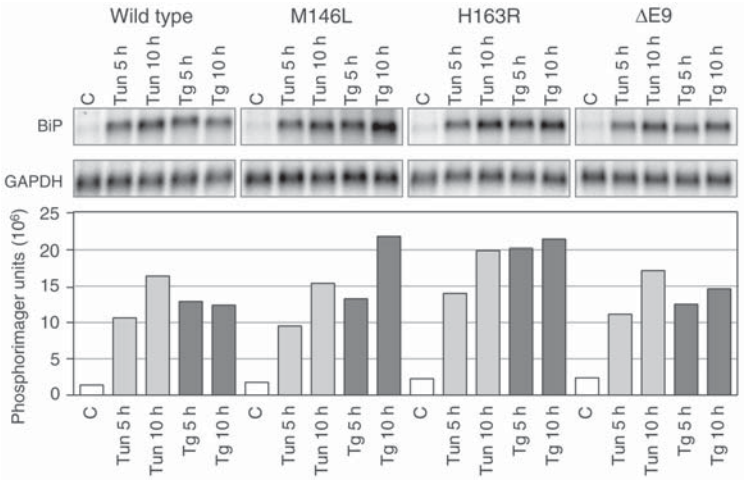

Fig. 3. Analysis of BiP expression in stable 293 pools. RNA was isolated from subconfluent Wt PS1 and mutant PS1 cultures treated for 5 or 10 h with tunicamycin (2 μg/mL) or thapsigargin (300 n*M*). The levels of *BiP* and *GAPDH* mRNA were analyzed by Northern blots. Hybridization signals were quantified by Phosphorimaging and *BiP* signals were normalized to *GAPDH* mRNA levels and plotted. Note that no obvious difference in the induction of *BiP* mRNA was observed between the different pools of cells analyzed.

293 cells also failed to show any defect in the induction of UPR in cells expressing mutant PS1 (**Fig. 3**).

In some experiments, mRNA levels were evaluated by semi-quantitative RT-PCR analysis (**Subheading 3.2.3.**). Standard protocols were used for reverse transcription (*see* **Subheading 3.2.2.**). To ensure that cDNA template amplification is within the linear range, control experiments were performed in which samples were incubated in polymerase chain reaction (PCR) for 16, 18, 20, or 22 cycles and the products were quantified by phosphorimage analysis. Appropriate cycle number for subsequent PCR is determined based on the results of this pilot experiment.

3.2.1. Northern Blot Analysis

1. Fractionate total RNA (20 μg/lane) in a 1.2% formaldehyde agarose gel.
2. Transfer the RNA to a nylon membrane in 20X SSC buffer.
3. Crosslink transferred RNA to the membrane using a Stratagene UV crosslinker.
4. Prehybridize the membrane for at least 1 h in RapiHhyb solution (Amersham).
5. Prepare [^{32}P]dATP-labeled *BiP*, and *GAPDH* cDNA probes (25 ng) by random prime labeling method.

6. Hybridize the membrane with *BiP* probe in RapidHyb buffer for 3–5 h at 65°C.
7. Wash the membrane in 2X SSC/0.1% SDS for 30 min and 0.1X SSC/0.1% SDS for 30 min at 60°C buffer.
8. Quantify hybridization signal by Phosphorimage analysis.
9. Remove the hybridized probe and repeat hybridization with *GAPDH* probe.
10. Normalize BiP signals to *GAPDH* signal intensity to adjust for minor differences in gel loading.

3.2.2. Reverse Transcription

1. Start with 1–5 μg of each RNA sample.
2. Add DEPC treated autoclaved water to a final volume of 13.5 μL in a 0.2-ml microcentrifuge tube.
3. Incubate the reaction at 65°C for 5 min.
4. Quick chill the reation on ice for 5 min.
5. While **steps 3** and **4** are occurring, prepare on ice a master mix containing the following reagents (volumes given are per reaction): 5 μL of 5X reverse transcriptase buffer, 1.25 μL dNTPs, 1 μL RNasIn, 2.5 μL DTT, 0.75 μL pd(N)6, and 1 μL reverse transcriptase enzyme.
6. Add 11.5 μL master mix to each of the reation tubes (final volume 25 μL).
7. Incubate the tubes at 42°C for 1 h.
8. Heat-inactivate the reverse transcriptase enzyme by incubating the reaction mixture at 100°C for 1 min.

3.2.3. Polymerase Chain Reaction

1. Add 100 μL sterile water to the 25 μL of cDNA obtained from the reverse transcription reation (a 1:5 final dilution).
2. Prepare a master mix containing 1.5 μL $MgCl_2$, 5 μL 10X PCR buffer, 2 μL dNTPs, and 32 μL dH_2O.
3. Pipette 42.5 μL of the master mix into each PCR reaction tube.
4. Add 5 μL of the appropriate diluted cDNA plus 1 μL of both the sense and antisense primers (20 pmoles). Add 2 pmoles of γ[^{32}P]-labeled sense or antisense primer (*see* **Note 4**). Finally add 0.5 μL of Taq DNA polymerase to each tube.
5. A typical thermal cycling program is given below. The cycle number is adjusted based on mRNA abundance (*see* above).
   Step 1: 2 min at 94°C.
   Step 2: 30 s at 92°C.
   Step 3: 30 s at 58°C (*see* **Note 5**).
   Step 4: 1 min at 72°C (extension/elongation; increase time for longer products).
   Step 5: Repeat **steps 2–4** for 24 cycles.
   Step 6: 10 min at 72°C.
   Step 7: Hold at 4°C.
6. Fractionate the PCR products by agarose gel electrophoresis. Quantify signal intensities by phosphorimage analysis of dried gels.

3.3. Quantification of BiP Promoter Activity

It has been previously shown that quantification of *BiP* promoter activity can be used as an independent measure of *BiP* expression. In this simple and quantitative assay, cells under investigation are transfected with a plasmid, termed *BiP*(–154CAT). This plasmid harbors a *BiP* promoter-chloramphenicol acetyltransferase (CAT) fusion gene consisting of 154 bp of BiP promoter, and retains all the ER stress-inducible properties of the rat *BiP* promoter ***(22)***. Cells are co-transfected with a control plasmid that encodes β-galactosidase so that differences in transfection efficiencies can be normalized based on β-galactosidase activity.

1. One day before initiating transfection, seed 0.5×10^6 stably transfected wt or mutant PS1 cells in each of nine 60-mm dishes containing 5 mL of growth medium (50% OptiMEM, 45% DMEM, 5% FCS).
2. Prepare a transfection mixture containing 1.5 μg *BiP* promoter/CAT fusion plasmid *BiP* (-154CAT), and 0.75 μg pSV40 β-galactosidase plasmid. Any lipid-based transfection method may be used in this step (*see* Chapter 16). Lipofectamine transfection method is routinely used in the author's laboratory to achieve maximum transfection efficiency in these studies.
3. Treat cells with 2 μg/mL tunicamycin for 10 or 20 h before harvesting. Three dishes are used for each time points and three dishes are left untreated.
4. β-galactosidase and CAT activities were determined by standard procedures as previously described ***(23)***. Convenient kits that are commercially available for assaying both activities from the same lysates may be used for this purpose. β-galactosidase activites are normalized between samples to adjust for differences in transfection efficiencies between cell lines.

As expected, treatment with tunicamycin causes a time-dependent increase in the *BiP* promoter activity. Notably, the promoter activity was induced to comparable levels in the Wt PS1 and C410Y PS1 stable lines, indicating that the UPR-mediated increase in *BiP* transcription is not influenced by the expression of FAD-linked PS1 variant (**Fig. 2**).

3.4. Western Blot Analysis of UPR Gene Expression

Although UPR is largely transcriptional, changes in the abundance of BiP, GRP94, and CHOP proteins can be readily monitored in cells undergoing ER stress. In general, the polypeptide levels of protein chaperones increase with slower kinetics relative to their mRNAs. On the other hand, CHOP protein levels increase within 4 h of treatment with tunicamycin.

1. Treat subconfluent cultures of cells in 60 mm dishes with tunicamycin or thapsigargin for predetermined periods of time.
2. Chill the cells on ice and wash twice with PBS.
3. Lyse cells in 400 μL of ice-cold protein lysis buffer. Use a sterile plastic cell scraper to scrape the cells from the bottom of the dish.

4. Transfer the lysate to a sterile microfuge tube. Briefly sonicate samples (30 s) to reduce viscosity. Store the lysates at –20°C.
5. Estimate protein concentration and fractionate 50 μg of protein by 10% sodium dodecyl sulfate polyacrylamide gel electrophoresis (SDS-PAGE).
6. Transfer the proteins to nylon membranes.
7. After blocking the membranes in 5% nonfat milk diluted in PBST, incubate with appropriate dilutions of primary antibodies. Anti KDEL (1:2500), CHOP (1:2500), and β-tubulin (1:50,000) antibodies were purchased from Santa Cruz Biotechnology, Inc., StressGen Biotechnologies Corp., and Amersham Pharmacia Biotechnologies, respectively. PS1 antibodies were generated in the author's laboratory.
8. Wash the membranes in PBST.
9. Incubate membranes with appropriate horseradish peroxidase (HRP)-coupled anti-rabbit or anti-mouse secondary antibody. Cleaner results may be obtained using HRP-coupled protein-A when using primary rabbit polyclonal antibodies (Pabs). For quantitative Western blots, substitute HRP-coupled antibodies with appropriate [^{125}I]-labeled IgG (DuPont NEN).

Results of Western-blot analyses show no significant difference in the increase in BiP, GRP94, and CHOP protein levels with respect to wt or mutant PS1 expression in stably transfected N2a cell lines (**Fig. 4**) or pooled stable 293 cells (**Fig. 5**).

3.5. Analysis of IRE1α and PERK Phosphorylation

One of the earliest responses to the accumulation of unfolded proteins is the autophosphorylation of transmembrane kinases IRE1α and PERK. To determine whether expression of mutant PS1 affects IRE1α or PERK activation, we examined the ER stress-induced phosphorylation of IRE1α in Wt and mutant PS1 cell lines following treatment with tunicamycin or thapsigargin. Activation by autophosphorylation of either kinases causes a small band-shift in their electrophoretic mobility through SDS gels ***(12,13)***. Owing to the low abundance of these kinases, we employed a combined immunoprecipiation/immunoblot method that has been described previously ***(24)***.

3.5.1. Cell Lysis and Immunoprecipitation/Western Blot Analysis

1. Prebind 1 μL of primary antibody (IRE1α or PERK) to 15 μL of protein A agarose beads in 200 μL of IP lysis buffer and mix the tubes on a nutator for 1 h at 4°C. Centrifuge at 1500*g* for 3 min to pellet the beads. Wash the beads twice in 500 μL of IP wash buffer. Collect the beads by centrifugation and aspirate the wash buffer. Prepare one tube per sample.
2. Lyse subconfluent culture of cells in 100-mm dishes in 500 μL of IP lysis buffer. Transfer the lysate to a microcentrifuge tube and incubate at 4°C for 15 min on a nutator.
3. Remove nuclei and cell debris by centrifugation at 10,000*g* for 5 min and save the clear supernatant.

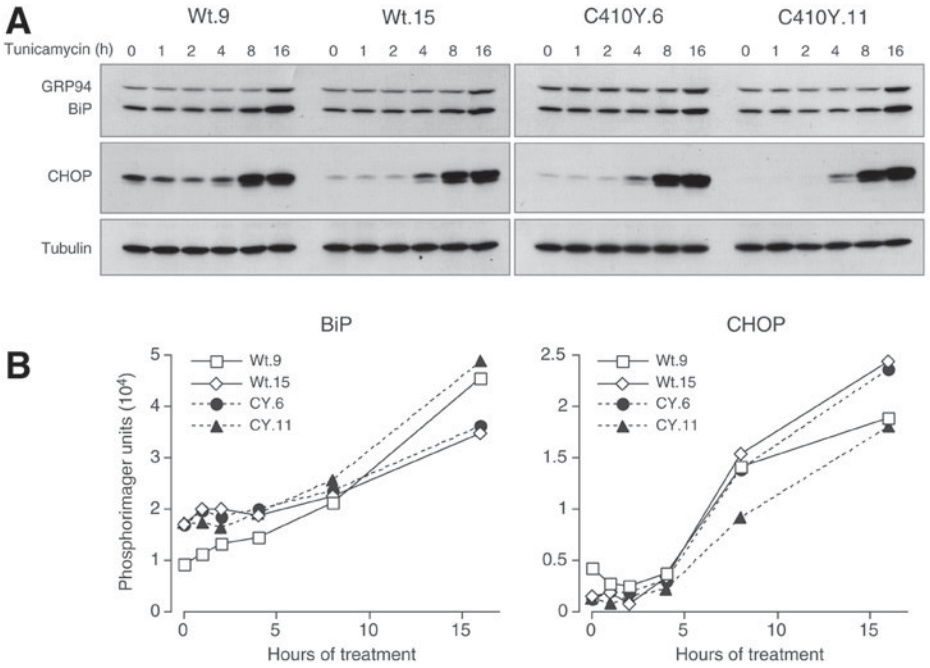

Fig. 4. Western-blot analysis of UPR gene expression in N2a cell lines. (**A**) Subconfluent cultures of Wt PS1 (Wt.9 and Wt.15) and PS1 C410Y mutant (C410Y.6 and C410Y.11) lines were incubated with tunicamycin (2 μg/mL) for various periods of time (0, 1, 2, 4, 8, or 16 h). Detergent lysates were prepared and analyzed by Western blotting with anti-KDEL (upper panel), anti-CHOP antibodies (middle panel). Blots were reprobed with anti-tubulin antibodies to confirm equal protein loading (lower panel). (**B**) To quantify the levels of BiP and CHOP polypeptides, blots containing primary antibodies were incubated with [^{125}I]-labeled secondary antibodies, and signal intensity was quantified by Phosphorimaging and plotted. In spite of the differences observed at time 0, the levels of BiP and CHOP uniformly increase after 8 and 16 h of tunicamycin treatment in Wt PS1 and mutant PS1 cultures.

4. Quantify protein content of the lysates to normalize between multiple samples. Typically the entire lysate is used for one immunoprecipitation.
5. Add the lysate to the tube containing washed beads prepared in **step 1** and mix the tubes on a nutator for 2 h at 4°C.
6. Collect the beads by centrifugation and wash three times with 500 μL of IP wash buffer. Carefully remove the wash buffer and resuspend the samples in 45 μL 2X Laemmli Buffer.
7. At this point the samples can be stored at –20°C for later use or boiled for 5 min. and loaded on 7% SDS-PAGE.
8. Proteins are transferred to nylon membranes and blotted with IRE1α (1:5000) or PERK (1:2000) antibodies.

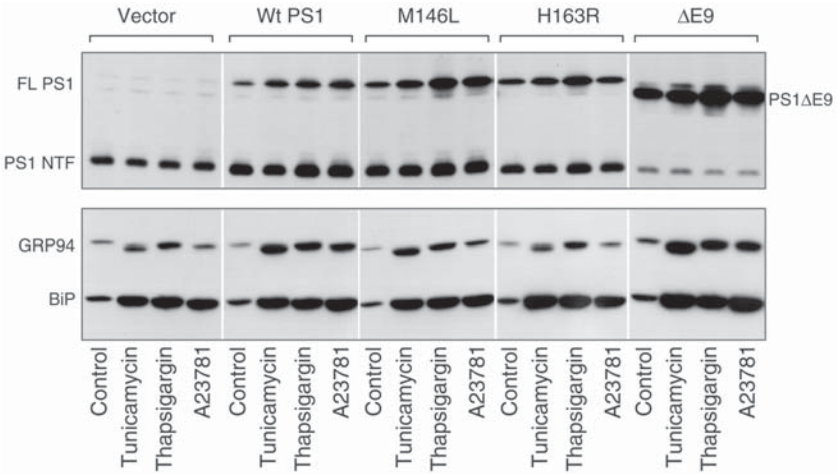

Fig. 5. Western-blot analysis of BiP and GRP94 induction in stable 293 cells. Stable pools of 293 cells that express Wt PS1 or FAD-linked mutant PS1 were incubated with tunicamycin (2 μg/mL), thapsigargin (300 nM), or the Ca^{2+} ionophore A23781 (7 μM) for 16 h. Detergent lysates were analyzed by blotting with PS1NT and anti-KDEL antibodies. Note that all three agents caused marked increases in the levels of BiP and GRP94 polypeptides regardless of the expression of Wt PS1 or mutant PS1.

3.5.2. Phosphatase Digestion of Immunoprecipitates

1. Perform **steps 1–5** as described in **Subheading 3.5.2.** and collect the immunoprecipitates by centrifugation. Wash once with PBS.
2. Resuspend the beads containing immunoprecipitates in 50 μL phosphatase digestion buffer and incubate with 10 U of alkaline phosphatase for 30 min at 37°C. The reaction is set on a nutator or the beads are mixed intermittently to ensure complete digestion.
3. Wash the beads once with 500 μL of IP wash buffer and resuspend in 45 μL 2X Laemmli Buffer.

A time-dependent increase in the levels of IRE1α polypeptides that exhibited retarded mobility was observed in cells upon treatment with tunicamycin. The shift in electrophoretic mobility of IRE1α is solely owing to phosphorylation because treatment of the immunoprecipitates with alkaline phosphatase restores these species to a molecular weight similar to that observed in untreated cells. Treatment with tunicamycin also resulted in a similar shift in PERK mobility. Notably, the migration of IRE1α and PERK were retarded in all lines tested, indicating ER stress-mediated activation of IRE1α or PERK was not impaired by expression of mutant PS1 (**Fig 6**).

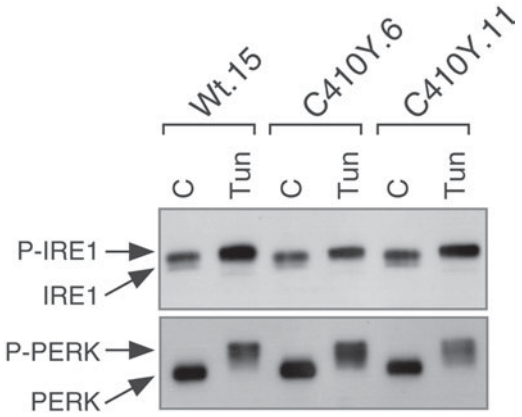

Fig. 6. ER stress-activated phosphorylation of endogenous IRE1α and PERK were analyzed by a combined immunoprecipitation/Western-blot analysis of lysates from stable N2a cell lines treated with tunicamycin (2 μg/mL) for 5 h. Migration of both ER kinases were retarded, indicative of phosphorylation, in tunicamycin treated Wt and C410Y cells. *P-IRE1*, phosphorylated IRE1α; *P-PERK*, phosphorylated PERK.

4. Notes

1. DEPC water should be prepared by adding 1 mL. DEPC to 1 L dH_2O in an evacuated hood. Shake the bottle vigorously for 1 min to homogenate and allow the bottle to sit in the hood for at least 8 h. DEPC water must then be autoclaved before it can be used for RNAse-free preparations.
2. The following set of primers have been successfully used in the author's laboratory to amplify UPR-related genes.

BiP,	5'-CTGGGTACATTTGATCTGACTGG-3' and 5'-GCATCCTGGTGGCTTTCCAGCCATTC-3';
Chop,	5'-GTCCAGCTGGGAGCTGGAAG-3' and 5'-CTGGTCAGGCGCTCGATTTCC-3'
Erp72,	5'-GCCATGGAGCCAGAGGAGTTTG-3' and 5'-GCTCAAATGCTCCAGATCTCTG-3'
DOC4,	5'-GTGATGTACAGTACAAGATG-3' and 5'-CATGTGGACAAGCTTGGTGAG-3';
GADD45,	5' -GAGCAGAAGACCGAAAGGATG-3' and 5'-CTTCAGTGCAATTTGGTTCAG-3';
GADD34,	5'-CTAGAGAAGAGGGAGTGGCTGA-3' and 5'-GGAAGGCATTTCCAGTACAGAC-3';
Mif1,	5'-GTCCAGAGGACCAGAGGTTA-3' and 5'-GTATCTCTTGTGCACTTGGTG-3';

3. PMSF and protease inhibitors should be added to the lysis buffer immediately before use.
4. Sense or antisense primers are labeled at the 5' end using T4 polynucleotide kinase and $\gamma[^{32}P]$-labeled ATP. Inclusion of small amounts (usually 1:20 of unlabeled primer) of labeled primer in the PCR results in radiolabeling of the amplified products, which facilitates accurate quantification. If optimal PCR cycle number is chosen as described to ensure that amplification still occurs within the linear range, then this method is as quantitative as Northern-blot hybridization.
   The annealing temperature depends on the choice of primer sequence. In general annealing at higher temperatures equates to greater fidelity but some primers will not anneal unless temperature is lowered, possibly to 55°C.

References

1. Tanzi, R. E. and Bertram, L. (2001) New frontiers in Alzheimer's disease genetics. *Neuron* **32,** 181–184.
2. Selkoe, D. J. (2001) Presenilin, Notch, and the genesis and treatment of Alzheimer's disease. *Proc. Natl. Acad. Sci. USA* **98,** 11,039–11,041.
3. Kaufman, R. J. (1999) Stress signaling from the lumen of the endoplasmic reticulum: coordination of gene transcriptional and translational controls. *Genes Dev.* **13,** 1211–1233.
4. Pahl, H. L. (1999) Signal transduction from the endoplasmic reticulum to the cell nucleus. *Physiol. Rev.* **79,** 683–701.
5. Shamu, C. E., and Walter, P. (1996) Oligomerization and phosphorylation of the Ire1p kinase during intracellular signaling from the endoplasmic reticulum to the nucleus. *EMBO J.* **15,** 3028–3039.
6. Sidrauski, C., and Walter, P. (1997) The transmembrane kinase Ire1p is a site-specific endonuclease that initiates mRNA splicing in the unfolded protein response. *Cell* **90,** 1031–1039.
7. Sidrauski, C., Chapman, R., and Walter, P. (1998) The unfolded protein response: an intracellular signalling pathway with many surprising features. *Trends Cell Biol.* **8,** 245–249.
8. Bertolotti, A., Zhang, Y., Hendershot, L. M., Harding, H. P., and Ron, D. (2000) Dynamic interaction of BiP and ER stress transducers in the unfolded- protein response. *Nat. Cell Biol.* **2,** 326–332.
9. Niwa, M., Sidrauski, C., Kaufman, R. J., and Walter, P. (1999) A role for presenilin-1 in nuclear accumulation of Ire1 fragments and induction of the mammalian unfolded protein response. *Cell* **99,** 691–702.
10. Price, B. D., and Calderwood, S. K. (1992) Gadd45 and Gadd153 messenger RNA levels are increased during hypoxia and after exposure of cells to agents which elevate the levels of the glucose-regulated proteins. *Cancer Res.* **52,** 3814–3817.
11. Wang, X. Z., Lawson, B., Brewer, J. W., Zinszner, H., Sanjay, A., Mi, L. J., et al. (1996) Signals from the stressed endoplasmic reticulum induce C/EBP-homologous protein (CHOP/GADD153) *Mol. Cell. Biol.* **16,** 4273–4280.

12. Urano, F., Wang, X., Bertolotti, A., Zhang, Y., Chung, P., Harding, H. P., and Ron, D. (2000) Coupling of stress in the ER to activation of JNK protein kinases by transmembrane protein kinase IRE1. *Science* **287,** 664–666.
13. Harding, H. P., Zhang, Y., and Ron, D. (1999) Protein translation and folding are coupled by an endoplasmic-reticulum- resident kinase. *Nature* **397,** 271–274.
14. Chen, C. and Okayama, H. (1987) High-efficiency transformation of mammalian cells by plasmid DNA. *Mol. Cell. Biol.* **7,** 2745–2752.
15. Thinakaran, G., Teplow, D. B., Siman, R., Greenberg, B., and Sisodia, S. S. (1996) Metabolism of the "Swedish" amyloid precursor protein variant in neuro2a (N2a) cells. Evidence that cleavage at the "β-secretase" site occurs in the golgi apparatus. *J. Biol. Chem.* **271,** 9390–9397.
16. Thinakaran, G., Regard, J. B., Bouton, C. M. L., Harris, C. L., Price, D. L., Borchelt, D. R., and Sisodia, S. S. (1998) Stable association of presenilin derivatives and absence of presenilin interactions with APP. *Neurobiol. Dis.* **4,** 438–453.
17. Thinakaran, G., Borchelt, D. R., Lee, M. K., Slunt, H. H., Spitzer, L., Kim, G., et al. (1996) Endoproteolysis of presenilin 1 and accumulation of processed derivatives in vivo. *Neuron* **17,** 181–190.
18. Thinakaran, G., Harris, C. L., Ratovitski, T., Davenport, F., Slunt, H. H., Price, D. L., et al. (1997) Evidence that levels of presenilins (PS1 and PS2) are coordinately regulated by competition for limiting cellular factors. *J. Biol. Chem.* **272,** 28,415–28,422.
19. Borchelt, D. R., Thinakaran, G., Eckman, C. B., Lee, M. K., Davenport, F., Ratovitsky, T., et al. (1996) Familial Alzheimer's disease-linked presenilin 1 variants elevate Abeta1-42/1-40 ratio in vitro and in vivo. *Neuron* **17,** 1005–1013.
20. Chomczynski, P., and Sacchi, N. (1987) Single-step method of RNA isolation by acid guanidinium thiocyanate-phenol-chloroform extraction. *Anal. Biochem.* **162,** 156–159.
21. Sambrook, J., Fritsch, E. F., and Maniatis, T. (1989) *Molecular Cloning: A Laboratory Manual*, 2nd ed. Cold Spring Harbor Laboratory Press, Cold Spring Harbor, NY.
22. Li, W. W., Alexandre, S., Cao, X., and Lee, A. S. (1993) Transactivation of the grp78 promoter by Ca2+ depletion. A comparative analysis with A23187 and the endoplasmic reticulum Ca(2+)-ATPase inhibitor thapsigargin. *J. Biol. Chem.* **268,** 12,003–12,009.
23. Li, M., Baumeister, P., Roy, B., Phan, T., Foti, D., Luo, S., and Lee, A. S. (2000) ATF6 as a transcription activator of the endoplasmic reticulum stress element: thapsigargin stress-induced changes and synergistic interactions with NF-Y and YY1. *Mol. Cell. Biol.* **20,** 5096–5106.
24. Harding, H. P., Zhang, Y., Bertolotti, A., Zeng, H., and Ron, D. (2000) *Perk* is essential for translational regulation and cell survival during the unfolded protein response. *Mol. Cell* **5,** 897–904.

18

Huntingtin Fragments Form Aggresome-Like Inclusion Bodies in Mammalian Cells

Annett Boeddrich, Rudi Lurz, and Erich E. Wanker

1. Introduction

The formation of large perinuclear inclusion bodies containing protein aggregates was first described in HeLa cells. Woijcik et al. ***(1)*** have shown that treatment of HeLa cells with the proteasome inhibitor PSI [*N*-benzyloxycarbonal-Ile-Glu(*O-t*-butyl)-Ala-leucinal] results in the accumulation of electron-dense material in the vicinity of the Golgi apparatus. These structures were termed proteolysis centers, because ubiquitin as well as components of the 26S proteasome are enriched in inclusion bodies, whereas carbohydrates, lipids, or nucleic acids are not present.

Recently, perinuclear inclusion bodies very similar to the ones described by Wojcik et al. ***(1)*** have been discovered in other mammalian cell-culture model systems ***(2–14)***. These structures were termed "aggresomes," because they mainly consist of high-molecular-weight protein aggregates ***(1–4,6,7,9–13)***. Aggresomes also contain proteasomal components and stress proteins, and they are located in close vicinity to the centrosome (rev. in **ref.** ***15***). Formation of aggresomes in mammalian cells is enhanced upon inhibition of proteasome activity, suggesting that they appear when the capacity of the proteasome is exceeded and the cell has lost the ability to degrade misfolded proteins ***(1–3,6–8,10,13)***. Ultrastructural studies using transmission electron microscopy with immunogold labeling revealed that aggresomes are large membrane-free, spherical structures (diameter approx 1–5 μm) composed of electron-dense material with an amorphous or fibrillar morphology ***(1,5,6,10,13)***. Interestingly, formation of aggresome structures is mostly accompanied by a redistribution of the intermediate filament protein vimentin, which forms a cage around the core of the aggregated, ubiquitinated protein ***(3,5–7,11,13)***.

From: *Methods in Molecular Biology, vol. 232: Protein Misfolding and Disease: Principles and Protocols*
Edited by: P. Bross and N. Gregersen © Humana Press Inc., Totowa, NJ

This chapter describes in detail biochemical and cell biological methods for the identification and characterization of aggresome-like perinuclear inclusion bodies containing insoluble huntingtin aggregates in a mammalian cell culture model system of Huntington's disease (HD).

2. Material

1. Media for culturing cells: L-glutamine-free modified Eagle's medium (MEM) with Earle's Salts (Life Technologies, Gaithersburg, MD), supplemented with 10% fetal bovine serum (FBS), 2 m*M* L-glutamine, 100 U/mL penicillin, 100 µg/mL streptomycin, 100 µg/mL G418, 150 µg/mL hygromycin B and 10 ng/mL doxycycline.
2. Poly-L-lysine treatment of cell-culture flasks: dilute poly-L-lysine solution (Sigma, St. Louis, MO) 1/10 in water, mix, and add an appropriate amount of the solution to the tissue-culture flask until it covers the flask surface. Incubate 5 min, aspirate the solution, and wash three times with water. Air-dry the flasks under a hood.
3. Cell lysis buffer: 50 m*M* Tris-HCl, pH 8.8, 100 m*M* NaCl, 5 m*M* $MgCl_2$, 0.5% NP-40, 2 m*M* phenylmethyl-sulfonyl fluoride (PMSF), 10 µg/mL leupeptin, 10 µg/mL pepstatin, 1 µg/mL aprotinin, and 50 µg/mL antipain.
4. Benzonase (Merck, Darmstadt, Germany).
5. Bradford protein assay (Bio-Rad, Munich, Germany).
6. 5X sodium dodecyl sulfate/polyacrylamide gel electrophoresis (SDS-PAGE) sample buffer: 250 m*M* Tris-HCl, pH 6.8, 500 m*M* DTT, 50% glycerol, 10% SDS, 0.5% bromophenol-blue.
7. Pellet buffer: 20 m*M* Tris-HCl, pH 8.0, 15 m*M* $MgCl_2$ containing 0.5 mg/mL DNaseI.
8. Blocking solution: 3% nonfat dry milk in 1X PBS containing 0.05% Tween 20.
9. Primary antibody for immunoblotting: anti-huntingtin antibody HD1 (diluted 1/1,000 in blocking solution) ***(16)***.
10. Secondary peroxidase-conjugated anti-rabbit antibody (diluted 1/5,000 in blocking solution; Sigma, St. Louis, MO).
11. Enhanced Chemiluminescence (Western Lighting™ Chemiluminescence Reagent Plus; PerkinElmer Life Sciences, Inc., Boston, MA).
12. Cellulose acetate membrane (0.2-µm, Schleicher & Schuell, Dassel, Germany).
13. Secondary alkaline phosphatase-conjugated anti-rabbit antibody (diluted 1/25,000, Sigma).
14. Alkaline phosphatase buffer: 0.5 *M* NaCl, 50 m*M* Tris-HCl, pH 9.0, 1 m*M* $MgCl_2$.
15. AttoPhos (JBL Scientific, San Luis Obispo, CA): 10 m*M* AttoPhos in 100 m*M* Tris-HCl, pH 9.0; light-sensitive, store at + 4°C.
16. Fixative for immunofluorescence microscopy: 4% paraformaldehyde (Sigma) in 1X PBS (prepare fresh before each use). Dissolve the paraformaldehyde in phosphate-buffered saline (PBS) by heating to 60°C. Cool down to room temperature and filter through folded filters (595½, Schleicher & Schuell).

17. *Clasto*-lactacystin β-lactone (Affiniti Research products).
18. Blocking solution for immunofluorescence analysis: 3% bovine serum albumin (BSA) (Sigma) in PBS; store at –20°C.
19. Secondary antibodies for immunofluorescence analysis: donkey anti-mouse or anti-rabbit IgG conjugated to either CY3 or FITC (diluted 1/200; Jackson ImmunoResearch, West Grove, PA), donkey anti-goat IgG conjugated to Alexa 546 (diluted 1/200; Molecular Probes, Eugene, OR).
20. Hoechst (Sigma): dissolve 1 mg Bisbenzimid in 1 mL H_2O; light-sensitive, store at + 4°C.
21. Mounting media: 1X PBS/glycerol (1/4, v/v) with 5% propyl gallate (Sigma); store at + 4°C.
22. Thermanox coverslips (13-mm diameter; Nunc, Naperville, IL).
23. Fixative for electron microscopy: 25% glutaraldehyde (Fluka, Buchs, CH) in H_2O; 10% paraformaldehyde (Sigma; prepare fresh before each use) in H_2O. Paraformaldehyde is dissolved in H_2O by adding 0.5% 1 *N* NaOH and heating to 60°C until the solution is clear. After centrifugation for 10 min at 10,000*g* the supernatant is used.
24. LR Gold Resin (London Resin Company, Berkshire, UK).
25. Spurr's low viscosity resin (EMS, Electron Microscopy Sciences, Fort Washington, USA; ***[17]***).
26. Buffer A: 20 m*M* Tris-HCl, pH 7.5, 150 m*M* NaCl.
27. Buffer B: Buffer A containing 6 mg/mL BSA-c (Aurion, Wageningen, The Netherlands).
28. Primary antibody for electron microscopy: rabbit polyclonal ubiquitin antibody (Dako A/S, Denmark).
29. Uranyl acetate (Electron Microscopy Sciences).
30. Secondary antibodies for electron microscopic analysis: goat anti-rabbit antibody conjugated with 10 nm gold (British Bio Cell, Cardiff, UK).
31. Osmium tetroxide, 2% aqueous solution (Electron Microscopy Sciences).
32. Propylene oxide (Merck).
33. Fluorescence microscope (e.g., Axioplan-2, Zeiss, Thornwood, NY).

3. Methods

The methods described here have been used in our laboratory for the analysis of aggresome- like inclusion bodies containing aggregated huntingtin protein in 293 Tet-Off cells by immunoblotting, filter retardation assay, immunofluorescence, and electron microscopy ***(13,18)***.

3.1. Analysis of Huntingtin Aggregates by Immunoblotting and a Filter Retardation Assay

In order to study the formation of huntingtin aggregates in mammalian cells, stable, inducible 293 Tet-Off cell lines expressing Flag-tagged huntingtin exon 1 proteins with 20 (HDQ20), 51 (HDQ51), and 83 (HDQ83) glutamines were

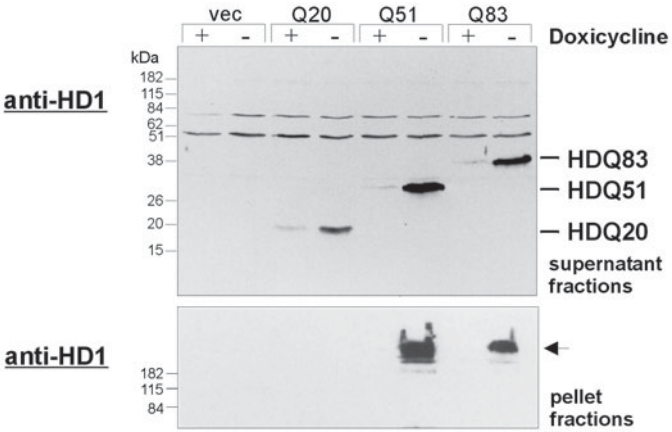

Fig. 1. Immunoblot analysis of soluble (supernatant) and insoluble (pellet) protein fractions prepared from induced and uninduced 293 Tet-Off cells. Proteins were resolved by SDS-PAGE, blotted onto nitrocellulose membranes, and probed with the anti-huntingtin antibody HD1. Reprinted from Molecular Biology of the Cell (**ref. *13***) with permission by the American Society for Cell Biology.

constructed ***(13)***. In the Tet-Off system, expression of recombinant proteins in the presence of doxycycline is inhibited, whereas in the absence of doxycycline it is induced. We have cultured the 293 Tet-Off cell lines for 3 d with and without doxycycline respectively. Whole-cell extracts were prepared, and after centrifugation the soluble (supernatant) and insoluble (pellet) fractions were analyzed by SDS-PAGE and Western blotting (**Fig. 1**). In addition, formation of insoluble protein aggregates was examined by a filter retardation assay. Using these methods, we found that the huntingtin exon 1 proteins with a polyglutamine sequence in the pathological range (HDQ51 and HDQ83), but not with a polyglutamine tract in the normal range (HDQ20), form SDS-insoluble protein aggregates. The methods used for the analysis of huntingtin aggregation are described in the following subheadings.

3.1.1. Culturing of Cell Lines

1. Grow 293 Tet-Off cell lines in the presence of doxycycline in L-glutamine-free MEM medium with Earle's Salts and supplements in poly-L-lysine-coated cell-culture flasks.
2. Thoroughly wash the cells with PBS and induce the expression of the FLAG-tagged huntingtin exon-1 proteins by the addition of fresh medium without doxycycline.
3. To remove the doxycycline completely change media on the following day.
4. Incubate the cells in doxycycline-free medium, e.g., for 3 d (*see* **Note 1**).

3.1.2. Preparation of Supernatant and Pellet Fractions

1. Wash cells, scrape in ice-cold PBS, and pellet by centrifugation.
2. Lyse the cells in cell lysis buffer for 30 min on ice.
3. Pellet insoluble material by centrifugation at 20,800*g* for 10 min at 4°C in an Eppendorf centrifuge (5417C).
4. Resuspend the pellet in 100 µL pellet buffer and incubate for 1 h at 37°C.
5. Determine the protein concentration of supernatant and pellet fraction using the Bradford protein assay.

3.1.3. Preparation of Whole-Cell Extracts

1. Wash cells, scrape in ice-cold PBS, and pellet by centrifugation.
2. Lyse the cells in cell lysis buffer containing 250 U/mL benzonase for 30 min on ice.
3. Determine the protein concentration using the Bradford protein assay.

3.1.4. Western Blot Analysis

1. Denature and reduce protein extracts with SDS-PAGE sample buffer.
2. Separate proteins by SDS-PAGE and transfer to nitrocellulose membrane.
3. Block the membrane with blocking solution for 30 min at room temperature.
4. Incubate the membrane with the anti-huntingtin antibody HD1 diluted in blocking solution for 1 h at room temperature.
5. Wash membrane in PBS containing 0.05% Tween 20 (Sigma) three times for 10 min.
6. Incubate the membrane with the secondary peroxidase-conjugated anti-rabbit antibody for 1 h at room temperature.
7. Wash in PBS containing 0.05% Tween 20 twice for 5 min and in PBS twice for 10 min.
8. Detect immunoreactive protein by using enhanced chemiluminescence.

3.1.5. Filter Retardation Assay

1. Heat whole-cell extracts in 2% SDS and 50 m*M* dithiothreitol (DTT) (Sigma) at 98°C for 3 min.
2. Pre-equilibrate the cellulose acetate membrane and 3 MM chromatography paper (Whatman) with 0.1% SDS.
3. Lay two pieces of preequilibrated 3 MM chromatography paper and the preequilibrated membrane on a Gibco-BRL dot-blot filtration unit (*see* **Note 2**).
4. Filter 20–30 µg cell extract through the cellulose acetate membrane.
5. Wash twice with 200 µL 0.1% SDS and remove the membrane from the dot-blot filtration unit.
6. Block the membrane with blocking solution for 30 min at room temperature.
7. Incubate the membrane with the HD1 antibody diluted in blocking solution for 1 h at room temperature.
8. Wash in PBS containing 0.05% Tween 20 (Sigma) three times for 10 min.

9. Incubate the membrane with the secondary alkaline phosphatase-conjugated antibody for 1 h at room temperature.
10. Wash membrane in PBS containing 0.05% Tween 20 twice for 5 min, in PBS twice for 10 min, and in alkaline phosphatase buffer once for 5 min.
11. Incubate the membrane with AttoPhos (diluted 1:250 in alkaline phosphatase buffer) for 5 min at room temperature, in the dark (*see* **Note 3**).
12. Quantify the amount of captured aggregates, e.g., with the Fuji-Imager LAS 2000 (Tokyo, Japan) (*see* **Note 4**).

3.2. Analysis of Huntingtin Aggresome Formation by Immunofluorescence Microscopy

The formation of huntingtin aggresomes in 293 Tet-Off cells was also analyzed by indirect immunofluorescence microscopy ***(13)***. We found that huntingtin exon 1 proteins with a polyglutamine stretch in the pathological range (HDQ51 or HDQ83 glutamines) form perinuclear inclusion bodies, whereas the huntingtin protein with a polyglutamine sequence in the normal range (HDQ20) showed a homogenous cytoplasmic staining (**Fig. 2A–C**). In the vast majority of cells, the perinuclear inclusion bodies appeared as spherical structures with a diameter of 1–3 μm. Comparison of the immunostaining of perinuclear inclusion bodies with the fluorescence of γ-tubulin, a known marker for the centrosome ***(19)***, revealed that both structures colocalize at least partially (**Fig. 2D**). In contrast, the fluorescence of the inclusion bodies did not overlap with the staining of α-mannosidase, a marker of the Golgi apparatus, indicating that these structures are distinct from each other (**Fig. 2E**). Interestingly, the accumulation of insoluble huntingtin aggregates caused the reorganization of the intermediate filament vimentin, which in normal cells extends to the periphery (**Fig. 2F**). Thus, the perinuclear inclusion bodies containing HDQ51 and HDQ83 are structurally very similar to the aggresomes that have been described for other aggregation-prone proteins ***(1,3,5–9,11,13)***.

3.2.1. Immunofluorescence Microscopy of 293 Tet-Off Cells

1. Grow induced cells on poly-L-lysine-coated Leighton tubes or comparable plastic ware (*see* **Note 5**).
2. Wash cells with PBS to remove cell-culture media.
3. Fix the cells in 4% paraformaldehyde for 15 min at room temperature (*see* **Note 6**).
4. Permeabilize cells in PBS containing 0.1% Triton X-100 three times for 5 min (*see* **Note 7**).
5. Block cells in blocking solution for immunofluorescence for 30 min (*see* **Note 8**).
6. Incubate cells with the appropriate primary antibody, diluted in 1X PBS, for 1 h at room temperature. The primary antibodies used for huntingtin aggresome analysis are listed in **Table 1** (*see* **Note 9**).
7. Wash cells in PBS containing 0.1% Triton X-100 three times for 10 min.

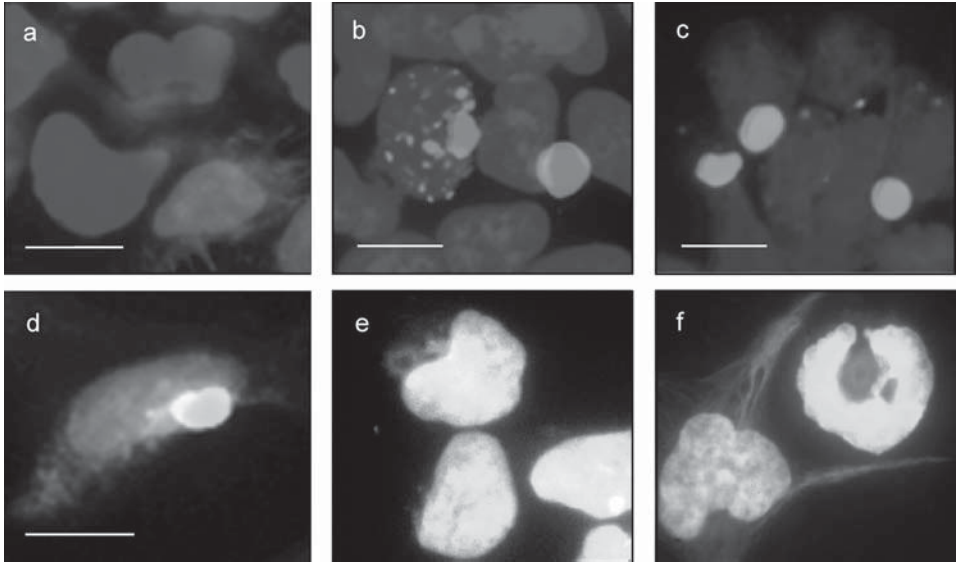

Fig. 2. HD exon 1 aggregates form at the centrosome and result in the redistribution of the intermediate filament vimentin. (**a–c**) Expression of the proteins HDQ20, HDQ51, and HDQ83 was induced for 3 d. Cells were processed for immunofluorescence using the anti-FLAG antibody followed by the CY3-coupled secondary antibody. Nuclei were counterstained with Hoechst. Cells expressing the HDQ20 protein showed a homogenous cytoplasmic staining (**a**), whereas in cells expressing the proteins HDQ51 (**b**) or HDQ83 (**c**), distinct inclusion bodies were observed. Immunofluorescence double labeling of cells reveals that FITC-labeled HDQ83 aggregates (green) partially colocalize with CY3-labeled γ-tubulin (red), a centrosomal marker (**d**), but not with CY3-labeled α-mannosidase II, a known Golgi marker (**e**). Induction of HDQ83 expression for 3 d also results in a redistribution of CY3-labeled vimentin to the perinuclear inclusion bodies (**f**). Bar, 10 μm. Reprinted from Molecular Biology of the Cell **ref.** ***13*** with permission by the American Society for Cell Biology.

Table 1
Primary Antibodies

Antigen	Compartment/ protein	Species	Dilution	Source
Flag	Flag-tag of the huntingtin exon 1 protein	Mouse mc	1/2000	Sigma
γ-tubulin	Centrosome	Mouse mc	1/100	Sigma
Vimentin (clone V9)	Intermediate filament protein (vimentin)	Mouse mc	1/20	Sigma

mc, monoclonal.

8. Incubate cells with the appropriate secondary antibody, diluted in PBS containing 3% BSA, for 1 h at room temperature.
9. Wash in PBS containing 0.1% Triton X-100 twice for 5 min and in PBS twice for 5 min.
10. Stain the cell nuclei with Hoechst for 20 s at room temperature.
11. Wash in PBS three times for 4 min.
12. Mount cells on microscope slides using mounting medium (*see* **Note 10**).
13. View the samples with a fluorescence microscope (*see* **Note 11**).

3.3 Analysis of Huntingtin Aggresomes by Electron Microscopy

To examine the perinuclear huntingtin aggresomes at an ultrastructural level, cells expressing the HDQ83 protein were immunogold-labeled with an antibody directed against huntingtin. We found that at the ultrastructural level, huntingtin aggresomes are large membrane-free, spherical structures with a diameter of 1–5 μm. The inclusion bodies are composed of individual filaments that have a diameter of approx 10 nm (**Fig. 3**). The inclusions were labeled selectively with anti-huntingtin and anti-ubiquitin antibodies supporting the hypothesis that the HDQ83 protein is ubiquitinated and tagged for degradation by the proteasome system ***(13)***. At the ultrastructural level, nuclear indentations and a clear disruption of the nuclear membrane was observed. Furthermore, accumulation of the filament vimentin was detected in the vicinity of aggresomes, confirming the results obtained by immunofluorescence microscopy (**Fig. 2**).

3.3.1. Ultrastructure of Huntingtin Aggresomes

1. Grow induced cells expressing HDQ83 on poly-L-lysine-coated Thermanox coverslips.

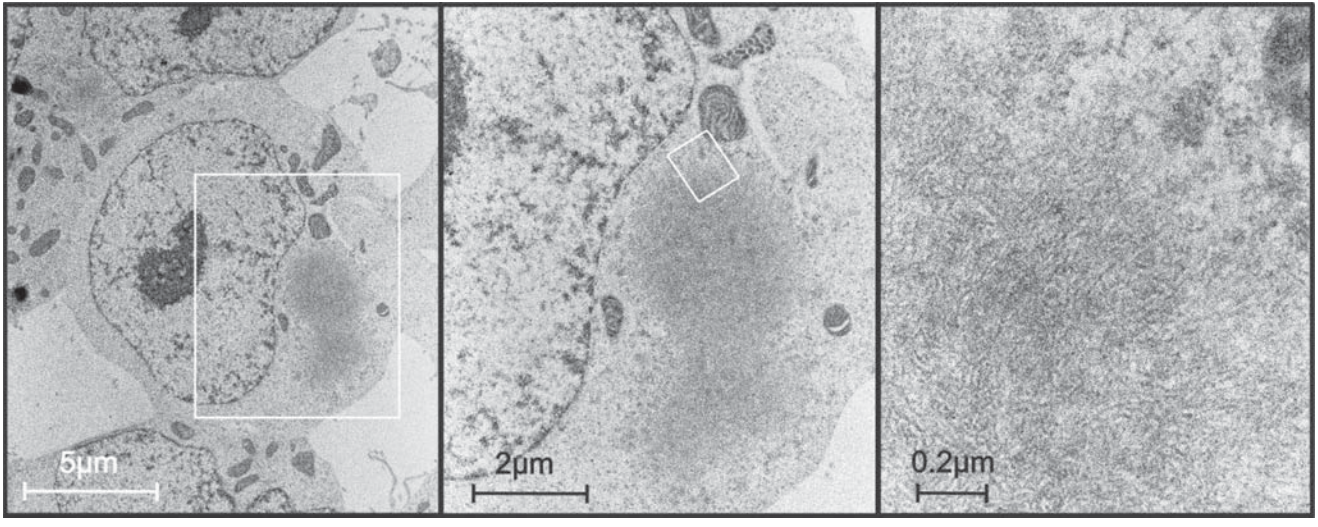

Fig. 3. Electron microscope picture of huntingtin-aggresomes. After HDQ83 was expressed for 3 d, cells were embedded in Spurr's resin and sectioned as described in **Subheading 3.3.** A 293 Tet-Off cell containing two adjacent perinuclear HDQ83 inclusion bodies is shown with increasing magnifications as indicated. The indentation of the nucleus caused by the aggresome and at the higher magnification the fibrillar morphology of the inclusion body can be observed.

2. Wash coverslips with cells in PBS and fix cells in a mixture of 2% paraformaldehyde and 0.2% glutaraldehyde in PBS for 1 h.
3. Dehydrate in ethanol series (10 min, 30% ethanol; 10 min, 50% ethanol; 10 min, 70% ethanol; 10 min, 90% ethanol; 10 min, 95% ethanol; two times 30 min, 100% ethanol).
4. Infiltrate cells in 50% LR Gold/50% ethanol for 1 h at +4°C, twice in 100% London Resin (LR) Gold for 12 h at + 4°C, and twice in 100% LR Gold (containing 0.1% benzil as photoinitiator for visible light) for 12 h at room temperature.
5. Polymerize in 100% LR Gold with 0.1% benzil under a projector halogen lamp at + 4°C for 2 d.
6. Prepare 50–60 nm thin sections on nickel grids (400 mesh, no support film).
7. Stabilize the sections from back with a thin layer of carbon by vacuum evaporation. Following steps are performed by floating the grids with the front on drops (50 μL) of solution on parafilm. During incubation, protect with a Petri dish against evaporation.
8. Incubate in buffer A for 10 min and in buffer B for 10 min.
9. Incubate samples with the anti-huntingtin antibody HD1 diluted 1/400 in buffer B or anti-ubiquitin antibody diluted 1/300 in buffer B for 2 h at room temperature.
10. Wash in buffer B four times for 10 min.
11. Incubate samples with the secondary gold-conjugated anti-rabbit antibody diluted 1/100 in buffer B for 2 h at room temperature.
12. Wash in buffer A four times for 1 min.
13. Poststain in 0.5% uranyl acetate for 1 min and with lead citrate for 45 s.
14. Samples are visualized in a transmission electron microscope (e.g., Philips CM100; FEI Company).

For better visualization of ultrastructural details of huntingtin aggresomes without immunolabeling, cells were fixed more strongly and embedded in an epoxy resin. The protocol that we used to study the ultrastructural details of the huntingtin aggresomes follows.

1. Fix induced cells on PBS washed coverslips with 2% glutaraldehyde in PBS for 2 h.
2. Wash three times in PBS for 10 min.
3. Treat the cells with 2% osmium tetroxide for 1 h.
4. Dehydrate in acetone series (10 min, 30% acetone; 10 min, 50% acetone; 10 min, 70% acetone; 10 min, 90% acetone; 10 min, 95% acetone; two times 30 min, 100% acetone).
5. Incubate cells in 100% propyleneoxide twice for 10 min.
6. Infiltrate Spurr's resin (50% Spurr/50% propylene oxide) for 1 h.
7. Incubate the sample in 100% resin for 3 d. Change the resin every day.
8. Polymerize at 60°C for 24 h.
9. Prepare 50–60-nm thin sections.
10. Stabilize the sections by vacuum evaporation with a thin layer of carbon.
11. Post-stain with lead citrate, 0.5% uranyl acetate, and lead citrate for 1 min each.

4. Notes

1. Expression can be induced for different times, depending on the experiment.
2. Remove all air bubbles from the membrane before closing the dot-blot filtration unit.
3. After incubation with AttoPhos, rinse membrane shortly with PBS to diminish background.
4. Probes can also be evaluated by enhanced chemiluminescence. Instead of a secondary alkaline phosphatase-conjugated antibody use a secondary peroxidase-conjugated antibody. After incubation for 1 h at room temperature, wash in PBS containing 0.05% Tween 20 twice for 5 min and in PBS twice for 10 min. Incubate the membrane with the chemiluminescence reagents and evaluate the amount of aggregates, e.g., with the Fuji-Imager.
5. Plastic ware may have an intrinsic fluorescence.
6. Other fixative procedures, such as –20°C methanol, can be used. But be aware that methanol fixation with some antibodies may show a different cellular localization than paraformaldehyde fixation.
7. After fixation, cells can be kept in PBS containing 0.05% sodium azide for 2–3 wk at + 4°C.
8. Be careful that during the following procedure the cells do not dry out.
9. Sometimes it is difficult to distinguish between centrosome and Golgi localization. Therefore, in addition to a centrosome marker a Golgi marker should also be used for the investigation of aggresomes.
10. Store prepared samples at + 4°C.
11. Fluorescence can bleach out very quickly when a too-strong UV-light is used.

Acknowledgments

The authors thank Klaus Genser for critical reading the manuscript. This work has been supported by grants from the Deutsche Forschungsgemeinschaft (WA 1151/4-1 and WA 1151/5-1), the Human Frontier Science Program Organization, and the Bundesministerium für Bildung, Wissenschaft, Forschung und Technologie (BioFuture project: 0311853).

References

1. Wojcik, C., Schroeter, D., Wilk, S., Lamprecht, J., and Paweletz, N. (1996) Ubiquitin-mediated proteolysis centers in HeLa cells: indication from studies of an inhibitor of the chymotrypsin-like activity of the proteasome. *Eur. J. Cell Biol.* **71,** 311–318.
2. Cardinale, A., Filesi, I., and Biocca, S. (2001) Aggresome formation by anti-Ras intracellular scFv fragments. The fate of the antigen-antibody complex. *Eur. J. Biochem.* **268,** 268–277.
3. Dul, J. L., Davis, D. P., Williamson, E. K., Stevens, F. J., and Argon, Y. (2001) Hsp70 and antifibrillogenic peptides promote degradation and inhibit intracellular aggregation of amyloidogenic light chains. *J. Cell Biol.* **152,** 705–716.

4. French, B. A., van Leeuwen, F., Riley, N. E., Yuan, Q. X., Bardag-Gorce, F., Gaal, K., et al. (2001) Aggresome formation in liver cells in response to different toxic mechanisms: role of the ubiquitin-proteasome pathway and the frameshift mutant of ubiquitin. *Exp. Mol. Pathol.* **71,** 241–246.
5. Garcia-Mata, R., Bebok, Z., Sorscher, E. J., and Sztul, E. S. (1999) Characterization and dynamics of aggresome formation by a cytosolic GFP- chimera. *J. Cell Biol.* **146,** 1239–1254.
6. Johnston, J. A., Ward, C. L., and Kopito, R. R. (1998) Aggresomes: a cellular response to misfolded proteins. *J. Cell Biol.* **143,** 1883–1898.
7. Kabore, A. F., Wang, W. J., Russo, S. J., and Beers, M. F. (2001) Biosynthesis of surfactant protein C: characterization of aggresome formation by EGFP chimeras containing propeptide mutants lacking conserved cysteine residues. *J. Cell Sci.* **114,** 293–302.
8. Ma, J. and Lindquist, S. (2001) Wild-type PrP and a mutant associated with prion disease are subject to retrograde transport and proteasome degradation. *Proc. Natl. Acad. Sci. USA* **98,** 14955–14960.
9. Riley, N. E., Li, J., Worrall, S., Rothnagel, J. A., Swagell, C., van Leeuwen, F. W., and French, S. W. (2002) The mallory body as an aggresome: in vitro studies. *Exp. Mol. Pathol.* **72,** 17–23.
10. Serrando, M., Casanovas, A., and Esquerda, J. E. (2002) Occurrence of glutamate receptor subunit 1-containing aggresome-like structures during normal development of rat spinal cord interneurons. *J. Comp. Neurol.* **442,** 23–34.
11. Shimohata, T., Sato, A., Burke, J. R., Strittmatter, W. J., Tsuji, S., and Onodera, O. (2002) Expanded polyglutamine stretches form an 'aggresome'. *Neurosci. Lett.* **323,** 215–218.
12. Stumptner, C., Fuchsbichler, A., Heid, H., Zatloukal, K., and Denk, H. (2002) Mallory body-A disease-associated type of sequestosome. *Hepatology* **35,** 1053–1062.
13. Waelter, S., Boeddrich, A., Lurz, R., Scherzinger, E., Lueder, G., Lehrach, H., and Wanker, E. E. (2001) Accumulation of mutant huntingtin fragments in aggresome-like inclusion bodies as a result of insufficient protein degradation. *Mol. Biol. Cell* **12,** 1393–1407.
14. Yao, R., Maeda, T., Takada, S., and Noda, T. (2001) Identification of a PDZ domain containing Golgi protein, GOPC, as an interaction partner of frizzled. *Biochem. Biophys. Res. Commun.* **286,** 771–778.
15. Kopito, R. R. (2000) Aggresomes, inclusion bodies and protein aggregation. *Trends Cell Biol.* **10,** 524–530.
16. Scherzinger, E., Lurz, R., Turmaine, M., Mangiarini, L., Hollenbach, B., Hasenbank, R., et al. (1997) Huntingtin-encoded polyglutamine expansions form amyloid-like protein aggregates in vitro and in vivo. *Cell* **90,** 549–558.
17. Spurr, A. R. (1969) A low-viscosity epoxy resin embedding medium for electron microscopy. *J. Ultrastruct. Res.* **26,** 31–43.
18. Wanker, E. E., Scherzinger, E., Heiser, V., Sittler, A., Eickhoff, H., and Lehrach, H. (1999) Membrane filter assay for detection of amyloid-like polyglutamine-containing protein aggregates. *Methods Enzymol.* **309,** 375–386.

19. Dictenberg, J.B., Zimmermann, W., Sparks, C.A., Young, A., Vidair, C., Zheng, Y., et al. (1998) Pericentrin and gamma-tubulin form a protein complex and are organized into a novel lattice at the centrosome. *J. Cell Biol.* **141,** 163–174.

19

Application of Chemical Chaperones to the Rescue of Folding Defects

Tip W. Loo and David M. Clarke

1. Introduction

Abnormal protein folding in the endoplasmic reticulum (ER) is the cause of more than 40 diseases such as cystic fibrosis (CF), familial hypercholesterolemia, long QT syndrome, diabetes insipidus, and Alzheimer's disease (AD) (reviewed in **refs.** ***1,2***). For diseases caused by protein misfolding, an important goal would be to develop drugs or small molecules to prevent misfolding.

The human multidrug resistance P-glycoprotein (P-gp) is an excellent model system for studying folding, trafficking, and ER associated degradation (ERAD). P-gp is clinically important because of its contribution to the phenomenon of "multidrug resistance" during AIDS and cancer chemotherapy. P-gp is a member of the ATP-binding cassette (ABC) family of transporters. A feature of the ABC transporters is that they consist of two hydrophobic domains (each containing a transmembrane segment) and two hydrophilic domains (each containing a nucleotide binding domain). During structure-function analysis of P-gp, numerous point mutations throughout the molecule (in transmembrane segments, in cytoplasmic loops, and in nucleotide-binding domains) were identified that inhibited protein folding and trafficking to the cell surface (misprocessed mutants) ***(3–5)***. These misprocessed mutants were retained in the ER in association with calnexin and Hsc70 chaperones ***(6,7)***, and were rapidly degraded by ER proteases ***(8)***. An important discovery was that substrates and modulators of P-gp (chemical chaperones or small molecules) could specifically correct the folding defects in all of these misprocessed mutants ***(9)***. After correction of the folding defect, the mutant proteins were processed through to the Golgi and then trafficked to the cell surface in an active form ***(9,10)***.

From: *Methods in Molecular Biology, vol. 232: Protein Misfolding and Disease: Principles and Protocols*
Edited by: P. Bross and N. Gregersen © Humana Press Inc., Totowa, NJ

Specific chemical chaperones have subsequently been identified that could rescue the folding defects in other proteins. Some of the proteins rescued include the HERG potassium channel (long QT syndrome) with the anti-arrhythmic drug E-4031 ***(11)***, α-galactosidase A (Fabry disease) with 1-deoxy-galactonojirimycin ***(12)***, in p53 with drugs CP31398 and CP257042 ***(13)***, and the vasopressin V2 receptor (diabetes insipidus) with drugs SR121463A or VPA985 ***(14)***. Therefore, a pharmacological approach to correct protein misfolding in any disease is feasible. In many diseases (e.g., CF), however, development of a drug therapy may be hindered by the lack of a specific substrate. But with the availability of high-throughput facilities, identification of specific compounds that can correct the folding defects in any protein may not be an obstacle ***(15)***.

This chapter will describe the techniques involved in "rescuing" a P-gp misprocessed mutant with a drug substrate, and its subsequent characterization. The most versatile expression system for studying P-gp mutants is transient expression in human embryonic kidney (HEK 293) cells. Expression is very rapid in these cells and the mutant proteins can be characterized 2–3 d after transfection. Several commercial sources have expression vectors for transient transfection (e.g., pcDNA3 from Invitrogen, San Diego, CA). To maintain expression for weeks to months, the Epstein-Barr virus (EBV) vectors such as pREP4 (Invitrogen) are useful because they can be maintained extrachromosomally in HEK 293 cells that constitutively express the EBNA-1 gene (the pREP and HEK293-EBNA-1 cells are available from Invitrogen).

2. Materials

2.1. Transient Transfection

1. HEK 293 cells (American Type and Culture Collection [ATCC]) (*see* **Note 1**).
2. Media: Dulbecco's modified Eagle's medium (DMEM) with high glucose and supplemented with nonessential amino acids, 4 m*M* L-glutamine, 10 IU/mL penicillin, 10 μg/mL streptomycin, and 10% (v/v) fetal bovine serum (FBS).
3. cDNA in the appropriate expression vector and purified using a Qiagen (Qiagen, Inc.) Maxi-Prep column and in sterile TE buffer (10 m*M* Tris-HCl, pH 8.0, and 1 m*M* ethylenediamine tetraacetic acid [EDTA]).
4. 2.5 *M* $CaCl_2$ stock in sterile water (tissue-culture grade $CaCl_2$; Sigma Cat. no. C-7902).
5. 2X BES: 50 m*M* BES [*N*,*N*-bis(2-hydroxyethyl)-2-aminoethanesulfonic acid; Sigma Cat no. B-4554], 280 m*M* NaCl, 1.5 m*M* Na_2HPO_4. Adjust pH to 6.96 with NaOH (*see* **Note 2**).
6. Endoglycosidase H_f and 10X Endo H_f buffer (New England Biolabs).

2.2. Pulse Labeling

1. S-minus media: DMEM with high glucose, without L-methionine or L-cysteine (Invitrogen).
2. [^{35}S]-Translabel (specific activity: 1180 Ci/mL; ICN Radiochemicals)
3. Buffer I: 25 m*M* Tris-HCl, pH 7.5, 150 m*M* NaCl, 1% (w/v) Triton X-100, 0.5% (w/v) sodium deoxycholate, and 1 m*M* EDTA.
4. Protein A Sepharose CL-4B (Amersham Biosciences).

2.3. Cell-Surface Labeling

1. Biotin hydrazide (Pierce).
2. Horse-radish peroxidase conjugated to streptavidin (Kirkegaard and Perry Laboratories).
3. PBSCM: PBS buffer, pH 7.4 with 1 m*M* $MgCl_2$ and 0.1 m*M* $CaCl_2$.
4. Acetate buffer: 100 m*M* sodium acetate, pH 5.5, 1 m*M* $MgCl_2$ and 0.1 m*M* $CaCl_2$.

2.4. Isolation of P-gp by Nickel-Chelate Chromatography and Assay of Activity

1. *N*-dodecyl-β-D-maltoside (Calbiochem).
2. Buffer A: 50 m*M* sodium phosphate, 5 m*M* Tris-HCl, pH 8.0, 150 m*M* NaCl.
3. Buffer B: 50 m*M* sodium phosphate, 5 m*M* Tris-HCl, pH 8.0, 150 m*M* NaCl, 2% (w/v) n-dodecyl-β-D-maltoside, 20% (v/v) glycerol.
4. Buffer C: 50 m*M* sodium phosphate, 5 m*M* Tris-HCl, pH 8.0, 500 m*M* NaCl, 50 m*M* imidazole (pH adjusted to 7.0), 0.1% (w/v) n-dodecyl-β-D-maltoside, 20% (v/v) glycerol.
5. Buffer D: 10 m*M* Tris-HCl, pH 7.5, 500 m*M* NaCl, 80 m*M* imidazole (pH adjusted to 7.0), 0.1% (w/v) n-dodecyl-β-D-maltoside, 20% (v/v) glycerol.
6. Buffer E: Buffer D but containing 300 m*M* imidazole, pH 7.0.
7. Ni-NTA spin columns (Qiagen).
8. Phosphatidylethanolamine (crude sheep brain, Sigma Type IIs, cat.no. P-4264) or *Escherichia coli* lipids (Avanti Polar Lipids, AL).
9. TBS: 10 m*M* Tris-HCl, pH 8.0, 150 m*M* NaCl.
10. Verapamil, vinblastine, colchicine, cyclosporin A (Sigma).
11. 2X ATPase buffer: 100 m*M* Tris-HCl, pH 7.5, 100 m*M* NaCl, 20 m*M* $MgCl_2$, 10 m*M* ATP, 5 m*M* dithiothreitol (DTT), 4 m*M* EGTA, pH 8.0, and 2 m*M* ouabain (Sigma). (Prepare fresh because ATP is not stable.)
12. Solution A: 12% (w/v) SDS (BioBasic, Inc., Scarborough, Ontario) (some sources of SDS have high inorganic phosphate that will interfere with the ATPase assay).
13. Solution B: 6% (w/v) L-ascorbic acid in 1 M HCl. (Unstable, prepare fresh.)
14. Solution D: 1% (w/v) ammonium molybdate.
15. Solution BD: Mix solutions B and D in 1/1 ratio. (Prepare fresh and store on ice.)

16. Solution E: 2% (w/v) sodium citrate, 2% (w/v) sodium meta-arsenite, 2% (w/v) acetic acid (*see* **Note 3**).
17. Branson Sonifier 450 with cup holder.

3. Methods

3.1 Small-Scale Expression of Processing Mutants and Rescue with a Chemical Chaperone

After a processing mutant has been identified, it can be subjected to rescue with a chemical chaperone. Many membrane proteins such as P-gp are normally glycosylated. The immature core-glycosylated form of wild-type P-gp (in the ER) and the misprocessed mutants migrate in sodium dodecyl sulfate (SDS) gels with an apparent mass of 150 kDa, while the fully functional mature form of P-gp migrates with an apparent mass of 170 kDa. Therefore, the glycosylation pattern of P-gp in SDS gels serves as an important preliminary tool for indicating whether a mutant protein has been processed after rescue with a chemical chaperone. Subsequent biochemical tests with endoglycosidases will indicate whether the P-gp has been fully processed. As the protein moves from the ER to the Golgi, their carbohydrates are modified and they become resistant to endoglycosidase H_f, but not to endoglycosidase F.

To identify the concentration of chemical chaperone required, the cells are first transfected with the mutant cDNA (in 24-well plates) and then incubated with different concentrations of the chaperone. Transfection using the calcium phosphate co-precipitation method ***(16)*** is relatively inexpensive and works well.

3.1.1. Transient Transfection

1. All procedures are done in a tissue-culture hood. In a 50-mL sterile polypropylene conical tube, mix 12 µg cDNA (in the chosen expression vector) and sterile water to give a volume of 540 µL. Then add 60 µL of 2.5 *M* $CaCl_2$ and mix. Then add slowly 600 µL 2X BES solution (drop-wise and with constant mixing) and let the mixture incubate at room temperature (21°C) for 10–15 min. During this interval, prepare the cells.
2. Remove the media from a 75-cm^2 flask of HEK 293 cells (grown to about 50–75% confluent). Give the flask a hard tap. This will dislodge the cells from the bottom of the flask. Add 5 mL of media. Pipet the cells up and down 3–4 times to break any clumps of cells and add another 55 mL of media. Take 12 mL of this cell suspension and add to the DNA/$CaPO_4$ mixture from **step 1**. Mix gently and immediately pipet 0.5 mL of this suspension into each well of a 24-well plate (*see* **Notes 4** and **5**).
3. Incubate the plate overnight at 37°C in 2.5% CO_2 (*see* **Note 6**).
4. Next day, prepare 10-fold serial dilutions of a drug in media, with 1 m*M* being the highest concentration (prepare drug stock of 100 m*M* in dimethyl sulfoxide [DMSO]). Remove the 24-well plate from the incubator and gently aspirate the media. Then add 1 mL of the diluted drug/media mixture to each well. Incubate

for 24–48 h at 37°C in 5% CO_2. Repeat this step on a plate of transfected cells but with no drug substrate (these are the mock-treated samples that will serve as controls). Another plate of cells that was transfected with cDNA for the wild-type P-gp should also be treated with and without different concentrations of drug substrate (these samples will indicate whether the chemical chaperone had an effect on the wild-type protein) (*see* **Note 7**).

5. Harvest the transfected cells by pipetting the media up and down several times to dislodge the cells and then transfer to a 1.5-mL microcentrifuge tube (*see* **Note 8**). Pellet cells by centrifugation at 2000*g* for 3 min at room temperature. Remove the supernatant and resuspend cells in 1 mL PBS. Pellet the cells again by centrifugation. Resuspend pellet in 25 µL of PBS, then add 175 µL 2X SDS sample buffer (125 m*M* Tris-HCl, pH 6.8, 4% [w/v] SDS, 4% [v/v] 2-mercaptoethanol, 20% [v/v] glycerol, and 50 m*M* EDTA) (*see* **Note 9**).
6. Load 15 µL on 5.5% SDS gels (minigels; 1.5-mm spacers and 15 wells). Electroblot the gel onto a piece of nitrocellulose (Western Blot) and do immunoblot analysis with anti-P-gp antibody (available commercially) followed by enhanced chemiluminescence ***(17)***. If the presence of drug substrate corrected the folding defect then P-gp will mature from the 150 kDa protein to the 170 kDa protein (*see* **Note 10**) (*see* **Fig. 1**).
7. P-gp can be tested for sensitivity to digestion by endoglycosidase H. Take 45 µL of the whole cell extract and add 5 µL 10X Endo H buffer (500 m*M* sodium citrate, pH 5.5, 5% [w/v] SDS, 100 m*M* EDTA, and 10% [v/v] 2-mercaptoethanol) and 1 µL of Endo H_f (1000 U/mL; New England Biolabs). Mix gently and incubate at 37°C for 15 min. Add 1 volume of 2X SDS sample buffer and load 10–20 µL onto 5.5% SDS-gels. Do Western-blot analysis.

3.2. Pulse Labeling to Monitor Time Course of Maturation

After a P-gp mutant that can be rescued with drug substrates is identified, its efficiency of maturation in the presence of drug substrate can be determined by pulse-chase experiments using radiolabeled [^{35}S]-methionine and cysteine. The steps described here involve the use of cyclosporin A as a chemical chaperone. Cyclosporin A is one of the most potent chemical chaperones for inducing maturation of misprocessed P-gp mutants ***(9)***.

1. HEK 293 cells are transfected on d 1. Take 50 mL of cells in media and add to 5 mL of (cDNA/$CaCl_2$/BES) mixture. (The cDNA will be wild-type P-gp, a misprocessed P-gp mutant and a control expression [mock-transfected].) Add 3.5 mL of this mixture to a 6-cm diameter culture dish (total of 12 dishes). Incubate the cells for 16–24 h at 37°C in a 2.5% CO_2 incubator.
2. Next day gently aspirate off the media from each plate and gently add 3 mL of S-minus media (no L-methionine or L-cysteine) and again remove media (*see* **Note 11**). Then add 3 mL of S-minus media with (+ 10 µ*M* cyclosporin A) or without (-cyclosporin A) and incubate cells for another 10 min at 37°C. While cells are incubating, prepare the radioactive label.

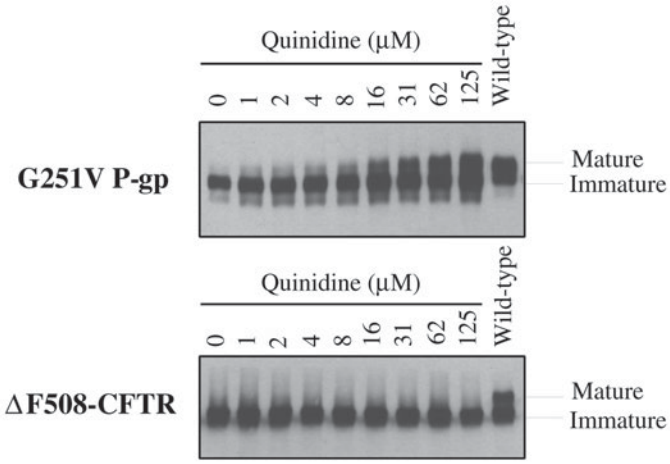

Fig. 1. Example of rescue of P-gp processing mutant by drug substrate/chemical chaperone. HEK 293 cells expressing the processing mutants, P-gp mutant G251V, or ΔF508-CFTR were incubated with media containing various concentrations of P-gp substrate, quinidine. After 48 h at 37°C, the cells were harvested and solubilized with SDS sample buffer containing 50 m*M* EDTA, and subjected to immunoblot analysis with anti-P-gp antibody or with anti-CFTR Antibody (Monoclonal Antibody M3A7; Dr. John Riordan, Mayo Clinic, Scottsdale, AZ). P-gp shows increasing amounts of the mature 170 kDa protein with increasing concentrations of quinidine. The effect is specific because quinidine had no effect on the ΔF508-CFTR mutant. Wild-type P-gp and CFTR were included as markers.

3. In a 50-mL conical tube, add 120 μL [^{35}S]-Translabel and 18 mL S-minus media with 10 μ*M* cyclosporin A. To start labeling, remove media from cells and add 1 mL of the radioactive media. Incubate the cells for 30 min at 37°C.
4. Remove radioactive media and add 3.5 mL of regular media (this is Time = 0 min, and the start of the chase part of the experiment).
5. At times 0, 1, 2, 4, 8, and 24 h, remove the media. Add 1 mL PBS and collect the cells in a 1-mL microfuge tube.
6. Collect cells by centrifugation at 2000*g* for 3 min and wash pelleted cells two more times with 1 mL PBS.
7. Suspend cells in 100 μL PBS containing 5 m*M* EDTA. Add 1 mL of buffer I, mix, and then centrifuge at 14,000*g* for 10 min at 4°C. Transfer the supernatant to a fresh microfuge tube and then add 10 μg of anti P-gp antibody. Incubate for 2 h to overnight at 4°C, and then add 50 μL of Protein A-Sepharose CL-4B beads (the Protein A Sepharose CL-4B beads are prepared as a 50% [v/v] slurry in Buffer I).

8. Incubate 1 h at 4°C on a rotator or platform shaker. Centrifuge at 4000*g* for 1 min to pellet the beads. Resuspend the beads in 1 mL of Buffer I, then centrifuge to pellet the beads. Wash the beads another 4 times with 1 mL Buffer I. Add 50 µL of 2X SDS sample buffer to the final pelleted beads (*see* **Note 12**). Load 15 µL of the supernatant onto a 5.5% minigel (1.5-mm thick). After gel electrophoresis, soak the gels in 10% (v/v) acetic acid for 15 min at room temperature. Rinse the gel twice with distilled water and soak the gel in Amplify (Amersham Biosciences) for 30–60 min at room temperature. Place the gel onto a piece of 3 MM filter paper and dry at 60–70°C for 1 h in a vacuum dryer (*see* **Note 13**).
9. Place the dried gel in a film cassette and expose to film for various times at –80°C (*see* **Note 14**).

3.3. Cell Surface Labeling

There are several ways to determine if a fully glycosylated (mature) protein has been transported from the Golgi to the cell surface. Immunofluorescence can be used to tell if the protein is at the cell surface. A biochemical method is cell-surface labeling of the carbohydrate group in the protein. When P-gp is at the cell surface, its carbohydrate groups are exposed to the outside of the cell and can be modified and labeled (*see* **Note 15**).

3.3.1. Modifying Carbohydrate Groups

1. Transfect HEK 293 cells with wild-type, misprocessed P-gp mutant or with expression vector (mock-transfected) in 10-cm^2 culture plates. Incubate overnight at 37°C in 2.5% CO_2 incubator.
2. Remove media from two plates. Add fresh plain media to one plate and fresh media with 10 µ*M* cyclosporin A to the other plate. Incubate for another 24–48 h at 37°C in a 5% CO_2 incubator.
3. The remaining steps are done at 4°C. Gently wash the cells 4 times with 3 mL PBSCM buffer (*see* **Note 16**).
4. Add 2 mL 10 m*M* $NaIO_4$ in PBSCM buffer and leave the plates in the dark for 30 min.
5. Wash the cells 3 times with 3 mL PBSCM buffer and once with 3 mL acetate buffer.
6. Add 2 mL 2 m*M* biotin hydrazide in acetate buffer and incubate for 30 min in the dark.
7. Wash cells four times with PBSCM. Collect cells in 1 mL PBS and transfer to a 1.5 mL microfuge tube. Pellet cells by centrifugation and suspend in 100 µL PBS and then add 1 mL of Buffer 1.
8. Centrifuge at 14,000*g* for 10 min. Transfer supernatant to a fresh microfuge tube and do immunoprecipitation as describe above.
9. Run immunoprecipitates on SDS-gels, transfer onto nitrocellulose, and develop with HRP-conjugated to streptavidin.

3.4. Large Scale Expression of the Rescued Mutant and Measurement of Drug-Stimulated ATPase Activity

A convenient method for testing whether the protein that is processed to the cell surface is active is to measure drug-stimulated ATPase activity. Isolation of the mutant can be performed on P-gp mutants containing a 10-histidine tag at the COOH-terminal end using nickel-chelate chromatography ***(9)***. The isolated mutant can then be reconstituted with lipids and its drug-stimulated ATPase activity measured and compared to that of wild-type P-gp (*see* **Notes 17** and **18**).

3.4.1. Large-Scale Transfection

1. Three different transfections are done: with histidine-tagged wild-type P-gp, with histidine-tagged misprocessed P-gp mutant, and with vector (control). Mix 200 μg of cDNA with sterile water to give a total volume of 9 mL. Add 1 mL of 2.5 *M* $CaCl_2$ and then add drop-wise 10 mL 2X BES solution. Let mixture sit at room temperature for 10–15 min. Prepare cells.
2. For each transfection remove the media from ten 75-cm^2 flasks of HEK 293 cells (about 75% confluent). Sharply tap the flask to dislodge the cells. Add 2 mL of media to each flask and transfer the cells to a bottle containing 600 mL of media. Mix the cells and dispense 200 mL of cell suspension into a 75-cm^2 flask. Add the DNA/$CaCl_2$/BES mix from **step 1**. Mix and dispense 9 mL onto a 10-cm diameter plate (total = 25 plates). Incubate overnight in a 2.5% CO_2 incubator.
3. Next day, remove the media and replace with fresh media containing a drug substrate (using the optimum concentration required to rescue the misprocessed mutant as determined in **Subheading 3.1.** of the Methods). Incubate at 37°C in a 5% CO_2 incubator for 24–48 h (*see* **Note 19**).
4. Harvest cells and use immediately or suspend in 3 mL of media containing 10% (v/v) DMSO and store in a –80°C freezer.

3.4.2. Isolation of Histidine-Tagged P-gp Mutants by Nickel-Chelate Chromatography

Histidine-tagged P-gp can be isolated from whole cell extracts of transfected HEK 293 cells using nickel-chelate chromatography ***(18)***. Background levels of endogenous ATPases are very low after one round of nickel-chelate chromatography (*see* **Note 20**). All steps are done at 4°C.

1. Wash transfected cells twice with Buffer A and suspend in a total volume of 0.75 mL (with Buffer A).
2. Add 1 volume of Buffer B, mix gently, and let sit on ice for 10 min (*see* **Note 21**).
3. Centrifuge at 14,000*g* for 15 min to remove insoluble material.
4. Transfer supernatant onto two Qiagen miniprep plasmid DNA spin columns and centrifuge at 14,000*g* for 1 min. (This removes some of the DNA that can interfere with subsequent binding to nickel column.)
5. Combine the pass-through fractions from both tubes (about 1300 μL) and add 150 μL 3 *M* NaCl and 50 μL 1 *M* imidazole. Mix gently and apply 0.5 mL to a

nickel-spin column (Qiagen). Centrifuge at 50*g* for 5 min. Repeat spin until the entire sample has been passed through the column (*see* **Note 22**).
6. Add 0.5 mL Buffer D and centrifuge 100*g* for 5 min. Repeat three more times.
7. Remove the nickel column and thoroughly wipe the outside with a tissue. Transfer the column to a fresh microfuge tube and add 100 µL Buffer E. Let column sit in ice for 10 min, then centrifuge at 50*g* for 5 min. Add another 100 µL of Buffer E and centrifuge again. Finally, spin for 1 min at 1000*g*. Combine the eluted material and use immediately or freeze at –80°C (*see* **Notes 23** and **24**).

3.4.3. Measuring Drug-Stimulated ATPase Activity

Drug substrates stimulate P-gp ATPase activity. The level of stimulation (up to 20-fold) varies with different substrates. Measurement of drug-stimulated ATPase activity is a convenient assay to test for drug interaction with P-gp. The ATPase assay measures the amount of inorganic phosphate released and is based on the method developed by Chifflet et al. ***(19)***.

1. To a microfuge tube add 10 mg of lipid and 0.5 mL of TBS buffer. Suspend the lipid with a plastic microfuge pestle. Transfer this suspension to a polycarbonate Oakridge centrifuge tube and mix with 30 mL of pre-chilled (4°C) TBS. Centrifuge at 45,000*g* for 30 min. Suspend the lipid pellet in 1 mL TBS and keep at 4°C (*see* **Notes 25** and **26**).
2. Add 100 µL of washed lipid (from above) to 100 µL of isolated histidine-tagged P-gp. This amount is sufficient to perform 10 duplicate assays.
3. Sonicate P-gp/lipid mixture for 45 s at 4°C at maximum setting.
4. To determine K_m and V_{max} values for drug-stimulated ATPase activity, prepare 2X ATPase buffer containing no drug (control) and 8 different drug concentrations. Place 10 µL of the sonicated samples into 10 pairs of microfuge tubes. To the first pair of tubes (blanks), add 12 µL of solution A (*see* **Note 27**).
5. Add 10 µL of 2XATPase buffer containing no drug (to blank and control tubes) or containing various concentrations of drug substrate.
6. Incubate the samples for 30 min at 37°C.
7. Stop the reaction by adding 12 µL of Solution A.
8. Add 30 µL of Solution BD and incubate 5–10 min at room temperature.
9. Add 45 µL of solution E and incubate for 10 min at 37°C.
10. Measure the absorbance at 850 nm using a microcuvet (Beckman Instruments).
11. Determine the amount of inorganic phosphate released using a standard curve prepared from known amounts of phosphate.
12. Do a Western-blot analysis on the isolated P-gp (load various amounts onto SDS-gels) and compare expression between wild-type and mutant P-gp.

4. Notes

1. The proper name for the cells is 293 cells. Although many laboratories use these cells for transfection studies, all are not morphologically similar. The reason is unknown. It may be that with prolonged passage, the cells may have altered characteristics because of their embryonic nature. Therefore, it is important to grow

and freeze many vials of cells as stock from the initial cell stock. Usually after about a year of continuous passage, transfection efficiency decreases. Then one will need to start a fresh vial of cells for transfection.

2. It is important that the pH is exact. Even the smallest deviation from this will adversely affect the level of expression.
3. Dissolve the solids in water first before adding acetic acid.
4. Expression is best if the cells are actively growing and very poor if the cells are 100% confluent.
5. HEK293 cells, unlike other cells (e.g., COS-1 cells), do not attach very well to the bottom of the flask. Therefore, one has to be gentle when moving the cells from the incubator to the culture hood. An advantage is that trypsin is not required to dislodge the cells from the bottom of the flask.
6. A 5% CO_2 incubator can also be used if a 2.5% CO_2 incubator is unavailable.
7. At the higher concentrations, some hydrophobic compounds will precipitate when mixed with the media. It is still worthwhile to add these mixtures to the cells. Alternatively, one could titrate the drug concentration that will remain in solution.
8. Many compounds are cytotoxic and will cause some cells to detach from the bottom of the plate. These floating cells should be harvested because they may contain mutant P-gp that has been rescued by drug/chemical chaperone.
9. Metal-dependent proteases seem to be present in HEK 293 cells that are resistant to SDS (Loo and Clarke, unpublished observations). The presence of EDTA protects P-gp from degradation after solubilization of whole cells.
10. The whole cell SDS extract is often too viscous to load onto the SDS gels because of the presence of genomic DNA. If this is the case, then pass the entire sample through a Qiagen miniprep plasmid DNA isolation column. Load the extract onto the spin column and centrifuge at 14,000*g* for 1 min at room temperature. Load the pass-through material onto the gel.
11. This step is essential as it removes residual media containing cold methionine and cysteine that if left will interfere with the efficiency of labeling.
12. Do not boil the sample! Membrane proteins, unlike the soluble proteins, will irreversibly aggregate upon heating. Once aggregation has occurred, nothing can be done to repair the damage. The whole experiment will have to be repeated.
13. Do not break the vacuum until the gel is dry. SDS gels will crack into many pieces if drying is interrupted.
14. Develop the film after 12–16 h exposure. In a good labeling experiment, a strong signal is easily present and you can decide whether to get a more or less intense signal by varying the exposure time. If signal is barely visible, then be prepared to repeat the experiment. A poor transfection (low expression) will also affect the intensity of signal obtained.
15. An alternative method for labeling cell-surface proteins is to use NHS-biotin (Pierce) which labels amino groups.
16. If HEK 293 cells detach too easily, then transfect COS-1 cells.
17. Tagging proteins with polyhistidine is a popular method for isolating mutant proteins and for purifying large amounts of proteins for structural studies. The posi-

tion of the histidine tag in the protein is important. In some membrane protein, the histidine tag is exposed only if placed at the NH_2- or COOH-terminal ends. In other cases, placing the tag a few residues away from the end is optimal.

18. One can use either a 6- or a 10-histidine tag. With a 10-histidine tag, the nickel column can be washed with a higher concentration of imidazole and the purified P-gp subsequently is more pure than if a 6-His tag was used.
19. Useful nontoxic chemical chaperones for P-gp mutants are 10 μ*M* cyclosporin A or 50 μ*M* verapamil ***(9)***. To inhibit P-gp maturation, use 1 μ*M* disulfiram ***(20)*** or 1 μ*M* MG-132 (Biomol Inc.) ***(21)*** in the media.
20. If highly purified P-gp is required, then membranes must be prepared from the transfected cells before solubilization with detergent. Also two rounds of nickel-chelate chromatography must be performed after solubilization with detergent.
21. Do not vortex as genomic DNA will be released from the nuclei.
22. Decrease the imidazole concentration to 20 m*M* at this step and in the wash buffers (Buffer D) when isolating the immature form of P-gp.
23. Residual phosphate at this step will interfere with the ATPase assay.
24. Repeated freezing and thawing will inactivate P-gp.
25. It is important to determine if the type of lipid used for reconstitution does not contain inorganic phosphate. This wash step removes any residual inorganic phosphate.
26. Lipids oxidize very rapidly in air. Prepare lipids fresh and use immediately.
27. A useful compound is verapamil (0.001–3 m*M*). It is one of the most potent stimulators of ATPase activity (about 20-fold).

Acknowledgments

This work was supported by funds from the United States National Institutes of Health (Grant CA 80900), the Canadian Institutes for Health Research, and the Canadian Cystic Fibrosis Foundation.

References

1. Thomas, P. J., Qu, B. H., and Pedersen, P. L. (1995) Defective protein folding as a basis of human disease. *Trends Biochem. Sci.* **20,** 456–459 .
2. Aridor, M. and Balch, W. E. (1999) Integration of endoplasmic reticulum signaling in health and disease. *Nat. Med.* **5,** 745–751.
3. Loo, T. W., and Clarke, D. M. (1993) Functional consequences of proline mutations in the predicted transmembrane domain of P-glycoprotein. *J. Biol. Chem.* **268,** 3143–3149.
4. Loo, T. W. and Clarke, D. M. (1993) Functional consequences of phenylalanine mutations in the predicted transmembrane domain of P-glycoprotein. *J. Biol. Chem.* **268,** 19,965–19,972.
5. Loo, T. W. and Clarke, D. M. (1994) Functional consequences of glycine mutations in the predicted cytoplasmic loops of P-glycoprotein. *J. Biol. Chem.* **269,** 7243–7248.

6. Loo, T. W. and Clarke, D. M. (1994) Prolonged association of temperature-sensitive mutants of human P- glycoprotein with calnexin during biogenesis. *J. Biol. Chem.* **269,** 28,683–28,689.
7. Loo, T. W. and Clarke, D. M. (1995) P-glycoprotein. Associations between domains and between domains and molecular chaperones. *J. Biol. Chem.* **270,** 21,839–21,844.
8. Loo, T. W. and Clarke, D. M.. (1998) Quality control by proteases in the endoplasmic reticulum. Removal of a protease-sensitive site enhances expression of human p-glycoprotein. *J. Biol. Chem.* **273,** 32,373–32,376.
9. Loo, T. W. and Clarke, D. M. (1997) Correction of defective protein kinesis of human P-glycoprotein mutants by substrates and modulators. *J. Biol. Chem.* **272,** 709–712.
10. Loo, T. W. and Clarke, D.M. (1998) Superfolding of the partially unfolded core-glycosylated intermediate of human P-glycoprotein into the mature enzyme is promoted by substrate- induced transmembrane domain interactions. *J. Biol. Chem.* **273,** 14,671–14,674.
11. Zhou, Z., Gong, Q., and January, C. T. (1999) Correction of defective protein trafficking of a mutant HERG potassium channel in human long QT syndrome. Pharmacological and temperature effects. *J. Biol. Chem.* **274,** 31,123–31,126.
12. Fan, J. Q., Ishii, S., Asano, N., and Suzuki, Y. (1999) Accelerated transport and maturation of lysosomal alpha-galactosidase A in Fabry lymphoblasts by an enzyme inhibitor. *Nat. Med.* **5,** 112–115.
13. Foster, B. A., Coffey, H. A., Morin, M. J., and Rastinejad, F. (1999) Pharmacological rescue of mutant p53 conformation and function. *Science* **286,** 2507–2510.
14. Morello, J. P., Salahpour, A., Laperriere, A., Bernier, V., Arthus, M. F., Lonergan, M., et al. (2000) Pharmacological chaperones rescue cell-surface expression and function of misfolded V2 vasopressin receptor mutants. *J. Clin. Invest.* **105,** 887–895.
15. Ma, T., Vetrivel, L., Yang, H., Pedemonte, N., Zegarra-Moran, O., Galietta, L. J. V., and Verkman, A. S. (2002) High-affinity activators of cystic fibrosis transmembrane conductance regulator (CFTR) chloride conductance identified by high-throughput screening. *J. Biol. Chem.* **277,** 37,235–37,241.
16. Chen, C. and Okayama, H. (1987) High-efficiency transformation of mammalian cells by plasmid DNA. *Mol. Cell Biol.* **7,** 2745–2752.
17. Loo, T. W. and Clarke, D. M. (1994) Reconstitution of drug-stimulated ATPase activity following co-expression of each half of human P-glycoprotein as separate polypeptides. *J. Biol. Chem.* **269,** 7750–7755 .
18. Loo, T. W. and Clarke, D. M. (1995) Rapid purification of human P-glycoprotein mutants expressed transiently in HEK 293 cells by nickel-chelate chromatography and characterization of their drug-stimulated ATPase activities. *J. Biol. Chem.* **270,** 21,449–21,452.
19. Chifflet, S., Torriglia, A., Chiesa, R., and Tolosa, S. (1988) A method for the determination of inorganic phosphate in the presence of labile organic phosphate and high concentrations of protein: application to lens ATPases. *Anal. Biochem.* **168,** 1–4.

20. Loo, T. W. and Clarke, D. M. (2000) Blockage of drug resistance in vitro by disulfiram, a drug used to treat alcoholism. *J. Natl. Cancer Inst.* **92,** 898–902.
21. Loo, T. W. and Clarke, D. M. (1999) The human multidrug resistance P-glycoprotein is inactive when its maturation is inhibited: potential for a role in cancer chemotherapy. *FASEB J.* **13,** 1724–1732.

20

Analysis of Defective Subunit Interactions Using the Two-Hybrid System

Belén Pérez, Lourdes R. Desviat, and Magdalena Ugarte

1. Introduction

The two-hybrid system exploits the ability of a pair of interacting proteins to bring a transcription factor activation domain into close proximity with a DNA-binding site that regulates the expression of a reporter gene. Many eukaryotic transcriptional activators consist of two physically and functionally separable domains: a DNA-binding domain (DNA-BD) that specifically binds a promotor and an activation domain (AD) that directs RNA polymerase II to transcribe the gene downstream of the DNA-binding site. The two hybrid system requires the construction of hybrid genes to encode: 1) the DNA binding domain fused to protein X, and 2) the activation domain fused to protein Y (**Fig. 1**). In the two-hybrid assay, the tether is the interaction between these two proteins (X and Y). There are two main systems: a yeast-based genetic assay usually used to identify proteins that bind to a protein of interest ***(1)*** and to delineate domains or residues critical for an interaction, and the mammalian two hybrid system aimed to the last application. The mammalian two-hybrid system is a strategy that has been applied to the study of a variety of protein–protein interactions and, in combination with deletional or site-directed mutagenesis, to the mapping of amino acids responsible for the interaction of two proteins ***(2,3)***. In our group we have applied the mammalian two-hybrid system successfully in the study of the effect of point mutations in the assembly of a cytosolic homotetrameric protein (phenylalanine hydroxylase; PAH) and in a heteromeric mitochondrial protein (propionyl-CoA carboxylase, PCC) ***(2,4,5)***. This chapter illustrates the approach employed to study the effect of missense mutations on the heteromeric and homomeric interaction using as model the β subunit of the PCC protein ***(4,5)***. The mitochondrial protein PCC (EC 6.4.1.3), one of the four human biotin-

From: *Methods in Molecular Biology, vol. 232: Protein Misfolding and Disease: Principles and Protocols*
Edited by: P. Bross and N. Gregersen © Humana Press Inc., Totowa, NJ

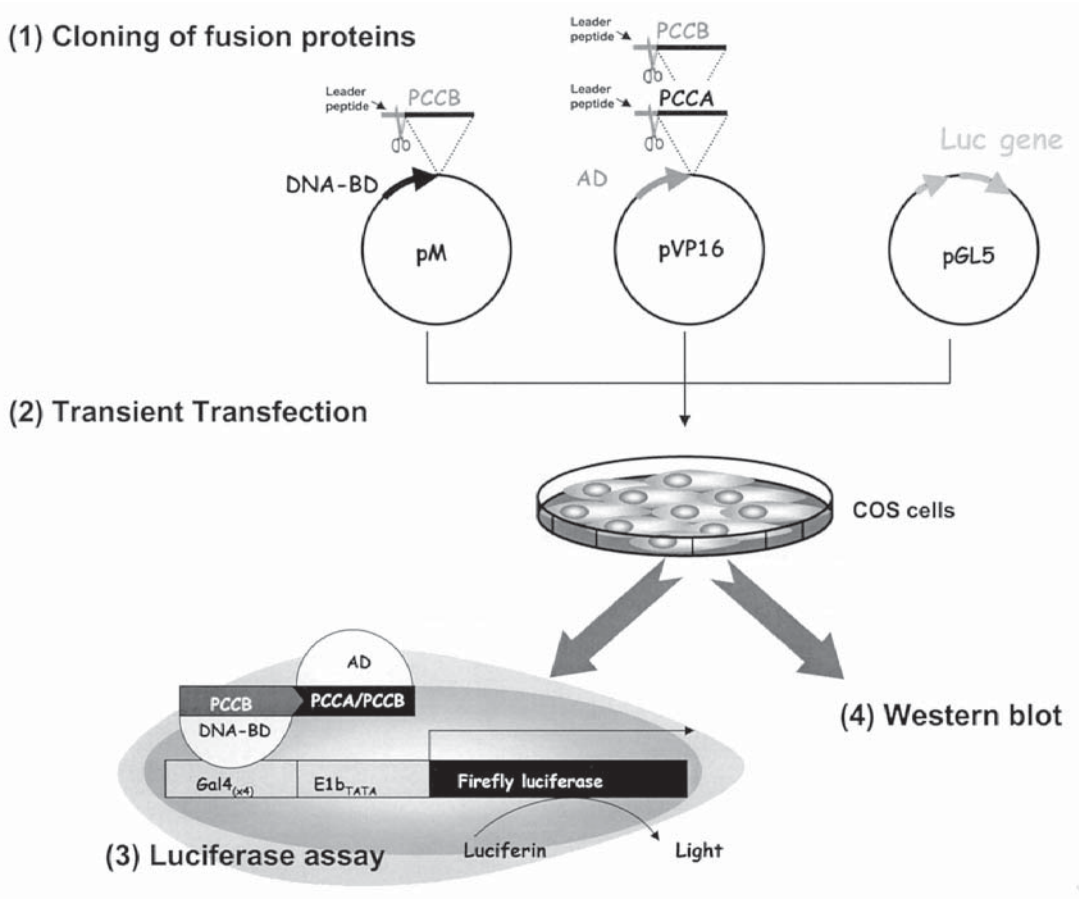

Fig. 1. Schematic diagram of the two-hybrid mammalian system described in this chapter. The β-PCC subunit was cloned in the AD and BD expression vectors and the α-PCC was cloned in the AD plasmid. The three plasmids (AD, BD, and luciferase vector) were cotransfected in COS-7 cells and the luciferase assay performed.

dependent enzymes, catalyses the carboxylation of propionyl-CoA to D-methylmalonyl-CoA and the native enzyme consists of two different subunits, α-PCC and β-PCC encoded by the *PCCA* and *PCCB* genes, respectively ***(6)***. Hereditary deficiency of *PCC* causes the clinically heterogeneous propionic acidemia (PA, MIM 232000, 232050). PA results from mutations in either *PCCA* or *PCCB* genes and up to now, 29 different mutations in the *PCCB* gene and 27 in the *PCCA* gene have been identified in different population studies ***(7,8)***.

2. Materials

1. Mammalian MATCHMAKER two-hybrid assay Kit (Clontech).
2. α-PCC cDNA (Accession number X14608) and β-PCC cDNA (accession number X73424).
3. Oligonucleotide primers.
4. Restriction enzymes (Roche, Indianapolis, IN) and polymerase chain reaction (PCR) reagents (Life Technologies, Rockville, MD)
5. QuickChange site-directed mutagenesis kit (Stratagene, La Jolla, CA).
6. Concert plasmid DNA purification kit (Promega, Madison, WI).
7. fmol DNA Sequencing System (Promega) and fluorescent *PCCB* gene primers (Pharmacia Biotech, Buckinghamshire, UK).
8. DNA electrophoresis equipment and DNA sequencing system (ALFexpress, Pharmacia Biotech).
9. *Escherichia coli*, XL1 Blue.
10. COS-7 cells.
11. CO_2 incubator and cell culture equipment.
12. Culture reagents: MEM and RPMI, inactivated fetal calf serum (FCS), glutamine. Antibiotics, ethylenediamine tetraacetic acid (EDTA)-trypsin, phosphate-buffered saline (PBS) (Life Technologies, Rockville, MD).
13. Hemocytometer-double chamber with Neubauer rulings.
14. Microscope, hand counter.
15. Lipofectins (Life Technologies).
16. Tris-HCl/dithiothreitol (DTT): 50m*M* Tris-HCl, pH 7.4, 2 m*M* DTT.
17. Luciferase assay system (Promega).
18. Luminometer (MonoLight 2010, Analytical Luminiscence Laboratoty, Ann Arbor, MI).
19. Protein electrophoresis and Western-blot transference equipment (Biorad, Hercules, CA).
20. Protan® nitrocellulose transfer membrane (Schleider and Schuell, Keene, NH).
21. Anti β-PCC Primary antibody: The primary antibody was produced in rabbit by immunization with purified PCCB protein expressed in *E. coli* and was affinity-purified using β-PCC ***(9)***.
22. Goat anti-rabbit secondary antibody conjugated with horseradish peroxidase (HRP) (Nordic, Immunological Laboratories, The Netherlands).
23. ECL® Western-blotting analysis system (Pharmacia Biotech).

3. Methods

The methods described here outline: 1) Construction and purification of the mutant and wild-type expression vectors, 2) transfection of the expression vectors, 3) luciferase assay, and 4) Western blot. This approach is shown schematically in **Fig. 1**.

3.1. Construction of Plasmids Expressing Hybrid Proteins

The construction of fusion genes has been performed using standard molecular-biology techniques ***(10)***. We have used the plasmids described in the Mammalian Matchmaker two-hybrid assay kit from Clontech Laboratories, Inc.

3.1.1. pM Gal4 DNA-Binding Domain and pVP16 Activation Domain Cloning Vectors and pGL-G5 Luciferase Reporter Vector

pM Gal4 DNA-binding domain cloning vector (BD) and pVP16-activation-domain cloning vector (AD) have been used to generate the fusion of the GAL4 DNA-BD (amino acids 1-14) and VP16 AD (amino acids 411-455), respectively, with the protein of interest (**Fig. 2**). The two-hybrid proteins are targeted to the nucleus by the SV40 nuclear localization sequences. Genes encoding proteins should be cloned, in the correct orientation and in reading frame, into one of the restriction sites of the multiple cloning site regions at the 3' end of the BD and AD domains. Transcription is initiated from the constitutive SV40 early promoter and the transcription is terminated at the SV40 poly A transcription termination signal.

The plasmid pGL-G5 was constructed and provided by P. Stäheli (University of Freiburg, Germany). It contains five Gal4 DNA-binding sites upstream of an E1b promoter and the luciferase gene (*see* **Note 1**).

These three plasmids confer ampicillin resistance for bacterial selectivity and we performed large-scale plasmid preparation using Concert DNA purification kit.

3.1.2. α-PCC and β-PCC cDNAs

The plasmid pCMVA45-12 containing the human *PCCA* cDNA and the plasmid pRC/CMVB52 containing human *PCCB* cDNA were kindly provided by Prof. Gravel and Dr. Leclerc (McGill University, Canada).

3.1.3. Cloning of Fusion Proteins

DNA manipulations were performed by standard recombinant DNA methods to construct the expression plasmid ***(10)***. Wild-type and mutant β-PCC peptides were expressed as N-terminal fused forms with the GAL4 DNA-BD and VP16 transactivation domain (AD). To eliminate the putative amino terminal mitochondrial transit peptide ***(11)***, which directs the protein towards the

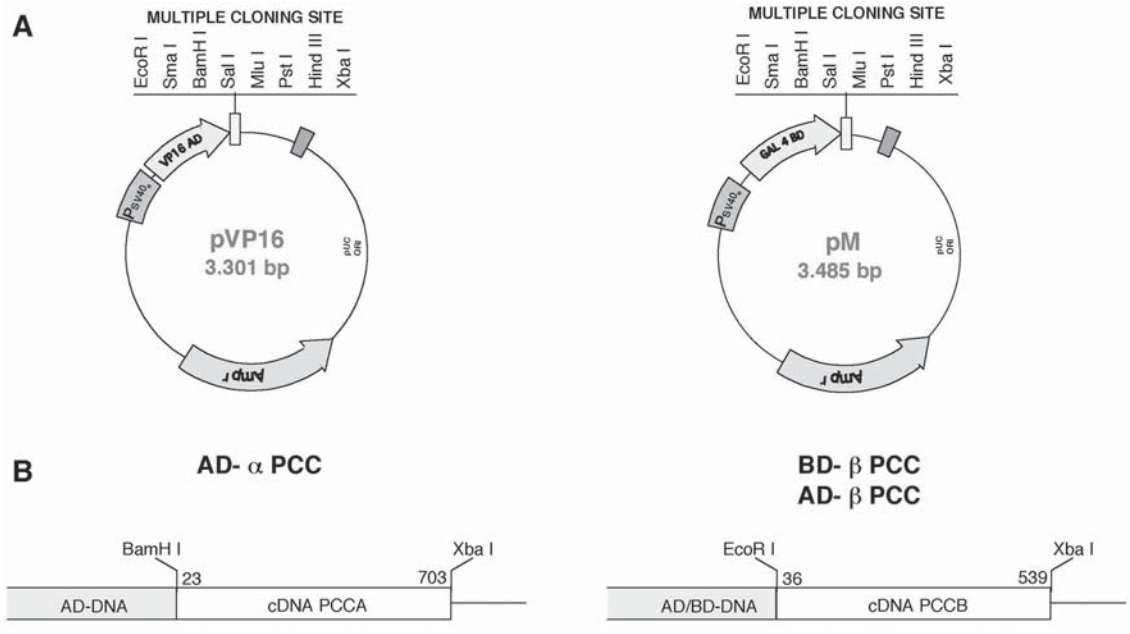

Fig. 2. (**A**) Schematic drawing of pM and pVP16 plasmid maps adapted from Clontech. (**B**) Schematic representation of the in frame cloning of α-PCC cDNA and β-PCC cDNA in the AD and DNA-BD eukaryotic expression vectors. The final products encode as fusion partner the respective subunits without the putative mitochondrial transit peptides (residues 1-36 in PCCB and 1-23 in PCCA).

mitochondrion, a wild-type β-PCC cDNA encoding the amino acids 36-539 [*Hinc*II (5') - *Xba*I (3')] was released from the vector pRC/CMV-*PCCB*, subcloned in pUC19, and finally ligated in frame to the expression plasmids pVP16 and pM [*Eco*RI (5') - *Xba*I (3')] (*see* **Note 2**). After the isolation of the plasmids (AD-PCCB and BD-PCCB), we checked for the presence of the insert in the correct orientation and reading frame by DNA cycle sequencing across the junctions of the fusion proteins using antisense oligonucleotide primer to read the N-terminal of the protein. The cycle sequencing was done using *fmol* DNA sequencing System (Promega) with fluorescent Cy5-primers and an automated ALF DNA Sequencer (Amersham, Pharmacia Biotech)

Cloning of the α-PCC cDNA in pVP16 (AD-PCCA) was performed following the same strategy previously employed with β-PCC, eliminating the putative mitochondrial transit peptide at the amino terminus, which directs the peptides to the mitochondria. α-PCC cDNA was PCR amplified using the sense primer 5´ATGGATCCGTAATCTTGGTTCA-3', which introduces a *BamH*I restriction site at its 5' end and hybridizes to nucleotides 69 to 84 in the *PCCA* cDNA and the antisense primer 5'-TAAAACCATCCCTGGTCTCT-3' hybridizing to nucleotides 652 to 633. The PCR product obtained was then digested with *BamH*I and *Stu*I and used in a triple ligation reaction with the *PCCA* cDNA fragment *Stu*I-*Xba*I, excised from vector pCMVA45-12, and the pVP16 vectors, properly digested. The final product encodes an α-PCC subunit in which the 23 amino-terminal residues have been deleted and substituted with the VP16 transactivation domain (AD).

3.1.4. Mutant Plasmids Constructs

To express mutant β-PCC proteins, a series of plasmid vectors were generated. The generation of the mutant constructs was performed by obtaining cDNAs carrying some mutations from the corresponding homozygous patients' fibroblasts by reverse transcription (RT)-PCR. After digestion of the amplified products with *Stu*I and *Xba*I, the resulting mutant fragments were used to replace their wild-type counterpart into the constructions AD-*PCCB* and BD-*PCCB*. In other cases cloning of mutations into the eukaryotic expression vectors AD-*PCCB* and BD-*PCCB* was performed by site-directed mutagenesis using QuickChange directed mutagenesis kit with the wild-type vectors. The presence of the desired mutation was confirmed by sequencing.

3.2. Mammalian COS-7 Cell Culture and Transfection

The next steps in this process involve the transient transfection of COS-7 cells with the three expression vectors followed by cell harvesting and luciferase assay. We use two different cultivation temperatures (37°C and 27°C) to explore, by the influence of this factor, defects directly affecting interaction or mutations disrupting it via misfolding.

3.2.1. Mammalian Cell Culture and Hemocytometer Counting

The cells were maintained in culture following standard protocols ***(12,13)***.

1. Frozen ampule for COS-7 cells is recovered from liquid nitrogen. The cells are cultured in MEM supplemented with 1% glutamine, 5% FCS and antibiotics at 95% humidity and 5% CO_2 in an incubator at 37°C (*see* **Note 3**).
2. At least 18 h before transfection, a total of 4×10^5 cells are plated into standard six-well dishes and grown in presence of MEM/FCS 5%. Total cell counts are done using an haemocytometer. Cell suspension prepared from a confluent COS-7 cell flask ($8–15 \times 10^6$ cells) is diluted to contain approx $1.5–2 \times 10^6$ cells/mL. The cell suspension is added to both chamber sides of the hemocytometer. The chamber coverslip should be firmly in place and the cells can be counted in any squares of the hemocytometer ***(12,13)***. Reproducibility is the key factor so that sufficient squares should be counted to obtain a count statistically representative of the population. Each large square (there are five on each chamber side) represents a volume of 0.1 mm^3. As an example, in 8 of 0.1 mm^3 squares (the four corners squares of each chamber side) 200 total cells are counted and if the original cell suspension had been diluted 1:8, the total cells numbers in the original suspension is:

$$\frac{200 \text{ (cells counted)} \times 8 \text{ (dilution)} \times 10^4 \text{ (mm}^3 \text{ in 1 cm}^3\text{)}}{8 \text{ (numbers of squares counted)}} = 2 \times 10^6 \text{ cells / mL}$$

3.2.2. COS-7 Cell Transfection

The three plasmids may be cotransfected into mammalian cells by any standard transfection method (*see* Chapter 16). We use a lipid-mediated method using lipofectin as transfection reagent (*see* **Note 4**). To study the effect of the mutations on the homomeric β-PCC assembly the cells are transiently transfected with wild-type AD-β-PCC and each of the different mutant BD β-PCC and vice versa. The study of the heteromeric assembly was done using the AD-PCCA and the different BD-PCCB mutant constructs. Each experiment should be done at least three times to evaluate the impact of the mutations precisely (*see* **Note 5**). For the lipid-mediated transfection proceed as follows:

1. Prepare the following solutions in polystirene tubes for each well of cells to be transfected:
   a. Solution A: Dilute 1 μg of each hybrid AD and BD expression plasmid and 1 μg of the reporter vector pGL-G5 in a final volume of 100 μL serum-free MEM.
   b. Solution B: For each transfection dilute 20 μL of lipofectin reagent in a final volume of 100 μL serum-free MEM.
2. After 45 min at room temperature, the two solutions are combined, mixed gently, and incubated further for 15 min.
3. While the lipofectin Reagent-DNA complexes are forming, the COS-7 cells plates are washed twice with serum-free MEM.

4. Add to each transfection tube 0.8-mL of serum-free medium. Mix gently and cover the cells with the solution.
5. After 5 h in a CO_2 incubator, replace the DNA containing medium with MEM supplemented with FCS and incubate the cells for 72 h.

3.3. Luciferase Assay

The gene encoding firefly luciferase is highly effective as reporter gene because the luciferase assay is extremely sensitive (*see* **Note 1**). The conventional assay for luciferase generates a "flash" of light that rapidly decays after enzyme and substrate are mixed, thus requiring automated injection luminometer for measurement of photon production. The luciferase activity is done at room temperature (the temperature optimum is 20–25°C) as follows:

1. Remove the growth medium from the cells to be assayed. Rinse the cells twice in PBS buffer and harvest the cells using 0.5 mL of EDTA-trypsin at 37ºC. If necessary, samples may be frozen at –70°C until the luciferase assay is performed.
2. Resuspend the cell pellet in 50 μL of Tris-HCl/DTT and disrupt the cells by three freeze/thaw cycles using liquid nitrogen and a water-bath at 37°C, alternatively.
3. Centrifuge the cell lysate at maximum speed in a microfuge 10 min to discard the cell debris. The total protein concentration in the supernatant is measured by Bradford assay (BioRad Laboratories, Hercules, CA)
4. Prepare one luminometer tube for each sample with 20 μL of supernatant and place the samples in an automated Luminometer in the presence of luciferin (Promega). It is important to thaw the luciferase reagent before beginning the experiment. After automatic injection of 10 μL luciferin the light produced for a period of 10 seconds is detected by a photomultiplier and the detected signal is converted to Relative Light Units (RLU).
5. Represent the data obtained as percentage of wild-type subunits interaction (**Fig. 3**). In the case of β-β homomeric interaction, both wild-type/mutant (AD-wild-type/BD-mutant and vice versa) and mutant-mutant pairs of hybrid proteins were tested and included in the mean and standard deviation (SD) calculated from the results.

   As illustrated in **Fig. 3** three different behaviors were found among the mutations expressed using this approach: (1) Mutations that affect the homomeric (β-β) and/or heteromeric (β-α) assembly independently of the cultivation temperature, reflecting their primary effect on the subunits interaction; (2) mutations that result in normal interaction levels only when expressed at the lower temperature, suggesting that these changes could be considered as temperature sensitive mutations; and (3) mutations that do not affect either heteromeric or homomeric assembly ***(4,5)***

3.4. Western-Blot Analysis

The expression of mutant AD-β-PCC and BD-β-PCC hybrid proteins was corroborated by Western-blot analysis ***(14)*** of the protein extract obtained from cotransfected COS-7 cells using anti-β-PCC antibodies (*see* **Note 6**).

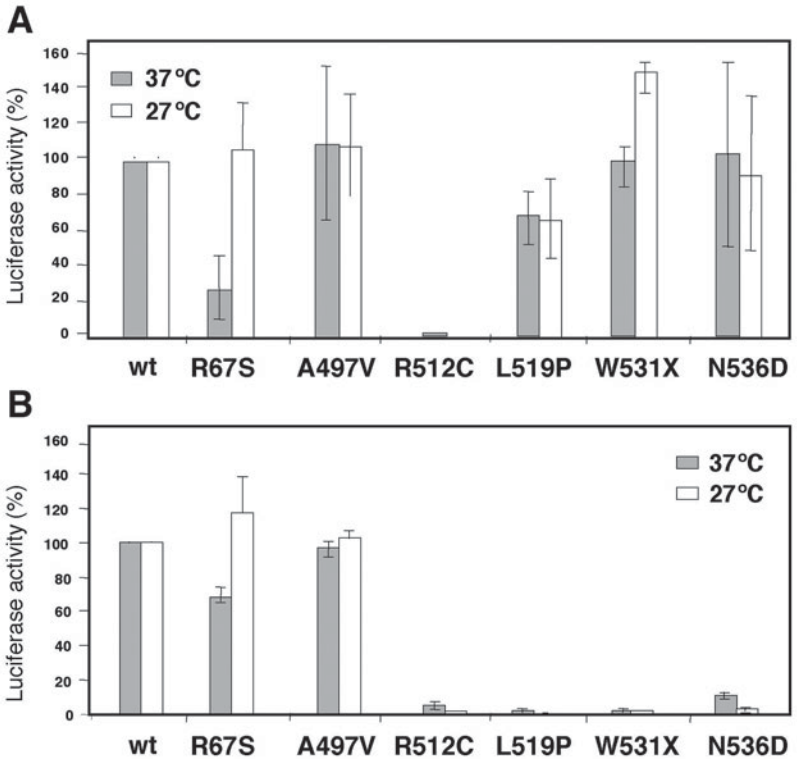

Fig. 3. This figure illustrates the effect of some *PCCB* mutations on the homomeric and heteromeric assembly using the two hybrid system at two different temperatures. (**A**) Effect of temperature on the assembly of α-β PCC subunits. The α-β heteromeric assembly was performed using the two-hybrid assay in COS-7 cells cultured at 37°C (blacks bar) and 27°C (white bars). The α subunit was expressed as fusion protein with VP16 activation domain (AD-PCCA) and the β-subunit fused to GAL4 binding domain (BD-PCCB). Co-transfection of the wild-type proteins AD-PCCA and BD-PCCB leads to the expression of cotransfected luciferase marker (100% interaction). The relative strength of the interaction between the wild-type AD-PCCA and the corresponding mutant BD-PCCB were measured as relative luciferase activity. The data represent the mean ± S.D. from three independent experiments. (**B**) Effect of temperature on the homomeric interaction between mutant β-PCC subunits. The β–β homomeric assembly was performed using the two-hybrid assay in COS-7 cells cultured at 37°C (white bars) and 27°C (gray bars). Co-transfection of the wild-type proteins AD-PCCB and BD-PCCB leads to the expression of cotransfected luciferase marker (100% interaction). The relative strength of the interaction between the normal AD-PCCB and the corresponding mutant BD-PCCB were measured as relative luciferase activity as previously described ***(5)***. The data represent the mean ± SD from three independent experiments.

1. At least 18 h before transfection, a total of 3×10^6 cells are plated into the standard T75 flask and grown as described in **Subheading 3.2.1.**
2. The transfection is done as described in **Subheading 3.2.2.** using 20 μg of one of the two plasmids (BD-PCCB or AD-PCCB) and 100 μL of lipofectins. The cells are grown in 4 mL of serum-free medium with the DNA-lipofectin mixture over 5 h.
3. Seventy-two h after transfection, cells are harvested and cell extracts are prepared in Tris-HCl/DTT as described in **Subheading 3.3.** The total protein concentration is measured by Bradford assay.
4. 200 μg of total protein are boiled in SDS buffer and are loaded in a 10% denaturing gel electrophoresis.
5. Transfer the proteins to Protan® Nitrocellulose transfer membrane by standard procedures ***(14)***.
6. Incubate with the primary antibody (anti β-PCC) at least 4 h.
7. Wash the membrane and incubate for 3 h with the goat anti-rabbit secondary antibody conjugated with HRP.
8. Cover and incubate the membrane 1 min with ECL® Western-blotting detection reagents at room temperature without agitation. Drain off excess detection reagent and place the blot in the film cassette with four sheets of autoradiographic film over 30 s.

4. Notes

1. pG5CAT mammalian reporter vector included in the MATCHMAKER kit could be used as cloramphenicol acetyl transferase (CAT) reporter plasmid for cotransfection into mammalian cells with AD and BD plasmids. The CAT assay most commonly used is radioactive ***(10)***, although there are several nonradiactive alternatives to provide interaction data (CAT enzyme-linked immunosorbent assay [ELISA] kit from Roche).
2. Methods such as cloning by PCR can be used to clone the protein in reading frame with the DNA-binding and AD domains.
3. The following modifications to the described methods have been done when growing the COS-7 cells at subphysiological temperature. Eighteen hours before transfection, a total of 600,000 cells are plated with RPMI/10% FCS media at 27°C. Cotransfection is done as described using RPMI instead of serum-free MEM (*see* **Subheading 3.2.2.**) to prepare the DNA and lipofectin solutions. The cell pellet is resuspended in 25 μL of Tris-HCl/DTT (50 m*M*, 2 m*M*, pH 7.4).
4. Several transfection methods can be used. After the transfection method is chosen, it should be optimized (cell number, amount and purity of DNA, media conditions, and transfection time).
5. It is convenient to use the negative and positive control vectors provided by Clontech in the initial experiment in order to optimize the two-hybrid experiments.
6. We recommend controlling the expression of fusion proteins to demonstrate that the decrease in the luciferase activity is not owing to reduced levels of mutant fusion protein.

Acknowledgment

This work was supported by grants of Fondo de Investigaciones Sanitarias (01/0405), and Comisión Interministerial de Ciencia y Tecnología (PM98-003 and SAF2001-0544). The financial support of Fundación Ramón Areces to the Centro de Biología Molecular "Severo Ochoa" is gratefully acknowledged.

References

1. Fields, S. and Sternglanz, R. (1994) The two-hybrid system: an assay for protein-protein interactions. *Trends Genet.* **10,** 286–292.
2. Gamez, A., Perez, B., Ugarte, M., and Desviat, L. R. (2000) Expression analysis of phenylketonuria mutations: effect on folding and stability of the phenylalanine hydroxylase protein. *J. Biol. Chem.* **275,** 29,737–29,742.
3. Zurcher, T., de la Luna, S., Sanz-Ezquerro, J. J., Nieto, A., and Ortin, J. (1996) Mutational analysis of the influenza virus A/Victoria/3/75 PA protein: studies of interaction with PB1 protein and identification of a dominant negative mutant. *J. Gen. Virol.* **77,** 1745–1749.
4. Muro, S., Pérez, B., Rodríguez-Pombo, P., Desviat, L. R., Pérez-Cerdá, C., and Ugarte, M. (2000) Mutations affecting the β–β homomeric interaction in propionic acidaemia: An approach to the determination of the β–propionyl-CoA carboxylase functional domains. *J. Inher. Metab. Dis.* **23,** 300–304.
5. Muro, S., Perez, B., Desviat, L.R., Rodriguez-Pombo, P., Perez-Cerda, C., Clavero, S., and Ugarte, M. (2001) Effect of PCCB Gene mutations on the heteromeric and homomeric assembly of propionyl-CoA carboxylase. *Mol. Genet. Metab.* **74,** 47–483.
6. Fenton, W. A., Gravel, R. A., and Rosenblatt, L. E. (2001) Disorders of propionate and methylmalonate metabolism, in *The Metabolic and Molecular Bases of Inherited Disease* (Scriver , B., Valle, Sly., eds.), II, Vol 8th ed. McGraw-Hill, New York, pp. 2165–2190.
7. Ugarte, M., Pérez-Cerdá, C., Rodríguez-Pombo, P., Desviat, L. R., Perez B., Richard, E., et al. (1999) Overview of mutations in the PCCA and PCCB genes causing propionic acidemia. *Hum. Mutat.* **14,** 275–282.
8. Muro, S., Rodríguez-Pombo, P., Perez B., Pérez-Cerdá, C., Desviat, L. R., Sperl, W., et al. (1999) Identification of Novel mutations in the PCCB gene in European propionic acidemia patients. *Hum. Mutat.* **14,** 89–90.
9. Richard, E., Desviat, L.R., Perez, B,. Perez-Cerda, C. and M. Ugarte. (1997). Three novel splice mutations in the PCCA gene causing identical exon skipping in propionic acidemia patients. *Hum. Genet.* **101,** 93–96.
10. Sambrook, J. and Russell, D. W. (2001) *Molecular Cloning: A Laboratory Manual*. Cold Spring Harbor Laboratory Press, Cold Spring Harbor, N.Y.
11. Kelson, T. L., Ohura, T., and Kraus, J. P. (1996) Chaperonin-mediated assembly of wild-type and mutant subunits of human propionyl-CoA carboxylase expressed in *Escherichia coli*. *Hum. Mol. Genet.* **5,** 331–337.

12. Masters, J. R. W. (2000) *Animal Cell Culture*. Oxford University Press, Oxford, UK.
13. Jakoby, W. B. and Pastan, I. H. (1979) Cell culture, in Colowich, S.P. and Kaplan, N.O. (eds.) *Methods in Enzymology*, Vol. LVIII, Academic Press, New York.
14. Harlow, E., and Lane, D. (1988) *Antibodies: A Laboratory Manual*. Cold Spring Harbor Laboratory, Cold Spring Harbor, NY.

21

Investigation of Folding and Degradation of In Vitro Synthesized Mutant Proteins in the Cytosol

Lourdes R. Desviat, Belén Pérez, and Magdalena Ugarte

1. Introduction

In many cases, the expression analysis of missense alleles renders reduced levels of protein with correspondingly reduced enzymatic activity. These results have been assumed to reflect accelerated degradation owing to instability of incorrectly folded mutant proteins. To test this hypothesis, we describe a simple approach combining in vitro synthesis using a rabbit reticulocyte lysate, with pulse-chase methodology, and analyzing protein turnover by determining the half-lives of normal and mutant proteins. The rabbit reticulocyte lysate is rich in proteases and components of the proteasome and thus is one of the systems commonly used to study the degradation of cytoplasmic proteins ***(1)***.

In our protocol (**Fig. 1**), starting from the cloned cDNA, it is first polymerase chain reaction (PCR)-amplified using a forward primer that introduces a T7 promoter and optimal Kozak translation initiation sequences ***(2,3)***. This modified cDNA is used for in vitro protein synthesis in the presence of labeled methionine and cysteine using a coupled transcription-translation assay. The pulse is stopped with excess cold methionine, Dnase, and RNase and labeled proteins are chased up to 24 h at 37°C and analyzed by sodium dodecyl sulfate polyacrylamide gel electrophoresis (SDS-PAGE) and autoradiography for labeled protein remaining at each time point. The cytosolic protein phenylalanine hydroxylase (PAH) is used as an example to illustrate the methods employed for the investigation of the accelerated proteolytic turnover of mutant proteins

From: *Methods in Molecular Biology, vol. 232: Protein Misfolding and Disease: Principles and Protocols*
Edited by: P. Bross and N. Gregersen © Humana Press Inc., Totowa, NJ

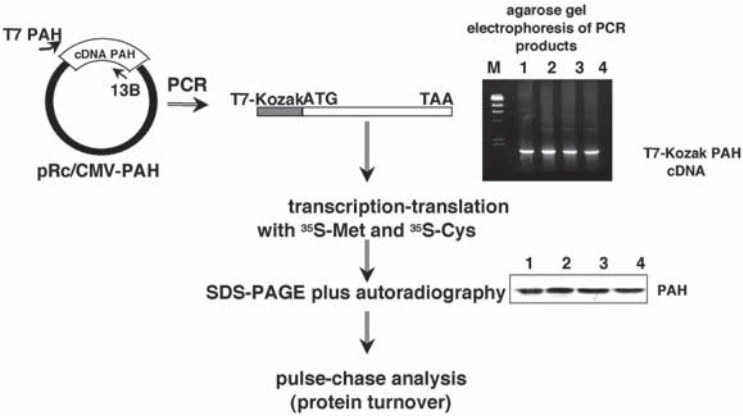

Fig. 1. Schematic diagram of the procedure outlined in this chapter for the in vitro protein synthesis using the TNT-T7 reaction and investigation of mutant protein degradation. Adapted from Promega.

in the cytosol. This enzyme, which catalyses the hydroxylation of phenylalanine to tyrosine, is defective in phenylketonuria (PKU, MIM 261600), with more than 400 mutations described in the *PAH* gene (http://data.mch.mcgill.ca/pahdb_new/), leading to variable degrees of enzyme impairment. In the last few years, many missense PKU mutations have been shown to cause defective folding and subsequent aggregation/degradation as a predominant disease mechanism ***(4,5)***.

2. Materials

1. T7-modified forward primer: The key feature of the amplification of cDNAs in general and the *PAH* cDNA specifically for in vitro synthesis using the TNT-T7 coupled transcription-translation system is a specifically designed, tailed forward primer (*see* **Fig. 2**). The 5' tail contains: (1) a T7 promoter sequence at the 5'-end, which directs the synthesis of RNA using the corresponding phage RNA polymerase; (2) a eukaryotic translation initiation or Kozak sequence, separated by a spacer of 2 bp (AG) from the T7 promoter. In the example, the forward primer further contains 18 bp of the *PAH* cDNA sequence in frame with the ATG codon from the Kozak sequence.
2. Reverse primer: The reverse primer hybridizes with the 3'-UTR *PAH* gene sequence (*see* **Fig. 2**).
3. PAH wild-type and mutant cDNA: Plasmid pRc/CMV-*PAH* comprising *PAH* cDNA was kindly provided by Dr. S.L.C. Woo ***(6)***. Point mutations were introduced in the *PAH* cDNA sequence using the PCR-based Quickchange site-

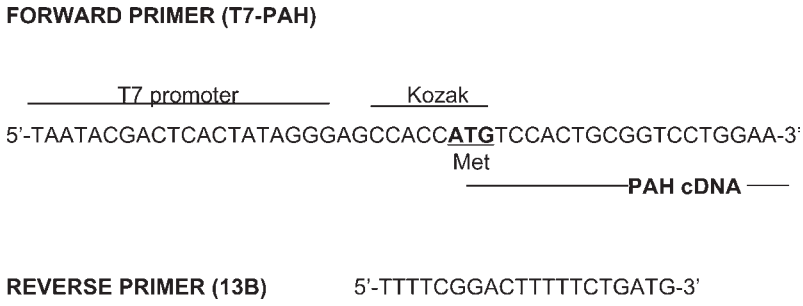

Fig. 2. Oligonucleotide primers used for the amplification of PAH cDNA for in vitro synthesis. The forward primer includes a T7 promoter and Kozak sequences preceding the bases hybridizing with the PAH cDNA sequence immediately downstream of the initiation codon.

directed mutagenesis kit. The presence of the desired mutation was verified by cycle sequencing using the *fmol* DNA Sequencing System with fluorescent Cy5-primers and an automated ALF DNA Sequencer. Plasmid DNA was purified using Concert DNA purification kit.

4. Quikchange site-directed mutagenesis kit (Stratagene, La Jolla, CA).
5. Concert plasmid DNA purification kit (Promega, Madison, WI).
6. *fmol* DNA Sequencing System (Promega) and fluorescent PAH gene primers.
7. Sequencing equipment (ALF DNA Automated Sequencer, Amersham Pharmacia Biotech, Buckinghamshire, UK).
8. PCR reagents: dNTP mix (10 m*M* each dNTP, stored at –20°C), 10m*M* $MgCl_2$.
9. Taq DNA polymerase (Perkin Elmer, Branchburg, NJ).
10. Thermal cycler.
11. Agarose gel electrophoresis equipment, ethidium bromide (EB), UV transilluminator.
12. DNA molecular-weight markers.
13. TNT-T7 coupled transcription-translation system (Promega), stored at –70°C.
14. L-[^{35}S]-methionine + L-[^{35}S]-Cysteine (14,3 mCi/mL) (*Promix* L-[^{35}S] in vitro cell-labeling mix; Amersham Pharmacia Biotech) and appropriate facilities to work with radioactive material.
15. Water bath.
16. L-Methionine: 100 m*M*, stored at –20°C.
17. DNase: 1 mg/mL, stored at –20°C.
18. RNase A: 1 mg/mL, stored at –20°C.
19. SDS sample buffer.
20. SDS-PAGE equipment.
21. Amplify reagent for flurographic detection (Amersham Pharmacia Biotech).
22. Autoradiography equipment.
23. Laser densitometer or Phosphorimager.

3. Methods

The methods described here outline: 1) PCR amplification of *PAH* cDNA using a sense primer that introduces the T7 promoter and Kozak sequences, 2) in vitro synthesis of labeled PAH protein using a rabbit reticulocyte lysate, 3) pulse-chase analysis of normal and mutant PAH proteins. An outline of the technique is schematically shown in **Fig. 1**. An alternative strategy is to clone the cDNA in an expression plasmid having a T7 promoter sequence upstream of the polylinker site and use this directly in the in vitro synthesis reaction (*see* **Note 1**).

3.1. PCR Amplification of PAH cDNA

1. Use 50–100 ng of plasmid DNA in a standard 100 µL PCR reaction *(7)* with 100 pmol of each primer, 200 µ*M* each dNTP, 1.5 m*M* $MgCl_2$, and 2.5 U of Taq polymerase.
2. The PCR amplification program is as follows: 1 cycle with 5 min at 94°C, 3 min at 50°C, and 1 min at 63°C; 40 subsequent cycles of 30 s at 94°C, 30 s at 50°C, and 30 sec at 63°C, and a final 5 min extension at 72°C (*see* **Note 2**).
3. Check an aliquot of the PCR product by standard 1% agarose gel electrophoresis and EB staining using a UV transiluminator *(7)*.
4. Quantify the PCR product by comparison with molecular-weight marker bands.

3.2. In Vitro Synthesis

1. Mix five microliters or 200 ngr of the PCR product (*see* **Note 3**) from the wild-type and mutant cDNAs with 10 µL of the reticulocyte lysate (TNT-T7 reaction mix) and 1 µL [^{35}S]-methionine+ [^{35}S]-cysteine.
2. Incubate 20–60 min at 30°C.
3. Boil samples in SDS buffer and load 2–5 µL on a denaturing polyacrylamide gel *(7)*.
4. After electrophoresis, soak the gel in Amplify reagent for 30 min, dry it, and expose it to an autoradiographic film for 2–24 h.
5. This experiment allows you to set the conditions for the pulse-chase analysis (*see* **Note 4**).

3.3. Pulse-Chase Analysis

After an initial confirmatory experiment of the in vitro synthesis of normal and mutant PAH proteins, pulse-chase analysis is performed to analyze protein turnover in the rabbit reticulocyte extract.

1. Perform a 30 min synthesis reaction with normal and mutant cDNAs as described in **Subheading 3.2.** Depending on the number of time points during the chase and the sample volume loaded on the SDS-PAGE gel, scale up the reaction volumes for each sample (*see* **Note 5**).

2. Stop the synthesis reaction adding 1 μL (per 10 μL reticulocyte lysate used) cold methionine (100 m*M*), 1 μL RNase A (1 mg/mL), and 1 μL DNase (1 mg/mL).
3. Incubate the reaction further at 37°C and remove 2–5 μL aliquots at different time points between 1 and 24 h (*see* **Note 6**).
4. Boil samples in SDS buffer and freeze until gel loading.
5. Separate samples by denaturing PAGE.
6. The labeled PAH protein is detected by fluorography (*see* **step 4** in **Subheading 3.2.)** (**Fig. 3**).
7. Quantitate the labeled protein in each lane by laser densitometry or Phosphorimaging.
8. Represent the data as percentage PAH proteins remaining vs time on a semilogarithmic plot to calculate the half-lives of normal and mutant *PAH* proteins (**Fig. 3**).

4. Notes

1. In some cases, relatively good results are obtained performing the in vitro synthesis reaction directly starting from the cloned cDNA in a vector such as pGEM-3Z (Promega) or any other containing T7 RNA polymerase promoter upstream of the multiple cloning site. This is the method used with the α-subunit of propionyl-CoA carboxylase ***(8)***. However, we have observed improved results when PAH cDNA is amplified with the T7-modified Kozak forward primer, probably owing to a combination of the effect of the proximity of the T7 promoter and the optimized consensus Kozak sequence compared to the natural one.
2. Other PCR programs and different concentrations of primers and PCR reagents can be used, after optimization of the conditions in each case. Care should be taken to include a first cycle with a long hybridization step at relatively low temperature to allow for hybridization of the tailed forward primer.
3. The volume of the PCR reaction used in the in vitro synthesis reaction depends on the efficiency of the amplification. As a general rule, if the PCR amplified band is quantitated, 200–300 ng of cDNA product are sufficient for the synthesis reaction. The same amount of amplified wild-type and mutant cDNAs should be used.
4. The length of the pulse has to be optimized in each case, but, in general, the minimum synthesis time to get a strong signal is 20–40 min.
5. In some cases it is better to perform several individual synthesis reactions for each sample and mix them after the addition of methionine, DNase and RNase for the chase incubation period. We have observed the protein synthesis reaction is sometimes less efficient when we scale up the volumes.
6. The length of the pulse depends on the half-lives in the cytosolic extract of the protein investigated. For PAH mutant proteins, many show reduced half-lives, of 5–6 h compared to 8.7 h of the wild-type protein.
7. The in vitro synthesis approach described may be used in combination with the isolation of functional rat liver mitochondria ***(9)*** to investigate the import and intramitochondrial stability of mitochondrial proteins, as was applied to the α-subunit of propionyl CoA carboxylase ***(8)*** (*see also* Chapter 23, this volume).

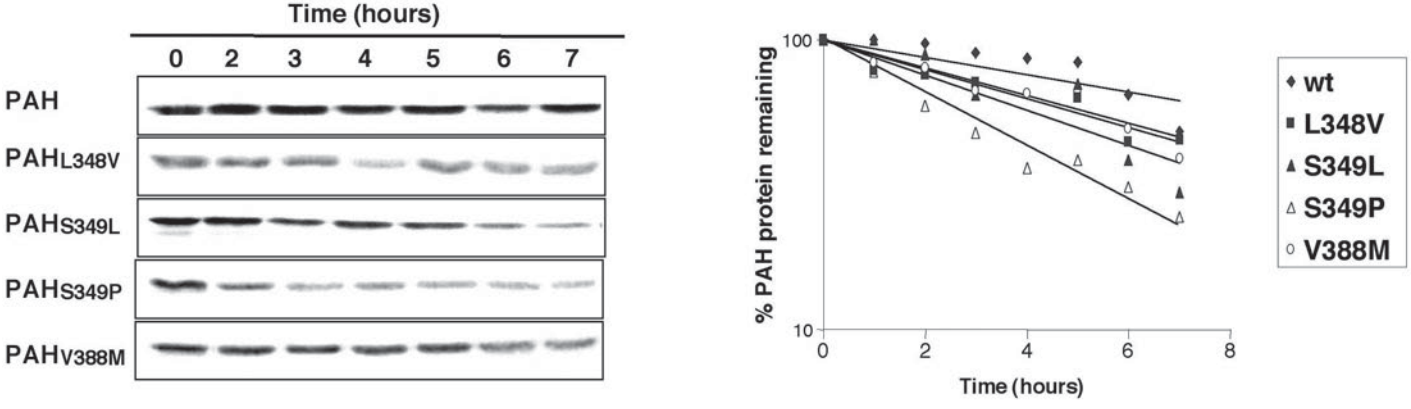

Fig. 3. (**Left**) Autoradiogram of SDS-PAGE analysis of pulse-chased extracts from the coupled in vitro transcription-translation system using wild-type PAH and different point mutants. (**Right**) Semilogarithmic plot of the degradation time courses of wild-type and mutant (L348V, S349L, S349P, and V388M) PAH proteins expressed by coupled in vitro transcription-translation. After pulse-chase, labeled PAH protein in the autoradiogram was quantitated by laser densitometry. Half-lives for the wild-type and mutant proteins were: wild-type, 8.7 h; L348V and V388M, 5.9 h; S349L, 4.9 h; and S349P, 3.1 h.

Acknowledgments

This work was supported by grants from Comisión Interministerial de Ciencia y Tecnología (PM98-003 and SAF2001-0544). The financial support of Fundación Ramón Areces to the Centro de Biología Molecular "Severo Ochoa" is gratefully acknowledged.

References

1. Qu, D., Teckman, J. H., Omura, S., and Perlmutter, D. H. (1996) Degradation of a mutant secretory protein, alpha1-antitrypsin Z, in the endoplasmic reticulum requires proteasome activity. *J. Biol. Chem.* **271,** 22,791–22,795.
2. Lo Ten Foe, J. R., Rooimans, M. A., Bosnoyan-Collins, L., Alon, N., Wijker, M., Parker, L., et al. (1996) Expression cloning of a cDNA for the major Fanconi anaemia gene, FAA. *Nat. Genet.* **14,** 320–323.
3. Sarkar, G. and Sommer, S. S. (1989) Access to a messenger RNA sequence or its protein product is not limited by tissue or species specificity. *Science* **244,** 331–334.
4. Gamez, A., Perez, B., Ugarte, M., and Desviat, L. R. (2000) Expression analysis of phenylketonuria mutations: effect on folding and stability of the phenylalanine hydroxylase protein. *J. Biol. Chem.* **275,** 29,737–29,742.
5. Waters, P. J., Parniak, M. A., Akerman, B. R., Jones, A. O., and Scriver, C. R. (1999) Missense mutations in the phenylalanine hydroxylase gene (*PAH*) can cause accelerated proteolytic turnover of PAH enzyme: a mechanism underlying phenylketonuria. *J. Inherit. Metab. Dis.* **22,** 208–212.
6. Kwok, S. C., Ledley, F. D., DiLella, A. G., Robson, K. J., and Woo, S. L. (1985) Nucleotide sequence of a full-length complementary DNA clone and amino acid sequence of human phenylalanine hydroxylase. *Biochem.* **24,** 556–561.
7. Sambrook, J. and Russell, D. W. (2001) *Molecular Cloning: A Laboratory Manual*. Cold Spring Harbor Laboratory Press, Cold Spring Harbor, NY.
8. Richard, E., Desviat, L. R., Pérez, B., Pérez-Cerdá, C., and Ugarte, M. (1999) Genetic heterogeneity in propionic acidemia patients with α-subunit defects. Identification of five novel mutations, one of them causing instability of the protein. *Biochim. Biophys. Acta* **1453,** 351–358.
9. Loewenstein, J., Scholte, H. R., and Wit-Peeters, E. M. (1970) A rapid and simple procedure to deplete rat-liver mitochondria of lysosomal activity. *Biochim. Biophys. Acta* **223,** 432–436.

22

Investigation of Folding and Degradation of In Vitro Synthesized Mutant Proteins in Microsomes

Alan W. Cuthbert and Will Fuller

1. Introduction

The ability of long polypeptide chains to form correctly folded and functional proteins in the intracellular environment is a complex process, requiring participation of other protein components and biased native-like interactions between residues. Failure to fold correctly can lead to a variety of disease states, in which proteins are deposited in highly organized aggregates or are degraded in the proteasome. Examples of the former are the amyloidoses, such as Alzheimer's disease (AD) and the spongioform encephalopathies, whereas in cystic fibrosis (CF) and some forms of nephrogenic diabetes insipidus, relevant misfolded protein molecules are degraded. Cell-free protein synthesis is used to examine gene expression, membrane insertion into microsomes or mitochondria, early endoplasmic reticulum (ER) folding events, exclusion mechanisms for misfolded proteins, effects of protein synthesis inhibitors, and even for the production of microgram quantities of proteins.

This chapter is concerned with methodology behind the translation of membrane proteins in the rabbit reticulocyte lysate (RRL) in the presence of microsomal membranes, which allow membrane insertion and early ER processing events to occur in a cell-free environment. We will use the example of the CF transmembrane conductance regulator (CFTR), a 12 transmembrane-spanning domain glycoprotein, and discuss the folding of a mutant of CFTR (ΔF508 CFTR) in which a single amino acid deletion leads to retention and degradation of the mutant protein in the ER.

Several types of system are available for cell-free protein synthesis. They are the RRL, wheat germ extract (WGE), and the recently described Xenopus egg extract (XEE) ***(1)***.

From: *Methods in Molecular Biology, vol. 232: Protein Misfolding and Disease: Principles and Protocols*
Edited by: P. Bross and N. Gregersen © Humana Press Inc., Totowa, NJ

The latter has been claimed to have an advantage over the other two in that it contains endoplasmic equivalent microsomes, whereas canine pancreatic microsomes need to be added to RRL and WGE. However the literature on XEE is still limited.

The choice of whether to use RRL or WGE needs careful consideration. Investigators should be aware that identical results may not be obtained using these two systems, although commonly they are so. For example, synthesis of the yeast protein Ure2p in RRL yielded a protein that was more rapidly proteolysed by proteinase K digestion than that synthesized by WGE. The opposite was found when chloramphenicol acetyl-transferase was synthesized in the two systems under identical conditions ***(2)***. Thus the outcome of cell-free protein synthesis depends on the nature of the translation process, the conditions used, and the presence of accessory factors and proteins. In another study, the p53 mutant 143ala was translated in both WGE and RRL. With RRL both the mutant and wild-type conformations were detectable immunologically, but only the former could be co-precipitated with the Hsp90 chaperone protein. Translation in WGE produced only wild-type p53, because this system is known to be deficient in heat-shock protein (Hsp)90. The mutated form of p53 could be formed in WGE if reconstituted to contain Hsp90. In this example the two systems have been used to demonstrate the role Hsp90 in the production of a particular protein ***(3)***.

Some proteins when synthesized in vitro are highly sensitive to proteolysis at the stage before the nascent protein is folded into its appropriate conformation. In another example, the cell-free synthesis of mitochondrial aspartate aminotranferase (pmAspAT) was studied. Synthesis of this protein in RRL gave a trypsin-resistant product that could be imported into mitochondria ***(4)***. In contrast, synthesis of pmAspAT in WGE did not give a trypsin-resistant product, although addition of RRL to the newly synthesized protein restored both folding and import capability. It was concluded that factors present in RRL, but not in WGE, are involved in the release of the nascent protein from Hsc70, with which it initially forms a complex, possibly cotranslationally ***(5)***. Others have studied the early stages of CFTR insertion into membranes using both RRL and WGE supplemented with canine pancreatic microsomes and find this can be achieved in both ***(6)***, but the deficiency in Hsp90 must be kept in mind if WGE is used. Thus in the example we have chosen for this chapter either RRL or WGE are suitable, although we will describe the conditions for RRL.

In simplest terms, the RRL is a protein-producing system: current systems will produce protein rapidly and directly from a circular DNA template. The lysate contains all of the machinery necessary for transcription and translation: RNA polymerase, initiation, and elongation factors; and mammalian ribosomes. Of relevance to membrane proteins, the signal recognition particle

(SRP), which binds to signal sequences on growing peptides to mediate co-translational membrane insertion of these proteins, is also present. The major difference between the RRL and a cellular system is that the superstructure of the cell is missing, including the cytoskeleton, and, of course, any membrane compartments (unless added).

Including a radiolabeled amino acid in a translation reaction radiolabels only the protein whose synthesis is directed by the added cDNA, and therefore this can be detected by separating the lysate mix by sodium dodecyl sulfate polyacrylamide gel electrophoresis (SDS-PAGE), drying the gel and exposing it to a phosphoscreen. Including microsomal membranes in the translation mix results in membrane incorporation and core glycosylation of membrane proteins such as CFTR.

The mechanisms directing translational control, post-translational oligomer assembly, protein folding, and protein degradation can all be examined in such a system. Indeed it was work carried out in such a system that allowed Schumacher and co-workers ***(7)*** to identify the cooperative actions of various molecular chaperones including Hsc70, Hsp90, and eukaryotic homologues of DnaJ such as Hsp40, and to identify the ATP-dependent nature of chaperone-mediated refolding of protein substrates ***(8)***. Prolonged protein synthesis, particularly important if producing tens of micrograms quantities of protein is desired, are best achieved by optimizing the conditions for the ATP generating system ***(9)***. Schumacher et al. ***(7)*** also identify high concentrations of molecular chaperone in the lysate. Hsc70 and Hsp90 are present at approx 50–150 μg/mL, with Hsp90 being twice as abundant. In the translation reactions described in this chapter, this implies that chaperone levels are approx 1–4 μg per 25 μL reaction, and hence that CFTR is translated in a chaperone-rich environment. An example was given earlier showing that WGE was deficient in Hsp90, whereas RRL contains a multiprotein chaperone system consisting of Hsc70 and Hsp90 together with Hop, Hsp40, Hip, p60, and p23. The former two are essential whereas the others are co-chaperones that optimize assembly. For example, in cell-free synthesis of the glucocorticoid receptor, Hop forms a complex Hsp90:Hop:Hsc70, with the stoichiometry 2:1:1, for opening the steroid binding site in the receptor. Note the stoichiometry requires Hsp90 to be more abundant than Hsc70 ***(10)***, the chaperones are found in both the RRL and cellular systems at this ratio, and in concert with the co-chaperones p60 and p23 form a complex sometimes referred to as the "foldosome" ***(11)***.

Renaturation (refolding) of denatured proteins is an ATP- and molecular chaperone-dependent process. For example, depletion of either Hsp90 or Hsc70 from the RRL severely compromises its ability to refold denatured firefly luciferase to a functional conformation ***(8)***. This process also appears to rely on cooperative interactions between the molecular chaperones Hsc70 and Hsp90;

again, both must be present and at a ratio of about 2:1 (Hsp90:Hsc70) for the most efficient protein folding.

Hence, the protein folding activity of the RRL is well characterized, and it has been used to examine the folding of several soluble proteins, including actin ***(12)***, tubulin ***(13,14)***, mitochondrial aspartate aminotransferase ***(4)***, and luciferase ***(15)***, and the membrane protein CFTR ***(16)***. The rich chaperoning environment offered is potentially ideal for the study of the misfolding phenotype of ΔF508 CFTR.

Some aspects of the processing of CFTR in the RRL are well-characterized ***(17–19***; *see also* Chapter 3*)*, and it has been shown to adopt the correct transmembrane structure ***(6)***. Briefly, wild-type and ΔF508 CFTR expression in the RRL produces proteins of identical electrophoretic mobility to unglycosylated CFTR expressed in cellular systems. Addition of microsomal membranes causes a decrease in this mobility owing to a form indistinguishable from glycosylated CFTR in the cell, which is sensitive to endoglycosidase H digestion (band B CFTR ***[17]***). Protease protection assays indicate that the proposed transmembrane structure ***(20)*** is adopted in the RRL ***(6)***. The mechanisms behind the assembly of the N terminus and preliminary transmembrane domain structure of CFTR have also been defined in the RRL ***(18)***. Most importantly, perhaps, the degradation of CFTR by the ubiquitin proteasome pathway has been shown to be intact in the RRL, and to occur at a similar rate to that observed in the cell ***(19)***. Incidentally, in another study ***(21)*** ubiquitination of misfolded proteins was not observed in the WGE system.

About 70% of persons with CF have at least one allele with the ΔF508 mutation. ΔF508 CFTR fails to achieve the stable B-form in the ER; which is the stable core glycosylated form that approx 25% of wild-type protein achieves before export from the ER ***(22,23)***. Therefore, all of the changes in the biogenesis of the protein as a result of the loss of phenylalanine at position 508 are manifested in the ER. Under such circumstances, the simplest and most effective system to study and manipulate the stability of the ΔF508 protein must be an in vitro system. This offers two primary options for examining the stability of the ΔF508 protein: detection of mature glycosylated (band C) protein as a marker of export to the Golgi apparatus in the intact cell, or direct measurement of stable B protein as it is formed in the ER. This chapter is concerned with the latter approach, and the evaluation of the role of the chaperones Hsc70 and Hsp90 in this process.

2. Materials

1. Promega TnT coupled transcription translation system containing rabbit reticulocyte lysate, TnT reaction buffer, T7 RNA polymerase, amino acid mixture (minus methionine), RNasin (ribonuclease inhibitor, 40 U/μL), (Promega, Madison, WI; *see* **Notes 1** and **2**).

2. CFTR cDNA in a suitable expression vector (*see* **Note 3**).
3. Canine pancreatic microsomal membranes (Promega, *see* **Note 4**).
4. Translation grade [^{35}S]-methionine (Amersham, UK or DuPont NEN, Boston, MA) (*see* **Notes 5** and **6**).
5. Cycloheximide (Sigma).
6. Nuclease-free water.
7. 0.5 *M* sucrose in PBS, pH 7.4.
8. RIPA buffer: 50 m*M* Tris-HCl pH 7.5, 150 m*M* NaCl, 1% nonidet P-40, 0.5% sodium deoxycholate, 0.1% SDS.
9. 10 m*M* Tris-HCl, pH 7.5, 0.1% nonidet P-40.
10. Hsp90 immunoprecipitation buffer: 50 m*M* NaCl, 20 m*M* Tris-HCl, pH 7.5, 10 m*M* sodium molybdate, 0.25% TWEEN 20.
11. Hsp90 immunoprecipitation wash buffer: 10 m*M* Tris-HCl pH 7.5, 10 m*M* sodium molybdate, 0.1% nonidet P-40.
12. Apyrase.
13. Triton X-100.
14. Sodium deoxycholate.
15. SDS.
16. $MgCl_2$.
17. Anti-Hsc70 antibody (Stressgen, San Diego, CA, clone 1B5).
18. Anti-Hsp90 antibody (Stressgen, clone 16F1).
19. Protein G sepharose.
20. Sodium molybdate.
21. 2X SDS sample buffer.

3. Methods

3.1. Transcription and Translation

Several variables must be tested before settling on an optimal translation procedure. These include the amount of DNA, microsomal membranes, and [^{35}S]-methionine to add to each reaction; the translation temperature; and the time the reaction should proceed. In some instances it may be necessary to modify the buffer composition to obtain ideal translation. The ideal ionic composition for RRL assays has been studied using a variety of alkali metal chlorides and acetates. Only salts of K^+, Rb^+, and NH_4^+ significantly support translation. The optimum concentration of salts varied being 40 m*M* for NH_4Ac, 80 m*M* for KCl and NH_4Cl, and 100 m*M* for RbCl and KAc ***(24)***.

3.1.1. Reagents

Final reaction volumes can be 25 µL upwards. Typically, it is necessary to use 5 µL of a reaction on an SDS-PAGE mini-gel to see a good signal for CFTR following 16–24 h exposure to a phosphoscreen. Unless more than five samples are required for analysis we routinely use a 25 µL reaction volume.

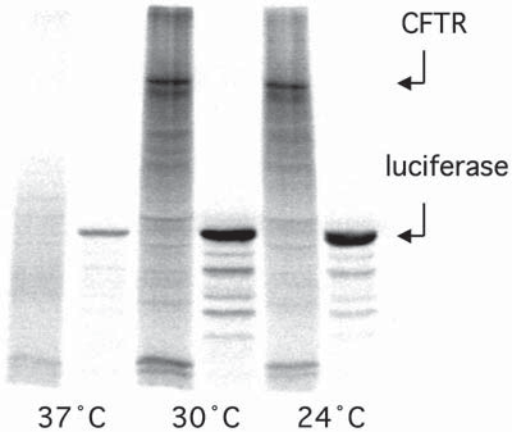

Fig. 1. Comparison of translation temperatures for luciferase and CFTR. Note that little luciferase and no CFTR is produced at 37°C for 45 min; however, at 30°C for 90 min and 24°C for 120 min, translation of both proteins is equally efficient.

The required amount of DNA and microsomal membranes are added to the RRL (*see* **Note 2**). Transcription and translation occur in the same tube. Translation may be halted at any point by the addition of 100 μg/mL cycloheximide (if post-translational events are to be studied) or 2X SDS PAGE sample buffer (for immediate analysis).

3.1.2. Reaction Temperature

Translation does not occur efficiently at 37°C in the RRL owing to dissociation of the ribosome complex leading to premature release of the nascent polypeptide. We have evaluated transcription and translation conditions for both CFTR and luciferase of 37°C for 45 min, 30°C for 90 min, and 24°C for 120 min (**Fig. 1**). The higher the temperature, the more is the cotranslational ubiquitination of CFTR (*see* **Subheading 3.2.2.**). Optimal expression of CFTR is achieved at 24°C, for 120 min. Other membrane proteins may be optimally translated under different conditions. Optimization is best carried out in the absence of microsomal membranes, to preserve reagents (*see* **Note 7**). Clearly, given that CFTR has 36 methionine residues, significantly less CFTR protein is made compared to luciferase. This is typically the case with complex hydrophobic membrane proteins. However, we are unable to improve expression even with increased translation times.

3.1.3. Plasmid Design and Concentration

Some features of plasmid design are discussed in **Note 3**. The most important feature is the presence of a KOZAK sequence (consensus A/GCCATGG,

where ATG is the first methionine codon of the cDNA) to optimize binding of the mRNA to the ribosome. It is possible to translate more than one protein from a single mRNA, as long as an internal ribosome entry site (IRES) precedes the second coding sequence. It is not necessary to cap mRNA: the RRL translates uncapped mRNA.

Plasmid DNA produced by alkaline lysis of bacteria (so called mini-prep) is generally sufficiently clean for expression in the RRL. However, it is important that all residual ethanol is removed because this will disrupt translation, and the DNA must be dissolved in nuclease-free water. It is not necessarily the case that the more DNA is added the more protein is produced. This should be optimized over the range 0.1–2 μg per 25 μL reaction. In our hands, optimal expression is achieved with 0.5 μg DNA per reaction.

3.1.4. How Much Microsomes?

CFTR possesses two putative *N*-linked glycosylation sites in the fourth extracellular loop. In general, increasing the amount of microsomal membranes added to a reaction increases the proportion of polypeptides translocated into vesicles, but decreases the total number of polypeptides synthesized. Up to 50% less protein may be expressed in the presence of the membranes. Hence it is necessary to strike a balance between processing and inhibition of translation. Between 0.3 μL and 3 μL of microsomal membranes may be added to a reaction. We find optimal processing when 1.5 μL is used in a 25 μL reaction (**Fig. 2**).

3.1.5. How Much Radiolabeled Amino Acid?

It is important that no reagents are present in rate-limiting amounts in the translation mix. However, given the significantly lower expression of CFTR compared to proteins such as luciferase (*see* **Subheading 3.1.2.**), it is necessary to use only 1 μL [^{35}S]-methionine per 25 μL reaction. Other proteins that may be expressed at higher levels by the RRL may require more.

3.1.6. Typical Reaction

The following reaction applies to the Promega TnT coupled transcription/translation system (*see* **Note 2**):

12.5 μL rabbit reticulocyte lysate.
1 μL TnT reaction buffer.
0.5 μL T7 RNA polymerase.
0.5 μL amino acid mixture (minus methionine).
1 μL [^{35}S]-methionine.
0.5 μL RNasin (ribonuclease inhibitor, 40 U/μL).
0.5 μL plasmid DNA (1 μg/μL in nuclease free water).

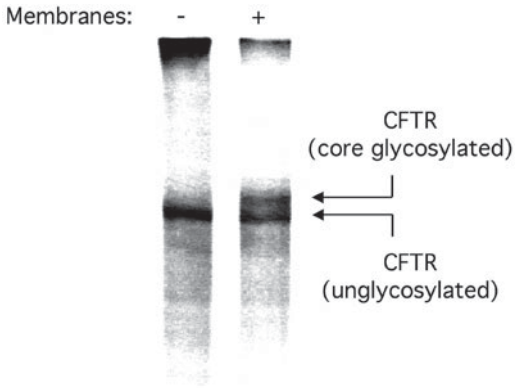

Fig. 2. Addition of microsomal membranes causes core glycosylation of CFTR. Addition of 1.5 μL microsomal membranes to the translation mix results in an increase in molecular weight of approx 5–6 kDa, consistent with two N-linked glycosylation events.

1.5 μL canine pancreatic microsomal membranes.
7 μL nuclease-free water.

Translate for 120 minutes at 24°C.

3.2. Post-Translational Events

3.2.1. Isolation of Membrane-Associated Proteins Through a Sucrose Cushion

If the molecular weight of a protein changes when it is inserted into microsomal membranes (for example, through glycosylation), one can readily distinguish successful insertions from uninserted polypeptides (for example, *see* **Fig. 2**). However, not all proteins are as easily identified as having been inserted successfully into the membrane. Measuring the stability of, or association of membrane-associated proteins with, molecular chaperones requires a homogeneous and membrane-associated starting material. If membrane-associated proteins cannot be distinguished from folding "accidents" in the RRL by their migration on SDS-PAGE, then the membranes (and associated proteins) must be isolated for analysis by themselves.

We have isolated membrane-incorporated proteins by centrifugation of the microsomal membranes through a sucrose cushion. When these proteins are resuspended in fresh RRL (identical in composition to the RRL in which they were translated), their characteristics are identical to those of membrane-associated proteins that have not been centrifuged.

Gently overlay samples of lysate onto 0.5 mL of 0.5 *M* sucrose in PBS, pH 7.4, at 4°C in reinforced microfuge tubes. Spin at 125,000*g* at 4°C for 15 min in a Beckman benchtop ultracentrifuge. The extracted microsomal membranes appear as a diffuse pellet following the spin (*see* **Note 8**).

3.2.2. Ubiquitination

Degradation of CFTR in the RRL (and the cell) is by ubiquitination ***(25,26)***. Ubiquitin monomers are attached to lysine residues on the polypeptide, and this targets it for proteolytic degradation by the 26S proteasome ***(27,28)***. Usually, multiple ubiquitin molecules are added to a protein substrate: multimeric chains of up to 20 ubiquitin monomers are formed, which can be added at multiple sites on the substrate ***(29,30)***.

Addition of ubiquitin retards the progress of CFTR through an SDS-PAGE minigel (**Fig. 3**). This does not necessarily reflect the true molecular weight of the polyubiquitinated protein; its mobility through the gel suggests a molecular weight of several hundred kDa. All CFTR is ubiquitinated at 37°C in the RRL, including incompletely translated protein (everything lower in molecular weight than core glycosylated CFTR). This high molecular-weight material is immunoprecipitated by an anti-ubiquitin antibody (**Fig. 3B**). The polyubiquitinated protein is not degraded by the RRL because the lysate contains hemin (20 μ*M*), which is required for optimal translation ***(31)***. Hemin is also a potent inhibitor of proteasomal activity ***(32)***, hence proteins expressed in the RRL can be ubiquitinated, but not degraded by the proteasome.

3.2.3. Formation of Stable B CFTR

Stable B CFTR is the stable form of the protein in the ER, which is competent for export to the Golgi apparatus and hence to the cell surface. It is formed with approx 25% efficiency in the cell. Wild-type CFTR does not form stable B in the RRL at 37°C (**Fig. 3A**). Indeed, few events occur efficiently at 37°C in the RRL. CFTR is co-translationally ubiquitinated in the RRL at 37°C ***(19)***, and translation is inefficient (**Fig. 1**). At a post-translational temperature of 30°C, wild-type CFTR does form stable B, with approx 25% efficiency. This is shown in **Fig. 4A**. All ΔF508 CFTR is ubiquitinated at this temperature: mean data for wild-type and mutant CFTR are shown in **Fig. 4B**.

We regard 30°C as the ideal temperature at which to use the RRL to examine protein-folding events. Only at this temperature does it appear to mimic the cell at 37°C. Why this may be is open to question. The lower temperature may allow a protein complex such as the "foldosome" to assemble and operate efficiently, whereas it cannot at 37°C. At 30°C, some amount of ordering may be possible either in the lysate, the added microsomal membranes, or the polypep-

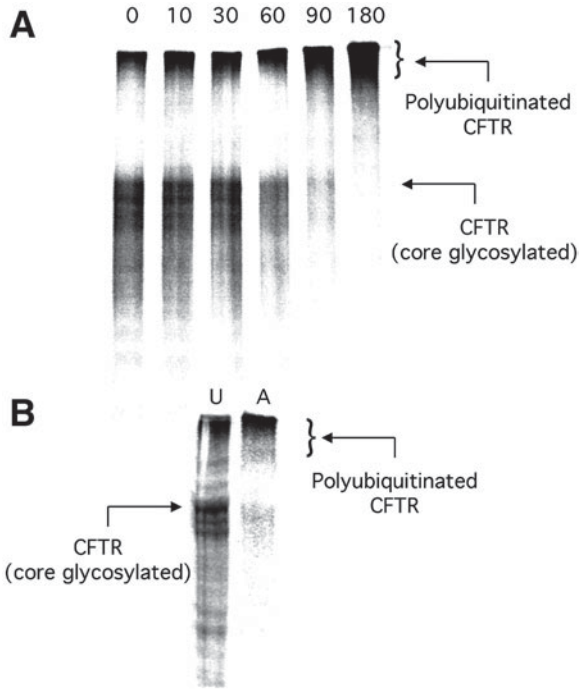

Fig. 3. CFTR is ubiquitinated in the RRL after incubation at 37°C. (**A**) shows the effect of incubating nascent CFTR at 37°C for the times indicated above the lanes (min) after translation. Polyubiquitinated CFTR is not degraded by the RRL. (**B**) shows immunoprecipitation of ubiquitin from the RRL with an anti-ubiquitin antibody. Lane U is material unassociated with ubiquitin, lane A is material associated with ubiquitin. Not all ubiquitin is immunoprecipitated by this protocol. The high molecular-weight material in lane A is polyubiquitinated CFTR.

tide chain of CFTR that leads to stable B being favored. Whatever the explanation, we would recommend that all folding events, regardless of the protein, be examined in the RRL at 30°C.

3.2.4. Addition of Drugs: Co-Translational and Post-Translational

The effect of drugs on the stability of the protein can readily be examined in the RRL. Because there is no cell membrane to cross, one can be confident that the concentration of drug seen by the polypeptide is indeed what is intended. In this way the effect of drugs on polypeptide stability may be assessed when the drug is present only post-translationally (add the drug after adding cycloheximide to halt translation), only co-translationally (translate in the presence of the drug, isolate membrane associated protein as described in **Subheading 3.2.1.**, and resuspend in fresh RRL), or both co- and post-translationally. In the

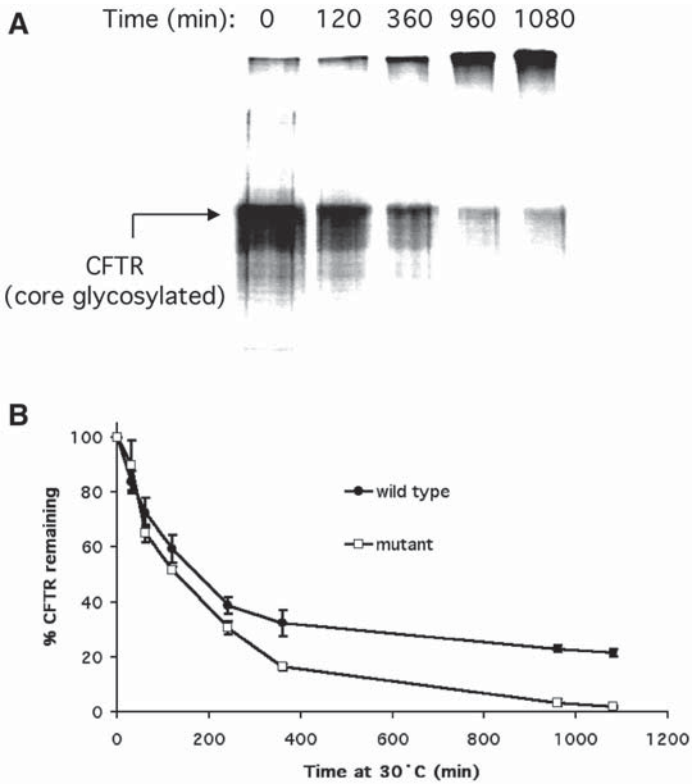

Fig. 4. Wild-type but not ΔF508 CFTR forms stable B at 30°C in the presence of microsomes. (**A**) shows a typical gel for wild type CFTR incubated at 30°C for the times indicated above the lanes. Approximately 20% of the wild-type protein is stable with respect to ubiquitination at this temperature. Mean data for wild type and mutant CFTR are shown in (**B**) (standard errors for *n* of at least four separate observations).

case of CFTR, we have assessed the effect of several drugs on the stability of the polypeptide. Stability in this case refers to the resistance of the polypeptide to ubiquitination (*see* **Subheading 3.2.2.**), and its association with molecular chaperones (*see* **Subheading 3.2.5.**).

Chemical chaperones are osmolytes, thought to stabilize protein structure, and are reported to stabilize ΔF508 CFTR in cellular systems ***(33,34)***. However, chemical chaperones by their very nature must be present at high concentrations (>1mol/L) to be effective, because they enhance stability by modifying protein hydration through changes in hydrogen bonding at the surface of protein molecules. The RRL is a very sensitive system, and does not tolerate the addition of drugs at such high concentrations. However, drugs binding to endogenous chaperones are active in the μmol/L range. Chaperone-binding

drugs such as geldanamycin, which binds to Hsp90, and 15-deoxyspergualin, which inhibits Hsc70, may be used to dissect the role of these chaperones in the folding of proteins in the RRL. We have used geldanamycin (11 μg/mL) to disrupt Hsp90 function in the RRL, and found that ΔF508 CFTR achieves a form analogous to stable B if the drug is added post-translationally, but not if it is present co-translationally ***(16)***. This implies that co-translational binding of Hsp90 to CFTR is necessary for the protein to reach a stable (and presumably correctly folded conformation), but that post-translational binding of the chaperone is associated with ubiquitination of CFTR.

The use of chaperone-binding drugs in the RRL, and the ability to restrict their presence to only co-translational or only post-translational, is an extremely powerful technique. The roles of the major molecular chaperones and their partners in mediating both protein folding and degradation can readily be assessed. Through immunoprecipitation of molecular chaperones from the lysate, their cooperative actions can be examined (**Subheading 3.2.5.**).

3.2.5. Immunoprecipitation of Molecular Chaperones

Achievement of the correctly folded state of a protein, which is stable with respect to degradation, can be detected most easily by SDS-PAGE analysis of the entire RRL at various times following the cessation of translation. However, another indication that this stable state has been reached is the release of the nascent protein from the molecular chaperones that are assisting folding. Immunoprecipitation of the chaperones Hsc70 and Hsp90 from the RRL following translation, and measurement of association with CFTR indicates whether part or all of the synthesized protein has been released. Release of substrate from the chaperones indicates folding is complete.

Chaperone proteins are immunoprecipitated from 10 μL aliquots of RRL under conditions that favor their continued association with substrate. Release of substrate from Hsc70 requires ATP binding, hence depletion of ATP throughout the immunoprecipitation "locks" Hsc70 in its substrate-bound state ***(35)***. Deplete ATP by adding 10 U/mL apyrase and incubating at 4°C in 0.1% Triton X-100, 5 mmol/L $MgCl_2$ for 15 min. Adjust the composition to 1% TX-100, 1% sodium deoxycholate, and 0.1% SDS; preclear the samples; and add 1 μg of anti-Hsc70 antibody (Stressgen, clone 1B5). After 2 h, harvest immune complexes with protein G sepharose by incubating for a further 2 h. Wash the beads twice for 5 min each in RIPA buffer, then once in 10 mmol/L Tris-HCl, pH 7.5, 0.1% nonidet P-40 for 20 min. This protocol yields two fractions: unassociated with Hsc70 (U), and associated with Hsc70 (A), which are shown in Fig. 5. The substrates shown in the gel in **Fig. 5A** is wild-type CFTR. Wild-type CFTR but ΔF508 CFTR is released by Hsc70 over the time shown (**Fig. 5B**). Release of CFTR by Hsc70 coincides with the cessation of ubiquitination

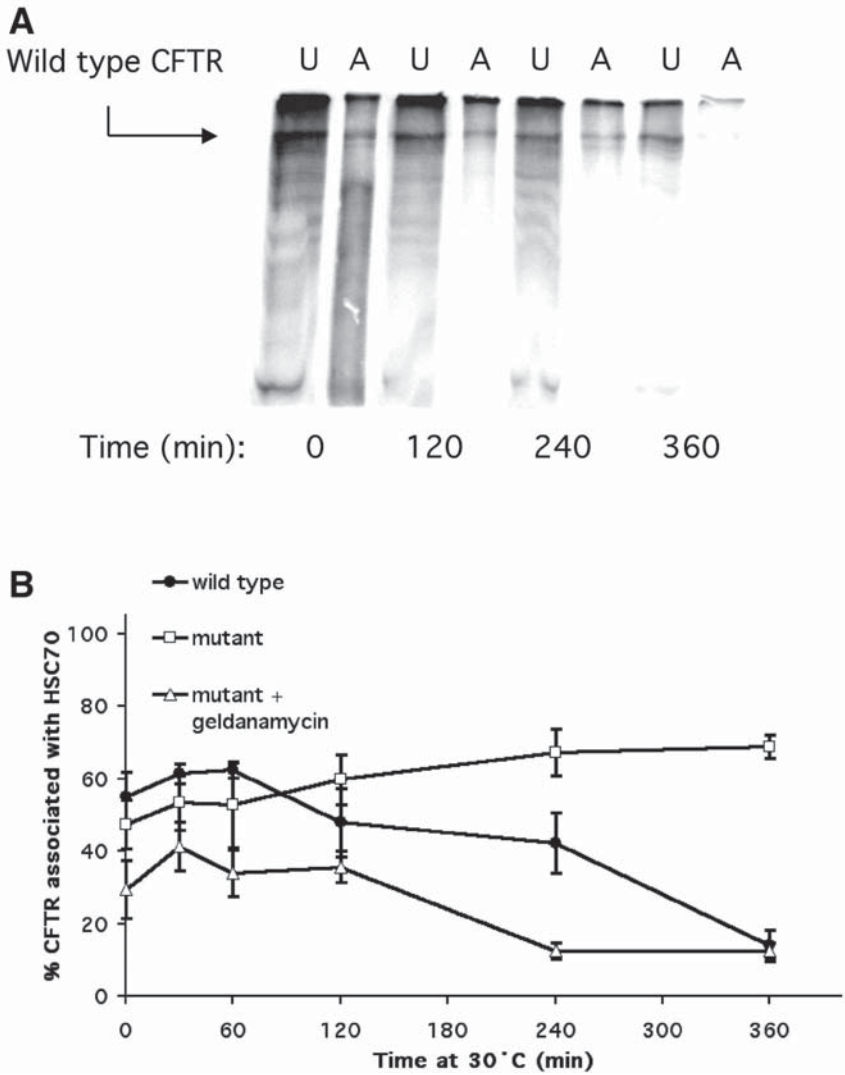

Fig. 5. Association of Hsc70 with wild-type and mutant CFTR. Immunoprecipitations are shown at various times after translation was halted. (**A**) shows a typical gel assessing association of Hsc70 with wild-type CFTR, following immunoprecipitation with an anti-Hsc70 antibody. Lanes U are protein not immunoprecipitated with Hsc70, lanes A are associated with Hsc70. (**B**) shows the change in the percentage of CFTR associated with Hsc70 over time. In the case of the wild-type protein, the proportion associated with Hsc70 reduces over time, as a stable and completely folded conformation is reached. ΔF508 CFTR cannot reach this conformation, so 6 h after translation is halted a high proportion is still bound to the chaperone (standard errors are for *n* of at least six separate observations).

of the protein, implying a role for this chaperone in mediating ubiquitination as well as folding of nascent proteins. Note that in **Fig. 5** polyubiquitinated CFTR is associated with Hsc70. Furthermore, addition of the Hsp90 binding agent geldanamycin to the mutant protein immediately after translation gradually reduces the association of this protein with Hsc70, indicating these chaperones are working cooperatively in the RRL ***(16)***.

Both phosphate-containing buffers and harsh detergent conditions disrupt the interaction between Hsp90 antibodies, Hsp90, and Hsp90 substrates. Hence milder conditions are used when immunoprecipitating Hsp90. Include 10 mmol/L sodium molybdate throughout in both lysis and wash buffers, because the molybdate ion stabilizes the interaction between Hsp90 and its substrates ***(36)***. Hsp90 immunoprecipitation buffer is 50 mmol/L NaCl, 20 mmol/L Tris-HCl, pH 7.5, 10 mmol/L sodium molybdate, 0.25% TWEEN 20. Preclear, then immunoprecipitate with 1 μg of anti-Hsp90 antibody (Stressgen, clone 16F1), following a similar protocol to that described in the previous paragraph for Hsc70, albeit using the milder detergent conditions described. After adsorption of antigen-antibody complexes, wash beads twice for 5 min and once for 20 min with immunoprecipitation wash buffer (*see* **Note 9**).

3.3. Analysis and Quantification

3.3.1. Quantification

High-quality digital images are obtained by exposing minigels to phosphoscreens after drying them. This generates images considerably more quickly than exposure to conventional films. In addition, the linear range of a phosphoscreen is considerably larger than any hyperfilm. This is crucial if large variations in band intensity are to be quantified from a single gel. Typically, exposing to the phosphoscreens overnight at room temperature gives images equivalent to several days exposure to hyperfilm at –70°C. Phosphoscreens are scanned and analyzed using the Molecular Dynamics ImageQuant system. Accurate quantification of bands on minigels is clearly essential. Inevitably when using the RRL, there are a considerable number of bands of lower molecular weight than the core glycosylated protein of interest. These represent both unglycosylated protein, and glycosylated protein that is not full-length. When quantitating core glycosylated CFTR, it is crucial that the investigator excludes these spurious bands. Hence, care must be taken both in drawing a baseline, and selecting the correct peak to quantify following densitometric analysis of a particular lane.

4. Notes

1. Even the most efficient RRLs will show batch-to-batch and even day-to-day variability. For this reason it is unwise to compare expression levels obtained on

different days. It is also important to test each new batch of RRL and microsomal membranes for activity before extensive use. It is common to find significant differences between batches.

2. In our experience the most suitable RRL is the TnT system sold by Promega. This offers the highest quality in terms of reproducibility and chaperone concentrations. Promega offer two types of RRL for sale: quick-coupled (e.g., L1170), or simply coupled (e.g., L4610). We have been unable to achieve significant expression of CFTR using the quick-coupled system (which is provided with all components for transcription and translation already added to the lysate). Best expression is achieved using the coupled system: use the amounts of the reagents recommended by the manufacturer. The RRL is provided in 200 μL aliquots; we routinely add the necessary amounts of amino acid, T7 RNA polymerase, reaction buffer, and RNase inhibitor RNasin (Promega) to an entire 200 μL aliquot, and divide this into 15 μL aliquots for storage at –70°C. This avoids freeze-thaw cycles (the lysate must not be freeze-thawed more than twice). When the time comes, add the required amount of DNA, radiolabeled amino acid, and microsomal membranes to a 15 μL aliquot, make the final volume up to 25 μL, and start the reaction.
3. Most expression vectors with a T7 promoter upstream of the cDNA give some expression. We noted over 10-fold variations in protein yield for the same cDNA using different plasmids (**Fig. 6**). In our hands, satisfactory expression is achieved with CFTR cDNA in both the pSP73 and pSI plasmids from Promega. Insertion of a run of 30 adenine residues immediately downstream of the cDNA (to give an artificial poly A tail on transcription) increases expression from the pSP73 backbone twofold (presumably through increasing the stability of the mRNA). Deleting a small part of the 3' untranslated region of the cDNA increases expression approx sevenfold from the pSI backbone, probably because some element in this region caused the mRNA to be destabilized. Hence it is worth testing several vectors before settling on one that gives the highest levels of expression. The amount of protein (particularly full-length membrane proteins) produced in the system is inevitably low, and it is best to start with the best vector possible.
4. Microsomal membranes (Promega Y4041) should be aliquoted and stored at –70°C.
5. The radiolabeled amino acid used must be of translation grade. Amersham and DuPont NEN are suitable suppliers. Methionine, leucine, or cysteine are suitable amino acids to choose to have radiolabeled. Unless there are very few in your protein of interest, methionine is probably the best choice. However, it is very susceptible to oxidation and must be stored in small aliquots at –70°C and freeze-thawed as few times as possible. Oxidation leads to the formation of sulfoxides, which inhibit translation in the RRL. Do not use after one half-life has passed.
6. Nonradioactive detection systems are available from Promega. One such (Transcend; L5070) uses biotinylated lysine residues, which are incorporated during translation and subsequently detected using streptavidin linked to alkaline phosphatase or horseradish peroxidase (HRP). Although the sensitivity of such a system is equivalent in sensitivity to using a radiolabeled amino acid, it may be unsuitable for studying folding and degradation of proteins such as CFTR, which

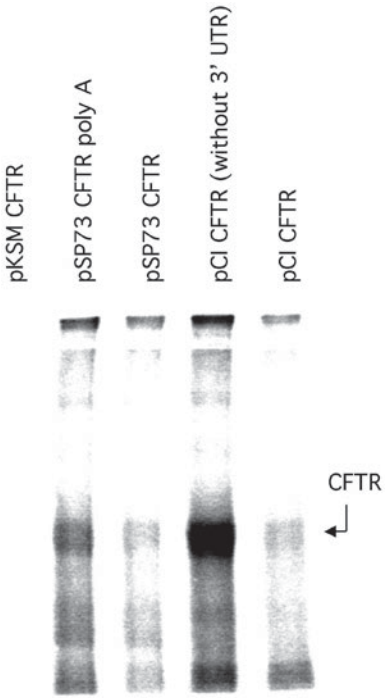

Fig. 6. Expression of CFTR in the RRL derived from various different vector backbones. Identical (0.5 μg) amounts of DNA were translated. Approximate band density ratios (reading left to right) are 0:2:1:7:1.

are degraded by the ubiquitin-proteasome pathway. Ubiquitination occurs at lysine residues in the polypeptide chain, and this may be disrupted if the lysines are already biotinylated.

7. In the absence of microsomal membranes, translation of some membrane proteins is poor ***(17)***. This probably represents translational arrest as a result of SRP binding to its recognition sequence as it emerges from the ribosome, a phenomenon overcome by the addition of 0.5% TX-100, which dissociates the SRP-recognition sequence complex.
8. Caution must be exercised when spinning radioactive material in an ultracentrifuge. The chamber of the centrifuge will be under vacuum. If seals fail or samples are inadvertently spilled, the rotor, vacuum pump, and ultimately the whole area surrounding the centrifuge will be contaminated. Ensure the rotor, all o-rings and the centrifuge itself are well-maintained, and vacuum grease is applied where necessary.
9. Because the RRL offers such a rich chaperoning environment, it is difficult to immunoprecipitate all of a particular chaperone without using large amounts of antibody. In addition, one cannot assume that the antibody used has an equal

affinity for the chaperone in its substrate-bound and substrate-free states. Hence it is difficult to estimate the absolute amount of substrate that is associated with a particular chaperone at a particular time. Nevertheless, the proportions bound and free can be estimated. Rather than attempt to immunoprecipitate all the molecular chaperones in a translation reaction, we prefer to conserve antibody, and therefore simply estimate the proportion of a substrate that is chaperone-associated at different times.

10. To ensure that translation is complete, and that full-length protein has been produced, immunoprecipitate the translated protein with an antibody specific for the final residues of the C terminus. In the case of CFTR, we use Genzyme anti-CFTR clone 2503-01.

Acknowledgments

Work reported in this chapter was supported by a grant from the Wellcome Trust (044441/Z/95/Z) and the Leverhulme Trust.

References

1. Zhou, X., Tsuda, S., Bala, N., and Arakaki, R. F. (2000) Efficient translocation and processing with Xenopus egg extracts of proteins synthesized in rabbit reticulocyte lysate. *In Vitro Cell Dev. Biol. Anim.* **36,** 293–298.
2. Komar, A. A., Lesnik, T., Cullin, C., Guillemet, E., Ehrlich, R., and Reiss, C. (1997) Differential resistance to proteinase K digestion of the yeast prion-like (Ure2p) protein synthesized in vitro in wheat germ extract and rabbit reticulocyte lysate cell-free translation systems. *FEBS Lett.* **415,** 6–10.
3. Blagosklonny, M. V., Toretsky, J., Bohen, S., and Neckers, L. (1996) Mutant conformation of p53 translated in vitro or in vivo requires functional Hsp90. *Proc. Natl. Acad. Sci. USA* **93,** 8379–8383.
4. Mattingly, J. R., Jr., Youssef, J., Iriarte, A., and Martinez-Carrion, M. (1993) Protein folding in a cell-free translation system. The fate of the precursor to mitochondrial aspartate aminotransferase. *J. Biol. Chem.* **268,** 3925–3937.
5. Lain, B., Iriarte, A., and Martinez-Carrion, M. (1994) Dependence of the folding and import of the precursor to mitochondrial aspartate aminotransferase on the nature of the cell-free translation system. *J. Biol. Chem.* **269,** 15,588–15,596.
6. Chen, M. and Zhang, J. T. (1996) Membrane insertion, processing, and topology of cystic fibrosis transmembrane conductance regulator (CFTR) in microsomal membranes. *Mol. Membr. Biol.* **13,** 33–40.
7. Schumacher, R. J., Hansen, W. J., Freeman, B. C., Alnemri, E., Litwack, G., and Toft, D. O. (1996) Cooperative action of Hsp70, Hsp90, and DnaJ proteins in protein renaturation. *Biochemistry* **35,** 14,889–14,898.
8. Schumacher, R. J., Hurst, R., Sullivan, W. P., McMahon, N. J., Toft, D. O., and Matts, R. L. (1994) ATP-dependent chaperoning activity of reticulocyte lysate. *J. Biol. Chem.* **269,** 9493–9499.

9. Kawarasaki, Y., Nakano, H., and Yamane, T. (1994) Prolonged cell-free protein synthesis in a batch system using wheat germ extract. *Biosci. Biotechnol. Biochem.* **58,** 1911–1913.
10. Murphy, P. J., Kanelakis, K. C., Galigniana, M. D., Morishima, Y., and Pratt, W. B. (2001) Stoichiometry, abundance, and functional significance of the hsp90/hsp70-based multiprotein chaperone machinery in reticulocyte lysate. *J. Biol. Chem.* **276,** 30,092–30,098.
11. Hutchison, K. A., Dittmar, K. D., and Pratt, W. B. (1994) All of the factors required for assembly of the glucocorticoid receptor into a functional heterocomplex with heat shock protein 90 are preassociated in a self-sufficient protein folding structure, a "foldosome". *J. Biol. Chem.* **269,** 27,894–27,899.
12. Gao, Y., Thomas, J. O., Chow, R. L., Lee, G. H., and Cowan, N. J. (1992) A cytoplasmic chaperonin that catalyzes beta-actin folding. *Cell* **69,** 1043–1050.
13. Yaffe, M. B., Farr, G. W., Miklos, D., Horwich, A. L., Sternlicht, M. L., and Sternlicht, H. (1992) TCP1 complex is a molecular chaperone in tubulin biogenesis. *Nature* **358,** 245–248.
14. Gao, Y., Vainberg, I. E., Chow, R. L., and Cowan, N. J. (1993) Two cofactors and cytoplasmic chaperonin are required for the folding of alpha- and beta-tubulin. *Mol. Cell. Biol.* **13,** 2478–2485.
15. Nimmesgern, E. and Hartl, F. U. (1993) ATP-dependent protein refolding activity in reticulocyte lysate. Evidence for the participation of different chaperone components. *FEBS Lett.* **331,** 25–30.
16. Fuller, W. and Cuthbert, A. W. (2000) Post-translational disruption of the delta F508 cystic fibrosis transmembrane conductance regulator (CFTR)-molecular chaperone complex with geldanamycin stabilizes delta F508 CFTR in the rabbit reticulocyte lysate. *J. Biol. Chem.* **275,** 37,462–37,468.
17. Gregory, R. J., Cheng, S. H., Rich, D. P., Marshall, J., Paul, S., Hehir, K., et al. (1990) Expression and characterization of the cystic fibrosis transmembrane conductance regulator. *Nature* **347,** 382–386.
18. Lu, Y., Xiong, X., Helm, A., Kimani, K., Bragin, A., and Skach, W. R. (1998) Co- and posttranslational translocation mechanisms direct cystic fibrosis transmembrane conductance regulator N terminus transmembrane assembly. *J. Biol. Chem.* **273,** 568–576.
19. Sato, S., Ward, C. L., and Kopito, R. R. (1998) Cotranslational ubiquitination of cystic fibrosis transmembrane conductance regulator in vitro. *J. Biol. Chem.* **273,** 7189–7192.
20. Riordan, J. R., Rommens, J. M., Kerem, B., Alon, N., Rozmahel, R., Grzelczak, Z., et al. (1989) Identification of the cystic fibrosis gene: cloning and characterization of complementary DNA. *Science* **245,** 1066–1073.
21. Iwamuro, S., Saeki, M., and Kato, S. (1999) Multi-ubiquitination of a nascent membrane protein produced in a rabbit reticulocyte lysate. *J. Biochem. (Tokyo)* **126,** 48–53.
22. Lukacs, G. L., Mohamed, A., Kartner, N., Chang, X. B., Riordan, J. R., and Grinstein, S. (1994) Conformational maturation of CFTR but not its mutant counterpart (delta F508) occurs in the endoplasmic reticulum and requires ATP. *EMBO J.* **13,** 6076–6086.

23. Ward, C. L. and Kopito, R. R. (1994) Intracellular turnover of cystic fibrosis transmembrane conductance regulator. Inefficient processing and rapid degradation of wild-type and mutant proteins. *J. Biol. Chem.* **269,** 25,710–25,718.
24. Hempel, R., Schmidt-Brauns, J., Gebinoga, M., Wirsching, F., and Schwienhorst, A. (2001) Cation radius effects on cell-free translation in rabbit reticulocyte lysate. *Biochem. Biophys. Res. Commun.* **283,** 267–272.
25. Jensen, T. J., Loo, M. A., Pind, S., Williams, D. B., Goldberg, A. L., and Riordan, J. R. (1995) Multiple proteolytic systems, including the proteasome, contribute to CFTR processing. *Cell* **83,** 129–135.
26. Ward, C. L., Omura, S., and Kopito, R. R. (1995) Degradation of CFTR by the ubiquitin-proteasome pathway. *Cell* **83,** 121–127.
27. Ciechanover, A. (1994) The ubiquitin-proteasome proteolytic pathway. *Cell* **79,** 13–21.
28. Hochstrasser, M. (1995) Ubiquitin, proteasomes, and the regulation of intracellular protein degradation. *Curr. Opin. Cell Biol.* **7,** 215–223.
29. Chau, V., Tobias, J. W., Bachmair, A., Marriott, D., Ecker, D. J., Gonda, D. K., and Varshavsky, A. (1989) A multiubiquitin chain is confined to specific lysine in a targeted short-lived protein. *Science* **243,** 1576–1583.
30. Deveraux, Q., Ustrell, V., Pickart, C., and Rechsteiner, M. (1994) A 26 S protease subunit that binds ubiquitin conjugates. *J. Biol. Chem.* **269,** 7059–7061.
31. Gross, M. (1980) The control of protein synthesis by hemin in rabbit reticulocytes. *Mol. Cell. Biochem.* **31,** 25–36.
32. Haas, A. L. and Rose, I. A. (1981) Hemin inhibits ATP-dependent ubiquitin-dependent proteolysis: role of hemin in regulating ubiquitin conjugate degradation. *Proc. Natl. Acad. Sci. USA* **78,** 6845–6848.
33. Brown, C. R., Hong-Brown, L. Q., Biwersi, J., Verkman, A. S., and Welch, W. J. (1996) Chemical chaperones correct the mutant phenotype of the delta F508 cystic fibrosis transmembrane conductance regulator protein. *Cell Stress Chap.* **1,** 117–125.
34. Sato, S., Ward, C. L., Krouse, M. E., Wine, J. J., and Kopito, R. R. (1996) Glycerol reverses the misfolding phenotype of the most common cystic fibrosis mutation. *J. Biol. Chem.* **271,** 635–638.
35. Beckmann, R. P., Mizzen, L. E., and Welch, W. J. (1990) Interaction of Hsp 70 with newly synthesized proteins: implications for protein folding and assembly. *Science* **248,** 850–854.
36. Hutchison, K. A., Stancato, L. F., Jove, R., and Pratt, W. B. (1992) The protein-protein complex between pp60v-src and hsp90 is stabilized by molybdate, vanadate, tungstate, and an endogenous cytosolic metal. *J. Biol. Chem.* **267,** 13,952–13,957.

23

Investigation of Folding and Degradation of In Vitro Synthesized Mutant Proteins in Mitochondria

Peter Bross, Vibeke Winter, Christina Bak Pedersen, and Niels Gregersen

1. Introduction

Missense mutations and one-amino acid deletions or insertions affect in a majority of cases folding and/or the stability of the native structure ***(1–3)***. Investigation of the biogenesis of the mutant protein after synthesis of the full-length polypeptide is therefore an essential starting point to evaluate the effect of a given mutation. Many disease-causing missense mutations cause retention of partly folded and misfolded intermediates in complexes with molecular chaperones or their premature degradation and these are hallmarks for folding deficiencies. For mitochondrial proteins, the use of in vitro transcription/translation followed by addition of isolated mitochondria presents a simple and efficient way to investigate the biogenesis of the mutant protein inside the organelle. The advantage of the method is that the protein of interest can be selectively labeled in vitro and subsequently its biogenesis can be investigated in its normal environment in the organelle without the need to use immunological methods to distinguish it from the other proteins. Mitochondria can easily be isolated from animal tissues, but can also be isolated from cultured cells ***(4)***.The mitochondrial protein is first synthesized in a coupled in vitro transcription/translation system using reticulocyte lysate. Subsequently, the synthesized polypeptide is added to freshly prepared mitochondria from rat liver. After a short import step at low temperature (20°C) the mitochondria are shifted to higher temperature and samples are taken at different time intervals. Mitochondria from the time-course samples are treated with protease to remove polypeptides that are not imported or stick to the outer surface of the organelle, and reisolated by centrifugation. After lysis, aliquots of the lysate are investigated by denaturing sodium

From: *Methods in Molecular Biology, vol. 232: Protein Misfolding and Disease: Principles and Protocols*
Edited by: P. Bross and N. Gregersen © Humana Press Inc., Totowa, NJ

dodecyl sulfate polyacrylamide gel electrophorersis (SDS-PAGE) to study the stability of the imported polypeptide. Samples are also investigated by native PAGE to monitor formation of complexes with chaperones and acquisition of the native structure. Using comparative analysis of wild-type and a disease-causing mutant variant (R22W) of human mitochondrial short-chain acyl-CoA dehydrogenase (SCAD) ***(5,6)*** as an example for this kind of study, we here describe the basic method and some variations that can be applied to refine the analysis.

2. Materials

1. Potter-Elvehjem tissue homogenizer.
2. Sonication water bath (e.g., Branson 200).
3. Heating block with shaker or shaking water bath.
4. Slab gel electrophoresis equipment.
5. Rotating shaker.
6. Vacuum gel drier with vacuum pump.
7. Mannitol buffer: 225 m*M* mannitol, 25 m*M* sucrose, 10 m*M* Tris-HCl, pH 7.8, 0.1 m*M* ethylenediamine tetraacetic acid (EDTA).
8. Protein assay dye reagent concentrate and bovine serum albumin (BSA) protein concentration standard (BioRad, Hercules, CA).
9. Lysis buffer: 50 m*M* Tris-HCl, pH 7.8, 5 m*M* EDTA, 1 m*M* dithiothreitol (DTT), 10 μg/mL aprotinin, 1 mg/mL soybean-Trypsin inhibitor, 250 m*M* sucrose.
10. TnT Quick-coupled reticulocyte transcription/translation kit (Promega, Madison, WI).
11. L-[^{35}S]Methionine in vivo cell-labeling grade (Amersham Biosciences, Piscataway, NJ), stored at –80°C.
12. Cycloheximide: 1.5 μg/μL in H_2O; store in aliquots at 4°C.
13. Malate: 180 m*M* in H_2O; store in aliquots at –20°C.
14. Pyruvate: 1 M in H_2O; store in aliquots at –20°C.
15. Trypsin: 5 μg/μL in H_2O; store in aliquots at –20°C.
16. Soybean trypsin inhibitor: 10 μg/μL in H_2O; store in aliquots at –20°C.
17. SDS sample buffer (6X): 3.5 mL 1 *M* Tris-HCl, pH 6.8, 3.0 mL 100% (v/v) glycerol, 1 g sodium-dodecyl sulfate (SDS), 0.93 g DTT, 1.2 mg bromophenol blue, fill up with H_2O to 10 mL; store in aliquots at –20°C.
18. Native loading buffer: 50% (v/v) Glycerol, 100 μg/mL bromophenol blue.
19. 10X SDS-PAGE running buffer: 250 *M* Tris base, 1.92 *M* glycine, 1% (w/v) SDS.
20. 10X Native PAGE running buffer: 250 m*M* Tris base, 1.92 m*M* glycine.
21. Precast 4–15% gradient gels and 12% gels, e.g., Tris-HCl Ready (15 slot) or Criterion Tris-HCl (26-slot) gels (BioRad).
22. Precision Protein standard SDS, prestained (BioRad).
23. Protein mw standard native (HMW Native Marker kit; Amersham Biosciences); resuspend contents of vial in 200 μL Native running buffer and add a few grains of bromophenol blue; store at –20°C.

24. Coomassie staining solution: 50% (v/v) ethanol, 10% (v/v) acetic acid, 0.5 g/L Coomassie R250.
25. Destaining solution: 5% (v/v) ethanol, 7% (v/v) acetic acid.

3. Methods

The methods describe the purification of mitochondria from rat liver (**Subheading 3.1.**), coupled in vitro transcription/translation and labeling of the protein (**Subheading 3.2.**), import of the in vitro translated protein into isolated mitochondria and a time course of folding (**Subheading 3.3.**), lysis of mitochondria (**Subheading 3.4.**), gel electrophoresis of samples from the different time points (**Subheading 3.5.**), and staining and phosphorimager analysis (**Subheading 3.6.**). An example for this type of analysis is shown in **Fig. 1**.

3.1. Isolation of Rat Liver Mitochondria

All steps are performed on ice or at 4°C. Rat liver is obtained from freshly killed rats.

1. The rat liver is immediately immersed in cold mannitol buffer.
2. Cut liver into small pieces using a scalpel on ice in a petri dish filled with mannitol buffer.
3. Homogenize liver tissue in 5 volumes of mannitol buffer using a Potter-Elvehjem glass-Teflon homogenizer with three strokes at 175v on power supply.
4. Transfer homogenisate to a 50-mL Falcon tube and Centrifuge at 400*g* for 10 min.
5. Transfer supernatant to a new Falcon tube and centrifuge at 8,000*g* for 10 min.
6. Discard supernatant, resuspend pellet containing the mitochondrial fraction in approx 15 mL mannitol buffer, and centrifuge at 8,000*g* for 10 min.
7. Repeat this wash step of the mitochondria pellet two times.
8. Resuspend final pellet in 600 µL mannitol buffer and store on ice.
9. Determination of the protein concentration: Dilute 10 µL of the mitochondria suspension 1:10 in an Eppendorf tube by adding 90 µL mannitol buffer. Make a dilution series of the standard (BSA).
10. Set up cuvet with the BSA standard dilution series and the two diluted samples from the mitochondria suspension as described in the manual for the Bradford protein dye reagent assay (microassay procedure), and calculate the protein concentration of the undiluted mitochondrial suspension.
11. Using the calculated protein concentration dilute the mitochondria suspension to 30 mg/mL using mannitol buffer.

3.2. Coupled Transcription/Translation Reaction

A DNA template with the cDNA under control of an appropriate promoter is used (*see* **Note 1**) to transcribe and translate the wild-type and mutant protein to be investigated. For all work with radiochemicals: Wear gloves, use filter pipet tips, collect used pipet tips and dispose as radioactive waste.

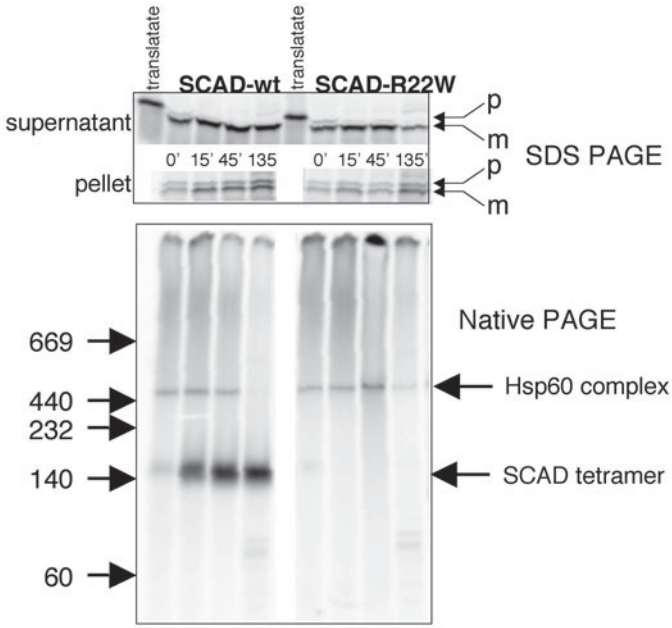

Fig. 1. Intramitochondrial biogenesis of wild-type human short-chain acyl-CoA dehydrogenase (SCAD) and the disease-causing mutant variant R22W. Plasmid-encoded cDNAs were transcribed and translated in the rabbit reticulocyte lysate system in the presence of [^{35}S]-methionine. Translated polypeptides were imported into isolated rat liver mitochondria for 10 min at 20°C. The reactions were shifted to 37°C and SCAD biogenesis was monitored by taking samples after the time intervals indicated. Samples were treated with trypsin to remove nonimported and partially imported polypeptides, and mitochondria were reisolated and lysed by freeze-thawing. Aliquots from the soluble extracts were subjected native PAGE and both soluble extracts and insoluble pellets were analyzed by SDS-PAGE. The radioactive bands were visualized by phosphorimaging. Translatate: samples of the translatates of wt and R22W SCAD before addition of mitochondria. The position of SCAD precursor (p) and mature (m) bands in the SDS gels, SCAD tetramer, and Hsp60 complex in native gels (inferred by comigration of the respective bands as shown by Western blotting; data not shown) are indicated on the right margin. Position and molecular masses of co-electrophoresed marker proteins are indicated on the left margin of the native gel.

1. For each protein variant to be analysed set up Eppendorf tubes with: 60 µL TnT Quick Master Mix with the appropriate RNA polymerase, 3 µL ^{35}S-met, 3 µL expression plasmid DNA (0.5 mg/mL), H_2O to a total volume of 75 µL.
2. Incubate in a shaking water bath at 30°C for 60–120 minutes (*see* **Note 2**).
3. Stop reaction by addition of 75 µL cycloheximide.
4. Store transcription/translation reaction on ice until use.

3.3. Import Into Mitochondria and Folding Time Course

A standard procedure with import at low temperature (20°C) for 10 min followed by a chase procedure at 37°C is given. Depending on the protein studied and the questions investigated, different conditions may be applied (*see* **Notes 3** and **4**).

1. Using the transcription/translation reaction from **Subheading 3.2.** set up (on ice) the following import mixture: 70 µL translatate, 35 µL mitochondria suspension, 0.6 µL malate, 1.1 µL, pyruvate (*see* **Note 5**).
2. Incubate in shaking water bath at 20°C for 10 min.
3. Shift reaction to a shaking water bath set to 37°C; after 0, 15, 45, and 135 min remove 20 µL aliquots from the reaction, transfer to fresh Eppendorf tubes, and place at 4°C.
4. To each 20 µL time sample, add 2 µL trypsin (5 µg/µL) and incubate for 10 min at 4°C.
5. Add 6 µL trypsin inhibitor, incubate for 10 min at 4°C, and subsequently centrifuge at 14,000*g* for 5 min at 4°C.
6. Discard supernatant and wash pellet once with 100 µL mannitol buffer.
7. Remove supernatant and freeze tube with mitochondria pellet at –80°C.

3.4. Lysis of Mitochondria

1. Thaw mitochondria pellets from time course on ice after addition of 20 µL ice cold lysis buffer (*see* **Note 6**).
2. Sonicate for 20 s in a sonication water bath at 4°C.
3. Centrifuge at maximum speed in a microcentrifuge for 20 min at 4°C.
4. Transfer supernatant (containing soluble matrix proteins) to a new tube and store at 4°C; also save tube with pellet (containing aggregated and membrane bound mitochondrial proteins) for SDS-PAGE analysis.

3.5. Electrophoresis of Samples

3.5.1. SDS-PAGE Analysis

The gel type applied depends on the molecular weight of the analyzed protein. Polyacrylamide gradient gels or gels with a constant acrylamide concentration may be used.

1. Prepare samples from each time point: mix 5µL of mitochondrial lysate (supernatant from **step 4**, **Subheading 3.4.**) with 1 µL of 6x SDS sample buffer in an Eppendorf tube; resuspend pellet from **step 4**, **Subheading 3.4.** with 25 µL 1x SDS sample buffer. Dilute 1 µL from the transcription/translation reaction (**step 4**, **Subheading 3.2.**) with 4 µL H_2O and add 1 µL 6x SDS sample buffer.
2. Boil the samples for 2 min at 95°C in a heating block; centrifuge briefly and keep at room temperature.

3. Pipet 6 μL of Precision Protein standard SDS into an Eppendorf tube. Keep all samples at room temperature and apply to a precast gel with the appropriate acrylamide concentration/gradient. Use 1x SDS Running buffer.
4. Run gel in the cold room at 200 V for 60 min or until the dye front is reaching the bottom of the gel.
5. Stain, dry, and process gel as described in **Subheading 3.6.**

3.5.2 Native PAGE Analysis

Native PAGE is dependent on the oligomeric molecular weight, shape, and net charge of the protein and its complexes. Proteins and protein complexes with a net positive charge at neutral pH will not migrate into the gel (*see* **Note 7**). Polyacrylamide gradient gels are used.

1. On ice mix 10 μL from the mitochondrial lysate (supernatant from **Subheading 3.4.**, **step 4**) from each time point with 1 μL of Native sample buffer. As molecular mass standard, use 5 μL of Protein MW standard native.
2. Set up a 4–15% gradient gel with 1X Native Running buffer (precooled to 4°C) and load the samples.
3. Run gel in the cold room at 200 V for 60 min or until the dye front is reaching the bottom of the gel.
4. Stain, dry, and process gel as described in **Subheading 3.6.**

3.6. Gel Staining and Phosphorimager Analysis

1. Remove gels from apparatus and stain for 15 min at room temperature using 25 mL Coomassie staining solution in a tray on a rotating shaker.
2. Remove staining solution, add 50 mL destaining solution, and destain for 1–2 h at room temperature on a rotating shaker; a small roll of a piece of coiled up paper towel attached with tape to the side of the tray may be added to accelerate destaining by adsorbing stain.
3. Place gels on damp Whatman 3M paper and dry on a vacuum/heat gel drier for 2 h at 80°C.
4. Pack dried gels into Saran wrap and expose over night to an erased phosphorimager screen (*see* **Note 8**).
5. Scan screen in the phosphorimager and analyze digital image.

4. Notes

1. The TnT system is available for expression using the T7, T3, or SP6 promoters. Many commercially available plasmids possess one or several of these promoter sequences preceding multiple cloning sites. A detailed treatise of different translation systems and the factors affecting transcription and translation can be found in Chapter 21 of this volume. The cDNA may be derived from EST clones and cloned into an appropriate vector. A DNA template containing an appropriate promoter and translational initiation site can also be produced by polymerase chain reaction (PCR) from cDNA (see Chapter 22, this volume, for a detailed procedure). The plasmid or PCR fragment used should contain (in this order):

one of the promoters supported by the reticulocyte extract system, a translation initiation site that is functional in eukaryotes and the cDNA coding for the protein/mutant variant to be expressed. The translational initiation (also termed "Kozak sequence") is defined by some context rules for the sequence up to approx six nucleotides upstream of the ATG start codon ***(7)***. Usually the original translational initiation site can be carried from the cDNA of the gene used. However, if low translational efficiency in the in vitro system is observed, it is advisable to change the sequence by PCR mutagenesis and add a "perfect Kozak" sequence.

2. The optimal incubation time for transcription/translation should be determined empirically for each protein. Run samples taken after different incubation times on an SDS-PAGE (*see* Chapter 22).
3. Import may be performed at temperatures between 14°C and 41°C. At low temperature, polypeptide folding appears to proceed very slowly while import still occurs. Import at low temperature thus allows importing the polypeptide under conditions where folding is stalled and these two processes can be partly separated. To ensure that no further import occurs valinomycin (100 m*M* stock in ethanol; dilute 1:50 in assay) can be added after the import incubation. However, we have observed that this negatively affects the biogenesis of SCAD proteins resulting in increased aggregation of the polypeptides and decreased formation of folded tetramers.
4. As a rule of thumb, incubation at 37°C for studies of the biogenesis results in a more dynamic picture than incubation at lower temperature, but the conditions applied depend on the investigated protein and should be optimized in each case. The temperature of the biogenesis reaction may be adjusted so that the effect of the mutation is enhanced, i.e., the difference in behavior between the wild-type and mutant protein is augmented. It is also advisable to compare the results from incubations at different temperature where a mutation effect increasing with temperature is indicative of a folding defect that may be modulatable by environmental conditions.
5. Malate and pyruvate are added to enhance membrane potential and spark mitochondrial ATP synthesis during the import step. Alternatively, sodium-succinate (10 m*M*) may be added ***(8)***. After addition of valinomycin, this has no more effect because the membrane potential is dissipated and therefore membrane potential driven ATP synthesis ceases. The reticulocyte lysate contains an ATP regenerating system (creatine kinase with phosphocreatine), which will function as a source for ATP that is able to enter the mitochondria. To ensure high ATP levels after addition of valinomycin, additional phosphocreatine may be added and the reverse (ATP consuming) reaction of ATP synthase blocked by adding oligomycin (2 μg/mL final concentration; 100X stock solution in ethanol).
6. The mitochondrial Hsp70 and Hsp60 chaperones are ATP-dependent and will in the presence of ATP cycle between high- and low-affinity conformations for the substrates (folding intermediates). In order to preserve the complexes, EDTA (5 m*M*) is present in the lysis buffer, which will chelate Mg ions and thereby freeze the chaperones in an ADP (high-affinity) conformation ***(9)***.

7. Running conditions for the native PAGE gels are critical. Precooled running buffer should be used. The described procedure is also not suited for all proteins, e.g., proteins with a basic native isoelectric point will not migrate to the anode. The migration in the polyacrylamide gradient gel is dependent on charge and shape. Another native gel procedure that is independent of the isoelectric point of the protein investigated is blue-native gel electrophoresis ***(10)***. The advantage of native PAGE is the possibility to quickly analyse many samples. As an alternative to using native PAGE for the display of complexes and the native conformation, co-immunoprecipitation may be applied with antibodies against the chaperones in question. A procedure can be found in Chapter 12 in this volume. This type of pull-down experiments should also be used to verify chaperone interactions, because the native gels only show co-migration. Another alternative to native PAGE is gel filtration chromatography of the samples to determine the oligomeric mass of the different conformations and complexes (*see* **ref. *11***).
8. Alternatively fluorography can be applied (*see* Chapter 12, this volume).

Acknowledgments

Development of the mitochondrial biogenesis assay has been supported by The Danish Medical Research Council; Karen Elise Jensen Foundation; and Institute of Experimental Clinical Research, Aarhus University.

References

1. Gregersen, N., Bross, P., Andresen, B. S., Pedersen, C. B., Corydon, T. J., and Bolund, L. (2001) The role of chaperone-assisted folding and quality control in inborn errors of metabolism: protein folding disorders. *J. Inherit. Metab Dis.* **24,** 189–212.
2. Bross, P., Corydon, T. J., Andresen, B. S., Jørgensen, M. M., Bolund, L., and Gregersen, N. (1999) Protein misfolding and degradation in genetic diseases. *Hum. Mutat.* **14,** 186–198.
3. Bross, P., Andresen, B. S., and Gregersen, N. (1998). Impaired folding and subunit assembly as disease mechanism: The example of medium-chain acyl-CoA dehydrogenase deficiency, in *Progress in Nucleic Acids Research and Molecular Biology* (Moldave, K., ed.), Academic Press, San Diego, pp. 301–337.
4. Pallotti, F. and Lenaz, G. (2001) Isolation and subfractionation of mitochondria from animal cells and tissue culture lines. *Methods Cell Biol.* **65,** 1–35.
5. Naito, E., Indo, Y., and Tanaka, K. (1990) Identification of two variant short chain acyl-coenzyme A dehydrogenase alleles, each containing a different point mutation in a patient with short chain acyl-coenzyme A dehydrogenase deficiency. *J. Clin. Invest.* **85,** 1575–1582.
6. Corydon, T. J., Bross, P., Jensen, T. G., Corydon, M. J., Lund, T. B., Jensen, U. B., et al. (1998) Rapid degradation of short-chain Acyl-CoA dehydrogenase variants with temperature-sensitive folding defects occurs after import into mitochondria. *J. Biol. Chem.* **273,** 13,065–13,071.

7. Kozak, M. (1996) Interpreting cDNA sequences: some insights from studies on translation. *Mamm. Genome* **7,** 563–574.
8. Ryan, M. T., Voos, W., and Pfanner, N. (2001) Assaying protein import into mitochondria. *Methods Cell Biol.* **65,** 189–215.
9. Ewalt, K. L., Hendrick, J. P., Houry, W. A., and Hartl, F. U. (1997) In vivo observation of polypeptide flux through the bacterial chaperonin system. *Cell* **90,** 491–500.
10. Schagger, H. (2001) Blue-native gels to isolate protein complexes from mitochondria. *Methods Cell Biol.* **65,** 231–244.
11. Saijo, T., Welch, W. J., and Tanaka, K. (1994) Intramitochondrial folding and assembly of medium-chain Acyl-CoA dehydrogenase (MCAD): demonstration of impaired transfer of K304E-variant MCAD from its complex with Hsp60 to the native tetramer. *J. Biol. Chem.* **269,** 4401–4408.

24

Investigation of Folding and Degradation of Mutant Proteins Synthesized in Semipermeabilized Cells

Cornelia M. Wilson and Neil J. Bulleid

1. Introduction

The endoplasmic reticulum (ER) is the site where most secretory proteins acquire their native conformation and gain access to the secretory pathway, and the cell surface. Proteins entering the secretory pathway are translocated across or inserted into the ER membrane either co-translationally or post-translationally through an aqueous pore in the ER membrane called the translocon ***(1)***. The emerging polypeptide chains may then interact with molecular chaperones to ensure their correct folding and assembly ***(2)***. Covalent modification of the polypeptide chain by the formation of native inter- and intrachain disulphide bonds stabilizes folded protein domains and cross-links subunits associated with oligomeric complexes. The ability of the ER-molecular chaperones and folding enzymes to recognize and bind to non-native substrates retains these proteins within the ER until they have reached their native state ***(3)***. The dissociation of the fully folded substrates from the ER chaperones facilitates the transport process, resulting in exit of the native protein from the ER. Therefore, the "quality-control" system of the ER allows export of only correctly folded and assembled proteins.

The folding process is not entirely efficient because folding can fail if amino acids are misincorporated as a result of genetic mutations such as cystic fibrosis (CF), or errors in transcription, mRNA processing, or translation. On the other hand, protein folding could fail, for example, when the cell is under conditions of thermal stress ***(4,5)***, and osmotic and oxidative stress ***(6)***, or in the

From: *Methods in Molecular Biology, vol. 232: Protein Misfolding and Disease: Principles and Protocols*
Edited by: P. Bross and N. Gregersen © Humana Press Inc., Totowa, NJ

presence of viral gene products *(7,8)*, which prevents the folding of newly synthesized polypeptides. Alternatively, inefficient synthesis of subunits that are part of a multimeric protein complex results in the production of unassembled polypeptide chains *(9)*. The quality-control process of the ER not only monitors for misfolding, but also targets non-native proteins for degradation. Proteins destined for degradation must be transported across the ER membrane to the cytosol, where they are degraded by a multicatalytic proteinase complex called the proteasome.

Most of the current data of ER-associated degradation (ERAD) in mammalian cells has been generated from studies that investigated the synthesis of Major Histocompability Complex (MHC) Class I molecules. Together, these studies have indicated that cytosolic proteasomes degrade proteins from the ER, and that ER export and import can use the same translocation machinery. This chapter will describe how an in-vitro system can be used to study the folding and degradation of MHC class I heavy chain in a functionally and morphologically intact ER.

2. Materials

1. CEM cells (from ECCAC) grown in Iscoves Modified Dulbeccos Media (IMDM) plus 10% (v/v) FCS.
2. IMDM (Sigma).
3. KHM buffer: 110 m*M* KOAc, 2 m*M* MgOAc, 20 m*M* HEPES, pH 7.2.
4. HEPES buffer: 50 m*M* KOAc, 50 m*M* HEPES, pH 7.2.
5. Phosphate-buffered saline (PBS) (Gibco-BRL).
6. 5X Transcription buffer: 400 m*M* HEPES buffer, pH 7.4, 60 m*M* $MgCl_2$, 10 m*M* spermidine stored at –80°C.
7. Endo H dissolution buffer: 0.1 *M* Tris-HCl, pH, 8.0, 1% (w/v) sodium dodecyl sulfate (SDS), 1% (v/v) β-mercaptoethanol.
8. 150 m*M* Sodium citrate buffer, pH 5.5.
9. Low-salt lysis buffer: 50 m*M* Tris-HCl, pH 7.5, containing 150 m*M* NaCl, 2 m*M* ethylenediamine tetraacetic acid (EDTA) and 1% v/v Triton X-100.
10. ATP-regeneration system: 40 m*M* Tris-HCl, pH 7.5, 0.5 m*M* ATP, 5 m*M* $MgCl_2$, 2 m*M* dithiothreitol (DTT), 1.6 mg/mL creatine phosphokinase, and 10 m*M* phosphocreatine, stored at –80°C.
11. Sample buffer: 0.0625 *M* Tris-HCl, pH 6.8, 2% SDS (w/v), 10% glycerol (v/v) and a few grains of bromophenol blue.
12. 40 mg/mL Digitonin in dimethyl sulfoxide (DMSO) stored at –80°C.
13. 0.4% (w/v) Trypan blue solution.
14. 0.1 *M* $CaCl_2$.
15. 0.4 *M* EGTA.
16. 1 *M* and 100 m*M* DTT (Sigma), stored at –20°C.
17. 2.5 *M* KCl (Promega).

18. 10% (v/v) Triton X-100 (Sigma).
19. Phenylmethylsulfonyl fluoride (PMSF) (0.1 *M* in isopropanol) (Sigma) stored at –20°C.
20. Cycloheximide (50 m*M*) (Sigma), stored at –20°C.
21. Clasta-lactacystin β-lactone (1 m*M* stock in DMSO) (Calbiochem), stored at –80°C.
22. MG132 and ALLN (1 m*M* stock in DMSO) (Sigma), stored at –20°C.
23. Nucleotide triphosphates (ATP, UTP, CTP, and GTP) (25 m*M* each) (Roche Diagnostics), stored at –20°C.
24. Amino acid mix (minus methionine) (Promega), stored at –20°C.
25. EasyTag™ L [^{35}S]-methionine (15 μCi/μL) (NEN Dupont).
26. 1mg/mL Micrococcal nuclease in sterile water (Roche Diagnostics), stored at –20°C.
27. 50 U/μL T7 RNA polymerase (Promega), stored at –80°C.
28. RNase inhibitor (Promega), stored at –80°C.
29. 2mg/mL Proteinase K in sterile H_2O (Roche Diagnostics), stored at –20°C.
30. 1 mU/μL Endoglycosidase H (Roche Diagnostics).
31. Monoclonal antibodies (MAbs) to MHC Class I molecule (HC10 and W6/32).
32. Polyclonal antibodies (PAbs) to β_2m (Serotec Ltd).
33. 10 μg linerized plasmid DNA in RNase-free water, containing gene of interest downstream from a viral polymerase promoter.
34. Flexi™ rabbit reticulocyte lysate (Promega), stored at –80°C.
35. Reticulocyte lysate (*see* **Note 14**), stored at –80°C.
36. Protein A-Sepharose 4B beads (10% [v/v] in PBS) (Zymed, Cambridge Bioscience).

3. Methods

The methods described here outline ***(1)*** the expression and characterization of expressed proteins in semi-permeabilized cells (SP-cells), and ***(2)*** the reconstitution of the degradation of mutant or malfolded proteins using isolated SP-cells and cytosol.

3.1. Protein Expression in SP-Cells

SP-cells allow the researcher to reconstitute the initial stages in the assembly and modification of proteins entering the secretory pathway, as they would occur in an intact cell. The procedure involves treating cells grown in culture with the detergent digitonin, and isolating the cells free of their cytosolic components. In subsequent experiments, mRNA transcripts can be translated in a cell-free translation supplemented with the SP-cells prepared as outlined in **Subheading 3.1.1.**

There are a number of distinct advantages to using this system. Because this is an in vitro system, the individual components can be manipulated easily,

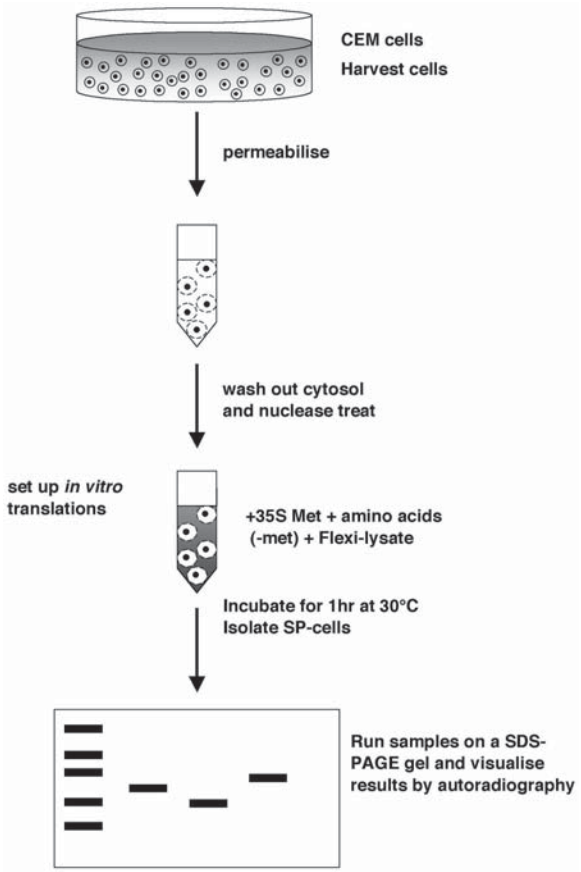

Fig. 1. Experimental approach for the preparation of SP-cells and in vitro translations.

providing a means by which cellular processes can be studied under a variety of conditions. In addition, membrane-permeable chemical cross-linking reagents can be added and have easy access to proteins within the ER lumen. Also, as the ER remains morphologically intact, the spatial localization of folding and transport processes within the reticular network may also be studied.

3.1.1. Preparation of SP-Cells

This procedure uses a modified protocol based on that of Plutner et al. ***(10)*** and Wilson et al. ***(11)***, which has been adapted for the cell-free expression of proteins ***(12)*** (*see* **Fig. 1** and **Note 1**).

1. Harvest CEM cells grown to confluence in 15-mL Falcon tube by centrifugation at 240*g* for 3 min at 4°C. Aspirate the supernatant from the cell pellet.

2. Resuspend the pelleted cells in 6 mL of ice-cold KHM and permeabilize by the addition of 6 µL digitonin (from 40 mg/mL stock) to a final concentration of 40 µg/mL and mix immediately by inversion and incubate on ice for 5 min (*see* **Note 2**).
3. Adjust the volume to 14 mL with ice-cold KHM and pellet cells by centrifugation as **step 1**.
4. Discard supernatant and resuspend cells in 14 mL ice-cold HEPES buffer. Incubate on ice for 10 min and pellet by centrifugation as **step 1**.
5. Discard the supernatant and resuspend cells carefully in 1 mL ice-cold KHM (use a 1 mL automatic pipet and pipet gently up and down). Place on ice.
6. Transfer a 10 µL aliquot to a separate 1.5 mL microcentrifuge tube and add 10 µL of Trypan blue.
7. At this stage, count the cells in a haemocytometer and check for permeabilization by trypan blue staining, i.e., cells should appear blue under the microscope.
8. Transfer cells to a 1.5 mL microcentrifuge tube and spin for 30 s at 15,700*g* in a microcentrifuge. Discard supernatant and resuspend the cells in 100 µL KHM using a pipet (approx 2×10^6 cells).
9. Remove endogenous mRNA from the cells by treating with a calcium-dependent nuclease. Add 1 µL of 0.1 *M* $CaCl_2$ and 1 µL of micrococcal nuclease (1 mg/mL) and incubate at room temperature for 12 min.
10. Add 1 µL of 0.4 *M* EGTA to chelate the calcium and inactivate the nuclease. Pellet the cells by centrifuging at 15,700*g* for 30 s in a microcentrifuge and resupend in 100 µL KHM.
11. Use approx 10^5 cells per 25 µL translation reaction (approx 4 µL of the 100 µL obtained).

3.1.2. Preparation of RNA Transcripts

The cDNA encoding the protein of interest is subcloned into a mammalian expression vector such as pBluescript and pSupK containing a viral promoter (for example, T7, T3, or SP6), allowing in vitro transcription with the corresponding viral RNA polymerase. The cDNA clone must be linearized downstream of the coding sequence by restriction endonuclease digestion to generate a template for RNA synthesis (*see* **Note 3**). This method is a modification of a method described previously ***(13)***.

1. Prepare a 100 µL transcription mixture containing 20 µL Transcription buffer (5X), 4 µL 0.1 *M* DTT, 28 µL linearized DNA (5–10 µg), 1 µL RNase inhibitor (40 U), 3 µL of each nucleotide (25 m*M* stock), and 42 µL H_2O.
2. Add 2 µL of the appropriate RNA polymerase (160 U) and incubate for 2 h at 37°C (*see* **Note 4**).
3. The RNA transcript can be purified by extraction with an equal volume of phenol/chloroform (1:1), then twice with chloroform. The RNA is precipitated from the final aqueous layer by adding 1/10th volume of 3 *M* NaOAc, pH 5.2, and 3 volumes of 100% ethanol. The RNA pellet is resuspended in 100 µL RNase-free H_2O containing 1 m*M* DTT and 1 µL RNase inhibitor. The RNA is stored at –80°C.

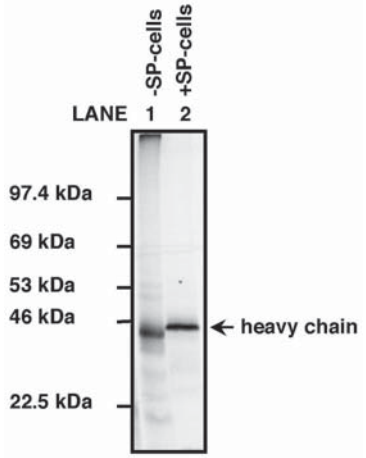

Fig. 2. Translocation of MHC Class I heavy chain. Translations were carried out in the absence (lane 1) or presence (lane 2) of SP-cells in rabbit reticulocyte lysate and incubated at 30°C for 60 min. Samples were heated at 100°C in SDS-PAGE sample buffer containing 50 m*M* DTT, and separated by 10% SDS-PAGE; radiolabeled proteins were visualized by autoradiography.

4. To assess the yield and integrity of the synthesized RNA, remove 1 µL and analyze on a 1% agarose gel (*see* **Note 5**).

3.1.3. Expression of the RNA Transcript In Vitro

The translation of proteins in vitro can be performed using either a wheat germ extract or a rabbit reticulocyte lysate that contain ribosomes, tRNAs, and a creatine phosphate-based energy regeneration system.

1. Prepare a 25 µL translation mixture containing 17.5 µL FlexiTM lysate, 0.5 µL amino acids, 0.5 µL KCl, 1 µL EasyTag™ [^{35}S]-methionine, 1 µL RNA, and 4 µL SP-cells (*see* **Notes 6** and **7**). Incubate the translation sample at 30°C for 60 min and then place on ice.
2. To prepare the samples for SDS-PAGE, add 2 µL of the product to 15 µL SDS-polyacrylamide gel electrophoresis (PAGE) sample buffer plus 2 µL DTT (1 *M*) and heat for 5 min at 100°C.
3. Separate samples through a SDS-PAGE gel appropriate for the expected molecular weight for the protein of interest. After electrophoresis, the SDS-PAGE gel should be dried and exposed to autoradiography film (Kodak X-Omat AR film) or phosphorimage screens (*see* **Note 8** and **Fig. 2**).

This approach can be best illustrated by following the expression of a particular secretory protein. The expression of a RNA transcript coding for the allele human leukocyte antigen (HLA)-B27 heavy chain can be followed in a

cell-free translation supplemented with the SP-cells prepared from the human cell line CEM, which is lymphoblastoid in origin and has been used previously to study MHC class I assembly ***(14)***. The following data demonstrate that, when added to the SP-cell translation system, RNA coding for heavy chain can be translated into polypeptides that are translocated into the lumen of the ER, fold, and assemble to form a trimeric complex with β_2-microglobulin and antigenic peptide.

To determine whether heavy chain undergoes translocation and *N*-glycosylation in the ER lumen of SP-cells, mRNA coding for the allele HLA-B27 heavy chain was translated in the presence and absence of SP-cells prepared from CEM cells. In the absence of SP-cells, the translated product migrates slightly faster than in the presence of SP-cells, which is owing to glycosylation of the translation product after translocation into the ER of the SP-cells (**Fig. 2**, compare lanes 1 and 2). This conclusion can be confirmed by removal of the oligosaccharide side chain following digestion with endoglycosidase H, as outlined in **Subheading 3.1.4.**

3.1.4. Endoglycosidase H Digestion of Translation Products

This treatment removes most of the oligosaccharide side chain, leaving GlcNAc attached to the asparagine residue of the protein. Denaturation of the glycoprotein by treating with SDS and β-mercaptoethanol increases the accessibility of oligosaccharide side-chains for digestion. N-linked oligosaccharides, attached to the amino group of some asparagine residues in the consensus sequence Asp-X-Ser/Thr, may contribute 3.5 kDa or more per structure. Therefore, Endo H treatment of the translated protein can be judged by the increased electrophoretic mobility of the protein on an SDS-PAGE gel. Enzymatic deglycosylation provides a mild and nondestructive method of removing carbohydrates.

1. Prepare a 50 µL (2X 25 µL) translation reaction including freshly prepared SP-cells. After translation, isolate the SP-cells from the translation reaction by centrifugation at 15,700*g* for 1 min.
2. Resuspend the isolated SP-cells in 30 µL Endo H dissolution buffer and heat at 100°C for 2 min.
3. Cool the heated sample on ice for 1 min and remove any insoluble material by centrifugation at 15,700*g* for 2 min.
4. Transfer the supernatant into a microcentrifuge tube and add 30 µL sodium citrate buffer (150 m*M*, pH 5.5).
5. Divide the sample equally into two aliquots (2X 30 µL) in fresh microcentrifuge tubes and add PMSF at a final concentration of 0.5 m*M*.
6. Incubate aliquots overnight at 37°C either in the presence or absence of 1 µL Endoglycosidase H (1 mU/µL) (*see* **Note 9** and **Fig. 3**).

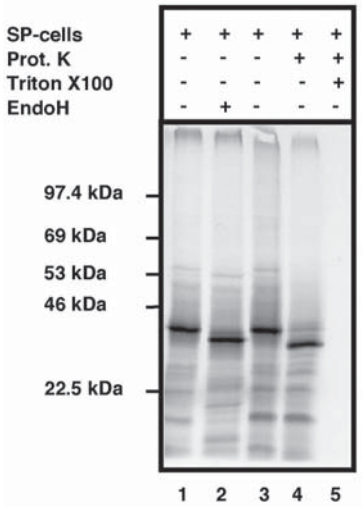

Fig. 3. *N*-glycosylation and integration into SP-cells. Translations were carried out in the presence (lanes 1–5) of SP-cells in rabbit reticulocyte lysate and incubated at 30°C for 60 min. For Endoglycosidase H (Endo H) treatment, SP-cells were isolated by centrifugation and solubilised in Endo H dissolution buffer and the pH was adjusted to 5.5 with sodium citrate. Samples were incubated overnight at 37°C with (lane 2) or without (lane 1) 1 mU of Endo H. Proteinase K treatment was carried out at 4°C for 25 min in either the absence (lane 4) or presence of (lane 5) Triton X-100. Samples were heated at 100°C in SDS-PAGE sample buffer containing 50 m*M* DTT, and separated by 10% SDS-PAGE; and radiolabeled proteins were visualized by autoradiography.

Following this treatment, the translation product was confirmed as being glycosylated, as judged by an increase in electrophoretic mobility (**Fig. 3**, compare lanes 1 and 2). To demonstrate that the synthesized heavy chain had indeed been translocated across and integrated into the ER membrane, a Proteinase K digestion was carried out as described in **Subheading 3.1.5.**

3.1.5. Proteinase K Protection Assay

A "protease protection" assay is a method used to determine whether the nascent chains are targeted to the ER membrane and translocated across or integrated into the ER membrane of SP-cells. The translation samples are treated post-translationally with Proteinase K, which digests any nontranslocated translation products. Fully translocated proteins (i.e., soluble proteins) are protected by the lipid bilayer of the ER membrane whilst proteins that are inserted into

the ER membrane (transmembrane proteins) are partially protected by this treatment. A control sample is incubated in the presence of Proteinase K and Triton X-100, which solubilizes the ER membrane and therefore enables the protein to be susceptible to Proteinase K digestion.

1. Prepare a 25 μL translation reaction including freshly prepared SP-cells. After translation, place the sample on ice and gently disperse the SP-cells using a pipet tip.
2. Divide the translation mixture into three microcentrifuge tubes containing 3 × 8 μL aliquots. One sample is used as a nontreated control. To the other two tubes, add 1 μL $CaCl_2$ (100 m*M*) and 1 μL Proteinase K (2.0 mg/mL). To one of these samples, also add Triton X-100 to a final concentration of 1% (v/v).
3. Incubate the samples on ice for 20 min, followed by a further incubation of the samples on ice for 5 min with 1 m*M* PMSF to inhibit the Proteinase K reaction.
4. Prepare the samples for electrophoresis by adding 5 μL of each reaction to 15 μL of SDS-PAGE buffer containing 2 μL DTT (1 *M*).
5. The samples should be separated through an SDS-PAGE gel appropriate for the expected molecular weight for the protein of interest. After running, the gel should be dried and exposed to autoradiography or to a phosphorimage screen (*see* **Note 10** and **Fig. 3**).

After Proteinase K treatment the translation product migrates with a slightly faster electrophoretic mobility (**Fig. 3**, compare lanes 3 and 4). This increase is caused by the removal of the cytoplasmic tail demonstrating that the translated heavy chain was translocated and integrated into the ER membrane. Addition of the detergent Triton X-100 followed by Proteinase K treatment leads to complete digestion (lane 5) demonstrating that the translated heavy chain is not intrinsically resistant to Proteinase K digestion.

Following translation the translation products can be characterized by carrying out immunoprecipitation with specific antibodies.

3.1.6. Immunoprecipitation of Translation Products

Immunoprecipitation is useful in studying novel interactions of newly synthesized proteins with ER components. This method is particularly useful in identifying proteins that react specifically with an antibody that can be removed from solution and examined by gel electrophoresis. Antibody-antigen complexes are removed from solution by the addition of an insoluble form of an antibody binding protein such as protein A or protein G. The choice of immobilized antibody-binding protein depends on the species that the antibody was raised in. Protein A binds well to rabbit, cat, human, pig, and guinea pig IgG as well as mouse IgG_{2a} and IgG_{2b}. Protein G binds strongly to IgG from cow,

goat, sheep, cow, horse, rabbit, and guinea pig and to mouse IgG_1 and IgG_3 (also binds to bovine serum albumin [BSA]).

The SP-cell membranes isolated post-translationally from a translation reaction can be solubilized in a low-salt lysis buffer (*see* **Note 11**), incubated with a matrix and an appropriate antibody.

1. Prepare a 50 μL (2X 25 μL) translation reaction including freshly prepared SP-cells. After translation, isolate the SP-cells from the translation reaction by centrifuging at 15,700*g* for 1 min.
2. Discard the supernatant and resuspend the cell pellet in 100 μL KHM buffer.
3. Add 900 μL of low-salt lysis buffer and 50 μL Protein A sepharose (10% v/v) to the SP-cells in order to remove proteins that bind nonspecifically to protein A sepharose. Incubate with end over end rotation for 30 min at 4°C (*see* **Note 12**).
4. After the incubation in **step 3**, isolate the Protein A beads and any material that has not been solubilized in the lysis buffer by centrifuging at 15,700*g* for 15 s.
5. Carefully, transfer approx 950 μL of the supernatant to a fresh microcentrifuge tube and divide the supernatant into four microcentrifuge tubes containing 4 × 235 μL aliquots. Add the antibodies to the individual samples; one sample is used as a pre-immune control and the other three samples add 1 μL β_2m, 1 μL W6/32, and 10 μL HC10 (all MHC Class I specific antibodies) along with 50 μL Protein A sepharose. Incubate the samples with end over end rotation for 16 h at 4°C (**Note 13**).
6. Isolate the Protein A sepharose beads by centrifuging at 15,700*g* for 15 s and aspirate the supernatant.
7. Wash the beads three times with 1 mL of lysis buffer at 15,700*g* for 15 s and finally resuspend the beads in 30 μL SDS-PAGE sample buffer containing DTT (50 m*M*) prior to analysis by electrophoresis.

The folding and assembly of MHC Class I heavy chain with unlabeled endogenous β_2-microglobulin can be assessed by carrying out immunoprecipitation with specific antibodies, as described in this subheading. When translation products were immunoprecipitated with antibodies to β_2m, the translated heavy chain was immunoprecipitated (**Fig. 4**, lane 2) demonstrating that correctly folded heavy chain forms a dimer with β_2m. This immunoprecipitate is specific because no translation product was immunoprecipitated with the pre-immune serum (**Fig. 4**, lane 4). Assembly into the complex could also be assessed by immunoprecipitating with the conformational specific antibody W6/32 ***(17)*** (**Fig. 4**, lane 3). Previous experiments have suggested that this immunoprecipitate represents peptide-loaded complexes, which are stable up to 55°C ***(16)***. Immunoprecipitation of heavy chain with the MAb HC10 (which recognizes unassembled chains) ***(17)*** demonstrates that there is an excess of unassembled heavy chain (**Fig. 4**, lane 1).

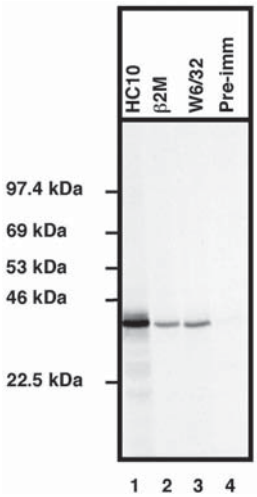

Fig. 4. Immunoprecipitation of MHC Class I heavy-chain complexes. Translations were carried out in the presence (lanes 1–4) of SP-cells in rabbit reticulocyte lysate and incubated at 30°C for 60 min. For immunoprecipitation, the SP-cells were washed and resuspended in KHM buffer. The pellets were then solubilized in lysis buffer and immunoprecipitated with HC10 (lane 1), β_2 microglobulin (β_2m) (lane 2), and W6/32 (lane 3) or preimmune (lane 4) antibodies. Samples were heated at 100°C in SDS-PAGE sample buffer containing 50 m*M* DTT, and separated by 10% SDS-PAGE; radiolabeled proteins were visualized by autoradiography.

3.2. Protein Degradation in SP-Cells

This method is a standard protocol to study MHC Class I heavy-chain degradation using SP-cells prepared from cultured mammalian CEM cells. This assay offers versatility in that other proteins of interest to the researcher can be studied using this assay. Cell-free assays have been used previously to demonstrate that the degradation process is proteasome-mediated, requires ATP, can involve ubiquitination of the substrate, and occurs after dislocation through the Sec61 complex ***(18–20)***. These approaches have mainly used microsomes prepared from wild-type or mutant yeast strains to study ERAD of pro-alpha factor. This ERAD assay in a mammalian SP-cell system allows the study of two closely related pathways, assembly and ERAD, which form an integral part of the quality-control function in the ER (*see* **Fig. 5**).

1. Prepare a 250 µL (10X 25 µL) translation reaction including freshly prepared SP-cells. After translation, inhibit further protein synthesis by adding 5 m*M*

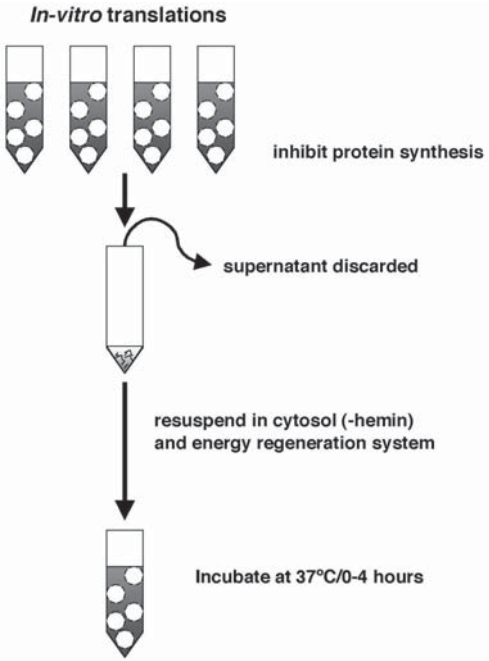

Fig. 5. A flow diagram to summarize the experimental approach for the set up of the ER-associated degradation assay.

cycloheximide and isolate the SP-cells from the translation reaction by centrifugation at 15,700*g* for 2 min. Aspirate the supernatant and resuspend the SP-cells in 1 mL KHM.

2. Divide the SP-cells into 7 × 140 µL aliquots and re-isolate the SP-cells by centrifuging at 15,700*g* for 2 min.
3. Resuspend the isolated SP-cells either in 10 µL KHM (1 × 4 h control for degradation in the absence of cytosol) or 5 µL reticulocyte lysate and 5 µL of energy regeneration system (0.5 m*M* ATP, 10 m*M* phosphocreatine, 1.6 mg/mL creatine phosphokinase, 40 m*M* Tris-HCl, 5 m*M* $MgCl_2$, and 2 m*M* DTT).
4. Incubate each sample for various times (i.e., 0, 0.5, 1, 2, 3, and 4 h) at 37°C up to 4 h (*see* **Note 15**).
5. For the proteasome inhibition studies, pretreat the reticulocyte lysate for 15 min at 37°C prior to degradation either with MG132 (25 µ*M*), ALLN (25 µ*M*), or clasta-lactacystin β-lactone (30 µ*M*) (*see* **Note 16**).

To study ER-associated degradation of MHC Class I heavy chain, mRNA coding for heavy chain was translated for 60 min in a rabbit reticulocyte lysate in the presence of SP-cells. The SP-cells were isolated from the translation mixture after inhibiting further protein synthesis by the addition of 5 m*M*

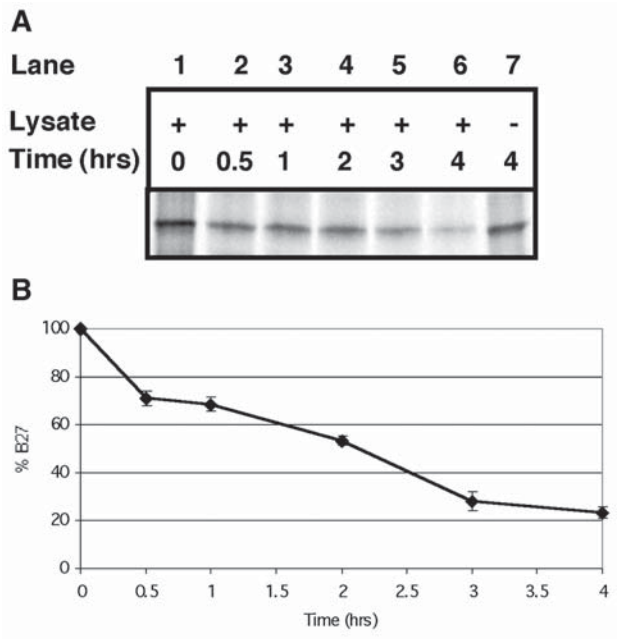

Fig. 6: ER-associated degradation assay of MHC class I heavy chain. (**A**) mRNA coding for heavy chain was translated for 60 min at 30°C in the presence of rabbit reticulocyte lysate. Protein synthesis was inhibited by the addition of cycloheximide (5 m*M*), and the SP-cells were isolated by centrifugation and washed in KHM buffer. Aliquots of SP-cells were resuspended either in untreated reticulocyte lysate and an ATP regeneration system (lanes 1–6) or in KHM buffer and an ATP regeneration system (lane 7). Degradation was terminated by the addition of SDS-PAGE sample buffer containing DTT (50 m*M*). Products were separated by 10% SDS-PAGE and analyzed by autoradiography. (**B**) Quantification analysis of degradation time courses of wild-type heavy chain. Band intensity at each point was quantified by phosphorimager analysis and plotted against time of assay. The starting point of the assay was taken as 100% total products at time 0. Each time point was calculated as a percentage of relative intensity (arbitrary units) to time 0 minus background intensity for each lane. Each data point represents an average value from three experiments, with the error bars representing S.E.

cycloheximide. The rabbit reticulocyte lysate used for translation contains added hemin, which is known to inhibit proteasomal activity ***(21)***. Therefore, the SP-cells were resuspended either in KHM buffer alone or in the presence of an untreated reticulocyte lysate that did not contain added hemin ***(22)***. When the SP-cells were resuspended in the presence of lysate, an ATP-regeneration system, and DTT, degradation of translated heavy chain was observed over the 4-h time course (**Fig. 6A**, lanes 1–6). When the SP-cells were resuspended in

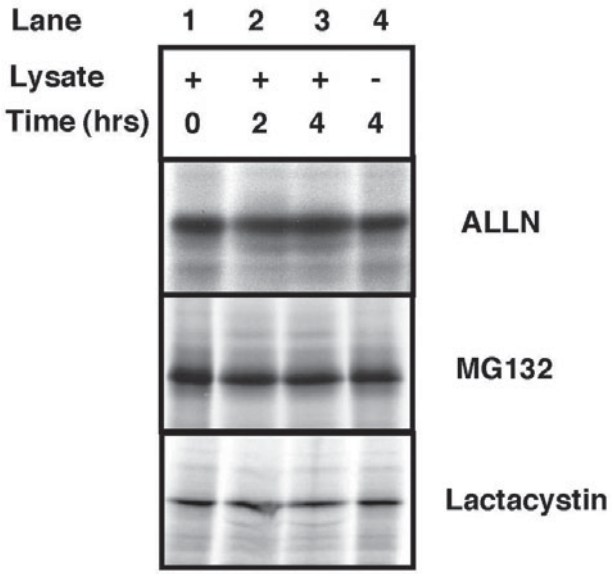

Fig. 7. Inhibition studies of ER-associated degradation. mRNA coding heavy chain was translated for 60 min in the presence of SP-cells. Further protein synthesis was inhibited with 5 m*M* cycloheximide, and the SP-cells were isolated by centrifugation and washed in KHM buffer. Aliquots of SP-cells were resuspended either in reticulocyte lysate (without hemin) treated with ALLN, MG132, or clasta-lactacystin β-lactone (lactacystin) and an ATP regeneration system containing DTT (lanes 1–3), or in KHM buffer and an ATP regeneration system containing DTT (lane 4). Degradation was terminated by the addition of SDS-PAGE sample buffer containing 50 m*M* DTT. Products were separated by 10% SDS-PAGE and analyzed by autoradiography.

buffer alone, no degradation was observed (**Fig. 6A**, lane 7). To assess whether heavy-chain degradation observed in this SP-cell system was mediated by the proteasome, the effects of proteasome inhibitors were examined. The first two inhibitors assessed were the synthetic peptide aldehyde inhibitors *N*-acetyl-L-leucinyl-L-leucinyl-norleucinal (ALLN) and Carbobenzoxy-L-Leucyl-L-Leucyl-L-Leucinal (MG132) inhibiting the activity of calpains (especially Class I), and cathepsins L and B ***(23,24)***. A third inhibitor called lactacystin (clasto-lactacystin β-lactone) is specific, modifying essential threonine residues of β-sububits within the catalytic core of the 20 S proteasome ***(25)***. All three inhibitors mentioned blocked degradation of heavy chain from SP-cells when incubated in the presence of untreated reticulocyte lysate, ATP-regeneration system, and DTT (**Fig. 7**, lanes 1–4). Thus, the SP-cell system faithfully reproduces the initial stages in folding, assembly, and ER-associated degradation of MHC Class I heavy chain.

4. Notes

1. The procedure takes approx 1 h and should be carried out immediately prior to using the SP-cells for translation in vitro. SP-cells can be stored at –80°C in 100 µL of sterile sucrose (0.2 *M*) and 1 µL of PMSF (0.1 *M*). The translocation of proteins in vitro must be assessed if this method of storage is chosen. It is advisable to use a minimum of one 75-cm^2 flask of cells because it proves difficult to work with a smaller quantity of cells. Note that the size of the cell pellet will decrease during the procedure owing to loss of the cell cytosol, which is accompanied by a decrease in cell volume.
2. The digitonin concentration has been optimized for permeabilization of CEM cells. If a different cell-line is used, the concentration of digitonin required for permeabilization should be assessed by titration.
3. In vitro transcription using a linearized template having a 3' overhang may inhibit translation or produce aberrant translation products. Try to use restriction endonucleases that generate a 5' overhang or blunt end prior to the transcription reaction. To avoid low mRNA yields or partially degraded mRNA, always use sterile pipet tips, microcentrifuge tubes, and RNase-free water.
4. The yield of mRNA can be increased by a further addition of RNA polymerase (1 µL) after 1 h.
5. Run 1 µL of RNA sample on a 1% agarose gel containing 2% ethidium bromide (EB). For running RNA, use either electrophoresis equipment that is for RNA only or run samples for a limited time, i.e., 30 min at 100 volts using ordinary DNA gel electrophoresis equipment.
6. The optimal salt concentration (KCl and MgOAc) used in the translation protocol should be optimized for each individual mRNA transcript. The optimal salt concentrations can increase translation as much as 10-fold.
7. To evaluate the translation efficiency of a new RNA sample, set up a single 25 µL reaction including 4 µL of sterile water instead of SP-cells.
8. If there are no products from translation, then the RNA may need to be heated to 60°C for 10 min prior to translation in order to denature any secondary structure. Additional products with molecular weights smaller than the major translation product may be observed owing to ribosomal binding to internal start sites downstream of the initiation codon.
9. The incubation time with Endo H overnight at 37°C can be reduced to 5 h at 37°C. This can be preferable if protein degradation is a problem.
10. The translocated and nontranslocated forms of the protein usually migrate differently on a reducing SDS-PAGE gel owing to modification of the nascent chain in the ER lumen. When transmembrane proteins are treated with Proteinase K, this results in an increase in electrophoretic mobility corresponding to loss of the cytoplasmic domain that is accessible to the enzyme. The translocated polypeptide may migrate faster than the nontranslocated form owing to signal peptide cleavage that occurs when the nascent chain enters the ER lumen. If the protein is a glycoprotein, the translocated polypeptide will exhibit decreased electrophoretic mobility owing to glycosylation. This is apparent in the case of MHC Class I heavy chain.

11. Detergents are present in the buffers to enable complete lysis of cell membranes and reduce hydrophobic interactions. The choice of detergents used in the low-salt lysis buffer may depend on a number of factors, including the efficiency of membrane solubilization and your expenditure. There are a number of detergents such as Triton X-100, IGEPAL, CA-630, Renex-30, or CHAPS. The authors recommend using Triton X-100 as a cheaper and effective source of detergent. If problems with solubilization are experienced, then use 2% CHAPS for lysis and incubations with antibody. Washes can be performed with a 1% CHAPS or 1% Triton X-100 lysis buffer.
12. If a high background is observed with immunoprecipitation, which could be owing to protein synthesis from a carryover of [^{35}S]-methionine or protein degradation, it is advisable to add 2 µL cold methionine (0.1 *M*) and 5 µL PMSF (0.1 *M*) to the immunoprecipitation reaction for longer incubations.
13. The dilution of antibody used in an immunoprecipitation reaction will have to be optimized. A general guide is to use 1:1000 dilution of antibody to start. The long incubation time of 16 h at 4°C can be reduced to 2–3 h at 4°C. Nonspecific binding can be a problem, especially if the proteins that are immunologically distinct from the antigen are trapped in the pellets formed during immunoprecipitation. To reduce nonspecific binding, a high salt wash should be included in **step 7** of the protocol, i.e., 1X low salt wash, 1X high salt (150 m*M* Tris-HCl, pH 7.5, 150 m*M* NaCl, 1% Triton X-100, and 2 m*M* EDTA) wash and 2X low-salt washes. Therefore, its always crucial to perform a control reaction where antibody is replaced by a nonrelevant immunoglobulin or if available a pre-immune (pre-bleed from a rabbit before injection of peptide).
14. The rabbit reticulocyte lysate for degradation assays was prepared as described previously; it was not treated with micrococcal nuclease, and did not contain added hemin ***(22)***. An alternative source of rabbit reticulocyte lysate that could be used instead is one that is commercially available from Promega.
15. The incubation time used to study protein degradation of a protein of interest will depend greatly on the protein used in the ERAD assay. For example, the degradation kinetics of adrenergic receptors can be by at least twice the rate of that of MHC Class I heavy chain.
16. Some of the proteasome inhibitors used have a short storage time; for example, lactacystin has a storage time of 1 mo at –80°C after reconstitution in DMSO.

Acknowledgments

The authors would like to thank Dr. Hidde Ploegh for providing the monoclonal antibody HC10. We are indebted to past and present members of the Bulleid Laboratory who have contributed to development of the methodologies described in this chapter; in particular Richard Wilson and Mark Farmery, who helped establish the SP-cell system for protein expression. The work was funded by the BBSRC (ref. C019198), Pfizer PLC, The Royal Society, and the Wellcome Trust (ref. 39078, 56493).

References

1. Crowley, K. S., Liao, S., Worrell, V. E., Reinhart, G. D., and Johnson A. E. (1994) Secretory proteins move through the endoplasmic reticulum membrane via an aqueous, gated pore. *Cell* **78,** 461–471.
2. Bergeron, J. J., Brenner, M. B., Thomas, D. Y., and Williams, D. B. (1994) Calnexin: a membrane-bound chaperone of the endoplasmic reticulum. *Trends Biochem. Sci.* **19,** 124–128.
3. Hammond, C. and Helenius, A. (1995) Quality control in the secretory pathway. *Curr. Opin. Cell Biol.* **7,** 523–529.
4. Knittler, M. R., Dirks, S., and Haas, I. G. (1995) Molecular chaperones involved in protein degradation in the endoplasmic reticulum: quantitative interaction of the heat shock cognate protein BiP with partially folded immunoglobulin light chains that are degraded in the endoplasmic reticulum. *Proc. Natl. Acad. Sci. USA* **92,** 1764–1768.
5. Vidair, C. A., Huang, R. N., and Doxsey, S. J. (1996) Heat shock causes protein aggregation and reduced protein solubility at the centrosome and other cytoplasmic locations. *Int. J. Hyperthermia* **12,** 681–695.
6. Buchner, J. (1996) Supervising the fold: functional principles of molecular chaperones. *FASEB J.* **10,** 10–19.
7. Wiertz, E. J., Jones, T. R., Sun, L., Bogyo, M., Geuze, H. J., and Ploegh, H. L. (1996) The human cytomegalovirus US11 gene product dislocates MHC class I heavy chains from the endoplasmic reticulum to the cytosol. *Cell* **84,** 769–779.
8. Levitskaya, J., Sharipo, A., Leonchiks, A., Ciechanover, A., and Masucci, M. G. (1997) Inhibition of ubiquitin/proteasome-dependent protein degradation by the Gly-Ala repeat domain of the Epstein-Barr virus nuclear antigen 1. *Proc. Natl. Acad. Sci. USA* **94,** 12,616–12,621.
9. Bonifacino, J. S., Suzuki, C. K., Lippincott Schwartz, J., Weissman, A. M., and Klausner, R. D. (1989) Pre-Golgi degradation of newly synthesized T-cell antigen receptor chains: intrinsic sensitivity and the role of subunit assembly. *J. Cell Biol.* **109,** 73–83.
10. Plutner, H., Davidson, H. W., Saraste, J., and Balch, W. E. (1992) Morphological analysis of protein transport from the ER to Golgi membranes in digitonin-permeabilised cells: role of the p58 containing compartment. *J. Cell Biol.* **119,** 1097–1116.
11. Wilson, R., Allen, A. J., Oliver, J., Brookman, J. L., High, S., and Bulleid, N. J. (1995) The translocation, folding, assembly and redox-dependent degradation of secretory and membrane proteins in semi-permeabilized mammalian cells. *Biochem. J.* **307,** 679–687.
12. Wilson, C. M., Farmery, M. R., and Bulleid, N. J. (2000) Pivotal role of calnexin and mannose trimming in regulating the endoplasmic reticulum-associated degradation of major histocompatibility complex class I heavy chain. *J. Biol. Chem.* **275,** 21,224–21,232.
13. Gurevich, V. V., Pokrovskaya, I. D., Obukhova, T. A., and Zozulya, S. A. (1991) Preparative in vitro mRNA synthesis using SP6 and T7 RNA polymerases. *Anal. Biochem.* **195,** 207–213.

14. Sadasivan, B. K., Cariappa, A., Waneck, G. L., and Cresswell, P. (1995) Assembly, peptide loading, and transport of MHC class I molecules in a calnexin-negative cell line. *Cold Spring Harb. Symp. Quant. Biol.* **60,** 267–275.
15. Barnstable, C. J., Bodmer, W. F., Brown, G., Galfre, G., Milstein, C., Williams, A. F., and Ziegler, A. (1978) Production of monoclonal antibodies to group A erythrocytes, HLA and other human cell surface antigens-new tools for genetic analysis. *Cell* **14,** 9–20.
16. Farmery, M. R., Allen, S., Allen, A. J., and Bulleid, N. J. (2000) The role of ERp57 in disulfide bond formation during the assembly of major histocompatibility complex class I in a synchronized semipermeabilized cell translation system. *J. Biol. Chem.* **275,** 14,933–14,938.
17. Stam, N. J., Spits, H., and Ploegh, H. L. (1986) Monoclonal antibodies raised against denatured HLA-B locus heavy chains permit biochemical characterization of certain HLA-C locus products. *J. Immunol.* **137,** 2299–2306.
18. Werner, E. D., Brodsky, J. L., and McCracken, A. A. (1996) Proteasome-dependent endoplasmic reticulum-associated protein degradation: an unconventional route to a familiar fate. *Proc. Natl. Acad. Sci. USA* **93,** 13,797–13,801.
19. McCracken, A. A. and Brodsky, J. L. (1996) Assembly of ER-associated protein degradation in vitro: dependence on cytosol, calnexin, and ATP. *J. Cell Biol.* **132,** 291–298.
20. Pilon, M., Schekman, R., and Romisch, K. (1997) Sec61p mediates export of a misfolded secretory protein from the endoplasmic reticulum to the cytosol for degradation. *EMBO J.* **16,** 4540–4548.
21. Haas, A. L., and Rose, I. A. (1981) Hemin inhibits ATP-dependent ubiquitin-dependent proteolysis: role of hemin in regulating ubiquitin conjugate degradation. *Proc. Natl. Acad. Sci. USA* **78,** 6845–6848.
22. Pelham, H. R. B. and Jackson, R. J. (1976) An efficient mRNA-dependent translation system from reticulocyte lysates. *Eur. J. Biochem.* **67,** 247–256.
23. Rock, K. L., Gramm, C., Rothstein, L., Clark, K., Stein, R., Dick, L., et al. (1994) Inhibitors of the proteasome block the degradation of most cell proteins and the generation of peptides presented on MHC class I molecules. *Cell* **78,** 761–771.
24. Lowe, J., Stock, D., Jap, R., Zwickl, P., Baumeister, W., and and Huber, R. (1995) Crystal-structure of the 20S proteasome from the archaeon T. acidoophilum at 3.4 angstrom resolution. *Science* **268,** 533–539.
25. Dick, L. R., Criukshank, A. A., Destree, A. T., Grenier, L., McCormack, T. A., Melandri, F. D., et al. (1997) Mechanistic studies on the inactivation of the proteasome by lactacystin in cultured cells. *J. Biol. Chem.* **272,** 182–188.